



COLORADO

Department of Transportation

Applied Research and Innovation Branch

Sensitivity of Dynamic Modulus and Flow Number of CDOT HMA Mixes in the Pavement Mechanistic-Empirical Design (PMED)

Md Rashadul Islam and Sylvester A. Kalevela

Report No. CDOT 2020-02

February 2020

The contents of this report reflect the views of the authors, who are responsible for the facts and accuracy of the data presented herein. The contents do not necessarily reflect the official views of the Colorado Department of Transportation or the Federal Highway Administration. This report does not constitute a standard, specification, or regulation

Technical Report Documentation Page

1. Report No. CDOT-2020-01	2. Government Accession No.	3. Recipient's Catalog No.	
4. Title and Subtitle Sensitivity of Dynamic Modulus and Flow Number of CDOT HMA Mixes in the Pavement Mechanistic-Empirical Design (PMED)		5. Report Date February 2020	
		6. Performing Organization Code	
7. Author(s) Md Rashadul Islam and Sylvester A. Kalevela		8. Performing Organization Report No.	
9. Performing Organization Name and Address Colorado State University – Pueblo Department of Engineering Technology 2200 Bonforte Blvd Pueblo, CO 81001		10. Work Unit No. (TRAIS)	
		11. Contract or Grant No. 417.01	
12. Sponsoring Agency Name and Address Colorado Department of Transportation - Research 2829 West Howard Place Denver, CO 80204		13. Type of Report and Period Covered Final	
		14. Sponsoring Agency Code	
15. Supplementary Notes Prepared in cooperation with the US Department of Transportation, Federal Highway Administration			
16. Abstract Colorado Department of Transportation (CDOT) has dynamic modulus (E^*), and flow number (N) database of different mixes from different regions of Colorado. The sensitivities of these mixes considering factors such as mix types, aggregates source, volumetric properties, contractors, preparation times, binders, etc. on E^* , and N , and on the pavement performances are investigated in this study. The effects of the mix factors were examined by statistical analysis, and using the Pavement Mechanistic-Empirical Design (PMED) software analysis. The mix, S(100) PG 76-28 is the most durable mix against rutting, and the mix, SX(75) PG 58-34 is the most durable mix against transverse cracking. On the other hand, SX(75) PG 64-28 mix is the most susceptible mix for rutting, and S(100) PG 64-22 is the most susceptible mix for transverse cracking. Performance of different mixes are mostly different from the CDOT default mixes. All distresses except rutting in HMA increase with the increase in air void, voids-in-mineral aggregates, voids filled with asphalt, and are insensitive to effective binder content, and asphalt content in the study range of these parameters. Rutting in HMA increases with the increase in voids-in-mineral aggregates, voids filled with asphalt, and is insensitive to effective binder content, air void, and asphalt content in the study range of these parameters. N -value can be statically different for different specimens of a mix prepared by a single contractor. N -value increases with the increase in effective binder content, air void, voids-in-mineral aggregates, voids filled with asphalt, and asphalt content in the study range of these parameters.			
17. Keywords Dynamic modulus, Flow number, Sensitivity, PMED, Pavement performance		18. Distribution Statement This document is available on CDOT's website http://www.coloradodot.info/programs/research/pdfs	
19. Security Classif. (of this report) Unclassified	20. Security Classif. (of this page) Unclassified	21. No. of Pages 191	22. Price

Acknowledgements

The Colorado State University–Pueblo (CSU–Pueblo) research team would like to express its sincere gratitude and appreciation to Jay Goldbaum (retired) and Michael Stanford for being the Study Panel Leaders, and Colorado Department of Transportation (CDOT), champions of this project for their regular support and suggestions. The research team members appreciate the valuable administration and support of David Reeves, Aziz Khan and Amanullah Mommandi. The CSU–Pueblo research team would also like to thank Melody Perkins, James Chang, Keith Uren, Vincent Battista, Craig Wieden, Tim Webb, and Skip Outcalt for their valuable suggestions during the project completion. The CSU-Pueblo research team appreciates the Federal Highway Administration (FHWA) – Colorado Division Contact, Dahir Egal, and the Research and Implementation Council (RIC) Sponsor, Bill Schiebel for giving us their valuable time. Special thanks also go to Roberto E. DeDios and Numan Mizyed for their keen interest in the research and timely organization.

Executive Summary and Implementation Statement

The Colorado Department of Transportation (CDOT) has a database of dynamic moduli (E^*) and flow numbers (N) for different mixes, aggregate gradations, and other hot asphalt properties. The influences of these mix parameters on E^* , N , and pavement performance are unknown to CDOT. Therefore, this research is conducted to identify the sensitivity of E^* to these mix parameters. Determining the sensitivity of the parameters to E^* may help in finding the most economic and durable mixes for pavement design in Colorado.

The E^* and N data are obtained from CDOT and grouped into eleven categories. For each group, the variations in E^* and N for different contractors, preparation times, binders, etc. are being assessed. Subsequently, the effects of the mix parameters are examined by the Pavement Mechanistic-Empirical Design (PMED) software analysis. Five types of distresses: International Roughness Index (IRI), total rutting, rutting in a hot-mix asphalt (HMA) layer, bottom-up fatigue cracking, and top-down longitudinal fatigue cracking are considered in the analysis.

Results show that S(100) PG 64-22 mixture has the highest value of E^* at low temperature or high reduced frequency, making it the most susceptible mix for transverse cracking. At high temperature or lower reduced frequency, S(100) PG 76-28 has the highest E^* value, making it the most durable mix against rutting. SX(75) PG 64-28 has the lowest E^* value at high temperature or lower reduced frequency. At low temperature or high reduced frequency, SX(75) PG 58-34 has the lowest E^* value. SMA mix has a lower E^* compared to S(100) and SX(100) mixes at low temperature, and thus, SMA is a better mix for reduced transverse cracking than S(100) and SX(100). The E^* increases with an increase in V_{be} , V_a , and VFA, and decreases with an increase in VMA and AC. However, the effects of VFA and AC on E^* are less sensitive compared to V_{be} , V_a , and VFA. The E^* of a mix can vary from 200 ksi to about 1,000 ksi, even if samples are from the same contractor. Similarly, the prediction of distresses using the PMED software may differ by up to 170%, although most data shows the difference is less than 100%. Using CDOT thermal cracking threshold values, the prediction of distresses using the PMED software for a mix prepared by a single contractor may differ by more than eleven years, although most of the data ranges from three to seven years. All distresses, except rutting, increase with air void (V_a), voids in mineral

aggregate (VMA), and voids filled with asphalt (VFA). These values are insensitive to the effective binder content (V_{be}) and asphalt content (AC) in the study range of these parameters. Rutting in HMA increases with an increase in VMA and VFA, and is insensitive to V_{be} , V_a , and AC in the study range of these parameters.

Flow numbers for different types of HMA used in Colorado vary from 47 to 2,272. The same mix may have statistically different flow numbers, regardless of contractor. Flow number increases with an increase in V_{be} , V_a , VMA, VFA, and AC in the study range of these parameters.

The developed dynamic moduli master curves may be used in the Colorado-calibrated AASHTOWare's PMED software while analyzing and designing pavement in Colorado. While selecting a contractor, binder source, and aggregate pit, care should be taken, or uniformity of the mix maintained. The conclusion obtained after analyzing the flow number can be directly used to choose a mixture for a particular volume of Equivalent Single Axle Load (ESAL).

Table of Contents

Acknowledgements.....	1
Table of Contents.....	v
List of Figures.....	viii
List of Tables.....	xii
SECTION 1: INTRODUCTION.....	1
Background.....	1
Objectives.....	1
SECTION 2: LITERATURE REVIEW.....	2
Dynamic Modulus.....	2
Flow Number (<i>N</i>).....	4
SECTION 3: LABORATORY TESTING.....	6
Dynamic Modulus (<i>E</i> *) Testing.....	6
Flow Number (<i>N</i>) Testing.....	6
SECTION 4: ANALYSIS OF DYNAMIC MODULUS.....	9
Dynamic Modulus Data.....	9
S(100) PG 64-22.....	10
S(100) PG 76-28.....	12
SMA PG 76-28.....	13
SX(75) PG 58-28.....	16
SX(75) PG 58-34.....	18
SX(75) PG 64-22.....	19
SX(75) PG 64-28.....	21
SX(100) PG 58-28.....	22
SX(100) PG 64-22.....	23
SX(100) PG 64-28.....	26
SX(100) PG 76-28.....	28
Summary of Comparison.....	31
Developing Dynamic Modulus Mastercurves for PMED.....	33
S(100) PG 64-22.....	35

S(100) PG 76-28	37
SMA PG 76-28	39
SX(75) PG 58-28	41
SX(75) PG 58-34	43
SX(75) PG 64-22	45
SX(75) PG 64-28	47
SX(100) PG 58-28	49
SX(100) PG 64-22	51
SX(100) PG 64-28	53
SX(100) PG 76-28	55
SECTION 5: ANALYSIS OF FLOW NUMBER	57
Effect on Flow Number	57
Same Mix by Same Contractor	57
Same Mix by Different Contractors.....	58
Groupwise Comparison	60
S(100) PG 64-22	60
S(100) PG 76-28	62
SMA PG 76-28	64
SX(75) PG 58-28	66
SX(75) PG 58-34	68
SX(75) PG 64-22	69
SX(75) PG 64-28	70
SX(100) PG 58-28	72
SX(100) PG 64-22	72
SX(100) PG 64-28	75
SX(100) PG 76-28	76
Flow Number Analysis Summary.....	80
SECTION 6: PERFORMANCE ANALYSIS USING THE PMED SOFTWARE.....	84
S(100) PG 64-22	85
S(100) PG 76-28	94
SMA PG 76-28	102

SX(75) PG 58-28	112
SX(75) PG 58-34	119
SX(75) PG 64-22	127
SX(75) PG 64-28	136
SX(100) PG 58-28	144
SX(100) PG 64-22	151
SX(100) PG 64-28	160
SX(100) PG 76-28	169
Analysis Summary	179
SECTION 7: CONCLUSIONS AND RECOMMENDATIONS	187
Conclusions.....	187
Recommendations for Future Studies.....	188
Implementation Plans.....	189
REFERENCES.....	190

List of Figures

Figure 1. Stress-strain Behaviors of Elastic and Viscoelastic Materials	2
Figure 2. Flow Number Test Setup.....	7
Figure 3. Relationship between Permanent Strain and Load Cycles [17]	8
Figure 4. Dynamic Modulus of S(100) PG 64-22 Mix.....	10
Figure 5. Dynamic Modulus of S(100) PG 76-28 Mix.....	12
Figure 6. Dynamic Modulus of SMA PG 76-28 Mix	14
Figure 7. Dynamic Modulus of SX(75) PG 58-28 Mix	17
Figure 8. Dynamic Modulus of SX(75) PG 58-34 Mix	19
Figure 9. Dynamic Modulus of SX(75) PG 64-22 Mix	19
Figure 10. Dynamic Modulus of SX(75) PG 64-28 Mix	21
Figure 11. Dynamic Modulus of SX(100) PG 58-28 Mix	23
Figure 12. Dynamic Modulus of SX(100) PG 64-22 Mix	24
Figure 13. Dynamic Modulus of SX(100) PG 64-28 Mix	26
Figure 14. Dynamic Modulus of SX(100) PG 76-28 Mix	28
Figure 15. Groupwise Comparison	32
Figure 16. Flow Number of Eight Specimens of SX(100) PG 64-28 Mix	58
Figure 17. Flow Number of a Mix by Different Contractors.....	59
Figure 18. Flow Numbers for S(100) PG 64-22 Mix.....	61
Figure 19. Flow Numbers for S(100) PG 76-28 Mix.....	63
Figure 20. Flow Numbers for SMA PG 76-28 Mix.....	64
Figure 21. Flow Numbers for SX(75) PG 58-28 Mix.....	66
Figure 22. Flow Numbers for SX(75) PG 58-34 Mix.....	68
Figure 23. Flow Numbers for SX(75) PG 64-22 Mix.....	69
Figure 24. Flow Numbers for SX(75) PG 64-28 Mix.....	71
Figure 25. Flow Numbers for SX(100) PG 64-22 Mix.....	73
Figure 26. Flow Numbers for SX(100) PG 64-28 Mix.....	75
Figure 27. Flow Numbers for SX(100) PG 76-28 Mix.....	77
Figure 28. Groupwise Average Flow Numbers	81
Figure 29. Geometry of the Trial Pavement for the PMED Analysis of All Groups	84
Figure 30. IRI Due to AADTT = 7,000 by S(100) PG 64-22 Mix	87
Figure 31. IRI Due to AADTT = 800 by S(100) PG 64-22 Mix	87
Figure 32. Total Rutting Due to AADTT = 7,000 by S(100) PG 64-22 Mix	88
Figure 33. Total Rutting Due to AADTT = 800 by S(100) PG 64-22 Mix	89
Figure 34. Rutting in Asphalt Layer Due to AADTT = 7,000 by S(100) PG 64-22 Mix.....	90
Figure 35. Rutting in Asphalt Layer Due to AADTT = 800 by S(100) PG 64-22 Mix.....	90
Figure 36. Bottom-up Fatigue Cracking Due to AADTT = 7,000 by S(100) PG 64-22 Mix.....	91
Figure 37. Bottom-up Fatigue Cracking Due to AADTT = 800 by S(100) PG 64-22 Mix.....	92

Figure 38. Longitudinal Cracking Due to AADTT = 7,000 by S(100) PG 64-22 Mix	93
Figure 39. Longitudinal Cracking Due to AADTT = 800 by S(100) PG 64-22 Mix	93
Figure 40. IRI Due to AADTT = 7,000 by S(100) PG 76-28 Mix	95
Figure 41. IRI Due to AADTT = 800 by S(100) PG 76-28 Mix	96
Figure 42. Total Rutting Due to AADTT = 7,000 by S(100) PG 76-28 Mix	97
Figure 43. Total Rutting Due to AADTT = 800 by S(100) PG 76-28 Mix	97
Figure 44. Rutting in Asphalt Layer Due to AADTT = 7,000 by S(100) PG 76-28 Mix.....	98
Figure 45. Rutting in Asphalt Layer Due to AADTT = 800 by S(100) PG 76-28 Mix.....	99
Figure 46. Bottom-up Fatigue Cracking Due to AADTT = 7,000 by S(100) PG 76-28 Mix.....	100
Figure 47. Bottom-up Fatigue Cracking Due to AADTT = 800 by S(100) PG 76-28 Mix.....	100
Figure 48. Longitudinal Cracking Due to AADTT = 7,000 by S(100) PG 76-28 Mix	101
Figure 49. Longitudinal Cracking Due to AADTT = 800 by S(100) PG 76-28 Mix	101
Figure 50. IRI Due to AADTT = 7,000 by SMA PG 76-28 Mix	104
Figure 51. IRI Due to AADTT = 800 by SMA PG 76-28 Mix	104
Figure 52. Total Rutting Due to AADTT = 7,000 by SMA PG 76-28 Mix	105
Figure 53. Total Rutting Due to AADTT = 800 by SMA PG 76-28 Mix	106
Figure 54. Rutting in Asphalt Layer Due to AADTT = 7,000 by SMA PG 76-28 Mix.....	107
Figure 55. Rutting in Asphalt Layer Due to AADTT = 800 by SMA PG 76-28 Mix.....	107
Figure 56. Bottom-up Fatigue Cracking Due to AADTT = 7,000 by SMA PG 76-28 Mix.....	108
Figure 57. Bottom-up Fatigue Cracking Due to AADTT = 800 by SMA PG 76-28 Mix.....	109
Figure 58. Longitudinal Cracking Due to AADTT = 7,000 by SMA PG 76-28 Mix	110
Figure 59. Longitudinal Cracking Due to AADTT = 800 by SMA PG 76-28 Mix	110
Figure 60. IRI Due to AADTT = 3,000 by SX(75) PG 58-28 Mix	113
Figure 61. IRI Due to AADTT = 800 by SX(75) PG 58-28 Mix	113
Figure 62. Total Rutting Due to AADTT = 3,000 by SX(75) PG 58-28 Mix	114
Figure 63. Total Rutting Due to AADTT = 800 by SX(75) PG 58-28 Mix	115
Figure 64. Rutting in Asphalt Layer Due to AADTT = 3,000 by SX(75) PG 58-28 Mix.....	115
Figure 65. Rutting in Asphalt Layer Due to AADTT = 800 by SX(75) PG 58-28 Mix.....	116
Figure 66. Bottom-up Fatigue Cracking Due to AADTT = 3,000 by SX(75) PG 58-28 Mix....	117
Figure 67. Bottom-up Fatigue Cracking Due to AADTT = 800 by SX(75) PG 58-28 Mix.....	117
Figure 68. Longitudinal Cracking Due to AADTT = 3,000 by SX(75) PG 58-28 Mix	118
Figure 69. Longitudinal Cracking Due to AADTT = 800 by SX(75) PG 58-28 Mix	118
Figure 70. IRI Due to AADTT = 7,000 by SX(75) PG 58-34 Mix	120
Figure 71. IRI Due to AADTT = 800 by SX(75) PG 58-34 Mix	121
Figure 72. Total Rutting Due to AADTT = 3,000 by SX(75) PG 58-34 Mix	122
Figure 73. Total Rutting Due to AADTT = 800 by SX(75) PG 58-34 Mix	122
Figure 74. Rutting in Asphalt Layer Due to AADTT = 3,000 by SX(75) PG 58-34 Mix.....	123
Figure 75. Rutting in Asphalt Layer Due to AADTT = 800 by SX(75) PG 58-34 Mix.....	123
Figure 76. Bottom-up Fatigue Cracking Due to AADTT = 3,000 by SX(75) PG 58-34 Mix....	124
Figure 77. Bottom-up Fatigue Cracking Due to AADTT = 800 by SX(75) PG 58-34 Mix.....	125

Figure 78. Longitudinal Cracking Due to AADTT = 3,000 by SX(75) PG 58-34 Mix	126
Figure 79. Longitudinal Cracking Due to AADTT = 800 by SX(75) PG 58-34 Mix	126
Figure 80. IRI Due to AADTT = 3,000 by SX(75) PG 64-22 Mix	129
Figure 81. IRI Due to AADTT = 800 by SX(75) PG 64-22 Mix	129
Figure 82. Total Rutting Due to AADTT = 3,000 by SX(75) PG 64-22 Mix	130
Figure 83. Total Rutting Due to AADTT = 800 by SX(75) PG 64-22 Mix	130
Figure 84. Rutting in Asphalt Layer Due to AADTT = 3,000 by SX(75) PG 64-22 Mix.....	131
Figure 85. Rutting in Asphalt Layer Due to AADTT = 800 by SX(75) PG 64-22 Mix.....	132
Figure 86. Bottom-up Fatigue Cracking Due to AADTT = 3,000 by SX(75) PG 64-22 Mix....	133
Figure 87. Bottom-up Fatigue Cracking Due to AADTT = 800 by SX(75) PG 64-22 Mix.....	133
Figure 88. Longitudinal Cracking Due to AADTT = 3,000 by SX(75) PG 64-22 Mix	134
Figure 89. Longitudinal Cracking Due to AADTT = 800 by SX(75) PG 64-22 Mix	135
Figure 90. IRI Due to AADTT = 3,000 by SX(75) PG 64-28 Mix	137
Figure 91. IRI Due to AADTT = 800 by SX(75) PG 64-28 Mix	137
Figure 92. Total Rutting Due to AADTT = 3,000 by SX(75) PG 64-28 Mix	138
Figure 93. Total Rutting Due to AADTT = 800 by SX(75) PG 64-28 Mix	139
Figure 94. Rutting in Asphalt Layer Due to AADTT = 3,000 by SX(75) PG 64-28 Mix.....	140
Figure 95. Rutting in Asphalt Layer Due to AADTT = 800 by SX(75) PG 64-28 Mix.....	140
Figure 96. Bottom-up Fatigue Cracking Due to AADTT = 3,000 by SX(75) PG 64-28 Mix....	141
Figure 97. Bottom-up Fatigue Cracking Due to AADTT = 800 by SX(75) PG 64-28 Mix.....	142
Figure 98. Longitudinal Cracking Due to AADTT = 3,000 by SX(75) PG 64-28 Mix	143
Figure 99. Longitudinal Cracking Due to AADTT = 800 by SX(75) PG 64-28 Mix	143
Figure 100. IRI Due to AADTT = 7,000 by SX(100) PG 58-28 Mix	145
Figure 101. IRI Due to AADTT = 800 by SX(100) PG 58-28 Mix	145
Figure 102. Total Rutting Due to AADTT = 7,000 by SX(100) PG 58-28 Mix	146
Figure 103. Total Rutting Due to AADTT = 800 by SX(100) PG 58-28 Mix	146
Figure 104. Rutting in Asphalt Layer Due to AADTT = 7,000 by SX(100) PG 58-28 Mix.....	147
Figure 105. Rutting in Asphalt Layer Due to AADTT = 800 by SX(100) PG 58-28 Mix.....	148
Figure 106. Bottom-up Fatigue Cracking Due to AADTT = 7,000 by SX(100) PG 58-28 Mix	149
Figure 107. Bottom-up Fatigue Cracking Due to AADTT = 800 by SX(100) PG 58-28 Mix...	149
Figure 108. Longitudinal Cracking Due to AADTT = 7,000 by SX(100) PG 58-28 Mix	150
Figure 109. Longitudinal Cracking Due to AADTT = 800 by SX(100) PG 58-28 Mix	151
Figure 110. IRI Due to AADTT = 7,000 by SX(100) PG 64-22 Mix	153
Figure 111. IRI Due to AADTT = 800 by SX(100) PG 64-22 Mix	153
Figure 112. Total Rutting Due to AADTT = 7,000 by SX(100) PG 64-22 Mix	154
Figure 113. Total Rutting Due to AADTT = 800 by SX(100) PG 64-22 Mix	155
Figure 114. Rutting in Asphalt Layer Due to AADTT = 7,000 by SX(100) PG 64-22 Mix.....	156
Figure 115. Rutting in Asphalt Layer Due to AADTT = 800 by SX(100) PG 64-22 Mix.....	156
Figure 116. Bottom-up Fatigue Cracking Due to AADTT = 7,000 by SX(100) PG 64-22 Mix	157
Figure 117. Bottom-up Fatigue Cracking Due to AADTT = 800 by SX(100) PG 64-22 Mix...	158

Figure 118. Longitudinal Cracking Due to AADTT = 7,000 by SX(100) PG 64-22 Mix	159
Figure 119. Longitudinal Cracking Due to AADTT = 800 by SX(100) PG 64-22 Mix	159
Figure 120. IRI Due to AADTT = 7,000 by SX(100) PG 64-28 Mix	162
Figure 121. IRI Due to AADTT = 800 by SX(100) PG 64-28 Mix	162
Figure 122. Total Rutting Due to AADTT = 7,000 by SX(100) PG 64-28 Mix	163
Figure 123. Total Rutting Due to AADTT = 800 by SX(100) PG 64-28 Mix	164
Figure 124. Rutting in the Asphalt Layer Due to AADTT = 7,000 by SX(100) PG 64-28 Mix	165
Figure 125. Rutting in the Asphalt Layer Due to AADTT = 800 by SX(100) PG 64-28 Mix...	165
Figure 126. Bottom-up Fatigue Cracking Due to AADTT = 7,000 by SX(100) PG 64-28 Mix	166
Figure 127. Bottom-up Fatigue Cracking Due to AADTT = 800 by SX(100) PG 64-28 Mix...	167
Figure 128. Longitudinal Cracking Due to AADTT = 7,000 by SX(100) PG 64-28 Mix	168
Figure 129. Longitudinal Cracking Due to AADTT = 800 by SX(100) PG 64-28 Mix	168
Figure 130. IRI Due to AADTT = 7,000 by SX(100) PG 76-28 Mix	172
Figure 131. IRI Due to AADTT = 800 by SX(100) PG 76-28 Mix	172
Figure 132. Total Rutting Due to AADTT = 7,000 by SX(100) PG 76-28 Mix	173
Figure 133. Total Rutting Due to AADTT = 800 by SX(100) PG 76-28 Mix	174
Figure 134. Rutting in the Asphalt Layer Due to AADTT = 7,000 by SX(100) PG 76-28 Mix	175
Figure 135. Rutting in the Asphalt Layer Due to AADTT = 800 by SX(100) PG 76-28 Mix...	175
Figure 136. Bottom-up Fatigue Cracking Due to AADTT = 7,000 by SX(100) PG 76-28 Mix	176
Figure 137. Bottom-up Fatigue Cracking Due to AADTT = 800 by SX(100) PG 76-28 Mix...	177
Figure 138. Longitudinal Cracking Due to AADTT = 7,000 by SX(100) PG 76-28 Mix	178
Figure 139. Longitudinal Cracking Due to AADTT = 800 by SX(100) PG 76-28 Mix	178

List of Tables

Table 1. Flow Number Criteria for HMA [11]	4
Table 2. List of Eleven Mixtures Used in this Study	9
Table 3. Generic Information of S(100) PG 64-22 Mix	11
Table 4. Generic Information of S(100) PG 76-28 Mix	13
Table 5. Generic Information of SMA(100) PG 76-28 Mix	15
Table 6. Generic Information of SX(75) PG 58-28 Mix	17
Table 7. Generic Information of SX(75) PG 64-22 Mix	20
Table 8. Generic Information of SX(75) PG 64-28 Mix	22
Table 9. Generic Information of SX(100) PG 64-22 Mix	25
Table 10. Generic Information of SX(100) PG 64-28 Mix	27
Table 11. Generic Information of SX(100) PG 76-28 Mix	29
Table 12. Summary of the Mix Parameters on Flow Number of HMA	31
Table 13. Summary of the Most Durable and Worst Mixes	33
Table 14. Average Raw Dynamic Moduli of S(100) PG 64-22 Mix.....	35
Table 15. Fitted Dynamic Modulus of S(100) PG 64-22 Mix.....	36
Table 16. Average Raw Dynamic Moduli of S(100) PG 76-28 Mix.....	37
Table 17. Fitted Dynamic Modulus of S(100) PG 76-28 Mix.....	38
Table 18. Average Raw Dynamic Moduli of SMA PG 76-28 Mix	39
Table 19. Fitted Dynamic Modulus of SMA PG 76-28 Mix	40
Table 20. Average Raw Dynamic Moduli of SX(75) PG 58-28 Mix.....	41
Table 21. Fitted Dynamic Modulus of SX(75) PG 58-28 Mix.....	42
Table 22. Average Raw Dynamic Moduli of SX(75) PG 58-34 Mix.....	43
Table 23. Fitted Dynamic Modulus of SX(75) PG 58-34 Mix.....	44
Table 24. Average Raw Dynamic Moduli of SX(75) PG 64-22 Mix.....	45
Table 25. Fitted Dynamic Modulus of SX(75) PG 64-22 Mix.....	46
Table 26. Average Raw Dynamic Moduli of SX(75) PG 64-28 Mix.....	47
Table 27. Fitted Dynamic Modulus of SX(75) PG 64-28 Mix.....	48
Table 28. Average Raw Dynamic Moduli of SX(100) PG 58-28 Mix.....	49
Table 29. Fitted Dynamic Modulus of SX(100) PG 58-28 Mix.....	50
Table 30. Average Raw Dynamic Moduli of SX(100) PG 64-22 Mix.....	51
Table 31. Fitted Dynamic Modulus of SX(100) PG 64-22 Mix.....	52
Table 32. Average Raw Dynamic Moduli of SX(100) PG 64-28 Mix.....	53
Table 33. Fitted Dynamic Modulus of SX(100) PG 64-28 Mix	54
Table 34. Average Raw Dynamic Moduli of SX(100) PG 76-28 Mix.....	55
Table 35. Fitted Dynamic Modulus of SX(100) PG 76-28 Mix.....	56
Table 36. Generic Information of 19655 Mix.....	57
Table 37. Pairwise Comparisons using t-tests to Determine Whether Statistically Different	59
Table 38. Generic Information of S(100) PG 64-22 Mix	61

Table 39. Generic Information of S(100) PG 76-28 Mix	63
Table 40. Generic Information of SMA PG 76-28 Mix.....	65
Table 41. Generic Information of SX(75) PG 58-28 Mix	67
Table 42. Generic Information of SX(75) PG 58-34 Mix	68
Table 43. Generic Information of SX(75) PG 64-22 Mix	70
Table 44. Generic Information of SX(75) PG 64-28 Mix	71
Table 45. Generic Information of SX(100) PG 64-22 Mix	74
Table 46. Generic Information of SX(100) PG 64-28 Mix	76
Table 47. Generic Information of SX(100) PG 76-28 Mix	78
Table 48. Groupwise Average Flow Numbers with 95% Boundaries.....	82
Table 49. Minimum Flow Number Requirements of HMA [11].....	82
Table 50. Summary of the Mix Parameters on Flow Number of HMA	83
Table 51. Climate Station Used for Different Mixes for the PMED Analysis	85
Table 52. Generic Information of S(100) PG 64-22 Mix	86
Table 53. Generic Information of S(100) PG 76-28 Mix	95
Table 54. Generic Information of SMA(100) PG 76-28 Mix.....	103
Table 55. Generic Information of SX(75) PG 58-28 Mix	112
Table 56. Generic Information of SX(75) PG 58-34 Mix	120
Table 57. Generic Information of SX(75) PG 64-22 Mix	128
Table 58. Generic Information of SX(75) PG 64-28 Mix	136
Table 59. Generic Information of SX(100) PG 64-22 Mix	152
Table 60. Generic Information of SX(100) PG 64-28 Mix	161
Table 61. Generic Information of SX(100) PG 76-28 Mix	170
Table 62. Summary of Region 1 Mixes Using the Statistical Analysis.....	180
Table 63. Summary of Region 2 Mixes Using the Statistical Analysis.....	181
Table 64. Summary of Region 3 Mixes Using the Statistical Analysis.....	183
Table 65. Summary of Region 4 Mixes Using the Statistical Analysis.....	184
Table 66. Summary of Region 5 Mixes Using the Statistical Analysis.....	185
Table 67. Summary of the Influence of Different Mix Parameters	186

SECTION 1: INTRODUCTION

Background

The Colorado Department of Transportation (CDOT) has developed dynamic modulus (E^*) and flow number (N) database for over a hundred mixes from locations throughout Colorado. This data set includes different mixes and testing parameters, such as aggregate gradations, replicates, operators, binders, binder sources, volumetric properties, etc. The effects of aggregate gradations and a binder's viscosity on E^* are well known to pavement engineers and researchers using the Witczak's viscosity-based E^* and the flow number (N) model. However, the effect of aggregate type, binder grade, binder source, contractors, etc. on E^* is still unknown. Additionally, the effects of the mix and testing parameters on the pavement performances using AASHTOWare's Pavement Mechanistic-Empirical Design (PMED) software are also unknown in the literature. Therefore, research is needed to identify which parameters are critical to a design, as well as the parameters that are less critical. Knowledge of how the various variables effect E^* , N , and/or the performance of pavements will be beneficial to the pavement designers. Comparing the effects of the range of parameters may allow the pavement designer to determine the most economic and durable mix for use on a project located in Colorado.

Objectives

The main objectives of the research project are:

1. Analyze the effect of aggregate type, binder grade, binder source, number of sample replicates, operator, other mixture and testing parameters on the E^* and N using Colorado database of asphalt mixtures available.
2. Identify critical mixture and testing parameters that are critical and determine their level or degree of impact on the long-term performance of asphalt pavements. Additionally, identify parameters that do not affect or have minimal effect on E^* .
3. Determine the most economic and durable hot-mix asphalt (HMA) mixtures for pavement design by comparing different mixtures parameters.

SECTION 2: LITERATURE REVIEW

Dynamic Modulus

HMA is a viscoelastic material. Viscoelasticity of a material is a property that exhibits both viscous and elastic characteristics when subjected to deformation. In purely elastic materials, stress and strain are in phase. In viscous material, there is a phase lag between applied stress and resulting strain. A 90° phase lag is observed for the strain in purely viscous material (Figure 1). In viscoelastic material, the behavior is somewhere in between that of purely elastic and purely viscous materials, exhibiting some phase lag less than that for purely viscous material. Upon applying stress (σ), the resulting cyclic strain (ε) can be expressed as:

$$\varepsilon = \varepsilon_o \sin(ft + \phi)$$

where ε_o is the strain amplitude, f is the frequency of strain oscillation, t is time, and ϕ is phase lag between stress and strain. The applied stress (σ) can be expressed as:

$$\sigma = \sigma_o \sin ft$$

where σ_o is the stress amplitude.

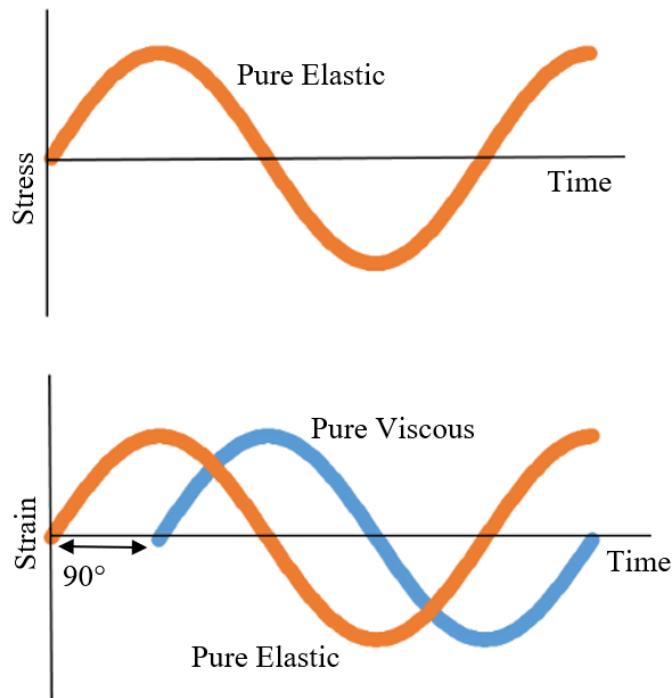


Figure 1. Stress-strain Behaviors of Elastic and Viscoelastic Materials

The storage modulus measures the stored energy representing the elastic portion of the response. The loss modulus represents the viscous response, measuring the energy dissipated as heat. The storage modulus (E'), and the loss modulus (E'') can be mathematically expressed as follows:

$$E' = \frac{\sigma_o}{\varepsilon_o} \cos \phi$$

$$E'' = \frac{\sigma_o}{\varepsilon_o} \sin \phi$$

The ϕ -value can be defined as shown in Eq. (5).

$$\phi = \tan^{-1} \left(\frac{E''}{E'} \right)$$

The complex modulus (E^*) is expressed as:

$$E^* = E' + iE''$$

The absolute value of this complex modulus is thus:

$$|E^*| = \sqrt{(E')^2 + (E'')^2} = \sqrt{\left(\frac{\sigma_o}{\varepsilon_o} \right)^2 (\sin^2 \delta + \cos^2 \delta)} = \frac{\sigma_o}{\varepsilon_o}$$

where $|E^*|$ is the dynamic modulus, σ_o is the peak dynamic stress and ε_o is the peak recoverable axial strain. Thus, the $|E^*|$ is defined mathematically as the ratio of σ_o and ε_o . The ϕ -value can also be determined as:

$$\phi = 2\pi f \Delta t$$

where ϕ is the phase angle in radians, f is the frequency in Hz, and Δt is the time lag between stress and strain in seconds. The $|E^*|$ of AC depends on many mix parameters: aggregate, binder, air voids, etc. Many empirical based $|E^*|$ models are available in the literature addressing these parameters on the dynamic modulus of HMA, such as the viscosity-based (η) Witczak model, the shear- modulus-based Witczak model, and the Hirsch model [1-10]. However, the effects of different mix parameters on the performance of asphalt pavement are not explored in the literature. Thus, this study focuses on the effect different mix parameters have on the performance of asphalt pavement using the PMED software.

Flow Number (N)

The flow number (N) is the number of load cycles at which tertiary flow begins. Tertiary flow can be differentiated from secondary flow by a marked departure from the linear relationship between cumulative strain and number of cycles in the secondary zone. It is assumed that in tertiary flow, the specimen's volume remains the constant. The N -value can be correlated with rutting potential. The final evaluation is an evaluation of the rutting resistance of the mixture using the flow number test defined by the American Association of State Highway, and Transportation Officials (AASHTO) TP 79 [11] using the Asphalt Mixture Performance Tester (AMPT). The test is conducted at the 'high' pavement temperature calculated by the LTPP Bind 3.1 software program for a specific project location. An unconfined flow number test with a repeated deviatoric stress of 87 psi (600 kPa) and a contact deviatoric stress of 4.4 psi (30 kPa) is used in this study. The test is conducted on specimens that are short-term conditioned for two hours at the compaction temperature to simulate the binder absorption and stiffening that occurs during construction. The flow number criteria for HMA as a function of traffic level are summarized in Table 1.

Table 1. Flow Number Criteria for HMA [11]

Traffic Level, Million Equivalent Single Axle Load (ESAL)	Flow Number
Less than 3.0	NA
3.0 to less than 10	50
10 to less than 30	190
More than 30	740

The effects of different mix parameters on the flow number have also been studied by different researchers [12 -15]. Kaloush [12] determined that the flow number increases with viscosity of binder and decreases with test temperature, effective binder content, and air voids. Kvasnak et al. [13] determined that the flow number increases with gyrations and viscosity of binder and decreases with voids in mineral aggregates (VMA) using Wisconsin dense graded mixtures. Both researchers determined that aggregate gradation also affects the flow number. Christensen [14]

applied various statistical techniques to relate the flow number with applied stress level and observed that the flow number decreases with an increase in the applied deviator stress. Rodezno et al. [15] determined that the flow number increases with viscosity of binder; however, it decreases with test temperature and air voids, and is affected by aggregate gradation. The current study does not intend to investigate viscosity of binder and test temperature. The other parameters such as VMA, VFA, effective binder content, contractors, testing time, mix gradation, and binder types are investigated.

SECTION 3: LABORATORY TESTING

Dynamic Modulus (E^*) Testing

The E^* testing on collected field cores is conducted by CDOT's Asphalt Material Unit using AASHTO TP 62 [16] test protocol and the AMPT testing device shown in Figure 2. The AASHTO TP 62 procedure is described below:

- a) Samples of 100-mm diameter and 150-mm height are prepared in the laboratory or field cores are collected.
- b) Attach the gauge points for the AMPT instrumentation.
- c) Run the full E^* test on each specimen at three different temperatures of 4 °C, 20 °C, and 40 °C. The testing frequencies are 0.1 Hz, 1 Hz, and 10 Hz at each temperature with the exception that another (4th) frequency of 0.01 Hz is adopted for 40 °C.
- d) Run N -value tests on two of the samples from each set of 5 at 50 °C.

Flow Number (N) Testing

The flow number (N) test procedure recommended in the National Cooperative Highway Research Program (NCHRP) project 9-19 is a simple performance test for rutting evaluation of asphalt mixtures. The test showed good correlation with rutting performance of mixtures from WesTrack, MnROAD, and FHWA's accelerated loading facility. Subsequent NCHRP studies allowed the development of a provisional standard. AASHTO TP 79 [11] includes test parameters for stress, temperature, specimen conditioning, and minimum flow number criteria that are established for HMA and for warm-mix asphalt (WMA) based on traffic level.

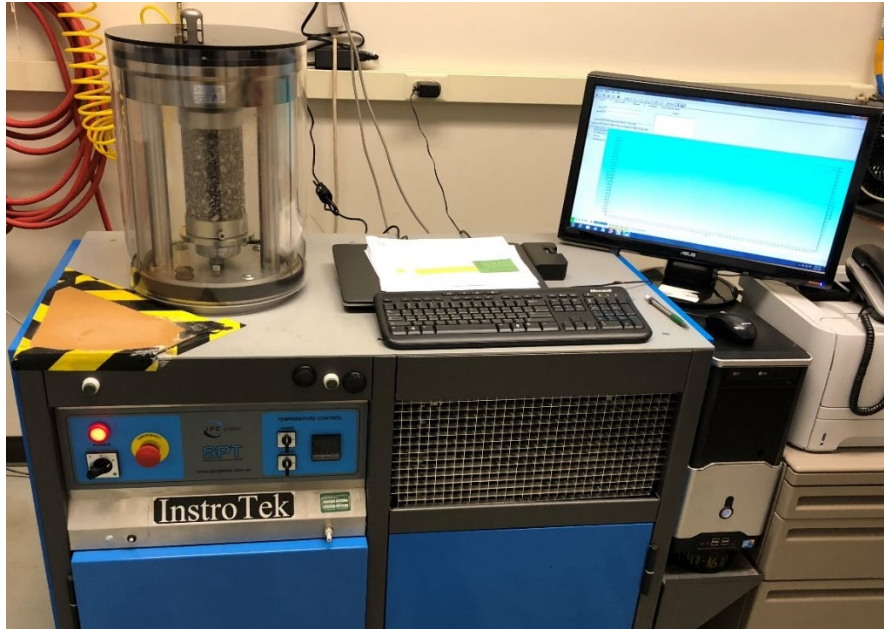


Figure 2. Flow Number Test Setup

In the flow number test, the permanent strain at each cycle is measured while a constant deviator stress is applied at each load cycle on the test sample (Figure 3). Permanent deformation of asphalt pavements has three stages [17]:

- a) Primary or initial consolidation
- b) Secondary, and
- c) Tertiary or shear deformation

Figure 3 shows the three stages of permanent deformation. The N -value is taken as the loading cycle, at which the tertiary stage begins following the secondary stage. Justification for selection of N -value criteria is determined using the Francken model, which is discussed below.

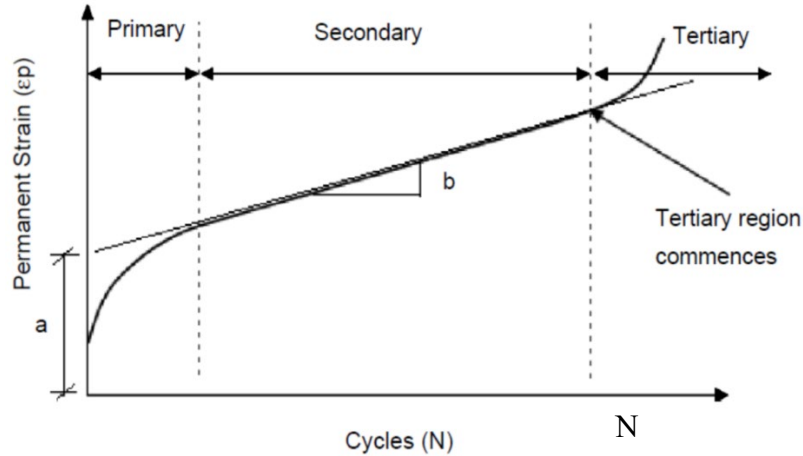


Figure 3. Relationship between Permanent Strain and Load Cycles [17]

The current study used testing conditions and criteria for N testing described in AASHTO TP 79 [11] for unconfined tests. The recommended test temperature, determined by LTPP Bind Version 3.1 software, is the average design high pavement temperature at 50% reliability for cities in Colorado. Tests are conducted at a temperature of 55 °C with an average deviator stress of 600 kPa and a minimum (contact) axial stress of 30 kPa. For conditioning, samples are kept in a conditioning chamber at the testing temperature for 12 hours prior to testing.

SECTION 4: ANALYSIS OF DYNAMIC MODULUS

Dynamic Modulus Data

This section presents the dynamic moduli data without determining the sensitivity of mix parameters. The dynamic moduli data is grouped into eleven types based on aggregate gradations and binder types. The average or representative dynamic modulus data for use in the PMED software has also been developed for each group. The development procedure of the average or representative dynamic modulus data is discussed later in this Section. The eleven types of mixtures being studied are listed in Table 2 along with their basic information such as Nominal Maximum Aggregate Size (NMAS), Performance Grade (PG) binder type, number of gyrations used while designing the mixes.

Table 2. List of Eleven Mixtures Used in this Study

Mix ID	NMAS (in.)	Binder	Number of Gyration
S(100) PG 64-22	0.75	PG 64-22	100
S(100) PG 76-28	0.75	PG 76-28	100
SMA PG 76-28	0.50	PG 76-28	100
SX(75) PG 58-28	0.50	PG 58-28	75
SX(75) PG 58-34	0.50	PG 58-34	75
SX(75) PG 64-22	0.50	PG 64-22	75
SX(75) PG 64-28	0.50	PG 64-28	75
SX(100) PG 58-28	0.50	PG 58-28	100
SX(100) PG 64-22	0.50	PG 64-22	100
SX(100) PG 64-28	0.50	PG 64-28	100
SX(100) PG 76-28	0.50	PG 76-28	100

The dynamic moduli of these eleven groups, their average dynamic moduli, the average best fit master curves, and statistical analysis of sensitivity are presented in this section.

S(100) PG 64-22

The dynamic modulus of S(100) PG 64-22 mix is presented in Figure 4. The dynamic modulus can differ by about 500 ksi from one contractor to another, especially at low temperature or high frequency of loading. The average dynamic modulus data of the mix is also shown in Figure 4.

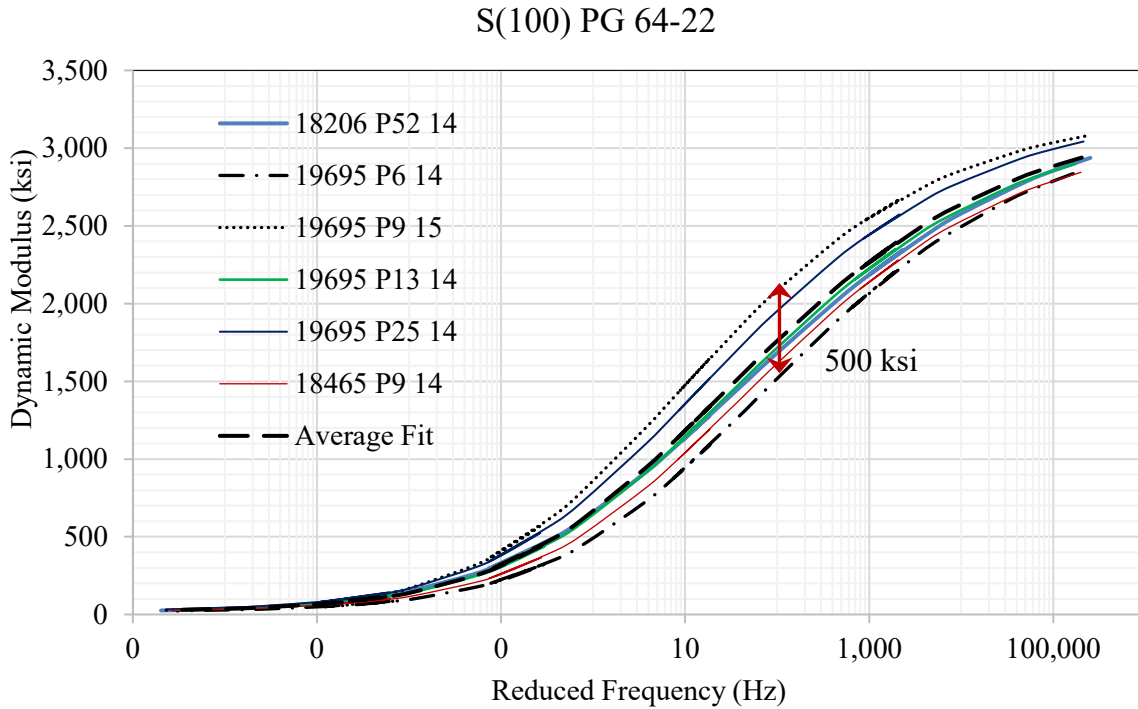


Figure 4. Dynamic Modulus of S(100) PG 64-22 Mix

Statistical *t*-test is conducted to determine whether the dynamic moduli are statistically different or not. The result shows that four mixes out of six mixes of S(100) PG 64-22 have statistically the equal dynamic moduli. Those four mixes (18206 P52 14, 18465 P9 14, 18695 P13 14, and 18695 P25 14) are highlighted in Table 3. Evaluation of mix parameters is required to find out the causes of this variation of dynamic moduli. The generic information of S(100) PG 64-22 mix is listed in Table 3 to compare the mix parameters. Table 3 shows that the mix parameters have many variables and hard to find out the sensitivity of each individual parameters. It can be found that two mixes (18695 P25 14 and 18695 P6 14) even though similar mix parameters have different dynamic moduli. These two mixes have the same paving contractor, same binder supplier, similar

volumetric properties, and aggregate sources. On the other hand, two mixes (18206 P52 14 and 18465 P9 14) with many different mix parameters (such as paving contractor, binder supplier, aggregate source) have statistically the equal dynamic modulus.

Table 3. Generic Information of S(100) PG 64-22 Mix

Mix ID	Paving Contractor	Binder Supplier	Region	Date	V_{be} (%)	V_a (%)	VMA (%)	VFA (%)	AC (%)	Pit
18206 P52 14	Aggregate Industries	Aggregate Industries	1	1/2015	12.09	6.78	15.8	72.5	5.00	Morrison, Platte River
18465 P9 14	Asphalt Paving	Frontier Cheyenne	4	7/2014	10.59	6.34	15.8	44.0	4.80	Ralston, Firestone, Lien
18695 P9 15	APC Southern	Suncor	1	4/2016	10.04	6.20	16.3	63.8	5.09	Ralston / Platteville
18695 P13 14	APC Southern	Holly Frontier	1	7/2014	10.78	6.12	17.0	63.7	5.00	Firestone, Ralston, Pete Lien
18695 P25 14	-	Holly Frontier	1	8/2014	10.26	5.84	15.8	63.2	5.00	Firestone, Ralston, Lien
18695 P6 14	-	Holly Frontier	1	4/2014	11.1	6.2	17.0	63.2	5.00	Firestone, Ralston, Pete Lien

Note: Purple highlighted mixes produce statistically the same dynamic modulus with each other.

A regression analysis is conducted to determine the influence of V_{be} , V_a , VMA, VFA, and AC, on E^* . The E^* in ksi at 10 Hz of loading at 20 °C is used as the dependent variable and the following correlation is obtained with the R^2 of 1.0. The regression equation below shows that the E^* increases with an increase in V_a , and VFA, and decreases with an increase in V_{be} , VMA, and AC.

$$E^* = 10,850.97 - 504.47 V_{be} + 446.1 V_a - 60.14 \text{ VMA} + 35.78 \text{ VFA} - 1,666.7 \text{ AC}$$

S(100) PG 76-28

The E^* of S(100) PG 76-28 mix is presented in Figure 5. The dynamic modulus can differ by about 200 ksi from one contractor to another, unless at high temperature or low frequency of loading. The average dynamic modulus data of the mix is also shown in Figure 5.

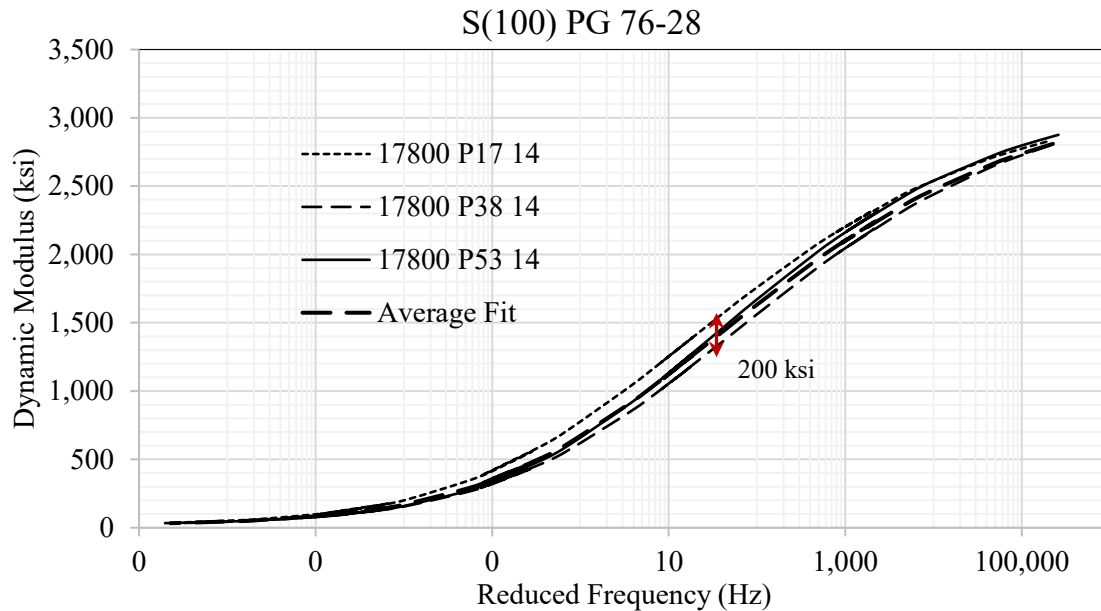


Figure 5. Dynamic Modulus of S(100) PG 76-28 Mix

Statistical t -test is conducted to determine whether the dynamic moduli are statistically different or not. The result shows that all four mixes have statistically the equal dynamic moduli and are highlighted in Table 4. Evaluation of mix parameters is required to find out the causes of this variation of dynamic moduli. The generic information of S(100) PG 76-28 mix is listed in Table 4 to compare the mix parameters. Table 4 shows that the mix parameters have similar variables and not feasible to find out the sensitivity of each individual parameters.

Table 4. Generic Information of S(100) PG 76-28 Mix

	Paving Contractor	Binder Supplier	Region	Date	V_{be} (%)	V_a (%)	VMA (%)	VFA (%)	AC (%)	Pit
17800 P17 14	Aggregate Industries	Jebro	4	7/2014	10.61	6.98	16.9	55.5	5.20	Distil, Lien
17800 P26 14	Aggregate Industries	Jebro	4	8/2014	10.61	6.58	16.8	58.6	5.20	Distil, Lien
17800 P38 14	Aggregate Industries	Jebro	4	9/2014	10.79	6.08	16.2	62.2	5.20	Distil, Lien
17800 P53 14	Aggregate Industries	Jebro	4	1/2015	10.61	6.72	16.6	59.3	5.20	Distil, Lien

Note: Purple highlighted mixes produce statistically the same dynamic modulus with each other.

A regression analysis is conducted to determine the influence of V_{be} , V_a , VMA, VFA, and AC, on E^* . The E^* in ksi at 10 Hz of loading at 20 °C is used as the dependent variable and the following correlation is obtained with the R^2 of 1.0. The regression equation below shows that the E^* increases with an increase in V_a , decreases with an increase in VMA, and VFA, and is insensitive to V_{be} and AC.

$$E^* = 7,970.5 + 168.5 V_a - 340.8 \text{ VMA} - 39.88 \text{ VFA}$$

SMA PG 76-28

The dynamic modulus of SMA PG 76-28 mix is presented in Figure 6. Apart from a single outlier, the dynamic modulus can differ by about 250 ksi from one contractor to another, unless at high temperature or low frequency of loading. The average dynamic modulus data of the mix is also shown in Figure 6.

SMA PG 76-28

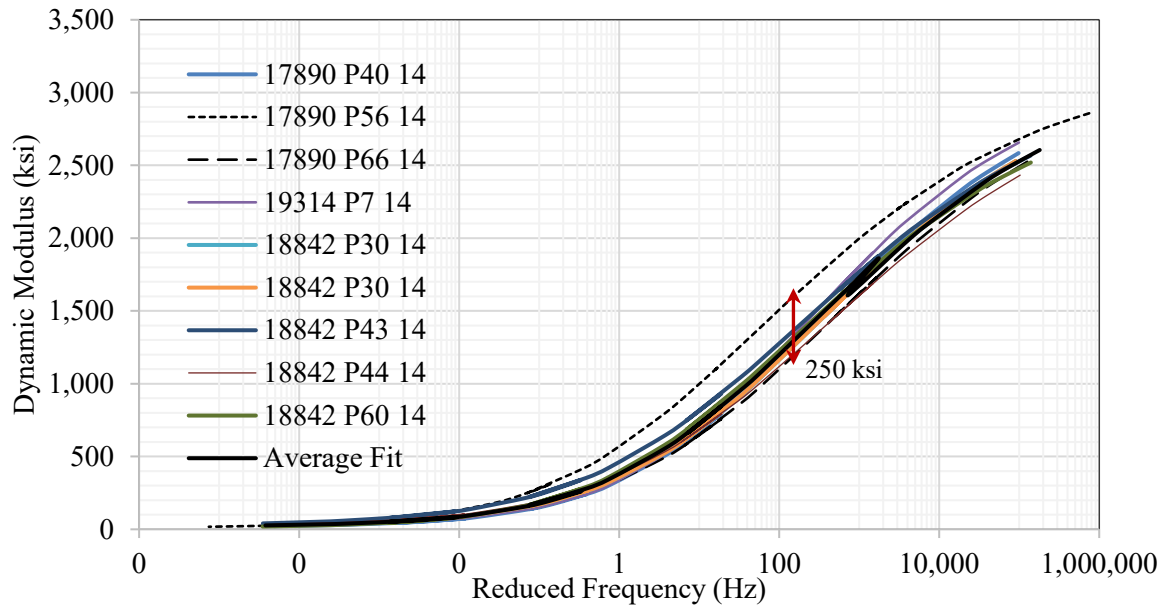


Figure 6. Dynamic Modulus of SMA PG 76-28 Mix

Table 5. Generic Information of SMA(100) PG 76-28 Mix

	Paving Contractor	Binder Supplier	Region	Date	V_{be} (%)	V_a (%)	VMA (%)	VFA (%)	AC (%)	Pit
17800 P70 14	Aggregate Industries	Jebro	4	5/2015	10.0	3.2	17.8	73.7	6.4	Morrison, Lien
17800 P85 14	Aggregate Industries	Jebro	4	10/2015	13.68	4.66	18.5	70.7	6.2	Morrison, Lien
17890 P40 14	Martin Marietta	Suncor	1	10/2014	15.17	4.24	18.0	77.5	6.40	Spec Agg
17890 P56 14	Martin Marietta	Suncor	1	1/2015	15.17	4.66	18.3	75.2	6.20	Spec Agg
17890 P66 14	Martin Marietta	Suncor	1	3/2015	15.17	4.20	17.9	76.8	6.20	Spec Agg
18842 P30 14	Kiewit Construction	Suncor	2	8/2014	13.64	4.64	18.4	75.7	6.3	Parkdale Tezak
18842 P43 14	Kiewit Construction	Suncor	2	11/2014	13.58	5.08	19.1	73.3	6.3	Parkdale Tezak
18842 P44 14	Kiewit Construction	Suncor	2	11/2014	13.29	3.4	18.8	75.0	6.3	Tezak, I-25 Millings
18842 P60 14	Kiewit Construction	Suncor	2	2/2015	13.31	3.4	19.8	65.1	5.2	Parkdale Tezak
18842 P83 14	Kiewit Construction	Suncor	2	9/2015	13.77	3.4	18.9	71.2	6.3	Parkdale Tezak
19314 P7 14	Martin Marietta	Suncor	4	6/2014	13.94	5.24	18.4	71.0	5.65	Granite Canyone, Lien
19807 P32 14	Brannan	Suncor	1	9/2014	13.80	3.0	16.0	74.9	6.3	Frei, Lein

Note: Purple highlighted mixes produce statistically the same dynamic modulus with each other.

Statistical t-test is conducted to determine whether the dynamic moduli are statistically different or not. The result shows that all mixes other than the three mixes (17890 P56 14, 18842 P43 14 and 19807 P32 14) have statistically the equal dynamic moduli. The highlighted mixes in Table 5

produce statistically the same dynamic modulus with each other. Evaluation of mix parameters is required to find out the causes of this variation of dynamic moduli. The generic information of SMA PG 76-28 mix is listed in Table 5 to compare the mix parameters. Table 5 shows that the mix parameters have many variables and hard to find out the sensitivity of each individual parameters. It can be found that Marin Marietta has four mixes (17890 P40 14, 17890 P56 14, 17890 P66 14 and 19314 P7 14) in this mix type. Of these four mixes, one mix (17890 P56 14) is not statistically the same with others although they all have similar mix parameters. This is similar to the mix, 18842 P43 14 produced by Kiewit. Other mixes (18842 P30 14, 18842 P44 14, 18842 P60 14, and 18842 P83 14) produced by Kiewit are statistically the same. On the other hand, mixes produced by different contractor (say, Aggregate Industries and Martin Marietta) are statistically the same.

A regression analysis is conducted to determine the influence of V_{be} , V_a , VMA, VFA, and AC, on E^* . The E^* in ksi at 10 Hz of loading at 20 °C is used as the dependent variable and the following correlation is obtained with the R^2 of 0.36. The regression equation below shows that the E^* increases with an increase in V_a , VFA, VMA, and AC, and decreases with an increase in V_{be} .

$$E^* = - 1,630 - 1.28 V_{be} + 27.3 V_a + 83.84 \text{ VMA} + 3.17 \text{ VFA} + 75.5 \text{ AC}$$

SX(75) PG 58-28

The dynamic modulus of SX(75) PG 58-28 mix is presented in Figure 7. The dynamic modulus can differ by about 500 ksi from one contractor to another, unless at high temperature or low frequency of loading. The average dynamic modulus data of the mix is also shown in Figure 7.

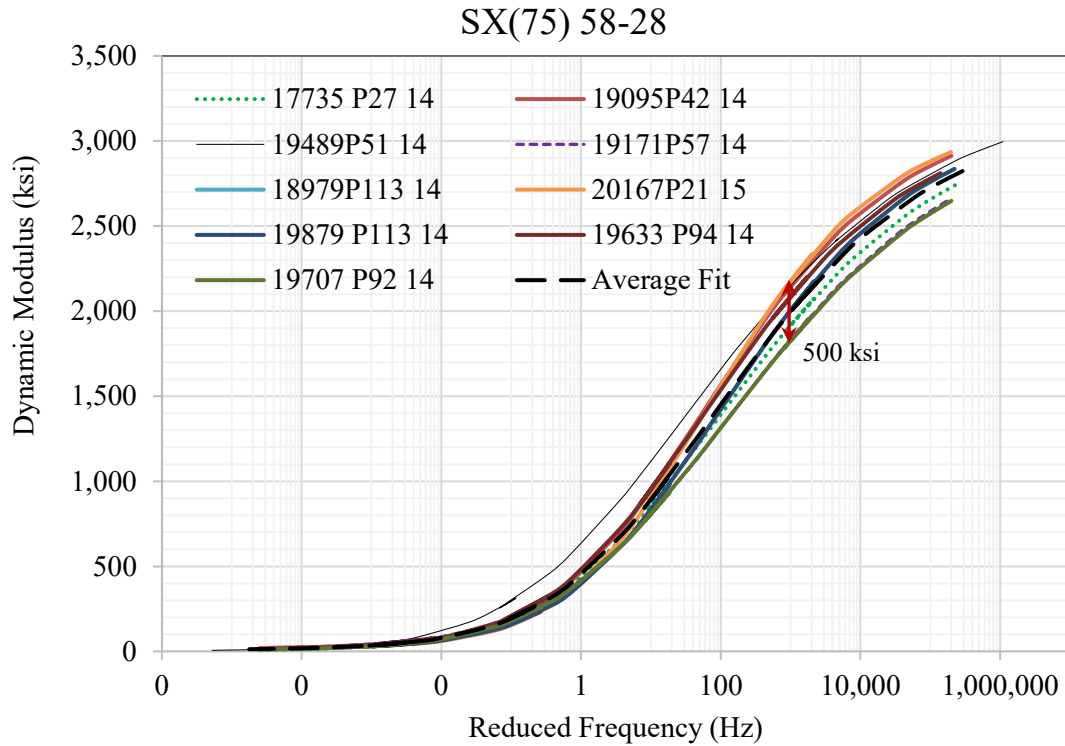


Figure 7. Dynamic Modulus of SX(75) PG 58-28 Mix

Table 6. Generic Information of SX(75) PG 58-28 Mix

	Paving Contractor	Binder Supplier	Region	Date	V_{be} (%)	V_a (%)	VMA (%)	VFA (%)	AC (%)	Pit
17735 P27 14	United Companies	Suncor	3	8/2014	13.23	5.60	18.1	69.5	6.40	Halderson
19095 P42 14	United Gypsum	Sinclair	3	10/2014	10.96	6.90	16.8	61.0	6.10	Lyster Camilletti
19171 P57 14	Everist Materials	Suncor	3	1/2015	12.58	6.90	18.6	62.8	5.80	Maryland Creek Ranch
19489 P51 14	Elam Construction	Sinclair	3	1/2015	11.25	5.00	15.8	67.5	5.10	Chambers
19633 P94 14	4 Corners	Suncor	5	11/2015	12.57	5.00	17.9	64.0	5.51	Cugnini Bayfield
19707 P92 14	Elam Construction	Suncor	5	11/2015	15.45	6.95	18.6	62.9	6.60	Agri-D Dillon Ranch
19879 P113 14	-	Suncor	1	2/2016	10.34	6.90	17.8	65.6	4.90	Ralston Firestone
20167 P21 15	Grand River	Peak	3	7/2016	9.81	5.90	17.7	65.1	4.94	Sievers

Note: Purple highlighted mixes produce statistically the same dynamic modulus with each other.

Statistical *t*-test is conducted to determine whether the dynamic moduli are statistically different or not. The result shows that all mixes except 19489 P51 14 have statistically the equal dynamic moduli and are highlighted in Table 6. Evaluation of mix parameters is required to find out the causes of this variation of dynamic moduli. The generic information of SX(75) PG 58-28 mix is listed in Table 6 to compare the mix parameters. Table 6 shows that the mix parameters have many variables and hard to find out the sensitivity of each individual parameters. It can be found that mixes by different contractors and produced by different aggregate sources have statistically the dynamic modulus.

A regression analysis is conducted to determine the influence of V_{be} , V_a , VMA, VFA, and AC, on E^* . The E^* in ksi at 10 Hz of loading at 20 °C is used as the dependent variable and the following correlation is obtained with the R^2 of 0.96. The regression equation below shows that the E^* increases with an increase in V_{be} and VFA, and decreases with an increase in V_a , VMA and AC.

$$E^* = 3028.8 + 29.83 V_{be} - 15.63 V_a - 139.9 \text{ VMA} + 3.04 \text{ VFA} - 28.9 \text{ AC}$$

SX(75) PG 58-34

The dynamic modulus of SX(75) PG 58-34 mix is presented in Figure 8. Only two mixture-dynamic modulus data are available from the database. At 10 Hz of loading, the dynamic modulus differs by about 1,000 ksi. Both moduli data are prepared from mixes by the same operator. The average dynamic modulus data of the mix is also shown in Figure 8.

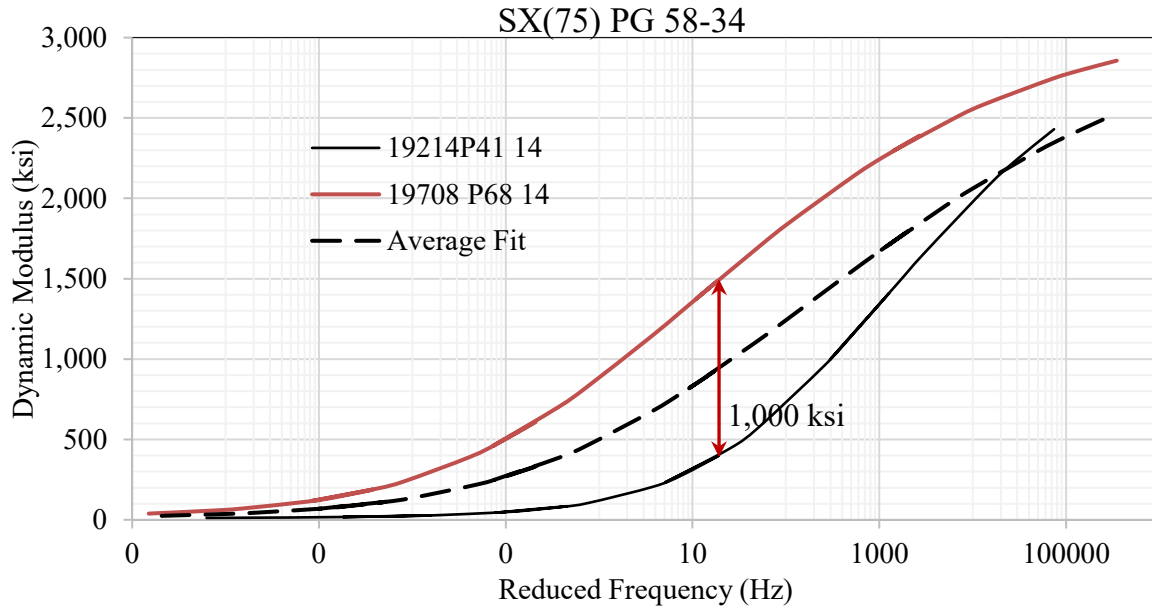


Figure 8. Dynamic Modulus of SX(75) PG 58-34 Mix

SX(75) PG 64-22

The dynamic modulus of SX(75) PG 64-22 mix is presented in Figure 9. The data shows a very consistent result. The dynamic modulus can differ by about 250 ksi from one contractor to another, unless at high temperature or low frequency of loading.

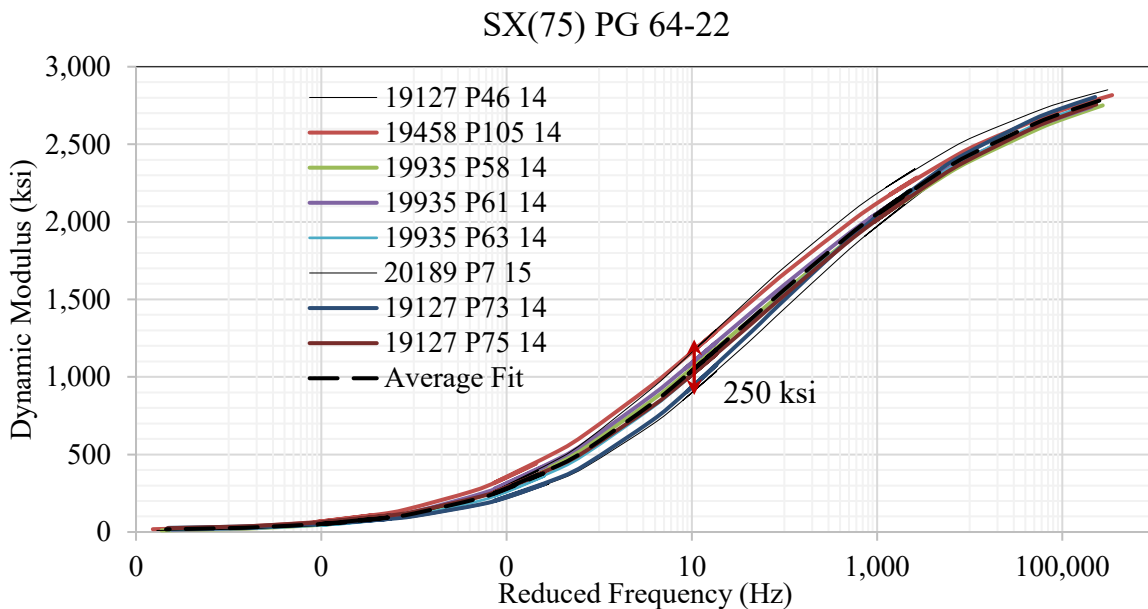


Figure 9. Dynamic Modulus of SX(75) PG 64-22 Mix

Statistical *t*-test is conducted to determine whether the dynamic moduli are statistically different or not. The result shows that all mixes except 19127 P73 14 have statistically the equal dynamic moduli and are highlighted in Table 6. Evaluation of mix parameters is required to find out the causes of this variation of dynamic moduli. The generic information of SX(75) PG 64-22 mix is listed in Table 7 to compare the mix parameters. Table 7 shows that the mix parameters have many variables and hard to find out the sensitivity of each individual parameters. It can be found that mixes by different contractors and produced by different aggregate sources have statistically the dynamic modulus.

Table 7. Generic Information of SX(75) PG 64-22 Mix

	Paving Contractor	Binder Supplier	Region	Date	V_{be} (%)	V_a (%)	VMA (%)	VFA (%)	AC (%)	Pit
19127 P73 14	Beltramo	Suncor	2	6/2015	13.53	7.10	18.4	61.2	5.70	Cesar/Transit Mix/Nepesta
19127 P75 14	Beltramo	Suncor	2	6/2015	13.55	6.93	17.9	61.6	5.70	Cesar/Transit Mix/Nepesta
19458 P105 14	Simon Construction	Suncor	4	12/2015	11.61	6.78	18.1	63.1	5.81	Granite Canyon, Julesburg, Ovid
19935 P58 14	A&S Construction	Suncor	2	2/2015	13.39	6.78	17.5	61.0	5.60	Rocky Ford South
19935 P61 14	A&S Construction	Suncor	2	2/2015	13.31	6.80	18.2	62.8	5.60	Rocky Ford South
19935 P63 14	A&S Construction	Suncor	2	3/2015	13.90	6.73	17.4	61.8	5.60	Rocky Ford South
20189 P7 15	McAtee	Suncor	4	4/2016	11.16	6.80	18.5	62.8	5.48	---

Note: Purple highlighted mixes produce statistically the same dynamic modulus with each other.

A regression analysis is conducted to determine the influence of V_{be} , V_a , VMA, VFA, and AC, on E^* . The E^* in ksi at 10 Hz of loading at 20 °C is used as the dependent variable and the following correlation is obtained with the R^2 of 0.96. The regression equation below shows that the E^* increases with an increase in V_{be} , VMA and AC, and decreases with an increase in V_a and VFA.

$$E^* = 9,366.6 + 14.89 V_{be} - 1,708 V_a + 433.1 \text{ VMA} - 121.2 \text{ VFA} + 506 \text{ AC}$$

SX(75) PG 64-28

The dynamic modulus of SX(75) PG 64-28 mix is presented in Figure 10. Generally, the data shows a very consistent result.

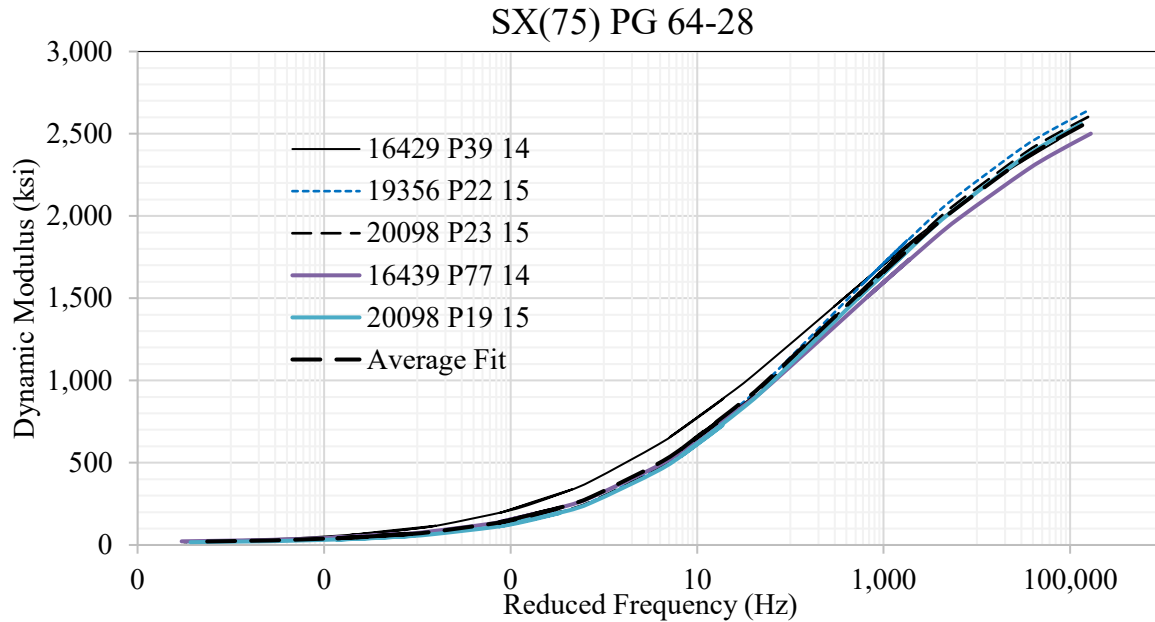


Figure 10. Dynamic Modulus of SX(75) PG 64-28 Mix

Statistical t-test is conducted to determine whether the dynamic moduli are statistically different or not. The result shows that all mixes of SX(75) PG 64-28 have statistically the equal dynamic moduli. Evaluation of mix parameters is required to find out the causes of this variation of dynamic moduli. The generic information of SX(75) PG 64-28 mix is listed in Table 8 to compare the mix parameters. Table 8 shows that the mix parameters have many variables and hard to find out the sensitivity of each individual parameters. It can be found that mixes by different contractors and produced by different aggregate sources have statistically the dynamic modulus.

Table 8. Generic Information of SX(75) PG 64-28 Mix

	Paving Contractor	Binder Supplier	Region	Date	V_{be} (%)	V_a (%)	VMA (%)	VFA (%)	AC (%)	Pit
16439 P77 14	Everist	Suncor	3	6/2015	12.73	7.08	18.9	62.5	5.80	Maryland Creek Ranch
19356 P22 15	Asphalt Specialties	Suncor	4	7/2016	10.92	5.30	17.7	60.9	5.51	Spec Agg, Turnpike, Bestway Firestone
20098 P19 15	Coulson	Suncor	4	5/2016	10.84	6.52	18.0	62.1	5.37	Bonser, Lien
20098 P23 15	Coulson	Suncor	4	8/2016	11.01	6.52	17.9	61.4	5.61	Bonser, Lien

Note: Purple highlighted mixes produce statistically the same dynamic modulus with each other.

A regression analysis is conducted to determine the influence of V_{be} , V_a , VMA, VFA, and AC, on E^* . The E^* in ksi at 10 Hz of loading at 20 °C is used as the dependent variable and the following correlation is obtained with the R^2 of 1.0. The regression equation below shows that the E^* increases with an increase in V_{be} and VFA, and decreases with an increase in V_a , and is insensitive to VMA and AC.

$$E^* = 385.4 + 9.02 V_{be} - 4.3 V_a + 2.2 \text{ VFA}$$

SX(100) PG 58-28

The dynamic modulus of SX(100) PG 58-28 mix is presented in Figure 11. Only one mixture's test data is available.

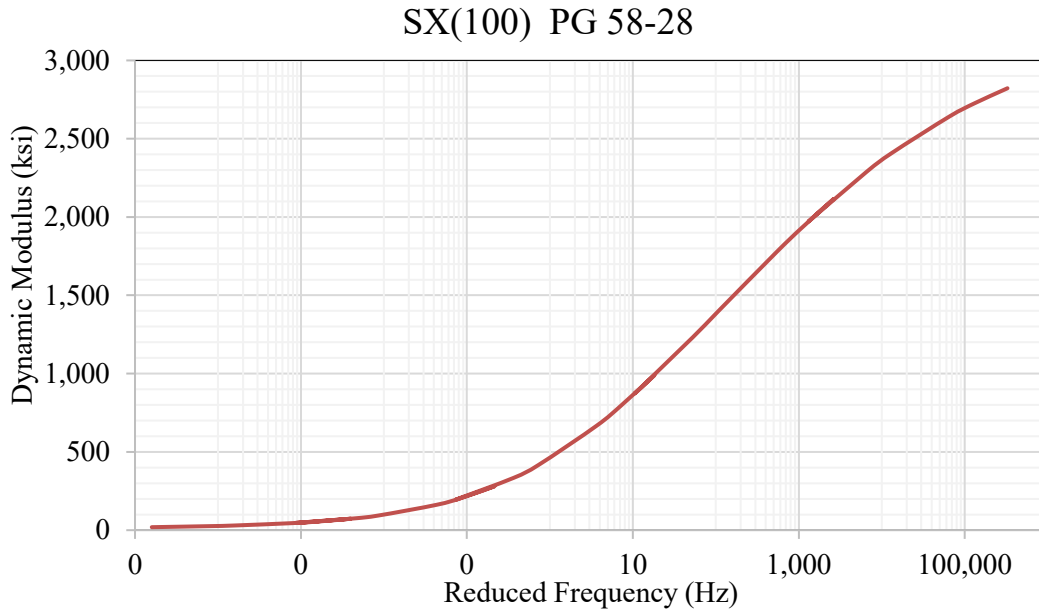


Figure 11. Dynamic Modulus of SX(100) PG 58-28 Mix

SX(100) PG 64-22

The dynamic modulus of SX(100) PG 64-22 mix is presented in Figure 12. The dynamic modulus can differ by about 700 ksi from one contractor to another, except for tests conducted at high temperature or low frequency of loading. The average dynamic modulus data of the mix is also shown in Figure 12.

SX(100) PG 64-22

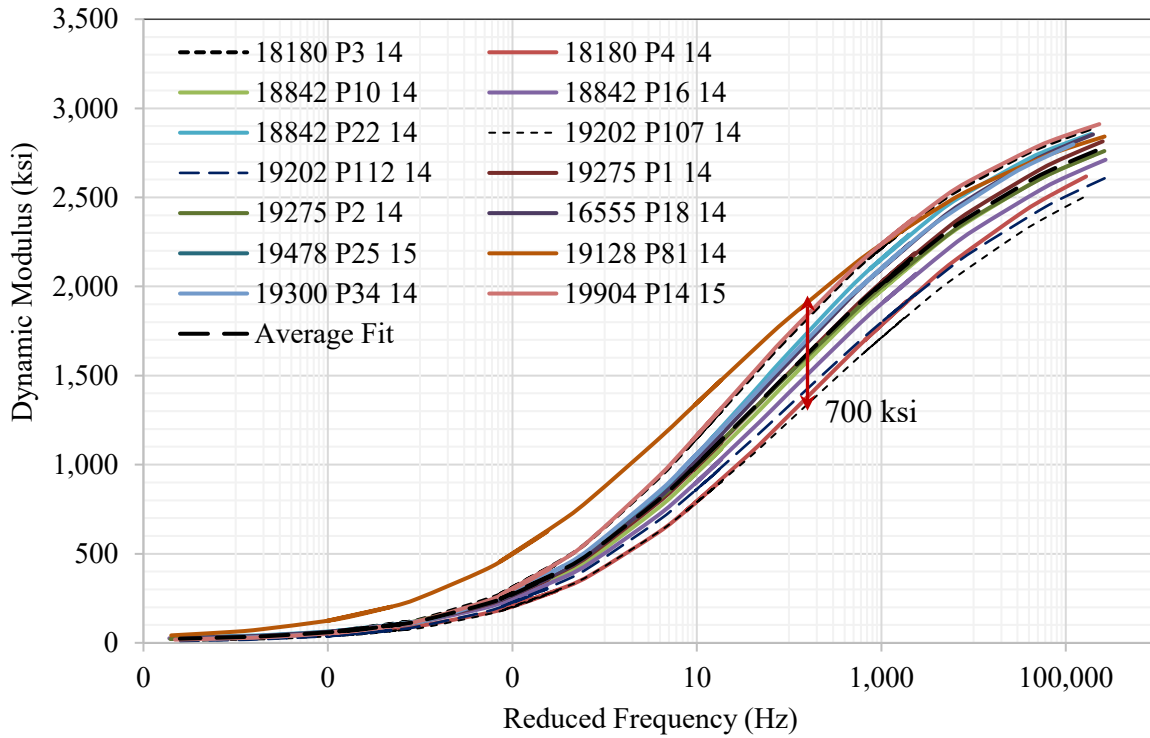


Figure 12. Dynamic Modulus of SX(100) PG 64-22 Mix

Statistical *t*-test is conducted to determine whether the dynamic moduli are statistically different or not. The generic information of SX(100) PG 64-22 mix is listed in Table 9 to compare the mix parameters. Table 9 shows that the mix parameters have many variables and hard to find out the sensitivity of each individual parameters. It can be found that mixes by different contractors and produced by different aggregate sources have statistically the dynamic modulus.

Table 9. Generic Information of SX(100) PG 64-22 Mix

	Paving Contractor	Binder Supplier	Region	Date	V_{be} (%)	V_a (%)	VMA (%)	VFA (%)	AC (%)	Pit
18180 P3 14	Aggregate Industries	Aggregate Industries	1	6/2014	12.24	6.66	17.1	61.2	5.00	Morrison, Plate River
18180 P4 14	Aggregate Industries	Suncor	--	6/2014	10.31	6.66	17.9	63.4	5.00	Morrison, Plate River
18842 P10 14	Kiewit Construction	Suncor	2	7/2014	11.63	5.00	18.3	62.8	5.30	Tezak Fountain / 125
18842 P16 14	Kiewit Construction	Suncor	2	7/2014	11.39	6.98	18.4	62.4	5.30	Tezak Fountain / 125
18842 P22 14	Kiewit Construction	Suncor	2	8/2014	11.44	6.52	18.1	64.3	5.30	Tezak Fountain / 125
19128 P81 14	Martin Marietta	Suncor	2	7/2015	13.18	6.90	17.6	60.8	5.50	Evans
19202 P107 14	Skanska	Suncor	5	1/2015	11.94	6.00	18.8	64.2	6.34	Four Corners
19202 P112 14	Skanska	Suncor	5	1/2015	11.29	6.00	18.3	61.2	5.95	Four Corners
19275 P1 14	APC Southern	Holly Frontier	2	6/2014	13.41	5.78	17.0	66.3	5.65	---
19275 P2 14	APC Southern	Holly Frontier	2	6/2014	13.41	6.60	18.1	65.9	5.65	---
19275 P5 14	Aggregate Industries	Holly Frontier	2	6/2014	13.41	6.14	17.3	65.2	5.65	---
19300 P34 14	United Companies	Suncor	3	9/2014	12.04	5.64	16.7	66.4	6.00	Craig Ranch
19655 P18 14	APC Southern	Holly Frontier	2	7/2014	11.05	6.06	16.7	64.3	5.60	Valardi
19904 P14 15	Martin Marietta	Suncor	1	5/2016	13.43	6.40	17.1	62.5	5.50	Spec Agg / Riverbend / Cottonwood

Note: Purple highlighted mixes produce statistically the same dynamic modulus with each other.

A regression analysis is conducted to determine the influence of V_{be} , V_a , VMA, VFA, and AC, on E^* . The E^* in ksi at 10 Hz of loading at 20 °C is used as the dependent variable and the following correlation is obtained with the R^2 of 0.62. The regression equation below shows that the E^* increases with an increase in V_{be} and V_a , and decreases with an increase in VMA, VFA and AC.

$$E^* = 3,938 + 63.91 V_{be} + 13.8 V_a - 91.9 \text{ VMA} - 31.4 \text{ VFA} - 41.6 \text{ AC}$$

SX(100) PG 64-28

The dynamic modulus of SX(100) PG 64-28 mix is presented in Figure 13. The dynamic modulus values can differ by more than 800 ksi from specimen to specimen, except for tests conducted at high temperature or low frequency of loading. Note that both the extreme moduli data (19655 P2014, and 19655 P2114) are produced from mixes manufactured by the same contractor. The average dynamic modulus data of the mix is also shown in Figure 13.

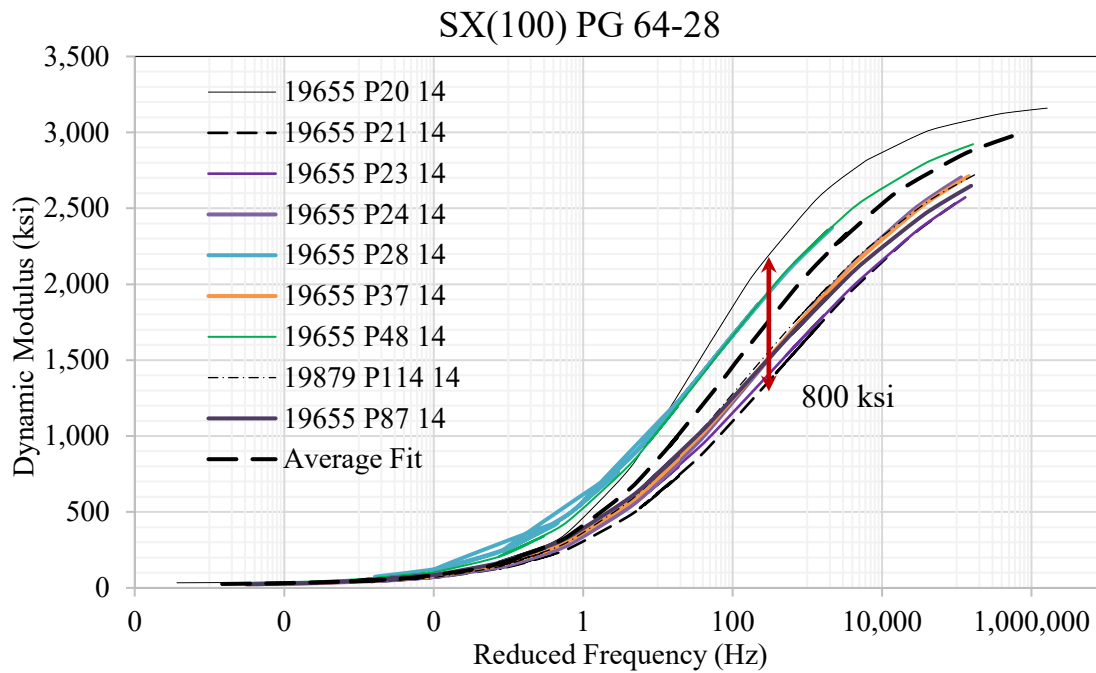


Figure 13. Dynamic Modulus of SX(100) PG 64-28 Mix

Statistical *t*-test is conducted to determine whether the dynamic moduli are statistically different or not. The generic information of SX(100) PG 64-28 mix is listed in Table 10 to compare the mix parameters. Table 10 shows that the mix parameters have many variables and hard to find out the sensitivity of each individual parameters. It can be found that mixes by different contractors and produced by different aggregate sources have statistically the dynamic modulus.

Table 10. Generic Information of SX(100) PG 64-28 Mix

	Paving Contractor	Binder Supplier	Region	Date	V_{be} (%)	V_a (%)	VMA (%)	VFA (%)	AC (%)	Pit
19655 P20 14	APC Southern	Suncor	2	7/2014	10.59	6.06	17.0	64.0	5.58	Valardi
19655 P21 14	APC Southern	Suncor	2	7/2014	10.85	6.06	17.1	63.5	5.80	Valardi
19655 P23 14	APC Southern	Suncor	2	8/2014	10.56	6.06	16.7	65.1	5.70	Valardi
19655 P24 14	APC Southern	Suncor	2	8/2014	10.97	6.06	16.0	64.2	5.78	Valardi
19655 P28 14	APC Southern	Suncor	2	8/2014	10.71	6.06	16.1	63.0	5.61	Valardi
19655 P37 14	APC Southern	Suncor	2	9/2014	10.48	6.06	15.8	62.4	5.65	Valardi
19655 P48 14	APC Southern	Suncor	2	12/2014	13.18	6.60	17.4	62.0	5.50	Valardi
19655 P87 14	APC Southern	Suncor	2	10/2015	13.18	6.30	17.1	63.2	5.50	Valardi
19879 P114 14	-	Suncor	1	3/2016	10.05	6.90	17.5	63.5	4.90	Ralston, Firestone

Note: Purple highlighted mixes produce statistically the same dynamic modulus with each other.

A regression analysis is conducted to determine the influence of V_{be} , V_a , VMA, VFA, and AC, on E^* . The E^* in ksi at 10 Hz of loading at 20 °C is used as the dependent variable and the following correlation is obtained with the R^2 of 0.74. The regression equation below shows that the E^* increases with an increase in V_{be} and V_a , and decreases with an increase in VMA, VFA and AC.

$$E^* = 1,681.9 + 31.82 V_{be} + 149.8 V_a - 63.4 \text{ VMA} - 16 \text{ VFA} - 35.7 \text{ AC}$$

SX(100) PG 76-28

The dynamic modulus of SX(100) PG 76-28 mix is presented in Figure 14. The dynamic modulus can differ by more than 600 ksi from one contractor to another, except for tests conducted at high temperature or low frequency of loading. The average dynamic modulus data of the mix is also shown in Figure 14.

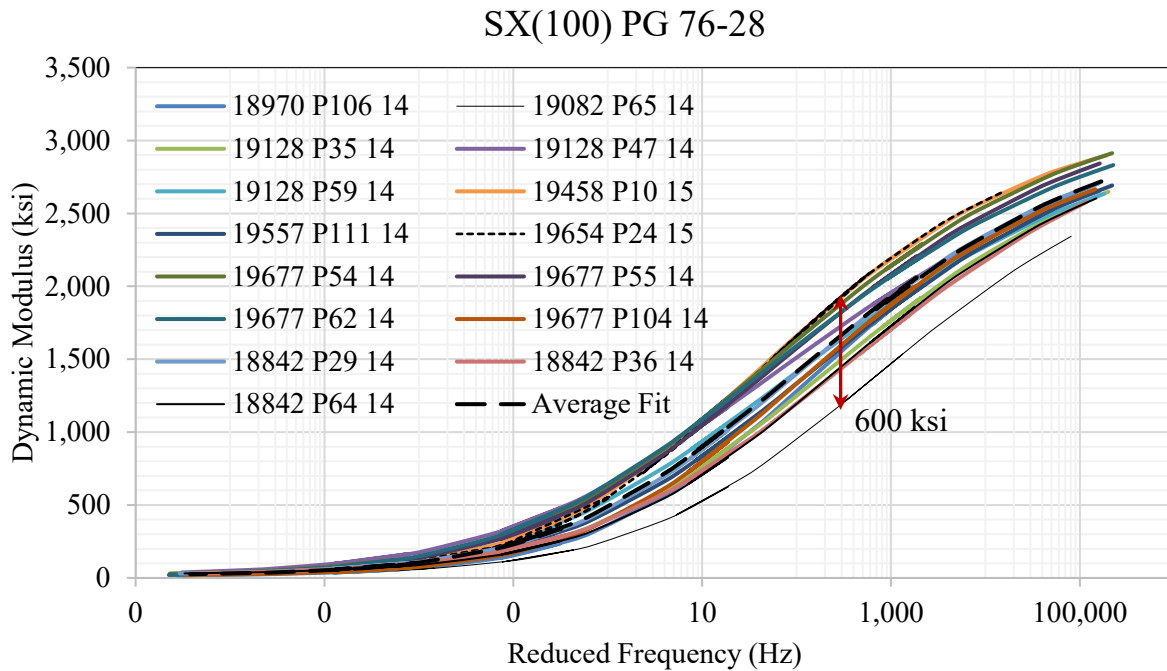


Figure 14. Dynamic Modulus of SX(100) PG 76-28 Mix

Statistical t-test is conducted to determine whether the dynamic moduli are statistically different or not. The generic information of SX(100) PG 76-28 mix is listed in Table 11 to compare the mix parameters. Table 11 shows that the mix parameters have many variables and hard to find out the sensitivity of each individual parameters. It can be found that mixes by different contractors and produced by different aggregate sources have statistically the dynamic modulus. Sometimes, mixes by the same producer are not statistically the same. For example, all mixes by the Kiewit are not statistically the same.

Table 11. Generic Information of SX(100) PG 76-28 Mix

	Paving Contractor	Binder Supplier	Region	Date	V_{be} (%)	V_a (%)	VMA (%)	VFA (%)	AC (%)	Pit
18842 P29 14	Kiewit Construction	Suncor	2	7/2014	12.61	6.68	18.1	64.3	6.30	Tezak / Fountain / I-25 Millings
18842 P36 14	Kiewit Construction	Suncor	2	8/2014	14.32	4.56	15.8	72.5	6.30	Parkdale/Tezak
18842 P45 14	Tezak	Suncor	2	8/2014	12.53	6.93	18.2	62.2	5.20	Tezak / Fountain / I-25 Millings
18842 P64 14	Kiewit Construction	Suncor	2	9/2014	12.53	6.85	18.2	62.4	6.30	Tezak / Fountain / I-25 Millings
18842 P71 14	Kiewit Construction	Suncor	2	10/2014	15.23	4.88	18.5	73.5	6.30	Parkdale/Tezak
18842 P82 14	Kiewit Construction	Suncor	2	10/2014	12.53	6.93	18.3	62.3	5.20	Tezak / Fountain / I-25 Millings
18970 P106 14	APC Southern	Suncor	5	11/2014	12.72	5.60	18.2	67.4	6.12	King Pit
19082 P65 14	ACA Buena Vista	Suncor	5	3/2015	13.84	6.85	18.8	63.2	5.70	Avery Pit, ACA Buena Vista
19128 P35 14	Martin Marietta	Suncor	2	8/2014	10.96	6.32	17.1	62.5	5.60	Evans
19128 P47 14	Evans	Suncor	2	8/2014	10.90	6.82	17.6	61.4	5.60	Evans
19128 P59 14	Martin Marietta	Suncor	2	9/2014	10.90	6.82	17.6	60.9	5.60	Evans
19128 P72 14	Martin Marietta	Suncor	2	9/2014	10.00	6.82	17.9	60.2	5.10	Evans
19128 P80 14	Martin Marietta	Suncor	2	10/2014	10.00	6.82	17.6	60.7	5.10	Evans/slate
19128 P88 14	Martin Marietta	Suncor	2	10/2014	10.82	6.83	17.6	61.6	5.60	Evans/slate
19458 P10 15	Simon Construction	Suncor	4	5/2015	9.90	5.30	16.8	61.5	5.05	Granite Canyon, Julesburg, Sedgwick
19458 P13 15	Simon Construction	Suncor	4	6/2015	9.47	5.30	16.5	61.7	4.96	Granite Canyon, Julesburg, Sedgwick
19458 P17 15	Simon Construction	Suncor	4	6/2015	9.55	5.30	16.1	60.7	4.93	Granite Canyon, Julesburg, Sedgwick
19458 P20 15	Simon Construction	Suncor	4	6/2015	10.32	4.40	16.6	60.0	5.30	Granite Canyon, Julesburg, Sedgwick
19458 P76 14	Simon Construction	Suncor	4	6/2015	11.57	6.43	17.3	62.6	5.20	Granite Canyon, Julesburg, Sedgwick

19458 P79 14	Simon Construction	Suncor	4	7/2015	11.57	6.80	17.6	61.4	5.20	Granite Canyon, Julesburg, Sedgwick
19458 P84 14	Simon Construction	Suncor	4	9/2015	11.57	6.75	17.6	61.2	5.20	Granite Canyon, Julesburg, Sedgwick
19458 P86 14	Simon Construction	Suncor	4	10/2015	11.57	6.78	17.6	61.3	5.20	Granite Canyon, Julesburg, Sedgwick
19557 P111 14	A&S Construction	Suncor	2	11/2014	11.71	5.00	17.7	64.6	5.38	Tezak/Transit Mix
19654 P24 15	Martin Marietta	Suncor	2	7/2015	10.31	5.00	17.6	60.6	5.25	Evans/slate
19669 P78 14	A&S Construction	Suncor	2	10/2014	10.72	6.93	17.7	61.0	5.40	Rocky Ford South/La Junta
19677 P54 14	Elam Construction	Suncor	3	1/2015	10.25	5.18	14.9	65.4	5.50	23 Road
19677 P55 14	Elam Construction	Suncor	3	1/2015	10.54	5.04	15.1	66.6	5.50	23 Road
19677 P62 14	Elam Construction	Suncor	3	2/2015	10.69	5.00	15.2	66.5	5.50	23 Road
19677 P69 14	Elam Construction	Suncor	3	5/2015	11.71	4.43	15.6	71.7	5.50	23 Road
19677 P89 14	Elam Construction	Suncor	3	10/2015	10.69	6.83	16.8	58.9	5.50	23 Road
19677 P90 14	Elam Construction	Suncor	3	10/2015	11.71	5.98	17.0	64.6	5.50	23 Road
19677 P91 14	Elam Construction	Suncor	3	11/2015	11.71	5.88	16.9	65.3	5.50	23 Road
19677 P104 14	Elam Construction	Suncor	3	11/2014	11.02	5.88	18.6	57.6	5.74	23 Road

Note: Purple highlighted mixes produce statistically the same dynamic modulus with each other.

A regression analysis is conducted to determine the influence of V_{be} , V_a , VMA, VFA, and AC, on E^* . The E^* in ksi at 10 Hz of loading at 20 °C is used as the dependent variable and the following correlation is obtained with the R^2 of 0.57. The regression equation below shows that the E^* increases with an increase in V_a and VFA, and decreases with an increase in V_{be} , VMA and AC.

$$E^* = 2,149 - 51.18 V_{be} + 1.42 V_a - 61.5 \text{ VMA} + 10.1 \text{ VFA} - 55.82 \text{ AC}$$

Summary of Comparison

The sensitivity analysis summary presented in Table 12 shows that the effects of V_{be} , V_a , VMA, VFA, and AC on the E^* are inconsistent. For example, five mixes show that the E^* increases with V_{be} , three mixes show the opposite, and three mixes show it is insensitive to V_{be} . This inconsistency is true for V_a , VMA, VFA, and AC as well. The reason behind this may be the effects of paving contractor, manufacture date, and/or aggregate source. Using the most scores, the E^* increases with an increase in V_{be} , V_a , and VFA, and decreases with an increase in VMA and AC. However, the effects of VFA and AC on E^* are less sensitive compared to V_{be} , V_a , and VFA.

Table 12. Summary of the Mix Parameters on Flow Number of HMA

	V_{be} (%)	V_a (%)	VMA (%)	VFA (%)	AC (%)
S(100) PG 64-22	Decreases	Increases	Decreases	Increases	Decreases
S(100) PG 76-28	--	Increases	Decreases	Decreases	--
SMA PG 76-28	Decreases	Increases	Increases	Increases	Increases
SX(75) PG 58-28	Increases	Decreases	Decreases	Increases	Increases
SX(75) PG 58-34	NA	NA	NA	NA	NA
SX(75) PG 64-22	Increases	Decreases	Increases	Decreases	Increases
SX(75) PG 64-28	Increases	Decreases	--	Increases	--
SX(100) PG 58-28	NA	NA	NA	NA	NA
SX(100) PG 64-22	Increases	Increases	Decreases	Decreases	Decreases
SX(100) PG 64-28	Increases	Increases	Decreases	Decreases	Decreases
SX(100) PG 76-28	Decreases	Increases	Decreases	Increases	Decreases
Summary	5 Increases 3 Decreases 1 Insensitive	6 Increases 3 Decreases	2 Increases 6 Decreases 1 Insensitive	5 Increases 4 Decreases	3 Increases 4 Decreases 2 Insensitive

The average fitted data from each group has been chosen and plotted together as shown in Figure 15 to compare among the group. The fitting procedure of the data is presented in the next article.

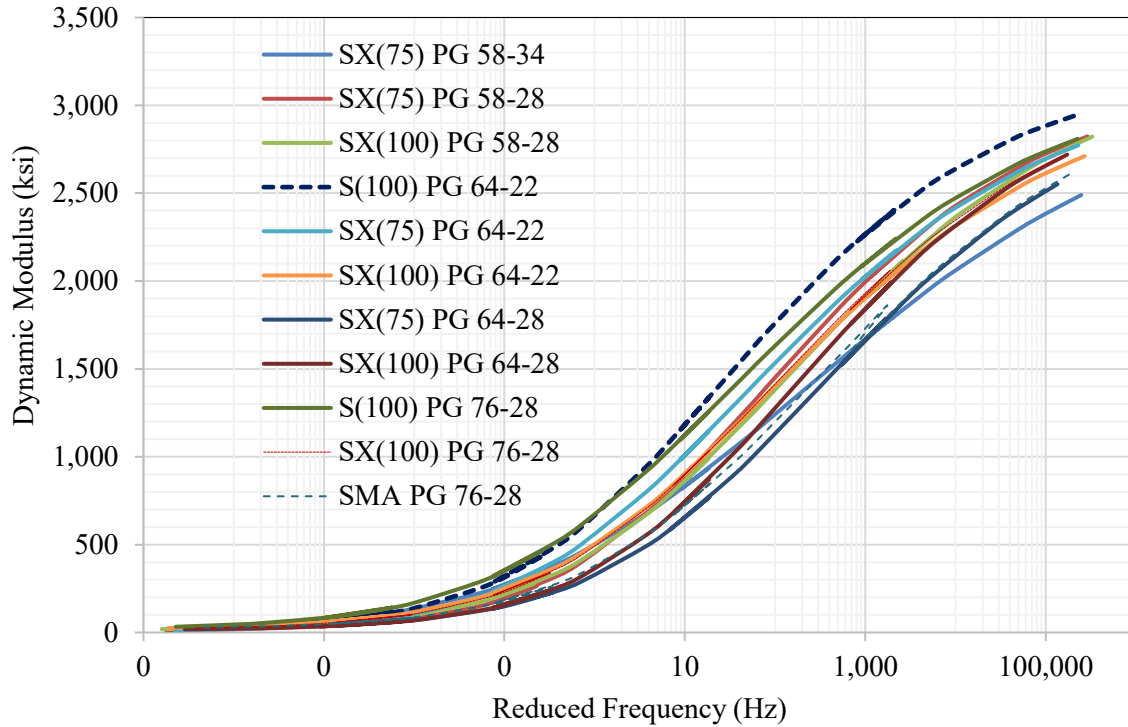


Figure 15. Groupwise Comparison

Figure 15 shows the E^* value varies greatly amongst the different binders. For example, at 10 Hz of loading, the E^* of SX(75) PG 64-28 mix is about 600 ksi; whereas the S(100) PG 64-22 mix has a value of 1,200 ksi (an increase of 100%). It is also apparent that the S(100) PG 64-22 mixture has the highest value of E^* , especially at low temperature or high reduced frequency. Thus, the S(100) PG 64-22 mix has the greatest potential for transverse cracking. At high temperature or lower reduced frequency, the S(100) PG 76-28 mix has the highest E^* value and is the best mix for minimal rutting. The SX(75) PG 64-28 mix has the lowest E^* value at high temperature or lower reduced frequency. At low temperature or high reduced frequency, the SX(75) PG 58-34 mix has the lowest E^* value. The average fitted SMA mix has a lower E^* value compared to the S(100) and SX(100) mixes at low temperature, and thus, would likely have lower predicted transverse cracking than S(100) and SX(100) mixes. A summary of the study's findings is presented in Table 13.

Table 13. Summary of the Most Durable and Worst Mixes

Mix Type	Property	Comments
S(100) PG 64-22	Highest at low temperature	Worst for transverse cracking
S(100) PG 76-28	Highest at high temperature	Best mix for rutting
SX(75) PG 58-34	Lowest at low temperature	Best for transverse cracking
SX(75) PG 64-28	Lowest at high temperature	Worst for rutting

Developing Dynamic Modulus Mastercurves for PMED

MasterSolver is used to determine the master curve of a dynamic modulus used in the PMED software. The dynamic modulus is determined using the following equation:

$$\log|E^*| = \log(\text{Min}) + \frac{(\log(\text{Max}) - \log(\text{Min}))}{1 + e^{\beta + \gamma \log \omega_r}}$$

where:

$|E^*|$ = dynamic modulus

ω_r = reduced frequency, Hz

Max = limiting maximum modulus, ksi

Min = limiting minimum modulus, ksi

β and γ = fitting parameters

The reduced frequency is computed using the Arrhenius equation given below:

$$\log(\omega_r) = \log \omega + \frac{\Delta E_a}{19.14714} \left(\frac{1}{T} - \frac{1}{T_r} \right)$$

where:

ω_r = reduced frequency at the reference temperature

ω = loading frequency at the test temperature

T_r = reference temperature, °K

T = test temperature, °K

ΔE_a = activation energy (treated as a fitting parameter)

The combination of the above two equations gives the following:

$$\log|E^*| = \log(\text{Min}) + \frac{(\log(\text{Max}) - \log(\text{Min}))}{1 + e^{\beta + \gamma \left\{ \log \omega + \frac{\Delta E_a}{19.14714} \left(\frac{1}{T} - \frac{1}{T_r} \right) \right\}}}$$

The shift parameters for each temperature are given by the following equation:

$$\log[a(T)] = \frac{\Delta E_a}{19.14714} \left(\frac{1}{T} - \frac{1}{T_r} \right)$$

where:

$a(T)$ = shift parameter at temperature T

The maximum limiting modulus is estimated from mixture volumetric properties using the Hrisch model shown below, and a limiting binder modulus of 1 GPa:

$$|E^*|_{\max} = P_c \left[4,200,000 \left(1 - \frac{VMA}{100} \right) + 435,000 \left(\frac{VMA \times VFA}{10,000} \right) \right] + \frac{1 - P_c}{\left[\frac{\left(1 - \frac{VMA}{100} \right)}{4,200,000} + \frac{VFA}{435,000} \right]}$$

where:

$$P_c = \frac{\left(20 + \frac{435,000 VFA}{VMA} \right)^{0.58}}{650 + \left(\frac{435,000 VFA}{VMA} \right)^{0.58}}$$

$|E^*|_{\max}$ limiting maximum dynamic modulus, psi

VMA = voids in mineral aggregates, %

VFA = voids filled with asphalt, %

To determine a recommended dynamic modulus from AMPT (master curve) data, the average raw dynamic moduli, VMA, and VFA of all eleven groups are combined, and the average value are calculated and fitted using the MasterSolver for each type of mixture listed at the beginning of this section. The test results are summarized below:

S(100) PG 64-22

The average raw dynamic modulus data are presented in Table 14 below:

Table 14. Average Raw Dynamic Moduli of S(100) PG 64-22 Mix

Temperature (°C)	Frequency (Hz)	Modulus (ksi)
4	0.1	1,206
4	1.0	1,750
4	10.0	2,316
20	0.1	322
20	1.0	638
20	10.0	1,110
35	0.01	34
35	0.1	54
35	1.0	117
35	10.0	288

The average VMA and VFA are 16.3% and 61.7%, respectively. After the execution of the MasterSolver program, the final fitting parameters are shown below. The PMED input moduli are listed in Table 15.

- Max. E^* (ksi): 3,237.2
- Min. E^* (ksi): 9.2
- Beta, β : - 0.91764
- Gamma, γ : -0.54361
- ΔE_a : 239,361
- Coefficient of Determination (R^2) = 0.993
- $S_e/S_y = 0.06$

Table 15. Fitted Dynamic Modulus of S(100) PG 64-22 Mix

No.	Temperature		Frequency (Hz)	<i>E*</i> ksi
	°C	°F		
1	-10.0	14	25	2,939
2	-10.0	14	10	2,867
3	-10.0	14	5	2,803
4	-10.0	14	1	2,613
5	-10.0	14	0.5	2,512
6	-10.0	14	0.1	2,227
7	4.4	40	25	2,404
8	4.4	40	10	2,234
9	4.4	40	5	2,091
10	4.4	40	1	1,717
11	4.4	40	0.5	1,544
12	4.4	40	0.1	1,137
13	21.1	70	25	1,338
14	21.1	70	10	1,108
15	21.1	70	5	942
16	21.1	70	1	607
17	21.1	70	0.5	489
18	21.1	70	0.1	284
19	37.8	100	25	443
20	37.8	100	10	325
21	37.8	100	5	255
22	37.8	100	1	144
23	37.8	100	0.5	113
24	37.8	100	0.1	68
25	54.4	130	25	118
26	54.4	130	10	87
27	54.4	130	5	70
28	54.4	130	1	45
29	54.4	130	0.5	38
30	54.4	130	0.1	28

S(100) PG 76-28

The average raw dynamic modulus data are presented in Table 16 below:

Table 16. Average Raw Dynamic Moduli of S(100) PG 76-28 Mix

Temperature (°C)	Frequency (Hz)	Modulus (ksi)
4	0.1	1,181
4	1.0	1,638
4	10.0	2,099
20	0.1	352
20	1.0	648
20	10.0	1,066
35	0.01	33
35	0.1	50
35	1.0	97
35	10.0	223

The average VMA and VFA are 16.63% and 58.9%, respectively. After the execution of the MasterSolver program, the final fitting parameters are shown below. The PMED input moduli are listed in Table 17.

- Max. E^* (ksi): 3,205.2
- Min. E^* (ksi): 5.6
- Beta, β : -0.99783
- Gamma, γ : -0.43172
- ΔE_a : 297534
- $R^2 = 0.981$
- $S_e/S_y = 0.10$

Table 17. Fitted Dynamic Modulus of S(100) PG 76-28 Mix

No.	Temperature		Frequency (Hz)	<i>E*</i>
	°C	°F		ksi
1	-10.0	14	25	2,810
2	-10.0	14	10	2,729
3	-10.0	14	5	2,658
4	-10.0	14	1	2,459
5	-10.0	14	0.5	2,357
6	-10.0	14	0.1	2,082
7	4.4	40	25	2,242
8	4.4	40	10	2,078
9	4.4	40	5	1,944
10	4.4	40	1	1,604
11	4.4	40	0.5	1,450
12	4.4	40	0.1	1,095
13	21.1	70	25	1,258
14	21.1	70	10	1,058
15	21.1	70	5	915
16	21.1	70	1	619
17	21.1	70	0.5	513
18	21.1	70	0.1	319
19	37.8	100	25	465
20	37.8	100	10	355
21	37.8	100	5	286
22	37.8	100	1	172
23	37.8	100	0.5	138
24	37.8	100	0.1	84
25	54.4	130	25	142
26	54.4	130	10	107
27	54.4	130	5	86
28	54.4	130	1	55
29	54.4	130	0.5	46
30	54.4	130	0.1	33

SMA PG 76-28

The average raw dynamic modulus data are presented in Table 18 below:

Table 18. Average Raw Dynamic Moduli of SMA PG 76-28 Mix

Temperature (°C)	Frequency (Hz)	Modulus (ksi)
4	0.1	716
4	1.0	1,152
4	10.0	1,686
20	0.1	181
20	1.0	367
20	10.0	696
35	0.01	27
35	0.1	35
35	1.0	57
35	10.0	128

The average VMA and VFA are 18.3% and 73%, respectively. After the execution of the MasterSolver program, the final fitting parameters are shown below. The PMED input moduli are listed in Table 19.

- Max. E^* (ksi): 3,193.1
- Min. E^* (ksi): 8.0
- Beta, β : - 0.47083
- Gamma, γ : -0.45889
- ΔE_a : 262810
- $R^2 = 0.976$
- $S_e/S_y = 0.11$

Table 19. Fitted Dynamic Modulus of SMA PG 76-28 Mix

No.	Temperature		Frequency (Hz)	E^*
	°C	°F		ksi
1	-10.0	14	25	2,605
2	-10.0	14	10	2,484
3	-10.0	14	5	2,380
4	-10.0	14	1	2,097
5	-10.0	14	0.5	1,958
6	-10.0	14	0.1	1,607
7	4.4	40	25	1,862
8	4.4	40	10	1,658
9	4.4	40	5	1,499
10	4.4	40	1	1,129
11	4.4	40	0.5	977
12	4.4	40	0.1	664
13	21.1	70	25	845
14	21.1	70	10	671
15	21.1	70	5	555
16	21.1	70	1	344
17	21.1	70	0.5	277
18	21.1	70	0.1	165
19	37.8	100	25	262
20	37.8	100	10	195
21	37.8	100	5	156
22	37.8	100	1	95
23	37.8	100	0.5	78
24	37.8	100	0.1	51
25	54.4	130	25	84
26	54.4	130	10	65
27	54.4	130	5	55
28	54.4	130	1	39
29	54.4	130	0.5	34
30	54.4	130	0.1	27

SX(75) PG 58-28

The average raw dynamic modulus data are presented in Table 20 below:

Table 20. Average Raw Dynamic Moduli of SX(75) PG 58-28 Mix

Temperature (°C)	Frequency (Hz)	Modulus (ksi)
4	0.1	928
4	1.0	1,451
4	10.0	2,026
20	0.1	202
20	1.0	445
20	10.0	856
35	0.01	22
35	0.1	39
35	1.0	95
35	10.0	262

The average VMA and VFA are 17.7% and 64.8%, respectively. After the execution of the MasterSolver program, the final fitting parameters are shown below. The PMED input moduli are listed in Table 21.

- Max. E^* (ksi): 3,182.9
- Min. E^* (ksi): 6.0
- Beta, β : - 0.79292
- Gamma, γ : - 0.57609
- ΔE_a : 200195
- $R^2 = 0.997$
- $S_e/S_y = 0.04$

Table 21. Fitted Dynamic Modulus of SX(75) PG 58-28 Mix

No.	Temperature		Frequency (Hz)	E^*
	°C	°F		ksi
1	-10.0	14	25	2,823
2	-10.0	14	10	2,739
3	-10.0	14	5	2,665
4	-10.0	14	1	2,449
5	-10.0	14	0.5	2,336
6	-10.0	14	0.1	2,026
7	4.4	40	25	2,181
8	4.4	40	10	1,994
9	4.4	40	5	1,839
10	4.4	40	1	1,449
11	4.4	40	0.5	1,276
12	4.4	40	0.1	889
13	21.1	70	25	1,031
14	21.1	70	10	821
15	21.1	70	5	677
16	21.1	70	1	404
17	21.1	70	0.5	316
18	21.1	70	0.1	171
19	37.8	100	25	265
20	37.8	100	10	186
21	37.8	100	5	142
22	37.8	100	1	76
23	37.8	100	0.5	59
24	37.8	100	0.1	34
25	54.4	130	25	58
26	54.4	130	10	42
27	54.4	130	5	33
28	54.4	130	1	21
29	54.4	130	0.5	18
30	54.4	130	0.1	13

SX(75) PG 58-34

The average raw dynamic modulus data are presented in Table 22 below:

Table 22. Average Raw Dynamic Moduli of SX(75) PG 58-34 Mix

Temperature (°C)	Frequency (Hz)	Modulus (ksi)
4	0.1	869
4	1.0	1,254
4	10.0	1,722
20	0.1	270
20	1.0	475
20	10.0	791
35	0.01	43
35	0.1	83
35	1.0	169
35	10.0	339

The average VMA and VFA are 17.12% and 60.65%, respectively. After the execution of the MasterSolver program, the final fitting parameters are shown below. The PMED input moduli are listed in Table 23.

- Max. E^* (ksi): 3,190
- Min. E^* (ksi): 4.9
- Beta, β : - 0.9138
- Gamma, γ : -0.42869
- ΔE_a : 196741
- $R^2 = 0.998$
- $S_x/S_y = 0.03$

Table 23. Fitted Dynamic Modulus of SX(75) PG 58-34 Mix

No.	Temperature		Frequency (Hz)	E^*
	°C	°F		ksi
1	-10.0	14	25	2,489
2	-10.0	14	10	2,382
3	-10.0	14	5	2,293
4	-10.0	14	1	2,059
5	-10.0	14	0.5	1,947
6	-10.0	14	0.1	1,668
7	4.4	40	25	1,818
8	4.4	40	10	1,655
9	4.4	40	5	1,527
10	4.4	40	1	1,226
11	4.4	40	0.5	1,098
12	4.4	40	0.1	818
13	21.1	70	25	936
14	21.1	70	10	783
15	21.1	70	5	675
16	21.1	70	1	461
17	21.1	70	0.5	385
18	21.1	70	0.1	247
19	37.8	100	25	347
20	37.8	100	10	269
21	37.8	100	5	219
22	37.8	100	1	136
23	37.8	100	0.5	110
24	37.8	100	0.1	68
25	54.4	130	25	112
26	54.4	130	10	85
27	54.4	130	5	69
28	54.4	130	1	44
29	54.4	130	0.5	37
30	54.4	130	0.1	25

SX(75) PG 64-22

The average raw dynamic modulus data are presented in Table 24 below:

Table 24. Average Raw Dynamic Moduli of SX(75) PG 64-22 Mix

Temperature (°C)	Frequency (Hz)	Modulus (ksi)
4	0.1	1,088
4	1.0	1,571
4	10.0	2,071
20	0.1	284
20	1.0	564
20	10.0	982
35	0.01	23
35	0.1	40
35	1.0	95
35	10.0	245

The average VMA and VFA are 18% and 62%, respectively. After the execution of the MasterSolver program, the final fitting parameters are shown below. The PMED input moduli are listed in Table 25.

- Max. E^* (ksi): 3,153.1
- Min. E^* (ksi): 3.0
- Beta, β : - 1.06853
- Gamma, γ : -0.48765
- ΔE_a : 245423
- $R^2 = 0.993$
- $S_e/S_y = 0.06$

Table 25. Fitted Dynamic Modulus of SX(75) PG 64-22 Mix

No.	Temperature		Frequency (Hz)	<i>E*</i>
	°C	°F		ksi
1	-10.0	14	25	2781
2	-10.0	14	10	2,701
3	-10.0	14	5	2,631
4	-10.0	14	1	2,431
5	-10.0	14	0.5	2,328
6	-10.0	14	0.1	2,048
7	4.4	40	25	2,204
8	4.4	40	10	2,036
9	4.4	40	5	1,897
10	4.4	40	1	1,545
11	4.4	40	0.5	1,386
12	4.4	40	0.1	1,020
13	21.1	70	25	1,177
14	21.1	70	10	972
15	21.1	70	5	826
16	21.1	70	1	534
17	21.1	70	0.5	431
18	21.1	70	0.1	250
19	37.8	100	25	378
20	37.8	100	10	277
21	37.8	100	5	216
22	37.8	100	1	119
23	37.8	100	0.5	92
24	37.8	100	0.1	52
25	54.4	130	25	93
26	54.4	130	10	67
27	54.4	130	5	52
28	54.4	130	1	31
29	54.4	130	0.5	26
30	54.4	130	0.1	17

SX(75) PG 64-28

The average raw dynamic modulus data are presented in Table 26 below:

Table 26. Average Raw Dynamic Moduli of SX(75) PG 64-28 Mix

Temperature (°C)	Frequency (Hz)	Modulus (ksi)
4	0.1	635
4	1.0	1,052
4	10.0	1,560
20	0.1	131
20	1.0	291
20	10.0	596
35	0.01	22
35	0.1	31
35	1.0	54
35	10.0	135

The average VMA and VFA are 18.1% and 61.7%, respectively. After the execution of the MasterSolver program, the final fitting parameters are shown below. The PMED input moduli are listed in Table 27.

- Max. E^* (ksi): 3,146.5
- Min. E^* (ksi): 8.3
- Beta, β : - 0.35155
- Gamma, γ : -0.53181
- ΔE_a : 221097
- $R^2 = 0.992$
- $S_e/S_y = 0.06$

Table 27. Fitted Dynamic Modulus of SX(75) PG 64-28 Mix

No.	Temperature		Frequency (Hz)	E^*
	°C	°F		ksi
1	-10.0	14	25	2,552
2	-10.0	14	10	2,427
3	-10.0	14	5	2,319
4	-10.0	14	1	2,026
5	-10.0	14	0.5	1,883
6	-10.0	14	0.1	1,521
7	4.4	40	25	1,787
8	4.4	40	10	1,579
9	4.4	40	5	1,416
10	4.4	40	1	1,042
11	4.4	40	0.5	890
12	4.4	40	0.1	584
13	21.1	70	25	772
14	21.1	70	10	603
15	21.1	70	5	493
16	21.1	70	1	296
17	21.1	70	0.5	234
18	21.1	70	0.1	136
19	37.8	100	25	228
20	37.8	100	10	167
21	37.8	100	5	133
22	37.8	100	1	79
23	37.8	100	0.5	64
24	37.8	100	0.1	41
25	54.4	130	25	71
26	54.4	130	10	54
27	54.4	130	5	45
28	54.4	130	1	30
29	54.4	130	0.5	26
30	54.4	130	0.1	20

SX(100) PG 58-28

The average raw dynamic modulus data are presented in Table 28 below:

Table 28. Average Raw Dynamic Moduli of SX(100) PG 58-28 Mix

Temperature (°C)	Frequency (Hz)	Modulus (ksi)
4	0.1	934
4	1.0	1,407
4	10.0	1,918
20	0.1	219
20	1.0	453
20	10.0	837
35	0.01	32
35	0.1	53
35	1.0	116
35	10.0	278

The average VMA and VFA are 15.8% and 66.3%, respectively. After the execution of the MasterSolver program, the final fitting parameters are shown below. The PMED input moduli are listed in Table 29.

- Max. E^* (ksi): 3,286
- Min. E^* (ksi): 8.5
- Beta, β : - 0.70528
- Gamma, γ : -0.53263
- ΔE_a : 202814
- $R^2 = 0.998$
- $S_e/S_y = 0.03$

Table 29. Fitted Dynamic Modulus of SX(100) PG 58-28 Mix

No.	Temperature		Frequency (Hz)	<i>E*</i>
	°C	°F		ksi
1	-10.0	14	25	2,823
2	-10.0	14	10	2,727
3	-10.0	14	5	2,643
4	-10.0	14	1	2,408
5	-10.0	14	0.5	2,289
6	-10.0	14	0.1	1,972
7	4.4	40	25	2,116
8	4.4	40	10	1,925
9	4.4	40	5	1,771
10	4.4	40	1	1,395
11	4.4	40	0.5	1,232
12	4.4	40	0.1	873
13	21.1	70	25	990
14	21.1	70	10	798
15	21.1	70	5	667
16	21.1	70	1	417
17	21.1	70	0.5	334
18	21.1	70	0.1	194
19	37.8	100	25	280
20	37.8	100	10	206
21	37.8	100	5	162
22	37.8	100	1	94
23	37.8	100	0.5	75
24	37.8	100	0.1	46
25	54.4	130	25	73
26	54.4	130	10	55
27	54.4	130	5	45
28	54.4	130	1	30
29	54.4	130	0.5	26
30	54.4	130	0.1	19

SX(100) PG 64-22

The average raw dynamic modulus data are presented in Table 30 below:

Table 30. Average Raw Dynamic Moduli of SX(100) PG 64-22 Mix

Temperature (°C)	Frequency (Hz)	Modulus (ksi)
4	0.1	1,030
4	1.0	1,496
4	10.0	1,997
20	0.1	288
20	1.0	560
20	10.0	956
35	0.01	29
35	0.1	46
35	1.0	100
35	10.0	239

The average VMA and VFA are 17.6% and 63.4%, respectively. After the execution of the MasterSolver program, the final fitting parameters are shown below. The PMED input moduli are listed in Table 31.

- Max. E^* (ksi): 3,180.6
- Min. E^* (ksi): 4.2
- Beta, β : -0.97082
- Gamma, γ : -0.46474
- ΔE_a : 250085
- $R^2 = 0.99$
- $S_e/S_y = 0.07$

Table 31. Fitted Dynamic Modulus of SX(100) PG 64-22 Mix

No.	Temperature		Frequency (Hz)	E^*
	°C	°F		ksi
1	-10.0	14	25	2,762
2	-10.0	14	10	2,674
3	-10.0	14	5	2,598
4	-10.0	14	1	2,383
5	-10.0	14	0.5	2,273
6	-10.0	14	0.1	1,977
7	4.4	40	25	2,157
8	4.4	40	10	1,982
9	4.4	40	5	1,839
10	4.4	40	1	1,482
11	4.4	40	0.5	1,323
12	4.4	40	0.1	964
13	21.1	70	25	1,137
14	21.1	70	10	937
15	21.1	70	5	795
16	21.1	70	1	515
17	21.1	70	0.5	417
18	21.1	70	0.1	247
19	37.8	100	25	378
20	37.8	100	10	281
21	37.8	100	5	222
22	37.8	100	1	128
23	37.8	100	0.5	101
24	37.8	100	0.1	60
25	54.4	130	25	105
26	54.4	130	10	78
27	54.4	130	5	62
28	54.4	130	1	39
29	54.4	130	0.5	33
30	54.4	130	0.1	23

SX(100) PG 64-28

The average raw dynamic modulus data are presented in Table 32 below:

Table 32. Average Raw Dynamic Moduli of SX(100) PG 64-28 Mix

Temperature (°C)	Frequency (Hz)	Modulus (ksi)
4	0.1	1,062
4	1.0	1,686
4	10.0	2,424
20	0.1	170
20	1.0	360
20	10.0	695
35	0.01	32
35	0.1	49
35	1.0	96
35	10.0	227

The average VMA and VFA are 16.8% and 63.7%, respectively. After the execution of the MasterSolver program, the final fitting parameters are shown below. The PMED input moduli are listed in Table 33.

- Max. E^* (ksi): 3,222.3
- Min. E^* (ksi): 19.0
- Beta, β : - 0.38919
- Gamma, γ : -0.65476
- ΔE_a : 213789
- $R^2 = 0.985$
- $S_e/S_y = 0.09$

Table 33. Fitted Dynamic Modulus of SX(100) PG 64-28 Mix

No.	Temperature		Frequency (Hz)	E^*
	°C	°F		ksi
1	-10.0	14	25	2,975
2	-10.0	14	10	2,906
3	-10.0	14	5	2,843
4	-10.0	14	1	2,651
5	-10.0	14	0.5	2,545
6	-10.0	14	0.1	2,242
7	4.4	40	25	2,333
8	4.4	40	10	2,135
9	4.4	40	5	1,969
10	4.4	40	1	1,542
11	4.4	40	0.5	1,349
12	4.4	40	0.1	921
13	21.1	70	25	991
14	21.1	70	10	769
15	21.1	70	5	622
16	21.1	70	1	360
17	21.1	70	0.5	280
18	21.1	70	0.1	156
19	37.8	100	25	212
20	37.8	100	10	152
21	37.8	100	5	120
22	37.8	100	1	73
23	37.8	100	0.5	60
24	37.8	100	0.1	42
25	54.4	130	25	56
26	54.4	130	10	46
27	54.4	130	5	40
28	54.4	130	1	31
29	54.4	130	0.5	29
30	54.4	130	0.1	25

SX(100) PG 76-28

The average raw dynamic modulus data are presented in Table 34 below:

Table 34. Average Raw Dynamic Moduli of SX(100) PG 76-28 Mix

Temperature (°C)	Frequency (Hz)	Modulus (ksi)
4	0.1	914
4	1.0	1,371
4	10.0	1,878
20	0.1	232
20	1.0	465
20	10.0	840
35	0.01	25
35	0.1	36
35	1.0	65
35	10.0	156

The average VMA and VFA are 17.2% and 63.2%, respectively. After the execution of the MasterSolver program, the final fitting parameters are shown below. The PMED input moduli are listed in Table 35.

- Max. E^* (ksi): 3,199.5
- Min. E^* (ksi): 5.0
- Beta, β : -0.76362
- Gamma, γ : -0.44588
- ΔE_a : 278405
- $R^2 = 0.981$
- $S_e/S_y = 0.10$

Table 35. Fitted Dynamic Modulus of SX(100) PG 76-28 Mix

No.	Temperature		Frequency (Hz)	<i>E*</i>
	°C	°F		ksi
1	-10.0	14	25	2,720
2	-10.0	14	10	2,619
3	-10.0	14	5	2,530
4	-10.0	14	1	2,284
5	-10.0	14	0.5	2,160
6	-10.0	14	0.1	1,834
7	4.4	40	25	2,061
8	4.4	40	10	1,872
9	4.4	40	5	1,719
10	4.4	40	1	1,348
11	4.4	40	0.5	1,187
12	4.4	40	0.1	837
13	21.1	70	25	1,035
14	21.1	70	10	840
15	21.1	70	5	706
16	21.1	70	1	447
17	21.1	70	0.5	360
18	21.1	70	0.1	212
19	37.8	100	25	340
20	37.8	100	10	252
21	37.8	100	5	200
22	37.8	100	1	116
23	37.8	100	0.5	93
24	37.8	100	0.1	57
25	54.4	130	25	101
26	54.4	130	10	76
27	54.4	130	5	62
28	54.4	130	1	40
29	54.4	130	0.5	34
30	54.4	130	0.1	25

SECTION 5: ANALYSIS OF FLOW NUMBER

Effect on Flow Number

In the supplied data of flow number, there are some mixes which have flow numbers of one or zero. Those data are discarded from the analysis.

Same Mix by Same Contractor

To investigate the variation of flow number by a single contractor for the same mix, the following mixes are selected randomly (Table 36). The paving contractor is APC Southern (APC), with the binder material provided by Suncor, and aggregate provided by Valardi. The mixes are manufactured in 2014.

Table 36. Generic Information of 19655 Mix

	19655 P20 14	19655 P21 14	19655 P23 14	19655 P24 14	19655 P28 14	19655 P37 14	19655 P48 14	19655 P87 14
Contractor	APC	APC	APC	APC	APC	APC	APC	APC
Refinery	Suncor	Suncor	Suncor	Suncor	Suncor	Suncor	Suncor	Suncor
Pit	Valardi	Valardi	Valardi	Valardi	Valardi	Valardi	Valardi	Valardi
Date	July 2014	July 2014	July 2014	July 2014	July 2014	Aug 2014	Sep 2014	Oct 2014

The N -values vary from 120 to 531 with an average value of 261, and standard deviation of 125, as shown in Figure 16. To determine whether this data is statistically significant or not, a one-sample t -test are conducted. The t -test requires the data to be normally distributed. Three normality tests (Cramer-von Mises, Anderson-Darling, and Shapiro-Wilk) are conducted, and all of them showed the data is normal. The t -test showed the 95% Confidence Interval (CI) boundaries to be 150 and 372, with the mean value of 261. This means all the mixes, except for 19655 P21 14 and 19655 P87 14, are statistically the same. Therefore, a conclusion can be made that the same mix may have statistically different flow numbers for the same contractor.

SX(100) PG 64-28

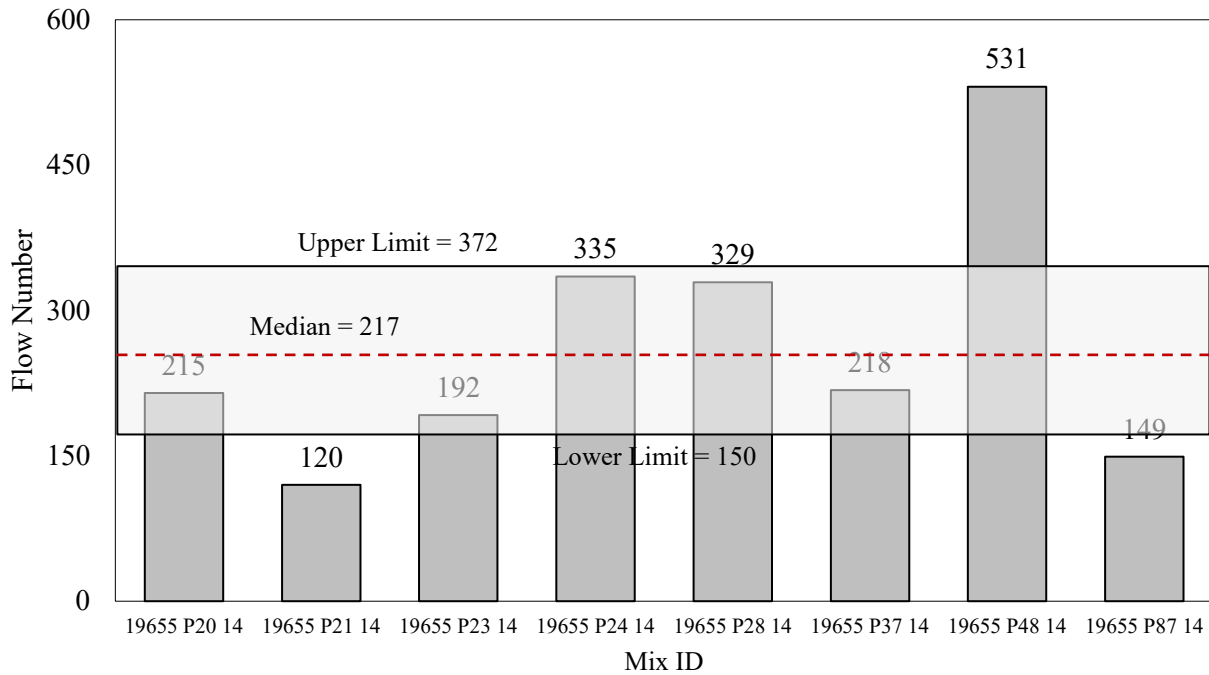


Figure 16. Flow Number of Eight Specimens of SX(100) PG 64-28 Mix

Same Mix by Different Contractors

To investigate the difference in flow number for the same mix prepared by different contractors, SX(100) PG 76-28 mix has been selected. The average flow numbers from four contractors, 19128, 18842, 19458, and 19677, are presented in Figure 17.

SX (100) PG 76-28

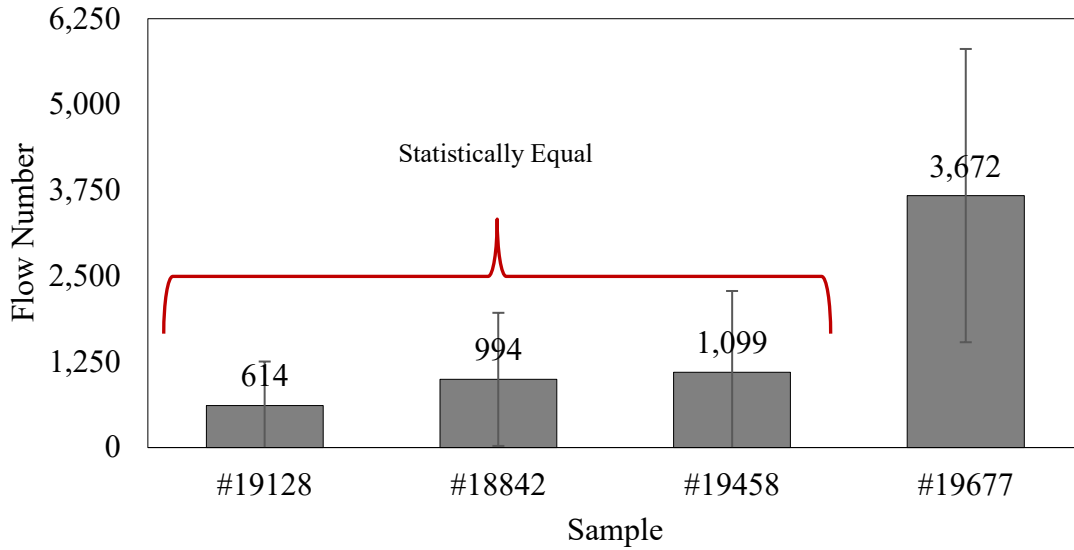


Figure 17. Flow Number of a Mix by Different Contractors

Normality tests (Cramer-von Mises, Anderson-Darling, and Shapiro-Wilk) show only projects #18842 and #19677 to be normal. The pairwise-comparisons test result shows mixes, 19128, 18842, and 19458 are statistically the same (Table 37). Therefore, a conclusion can be made that the same mix may have statistically different flow numbers for different contractors.

Table 37. Pairwise Comparisons using t-tests to Determine Whether Statistically Different

	19128	18842	19458
18842	Equal	-	-
19458	Equal	Equal	-
19677	Different	Different	Different

Groupwise Comparison

Eleven types of mixtures are classified as follows:

- 1) S(100) PG 64-22
- 2) S(100) PG 76-28
- 3) SMA PG 76-28
- 4) SX(75) PG 58-28
- 5) SX(75) PG 58-34
- 6) SX(75) PG 64-22
- 7) SX(75) PG 64-28
- 8) SX(100) PG 58-28
- 9) SX(100) PG 64-22
- 10) SX(100) PG 64-28
- 11) SX(100) PG 76-28

S(100) PG 64-22

The flow numbers for S(100) PG 64-22 mix by different contractors are presented in Figure 18, which shows that the flow number varies from 110 to 252, with an average number of 155, median of 130 and standard deviation of 59. As per AASHTO [11], a mix is good for 3 to 10 million ESALs if it has a flow number greater than 50. The current mix has an average flow number of 103, however, about one-third of the test results indicate flow numbers less than 50. Despite this, the S(100) PG 64-22 mix would be considered good for pavement designs with a traffic between 3 to 10 million ESALs. Shapiro-Wilk normality shows the data to be normal. The t -test shows the 95% CI boundaries to be 47 and 262.

S(100) PG 64-22

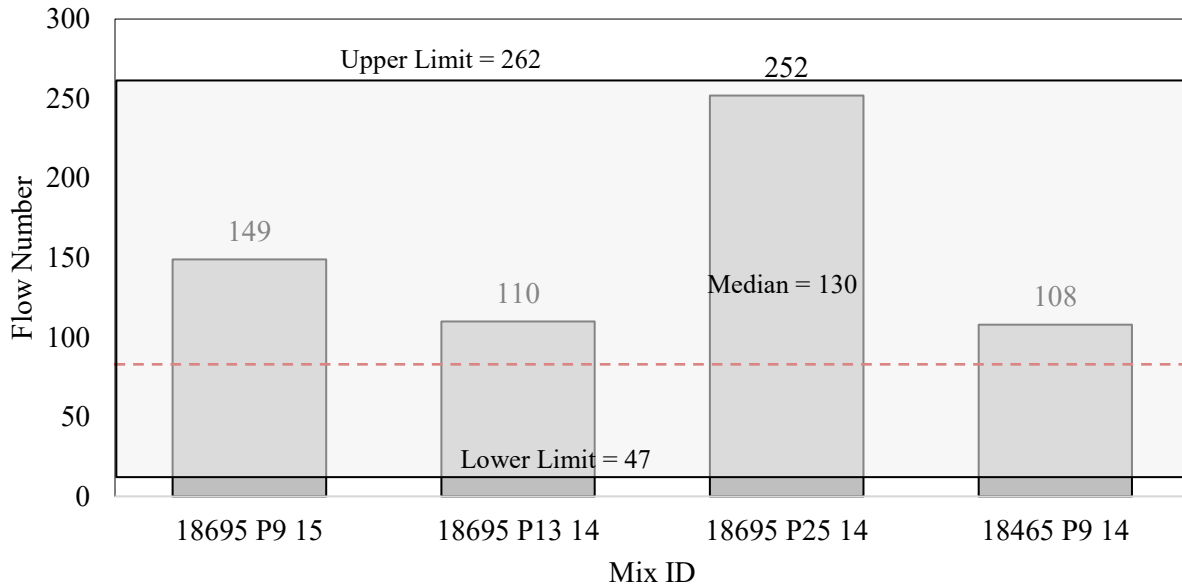


Figure 18. Flow Numbers for S(100) PG 64-22 Mix

Four mixes, 18695 P9 15, 18695 P13 14, 18695 P25 14, and 18465 P9 14, are being found to be statistically the same, although the paving contractors, binder supplier, and production dates differ (Table 38). The 18465 P9 14 mix, for example, has a much lower VFA compared to the others. Thus, definitive conclusions cannot be made from this mix.

Table 38. Generic Information of S(100) PG 64-22 Mix

	Paving Contractor	Binder Supplier	Region	Date	V_{be} (%)	V_a (%)	VMA (%)	VFA (%)	AC (%)	Pit
18465 P9 14	Asphalt Paving	Frontier Cheyenne	4	7/2014	10.59	6.34	15.8	44.0	4.80	Firestone, Ralston, Lien
18695 P9 15	APC Southern	Suncor	1	4/2016	10.04	6.20	16.3	63.8	5.09	Ralston / Platteville
18695 P13 14	APC Southern	Holly Frontier	1	7/2014	10.78	6.12	17.0	63.7	5.00	Firestone, Ralston, Pete Lien
18695 P25 14	-	Holly Frontier	1	8/2014	10.26	5.84	15.8	63.2	5.00	Firestone, Ralston, Lien

Note: Green highlighted mixes produce statistically the same flow number.

To determine the influence of V_{be} , V_a , VMA, VFA, and AC, a regression analysis is conducted, and the following correlation is obtained with the R^2 of 1.0. The regression equation below shows that the flow number increases with an increase in V_a , VMA, and VFA, and decreases with an increase in V_{be} and AC.

$$N = 13176.37 - 470.686 V_{be} + 769.3063 V_a + 97.8547 \text{ VMA} + 41.8502 \text{ VFA} - 3405.98 \text{ AC}$$

S(100) PG 76-28

The flow numbers for S(100) PG 76-28 mix by different contractors are presented in Figure 19. Data shows the flow number varies from 626 to 2,065 with an average number of 1,223, median of 1,101 and standard deviation of 528. As per AASHTO [11], a mix is good for more than 30 million ESALs if it has flow number greater than 740. The current mix has the average flow number of 1,223. All the test results show flow number greater than 740. Therefore, this mix is considered good for traffic greater than 30 million ESALs based on the criteria listed in Table 1.

The Shapiro-Wilk normality test is conducted and results in data to be considered normal. The t -test shows the 95% CI boundaries to be 253 and 2,193. All the values are within the 95% CI boundaries, thus statistically equal. The generic information listed in Table 39 shows the mix parameters of all mixes are very close to each other.

S(100) PG 76-28

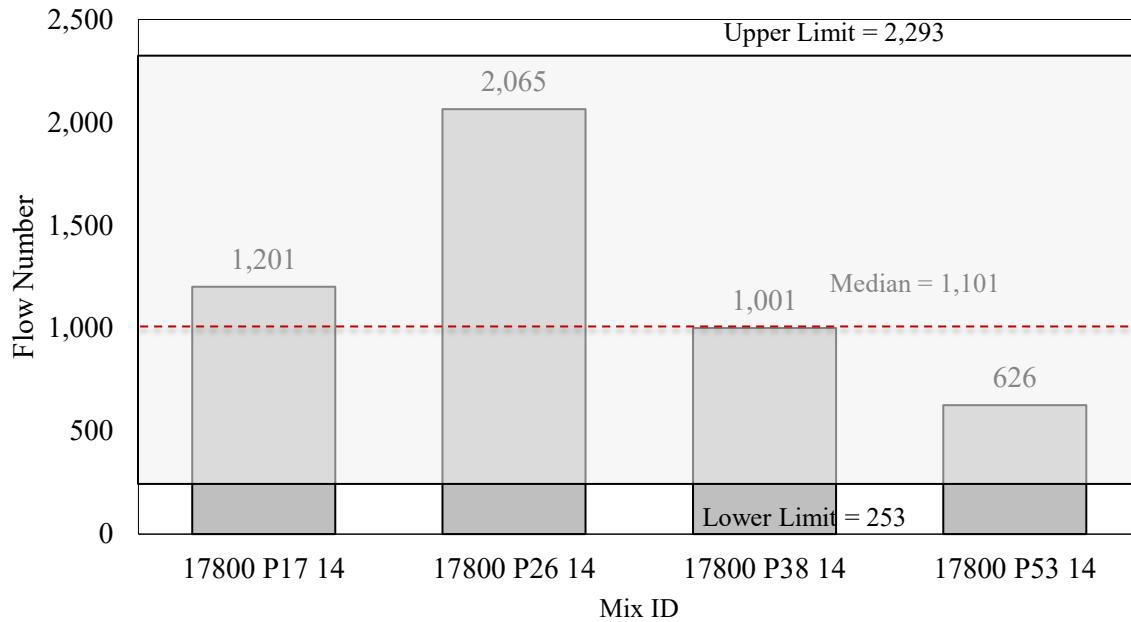


Figure 19. Flow Numbers for S(100) PG 76-28 Mix

Comparing the above two mixtures, S(100) PG 64-22, and S(100) PG 76-28, both have the same aggregate size; the only difference is the binder type. With an increase in binder grade, the flow number increases. The mix parameters listed in Table 39 show that all four mixes (17800 P17 14, 17800 P26 14, 17800 P38 14, and 17800 P53 14) have similar properties, and their flow numbers are statistically equal.

Table 39. Generic Information of S(100) PG 76-28 Mix

	Paving Contractor	Binder Supplier	Region	Date	V_{be} (%)	V_a (%)	VMA (%)	VFA (%)	AC (%)	Pit
17800 P17 14	Aggregate Industries	Jebro	4	7/2014	10.61	6.98	16.9	55.5	5.20	Distil, Lien
17800 P26 14	Aggregate Industries	Jebro	4	8/2014	10.61	6.58	16.8	58.6	5.20	Distil, Lien
17800 P38 14	Aggregate Industries	Jebro	4	9/2014	10.79	6.08	16.2	62.2	5.20	Distil, Lien
17800 P53 14	Aggregate Industries	Jebro	4	1/2015	10.61	6.72	16.6	59.3	5.20	Distil, Lien

Note: Green highlighted mixes produce statistically the same flow number.

Regression analysis is conducted using the mix parameters listed in Table 27. The following regression equation is obtained with an R^2 of 1.0. The equation shows that the flow number increases with an increase in VMA, decreases with an increase in V_a and VFA, and is insensitive to V_{be} , and AC.

$$N = - 48144.5 - 3600.27 V_a + 4536.5 \text{ VMA} - 39.5 \text{ VFA}$$

SMA PG 76-28

The flow numbers for SMA PG 76-28 mix by different contractors are presented in Figure 20. The graph shows that the flow number varies from 426 to 4,311, with an average number of 2,272, median of 2,219 and a standard deviation of 1,182. All the test results, with the exception of one outlier judged by visual inspection, show the flow number to be greater than 740. Therefore, this mix is considered good for traffic greater than 30 million ESALs. Three normality tests, Cramer-von Mises, Anderson-Darling, and Shapiro-Wilk did not show sufficient evidence of the data to not be normal. The t -test showed the 95% CI boundaries to be 1,487 and 3,057.

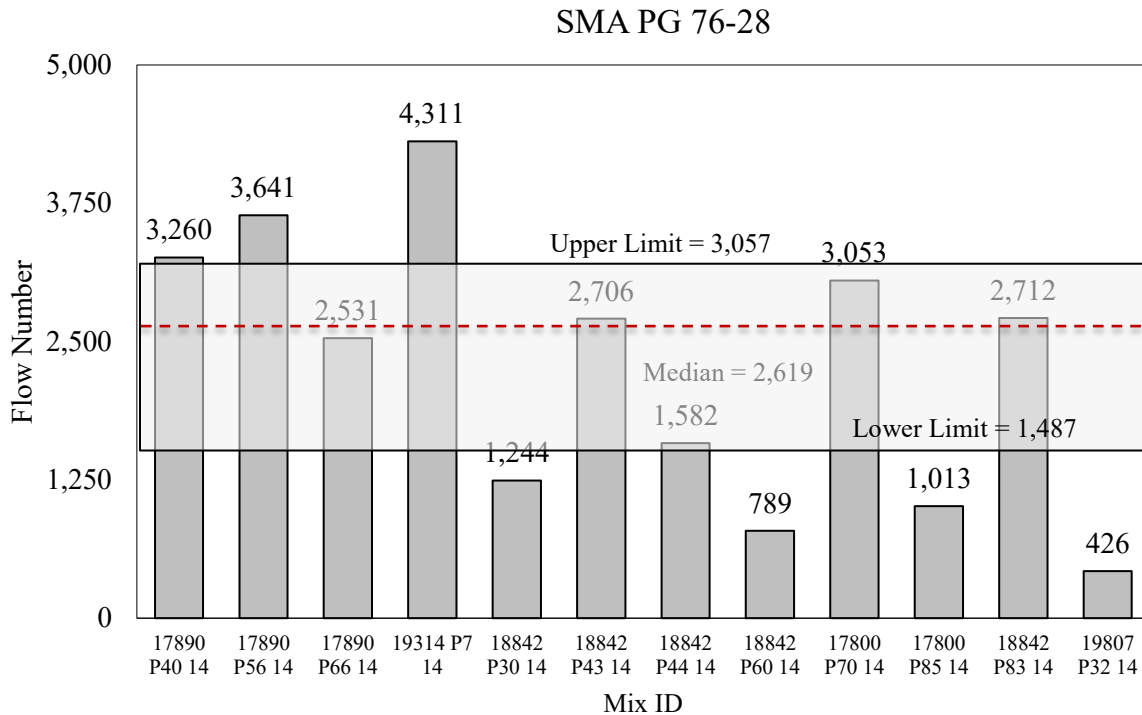


Figure 20. Flow Numbers for SMA PG 76-28 Mix

Comparing the two mixtures, S(100) PG 76-28 and SMA PG 76-28, both have the same binder, but have different aggregate size. An increase in aggregate size increases the flow number as observed from these two mixtures. The coarser aggregate shows better resistance to the deformation due to aggregate-to-aggregate interlocking. Mix parameters listed in Table 40 show that mixes with similar properties (such as V_{be} , V_a , VMA, VFA, AC) have statistically different flow numbers.

Table 40. Generic Information of SMA PG 76-28 Mix

	Paving Contractor	Binder Supplier	Region	Date	V_{be} (%)	V_a (%)	VMA (%)	VFA (%)	AC (%)	Pit
17800 P70 14	Aggregate Industries	Jebro	4	5/2015	10.0	3.2	17.8	73.7	6.4	Morrison, Lien
17800 P85 14	Aggregate Industries	Jebro	4	10/2015	13.68	4.66	18.5	70.7	6.2	Morrison, Lien
17890 P40 14	Martin Marietta	Suncor	1	10/2014	15.17	4.24	18.0	77.5	6.40	Spec Agg
17890 P56 14	Martin Marietta	Suncor	1	1/2015	15.17	4.66	18.3	75.2	6.20	Spec Agg
17890 P66 14	Martin Marietta	Suncor	1	3/2015	15.17	4.20	17.9	76.8	6.20	Spec Agg
18842 P30 14	Kiewit Construction	Suncor	2	8/2014	13.64	4.64	18.4	75.7	6.3	Parkdale Tezak
18842 P43 14	Kiewit Construction	Suncor	2	11/2014	13.58	5.08	19.1	73.3	6.3	Parkdale Tezak
18842 P44 14	Kiewit Construction	Suncor	2	11/2014	13.29	3.4	18.8	75.0	6.3	Tezak, I-25 Millings
18842 P60 14	Kiewit Construction	Suncor	2	2/2015	13.31	3.4	19.8	65.1	5.2	Parkdale Tezak
18842 P83 14	Kiewit Construction	Suncor	2	9/2015	13.77	3.4	18.9	71.2	6.3	Parkdale Tezak
19314 P7 14	Martin Marietta	Suncor	4	6/2014	13.94	5.24	18.4	71.0	5.65	Granite Canyone, Lien
19807 P32 14	Brannan	Suncor	1	9/2014	13.80	3.0	16.0	74.9	6.3	Frei, Lein

Note: Green highlighted mixes produce statistically the same flow number.

To determine the influence of V_{be} , V_a , VMA, VFA, and AC, a regression analysis is conducted using the mix parameters listed in Table 40 and the following correlation is obtained with a R^2 of

0.32. The regression equation shows the flow number increases with an increase in V_a , VMA, and VFA, and decreases with an increase in V_{be} and AC.

$$N = -12065.8 - 225.114 V_{be} + 699.781 V_a + 255.266 VMA + 217.2518 VFA - 984.631 AC$$

SX(75) PG 58-28

The flow numbers for SX(75) PG 58-28 mix by different contractors are presented in Figure 21. The graph shows that the flow number varies from 29 to 220, with an average number of 91, median of 81 and standard deviation of 55. All the test results, apart from one outlier, show a flow number greater than 50. The current mix has an average flow number of 91; therefore, per AASHTO, this mix is considered good for traffic of 3 to 10 million ESALs. Normality tests Cramer-von Mises, Anderson-Darling, and Shapiro-Wilk showed sufficient evidence of the data to be normal. The t -test showed the 95% CI boundaries to be 42 and 140.

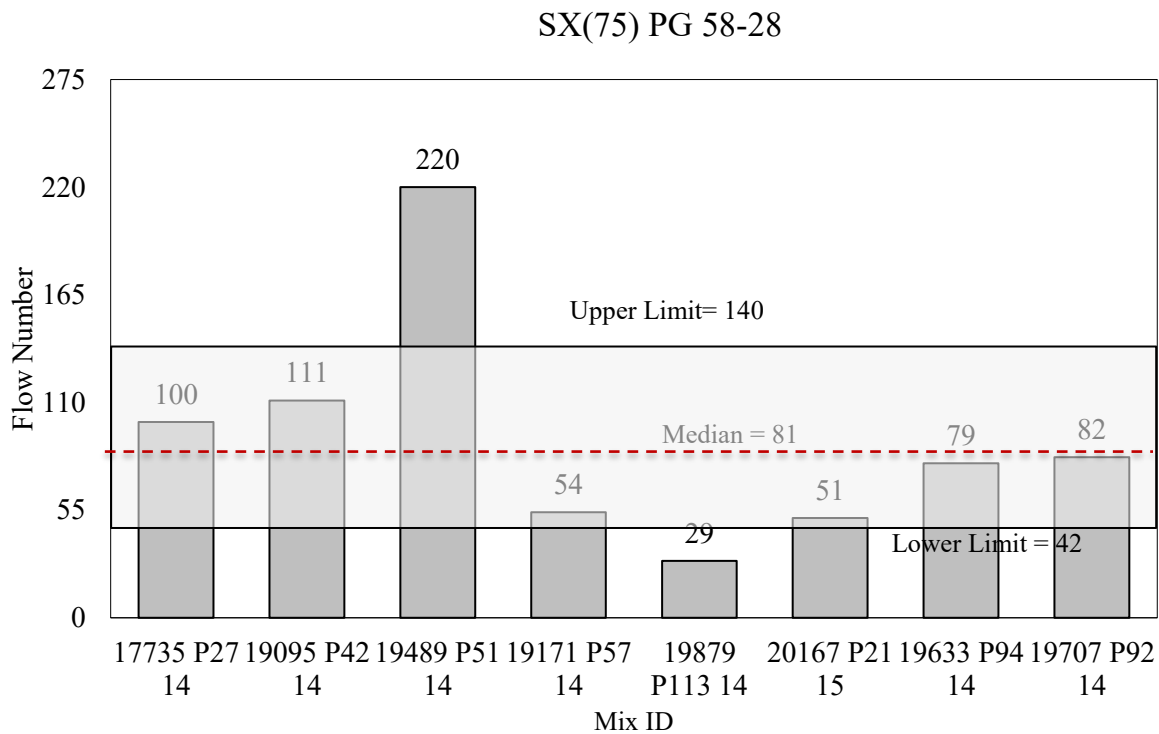


Figure 21. Flow Numbers for SX(75) PG 58-28 Mix

All mixes except 19489 P51 14 and 19879 P113 14 do not statistically have the same flow numbers. One mix (19489 P51 14) has a unique aggregate source (Chambers), and another mix (19879 P113 14) has a unique contractor (Kraemer and Sons) and aggregate source (Ralston, Firestone). All the other properties are similar to the mixes whose flow numbers are statistically the same. Therefore, contractor or aggregate source may be a parameter for the variation of the flow number.

Table 41. Generic Information of SX(75) PG 58-28 Mix

	Paving Contractor	Binder Supplier	Region	Date	V_{be} (%)	V_a (%)	VMA (%)	VFA (%)	AC (%)	Pit
17735 P27 14	United Companies	Suncor	3	8/2014	13.23	5.60	18.1	69.5	6.40	Halderson
19095 P42 14	United Gypsum	Sinclair	3	10/2014	10.96	6.90	16.8	61.0	6.10	Lyster Camilletti
19171 P57 14	Everist Materials	Suncor	3	1/2015	12.58	6.90	18.6	62.8	5.80	Maryland Creek Ranch
19489 P51 14	Elam Construction	Sinclair	3	1/2015	11.25	5.00	15.8	67.5	5.10	Chambers
19633 P94 14	4 Corners	Suncor	5	11/2015	12.57	5.00	17.9	64.0	5.51	Cugini Bayfield
19707 P92 14	Elam Construction	Suncor	5	11/2015	15.45	6.95	18.6	62.9	6.60	Agri-D Dillon Ranch
19879 P113 14	-	Suncor	1	2/2016	10.34	6.90	17.8	65.6	4.90	Ralston Firestone
20167 P21 15	Grand River	Peak	3	7/2016	9.81	5.90	17.7	65.1	4.94	Sievers

Note: Green highlighted mixes produce statistically the same flow number.

To determine the influence of V_{be} , V_a , VMA, VFA, and AC, a regression analysis is conducted using data from Table 41, and the following correlation is obtained with a R^2 of 0.96. The equation shows the flow number increases with an increase in VFA and AC, and decreases with an increase in V_{be} , V_a , and VMA.

$$N = 910.4758 + 19.12665 V_{be} - 6.097 V_a - 66.5327 \text{ VMA} + 2.2497 \text{ VFA} + 3.0182 \text{ AC}$$

SX(75) PG 58-34

The flow numbers for SX(75) PG 58-34 mix by different contractors are presented in Figure 22. The graph shows that the flow number varies from 19 to 75, with an average flow number of 47 and standard deviation of 28. As per AASHTO, a mix is considered good for traffic less than 3 million ESALs if it has a flow number less than 50. The current mix has an average flow number of 47; therefore, this mix is good for traffic less than 3 million ESALs. However, the current mix has only data for two mixes as shown in Table 42. Therefore, no sensitivity analysis is conducted on this mix.

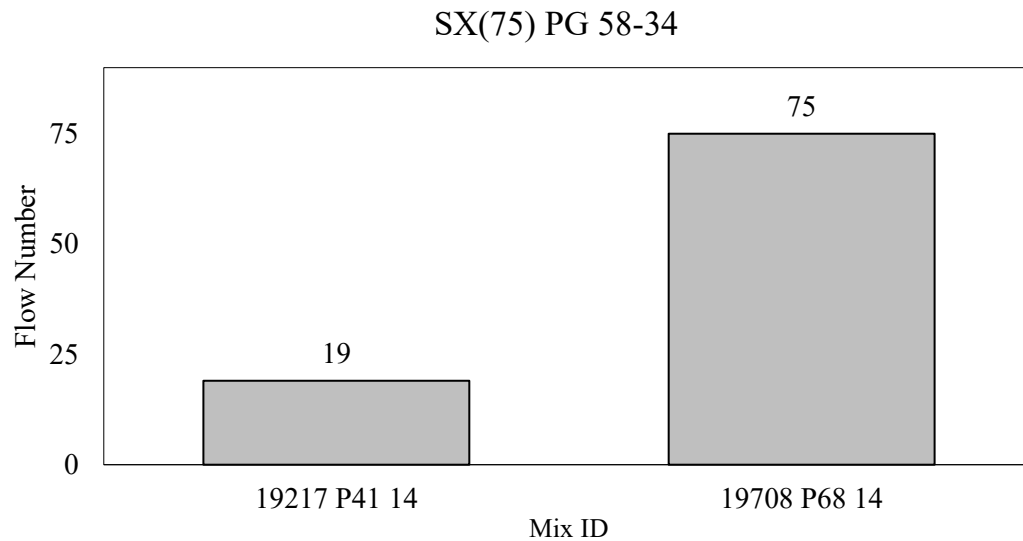


Figure 22. Flow Numbers for SX(75) PG 58-34 Mix

Table 42. Generic Information of SX(75) PG 58-34 Mix

	Paving Contractor	Binder Supplier	Region	Date	V_{be} (%)	V_a (%)	VMA (%)	VFA (%)	AC (%)	Pit
19217 P41 14	Connell Resources	Suncor	3	10/2014	10.94	6.60	16.5	60.5	5.60	Lyster & Camilletti
19708 P68 14	Connell Resources	Suncor	3	5/2015	11.69	6.90	17.8	60.8	5.50	Camilletti/Duckles

Note: Green highlighted mixes produce statistically the same flow number.

SX(75) PG 64-22

The flow numbers for SX(75) PG 64-22 mix by different contractors are presented in Figure 23. The graph shows that the flow number varies from 19 to 123, with an average number of 59, median of 49 and standard deviation of 34. As per AASHTO, a mix is considered good for traffic between 3 to 10 million ESALs if it has flow number greater than 50. The current mix has an average flow number of 59; therefore, this mix is considered good for traffic between 3 to 10 million ESALs. Normality tests Cramer-von Mises, Anderson-Darling, and Shapiro-Wilk showed sufficient evidence of the data to be normal. The *t*-test showed the 95% CI boundaries to be 28 and 90.

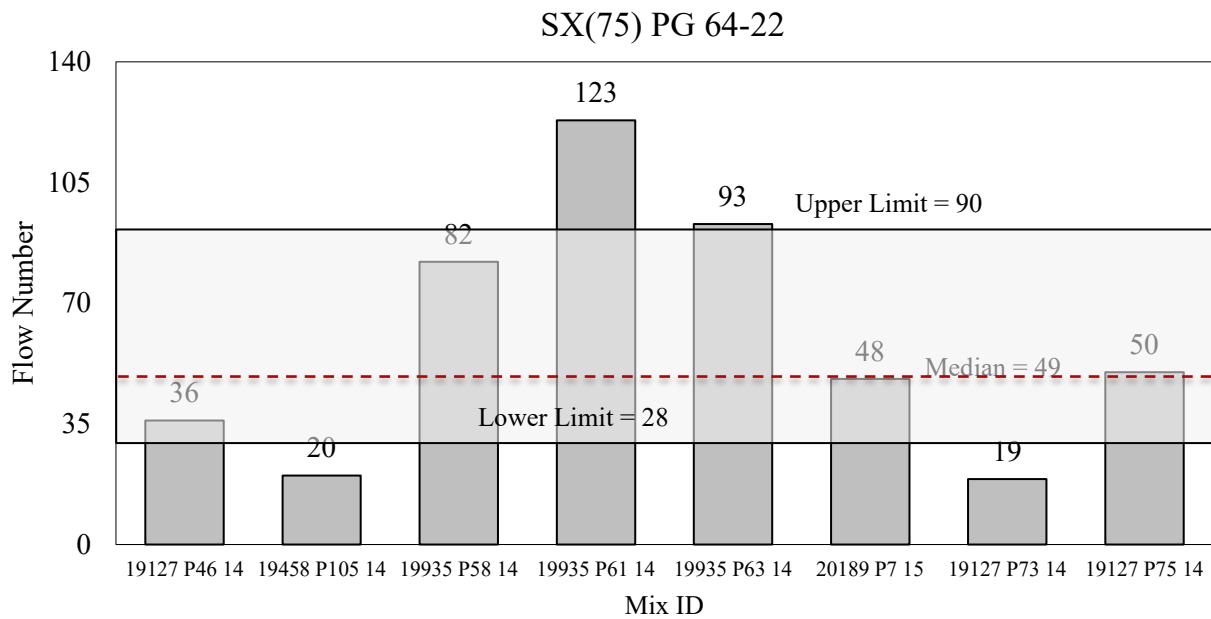


Figure 23. Flow Numbers for SX(75) PG 64-22 Mix

The mix parameters listed in Table 43 show that mixes with similar properties have statistically different flow numbers. For example, mixes with the prefix 19935 have the same binder supplier, aggregate source, region, and volumetric properties, though they have statistically different flow numbers.

Table 43. Generic Information of SX(75) PG 64-22 Mix

	Paving Contractor	Binder Supplier	Region	Date	V_{be} (%)	V_a (%)	VMA (%)	VFA (%)	AC (%)	Pit
19127 P73 14	Beltramo	Suncor	2	6/2015	13.53	7.10	18.4	61.2	5.70	Cesar/Transit Mix/Nepesta
19127 P75 14	Beltramo	Suncor	2	6/2015	13.55	6.93	17.9	61.6	5.70	Cesar/Transit Mix/Nepesta
19458 P105 14	Simon Construction	Suncor	4	12/2015	11.61	6.78	18.1	63.1	5.81	Granite Canyon, Julesburg, Ovid
19935 P58 14	A&S Construction	Suncor	2	2/2015	13.39	6.78	17.5	61.0	5.60	Rocky Ford South
19935 P61 14	A&S Construction	Suncor	2	2/2015	13.31	6.80	18.2	62.8	5.60	Rocky Ford South
19935 P63 14	A&S Construction	Suncor	2	3/2015	13.90	6.73	17.4	61.8	5.60	Rocky Ford South
20189 P7 15	McAtee	Suncor	4	4/2016	11.16	6.80	18.5	62.8	5.48	---

Note: Green highlighted mixes produce statistically the same flow number.

To determine the influence of V_{be} , V_a , VMA, VFA, and AC, a regression analysis is conducted using data from Table 31, and the following correlation is obtained with a R^2 of 0.98. The regression equation shows the flow number increases with an increase in VMA and AC, and decreases with an increase in V_{be} , V_a , and VFA.

$$N = 2680.341 + 55.39143 V_{be} - 662.65 V_a + 167.6587 \text{ VMA} - 32.7239 \text{ VFA} + 38.077 \text{ AC}$$

SX(75) PG 64-28

The flow numbers for SX(75) PG 64-28 mix by different contractors are presented in Figure 24. The graph shows that the flow number varies from 32 to 311, with an average number of 106, median of 41 and standard deviation of 118. As per AASHTO, a mix is considered good for traffic between 3 to 10 million ESALs if it has a flow number greater than 50. The current mix has an average flow number of 99; therefore, this mix is considered good for traffic between 3 to 10 million ESALs. The same observation are found for binders SX(75) PG 58-28 and SX(75) PG 58-

34. The Shapiro-Wilk normality test did not show sufficient evidence of the data to be normal. The one-sample *t*-test showed the 95% CI boundaries to be 0 and 323.

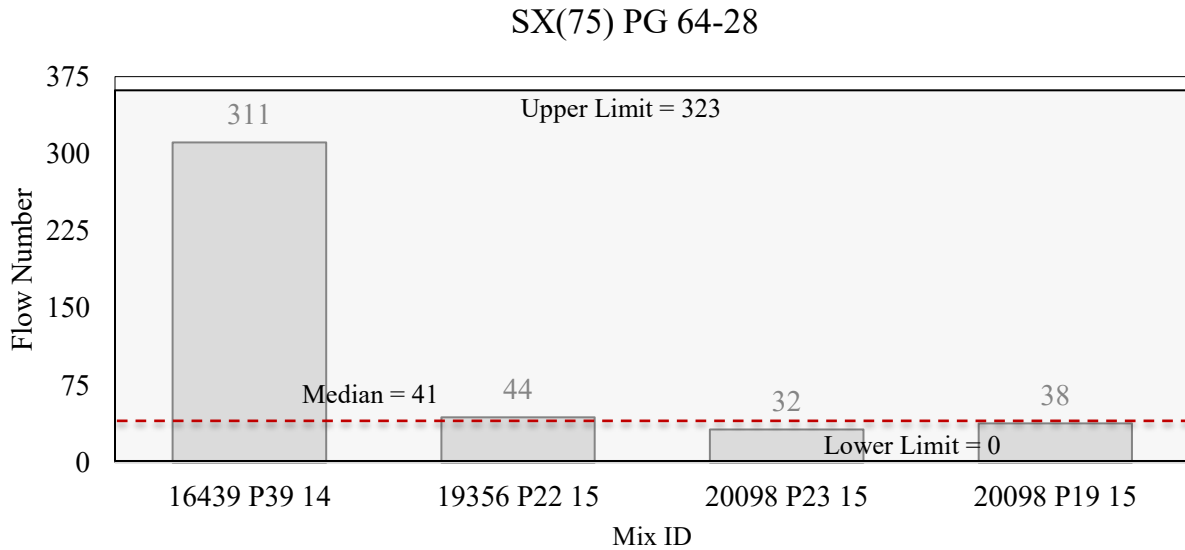


Figure 24. Flow Numbers for SX(75) PG 64-28 Mix

The mix parameters listed in Table 44 show that mixes with different properties have statistically same flow numbers.

Table 44. Generic Information of SX(75) PG 64-28 Mix

	Paving Contractor	Binder Supplier	Region	Date	V_{be} (%)	V_a (%)	VMA (%)	VFA (%)	AC (%)	Pit
16439 P77 14	Everist	Suncor	3	9/2014	9.16	6.52	--	--	5.80	Maryland Creek Ranch
19356 P22 15	Asphalt Specialties	Suncor	4	7/2016	10.92	5.30	17.7	60.9	5.51	Spec Agg, Turnpike, Firestone
20098 P19 15	Coulson	Suncor	4	5/2016	10.84	6.52	18.0	62.1	5.37	Bonser, Lien
20098 P23 15	Coulson	Suncor	4	8/2016	11.01	6.52	17.9	61.4	5.61	Bonser, Lien

Note: Green highlighted mixes produce statistically the same flow number.

The regression analysis using data from Table 32 obtained a regression equation with a R^2 of 1.0. The regression equation shown below shows the flow number increases with an increase in V_{be} and VFA, decreases with an increase in V_a , and is insensitive to VMA and AC.

$$N = -853.827 + 18.0133 V_{be} - 16.47 V_a + 12.946 \text{ VFA}$$

SX(100) PG 58-28

Only a single sample has been tested for this mix with the flow number of 128. No statistical test or sensitivity analysis are conducted on this mix due to insufficient data.

SX(100) PG 64-22

The flow numbers for SX(75) PG 64-22 mix by different contractors are presented in Figure 25. The graph shows that the flow number varies from 23 to 388, with an average number of 112, median of 97 and standard deviation of 92. As per AASHTO, a mix is considered good for traffic between 3 to 10 million ESALs if it has a flow number greater than 50. The current mix has the average flow number of 112; therefore, this mix is considered good for traffic between 3 to 10 million ESALs. Normality tests Cramer-von Mises, Anderson-Darling, and Shapiro-Wilk did not show sufficient evidence of the data to be normal. Nonetheless, a t -test is conducted, and the results show the 95% CI boundaries to be 59 and 164.

SX(100) PG 64-22

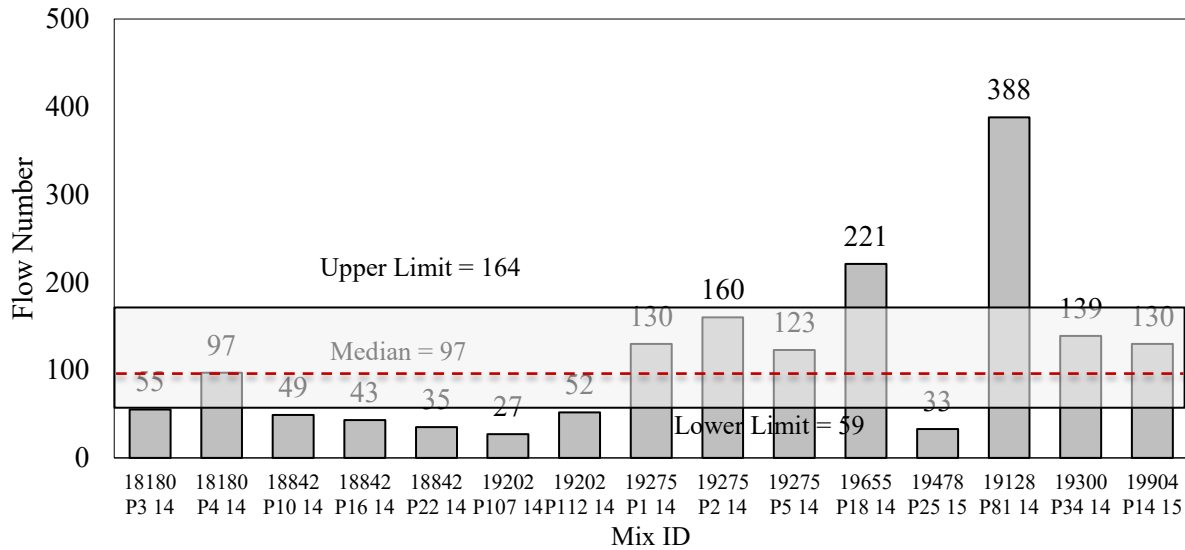


Figure 25. Flow Numbers for SX(100) PG 64-22 Mix

The mix parameters listed in Table 45 show that mixes with different properties have statistically the same flow numbers. On the other hand, mixes by the same contractor with the same aggregate source have statistically different flow numbers.

Using the data listed in Table 45, regression analysis is conducted, which obtained the following regression equation with a R^2 of 0.40. The regression equation shows the flow number increases with an increase in V_{be} , V_a , and AC, and decreases with an increase in VMA and VFA.

$$N = 11733 + 21.71 V_{be} + 50.56 V_a - 68.37 \text{ VMA} - 11.73 \text{ VFA} + 57.59 \text{ AC}$$

Table 45. Generic Information of SX(100) PG 64-22 Mix

	Paving Contractor	Binder Supplier	Region	Date	V_{be} (%)	V_a (%)	VMA (%)	VFA (%)	AC (%)	Pit
18180 P3 14	Aggregate Industries	Aggregate Industries	1	6/2014	12.24	6.66	17.1	61.2	5.00	Morrison, Plate River
18180 P4 14	Aggregate Industries	Suncor	---	6/2014	10.31	6.66	17.9	63.4	5.00	Morrison, Plate River
18842 P10 14	Kiewit Construction	Suncor	2	7/2014	11.63	5.00	18.3	62.8	5.30	Tezak Fountain / I25
18842 16 14	Kiewit Construction	Suncor	2	7/2014	11.39	6.98	18.4	62.4	5.30	Tezak Fountain / I25
18842 P22 14	Kiewit Construction	Suncor	2	8/2014	11.44	6.52	18.1	64.3	5.30	Tezak Fountain / I25
19128 P81 14	Martin Marietta	Suncor	2	7/2015	13.18	6.90	17.6	60.8	5.50	Evans
19202 P107 14	Skanska	Suncor	5	1/2015	11.94	6.00	18.8	64.2	6.34	Four Corners
19202 P112 14	Skanska	Suncor	5	1/2015	11.29	6.00	18.3	61.2	5.95	Four Corners
19275 P1 14	APC Southern	Holly Frontier	2	6/2014	13.41	5.78	17.0	66.3	5.65	---
19275 P2 14	APC Southern	Holly Frontier	2	6/2014	13.41	6.60	18.1	65.9	5.65	---
19275 P5 14	Aggregate Industries	Holly Frontier	2	6/2014	13.41	6.14	17.3	65.2	5.65	---
19300 P34 14	United Companies	Suncor	3	9/2014	12.04	5.64	16.7	66.4	6.00	Craig Ranch
19655 P18 14	APC Southern	Holly Frontier	2	7/2014	11.05	6.06	16.7	64.3	5.60	Valardi
19904 P14 15	Martin Marietta	Suncor	1	5/2016	13.43	6.40	17.1	62.5	5.50	Spec Agg / Riverbend / Cottonwood

Note: Green highlighted mixes produce statistically the same flow number.

SX(100) PG 64-28

The flow numbers for SX(100) PG 64-28 mix by different contractors are presented in Figure 26. The graph shows that the flow number varies from 19 to 123, with an average number of 241, median of 215 and standard deviation of 131. As per AASHTO, a mix is considered good for traffic between 10 to 30 million ESALs if it has a flow number greater than 190. The current mix has an average flow number of 240; therefore, this mix is considered good for traffic between 10 to 30 million ESALs. Normality tests Cramer-von Mises, Anderson-Darling, and Shapiro-Wilk showed sufficient evidence of the data to be normal. The *t*-test showed the 95% CI boundaries to be 134 and 347.

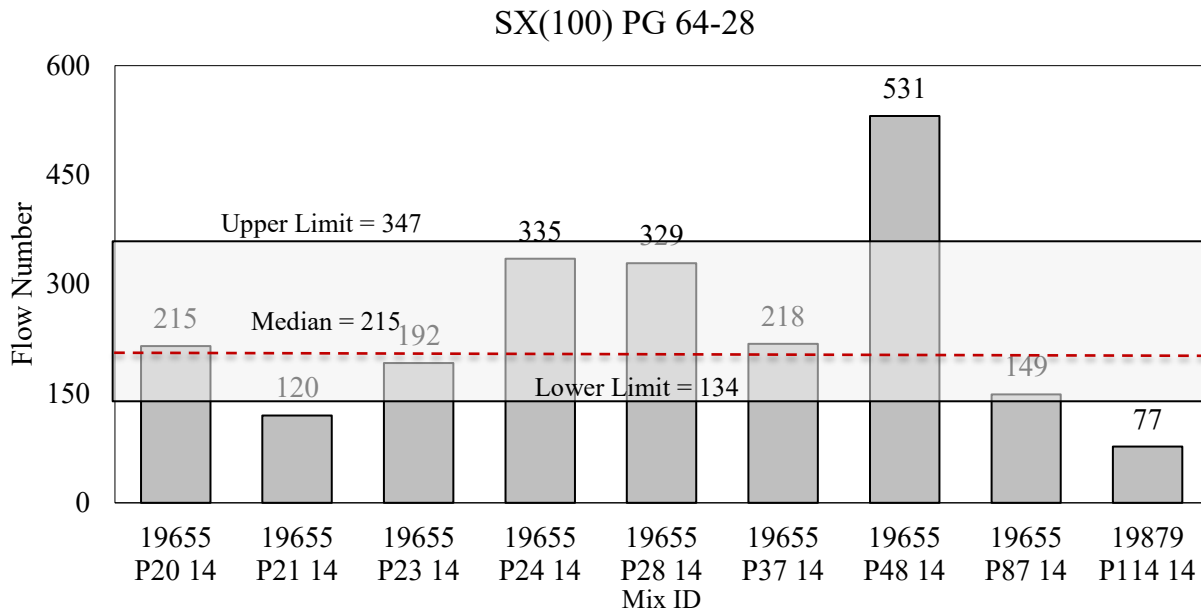


Figure 26. Flow Numbers for SX(100) PG 64-28 Mix

Table 46 highlights the mixes with flow numbers that are statistically the same. Three mixes, 19655 P 21 14, 19655 P48 14, and 19879 P114 14, are not statistically the same, however, two mixes, 19655 P 21 14, and 19655 P48 14, have similar properties with the statistically similar mixes. Therefore, flow numbers can be statistically different for the same mix by the same contractor.

Table 46. Generic Information of SX(100) PG 64-28 Mix

	Paving Contractor	Binder Supplier	Region	Date	V_{be} (%)	V_a (%)	VMA (%)	VFA (%)	AC (%)	Pit
19655 P20 14	APC Southern	Suncor	2	7/2014	10.59	6.06	17.0	64.0	5.58	Valardi
19655 P21 14	APC Southern	Suncor	2	7/2014	10.85	6.06	17.1	63.5	5.80	Valardi
19655 P23 14	APC Southern	Suncor	2	8/2014	10.56	6.06	16.7	65.1	5.70	Valardi
19655 P24 14	APC Southern	Suncor	---	8/2014	10.97	6.06	16.0	64.2	5.78	Valardi
19655 P28 14	APC Southern	Suncor	2	8/2014	10.71	6.06	16.1	63.0	5.61	Valardi
19655 P37 14	APC Southern	Suncor	2	9/2014	10.48	6.06	15.8	62.4	5.65	Valardi
19655 P48 14	APC Southern	Suncor	2	12/2014	13.18	6.60	17.4	62.0	5.50	Valardi
19655 P87 14	APC Southern	Suncor	2	10/2015	13.18	6.30	17.1	63.2	5.50	Valardi
19879 P114 14	-	Suncor	1	3/2016	10.05	6.90	17.5	63.5	4.90	Ralston, Firestone

Note: Green highlighted mixes produce statistically the same flow number.

A regression analysis is conducted to determine the influence of V_{be} , V_a , VMA, VFA, and AC using data from Table 46. The following correlation is obtained with a R^2 of 0.56. The regression equation shows the flow number increases with an increase in V_{be} , V_a , and AC, and decreases with an increase in VMA and VFA.

$$N = -3944 + 25.85 V_{be} + 579.6 V_a - 106.93 \text{ VMA} - 20.44 \text{ VFA} + 605.78 \text{ AC}$$

SX(100) PG 76-28

The flow numbers for SX(100) PG 76-28 mix by different contractors are presented in Figure 27. The graph shows that the flow number of this mix varies from 82 to 6,343, with an average number of 1,578, median of 810 and a standard deviation of 1,837. As per AASHTO, a mix is considered good for traffic greater than 30 million ESALs if it has a flow number greater than 740. Although

the average flow number is 1,482, nearly half of the samples had a flow number less than 740. Therefore, it is very difficult to conclude whether this mix is considered good for traffic greater than 30 million ESALs. Comparing this result with the previous binders, the flow number increases with an increase in high-temperature grade of the binder. A similar observation are found for the SX(75) mix. Normality tests Cramer-von Mises, Anderson-Darling, and Shapiro-Wilk did not show sufficient evidence of the data to be normal. The *t*-test showed the 95% CI boundaries to be 893 and 2,262. Out of 33 specimens, only 7 specimens are within the 95% CI boundaries.

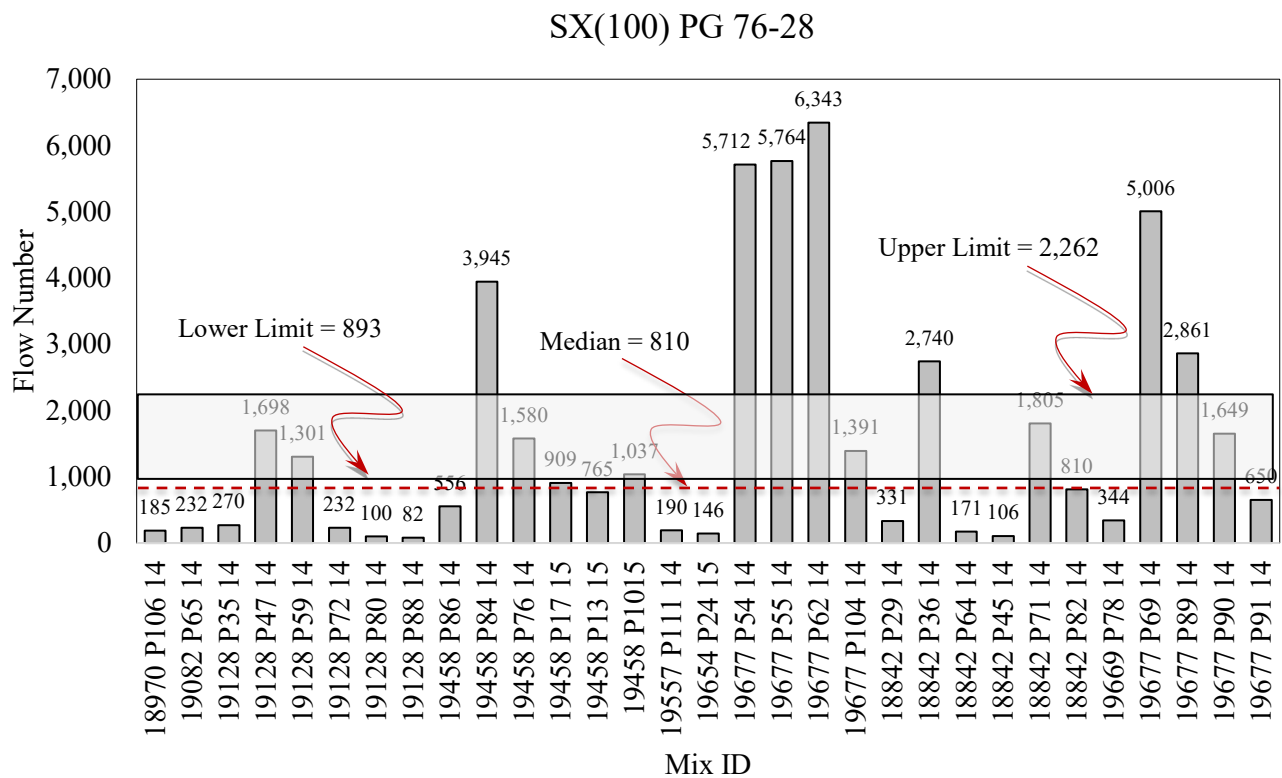


Figure 27. Flow Numbers for SX(100) PG 76-28 Mix

As listed in Table 35, there are seven mixes whose mix parameters are the same, but their flow numbers are not statistically the same. To clarify, the mixes by Kiewit, Martin Marietta, or Simon Construction have similar mix parameters in every category, but the flow numbers are statistically different. Table 47 also shows that mixes with different properties have statistically the same flow numbers.

Table 47. Generic Information of SX(100) PG 76-28 Mix

	Paving Contractor	Binder Supplier	Region	Date	V_{be} (%)	V_a (%)	VMA (%)	VFA (%)	AC (%)	Pit
18842 P29 14	Kiewit Construction	Suncor	2	7/2014	12.61	6.68	18.1	64.3	6.30	Tezak / Fountain / I-25 Millings
18842 P36 14	Kiewit Construction	Suncor	2	8/2014	14.32	4.56	15.8	72.5	6.30	Parkdale/Tezak
18842 P45 14	Tezak	Suncor	2	8/2014	12.53	6.93	18.2	62.2	5.20	Tezak / Fountain / I-25 Millings
18842 P64 14	Kiewit Construction	Suncor	2	9/2014	12.53	6.85	18.2	62.4	6.30	Tezak / Fountain / I-25 Millings
18842 P71 14	Kiewit Construction	Suncor	2	10/2014	15.23	4.88	18.5	73.5	6.30	Parkdale/Tezak
18842 P82 14	Kiewit Construction	Suncor	2	10/2014	12.53	6.93	18.3	62.3	5.20	Tezak / Fountain / I-25 Millings
18970 P106 14	APC Southern	Suncor	5	11/2014	12.72	5.60	18.2	67.4	6.12	King Pit
19082 P65 14	ACA Buena Vista	Suncor	5	3/2015	13.84	6.85	18.8	63.2	5.70	Avery Pit, ACA Buena Vista
19128 P35 14	Martin Marietta	Suncor	2	8/2014	10.96	6.32	17.1	62.5	5.60	Evans
19128 P47 14	Evans	Suncor	2	8/2014	10.90	6.82	17.6	61.4	5.60	Evans
19128 P59 14	Martin Marietta	Suncor	2	9/2014	10.90	6.82	17.6	60.9	5.60	Evans
19128 P72 14	Martin Marietta	Suncor	2	9/2014	10.00	6.82	17.9	60.2	5.10	Evans
19128 P80 14	Martin Marietta	Suncor	2	10/2014	10.00	6.82	17.6	60.7	5.10	Evans/slate
19128 P88 14	Martin Marietta	Suncor	2	10/2014	10.82	6.83	17.6	61.6	5.60	Evans/slate
19458 P10 15	Simon Construction	Suncor	4	5/2015	9.90	5.30	16.8	61.5	5.05	Granite Canyon, Julesburg, Sedgwick
19458 P13 15	Simon Construction	Suncor	4	6/2015	9.47	5.30	16.5	61.7	4.96	Granite Canyon, Julesburg, Sedgwick
19458 P17 15	Simon Construction	Suncor	4	6/2015	9.55	5.30	16.1	60.7	4.93	Granite Canyon, Julesburg, Sedgwick
19458 P20 15	Simon Construction	Suncor	4	6/2015	10.32	4.40	16.6	60.0	5.30	Granite Canyon, Julesburg, Sedgwick
19458 P76 14	Simon Construction	Suncor	4	6/2015	11.57	6.43	17.3	62.6	5.20	Granite Canyon, Julesburg, Sedgwick

19458 P79 14	Simon Construction	Suncor	4	7/2015	11.57	6.80	17.6	61.4	5.20	Granite Canyon, Julesburg, Sedgwick
19458 P84 14	Simon Construction	Suncor	4	9/2015	11.57	6.75	17.6	61.2	5.20	Granite Canyon, Julesburg, Sedgwick
19458 P86 14	Simon Construction	Suncor	4	10/2015	11.57	6.78	17.6	61.3	5.20	Granite Canyon, Julesburg, Sedgwick
19557 P111 14	A&S Construction	Suncor	2	11/2014	11.71	5.00	17.7	64.6	5.38	Tezak/Transit Mix
19654 P24 15	Martin Marietta	Suncor	2	7/2015	10.31	5.00	17.6	60.6	5.25	Evans/slate
19669 P78 14	A&S Construction	Suncor	2	10/2014	10.72	6.93	17.7	61.0	5.40	Rocky Ford South/La Junta
19677 P54 14	Elam Construction	Suncor	3	1/2015	10.25	5.18	14.9	65.4	5.50	23 Road
19677 P55 14	Elam Construction	Suncor	3	1/2015	10.54	5.04	15.1	66.6	5.50	23 Road
19677 P62 14	Elam Construction	Suncor	3	2/2015	10.69	5.00	15.2	66.5	5.50	23 Road
19677 P69 14	Elam Construction	Suncor	3	5/2015	11.71	4.43	15.6	71.7	5.50	23 Road
19677 P89 14	Elam Construction	Suncor	3	10/2015	10.69	6.83	16.8	58.9	5.50	23 Road
19677 P90 14	Elam Construction	Suncor	3	10/2015	11.71	5.98	17.0	64.6	5.50	23 Road
19677 P91 14	Elam Construction	Suncor	3	11/2015	11.71	5.88	16.9	65.3	5.50	23 Road
19677 P104 14	Elam Construction	Suncor	3	11/2014	11.02	5.88	18.6	57.6	5.74	23 Road

Note: Green highlighted mixes produce statistically the same flow number.

To determine the influence of V_{be} , V_a , VMA, VFA, and AC, a regression analysis is conducted using data from Table 47, and the following correlation is obtained with a R^2 of 0.62. The regression equation shows the flow number increases with an increase in V_{be} , V_a , VFA, and AC, and decreases with an increase in VMA.

$$N = 18427.9 + 225.75 V_{be} + 413.82 V_a - 1600.7 \text{ VMA} + 60.9 \text{ VFA} + 314.43 \text{ AC}$$

Flow Number Analysis Summary

The flow number for each group, their variations, 95% CI boundaries, etc. are presented in Figure 28, and Table 48. They show that SX(75) PG 58-34 has the lowest flow number and SMA PG 76-28 has the highest flow number. Comparing the average flow number with the above-listed values, the following may be concluded:

- Only two types of mixtures, SX(100) PG 76-28 and SMA PG 76-28, have flow numbers greater than 740. Thus, only these mixtures are considered good for traffic greater than 30 million ESALs.
- S(100) PG 76-28 has an average flow number of more than 190; thus, it is considered good for traffic between 10 to 30 million ESALs.
- SX(100) PG 64-22, SX(100) PG 64-28 and SX(100) PG 58-28 are considered good for traffic between 3 to 10 million ESALs.
- Other five mixtures: S(100) PG 64-22, SX(75) PG 58-28, SX(75) PG 58-34, SX(75) PG 64-22 and SX(75) PG 64-28 have a flow number less than 50; thus, they are considered good for traffic less than 3 million ESALs.
- Comparing SX(100) PG 64-28 and SX(100) PG 76-28, the flow number of HMA increases with an increase in high-temperature grade of the binder.
- Variable results are observed whether the flow number increases or decreases with an increase in low-temperature grade of the binder. For example, when comparing SX(75) PG 64-22 and SX(75) PG 64-28, the flow number increases with an increase in low-temperature grade of the binder, however, when comparing SX(75) PG 58-34 and SX(75) PG 58-28, the flow number decreases with an increase in low-temperature grade of the binder.
- An SX mix has 0.5-in. nominal aggregate size, and an S mix is 0.75-in. nominal aggregate size. SX mix has larger flow number, i.e., smaller aggregate size produces larger flow number from the comparisons of flow number of SX(100) PG 64-22 with S(100) PG 64-22, and SX(100) PG 76-28 with S(100) PG 76-28. However, the differences between these pairs are not statistically significant.

- The (75) and (100) refer to the number of gyrations during design. Greater number of gyrations produce greater number of flow number as shown from the comparison of SX(75) PG 58-28 with SX(100) PG 58-28, SX(75) PG 64-22 with SX(100) PG 64-22, and SX(75) PG 64-28 with SX(100) PG 64-28. However, the differences between these pairs are not statistically significant.

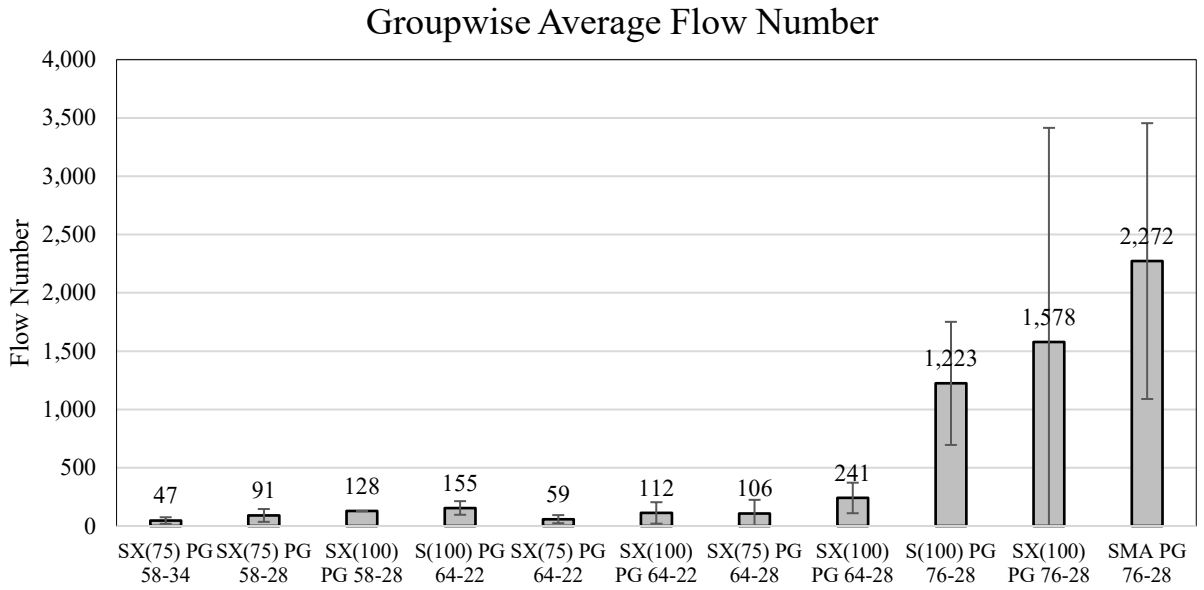


Figure 28. Groupwise Average Flow Numbers

Table 48. Groupwise Average Flow Numbers with 95% Boundaries

Mixes	95% CI Lower Limit	95% CI Upper Limit	Average
S(100) PG 64-22	47	262	155
S(100) PG 76-28	253	2,193	1,223
SMA PG 76-28	1,487	3,057	2,272
SX(75) PG 58-28	42	140	91
SX(75) PG 58-34	0	403	47
SX(75) PG 64-22	28	90	112
SX(75) PG 64-28	0	323	106
SX(100) PG 58-28	--	--	128
SX(100) PG 64-22	59	164	112
SX(100) PG 64-28	134	347	241
SX(100) PG 76-28	893	2,263	1,578

The minimum flow number, as recommended by AASHTO, depends on the traffic level listed in Table 49 below:

Table 49. Minimum Flow Number Requirements of HMA [11]

Traffic Level, Million ESAL	Min. Flow Number
Less than 3.0	NA
3.0 to less than 10	50
10 to less than 30	190
More than 30	740

The sensitivity analysis summary presented in Table 50 shows that the effects of V_{be} , V_a , VMA, VFA, and AC on the flow number are inconsistent. For example, six mixes show that the flow number increases with V_{be} , two mixes show the opposite, and one mix shows it is insensitive to V_{be} . This inconsistency is true for V_a , VMA, VFA, and AC as well. The reason behind this may be

the effects of paving contractor, manufacture date, and/or aggregate source. Using the most scores, the flow number increases with an increase in V_{be} , V_a , VMA, VFA, and AC.

Table 50. Summary of the Mix Parameters on Flow Number of HMA

	V_{be} (%)	V_a (%)	VMA (%)	VFA (%)	AC (%)
S(100) PG 64-22	Decreases	Increases	Increases	Increases	Decreases
S(100) PG 76-28	--	Decreases	Increases	Decreases	--
SMA PG 76-28	Decreases	Increases	Increases	Increases	Decreases
SX(75) PG 58-28	Increases	Decreases	Decreases	Increases	Increases
SX(75) PG 58-34	NA	NA	NA	NA	NA
SX(75) PG 64-22	Increases	Decreases	Increases	Decreases	Increases
SX(75) PG 64-28	Increases	Decreases	--	Increases	--
SX(100) PG 58-28	NA	NA	NA	NA	NA
SX(100) PG 64-22	Increases	Increases	Decreases	Decreases	Increases
SX(100) PG 64-28	Increases	Increases	Decreases	Decreases	Increases
SX(100) PG 76-28	Increases	Increases	Decreases	Increases	Increases
Summary	6 Increases 2 Decreases 1 Insensitive	5 Increases 4 Decreases 2 N/A	5 Increases 4 Decreases 1 Insensitive	5 Increases 4 Decreases 2 N/A	5 Increases 2 Decreases 2 Insensitive

SECTION 6: PERFORMANCE ANALYSIS USING THE PMED SOFTWARE

The effects of different mix parameters on the dynamic modulus are determined using the Colorado-calibrated PMED software analysis. The most recent version (Version 2.3 Revision 66) of the PMED software are used to predict the performance of the trial pavements. A trial section (Figure 29) with a 6-in. single layer of HMA, 6-in. of A-1-b base course, and A-6 sub-grade is used for all analysis. The resilient moduli (M_r) of the base, and the sub-grade are 38,000 psi, and 14,000 psi, respectively. In addition to the mix data, the CDOT-default mix data and the average-fit data (discussed in Section 4) is used in the PMED analysis.

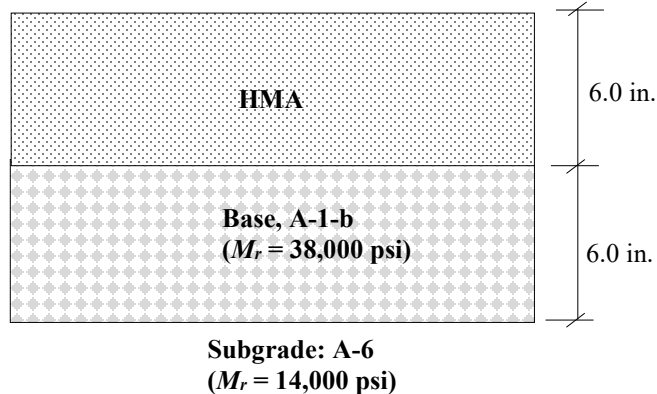


Figure 29. Geometry of the Trial Pavement for the PMED Analysis of All Groups

Two types of traffic data are used for each group. For the SX (100), S(100), and SMA mixes, the traffic Annual Average Daily Truck-Traffic (AADTT) are 7,000 and 800. For the SX (75) mixes, an AADTT of 3,000 and 800 are used as listed in Table 28. Other than dynamic modulus, the material properties are adopted from the CDOT 2017 M-E Pavement Design Manual, available at <https://www.codot.gov/business/designsupport/materials-and-geotechnical/manuals/pdm/2017-m-e-pavement-design-manual>. The analysis period is 20 years starting on May 2018. Climate has been selected based on the region where the mixes are collected and is shown on Table 51.

Table 51. Climate Station Used for Different Mixes for the PMED Analysis

Groups	Climate Station	AADTT
S(100) PG 64-22	Denver 12342	7,000, and 800
S(100) PG 76-28	Denver 12342	7,000, and 800
SMA PG 76-28	Denver 12342	7,000, and 800
SX(75) PG 58-28	Gunnison 93007	3,000, and 800
SX(75) PG 58-34	Gunnison 93007	3,000, and 800
SX(75) PG 64-22	Pueblo 93058	3,000, and 800
SX(75) PG 64-28	Gunnison 93007	3,000, and 800
SX(100) PG 58-28	Gunnison 93007	7,000, and 800
SX(100) PG 64-22	Colorado Spring 93037	7,000, and 800
SX(100) PG 64-28	Pueblo 93058	7,000, and 800
SX(100) PG 76-28	Trinidad 23070	7,000, and 800

The following five distresses at 90% reliability are analyzed to compare differences in mix performance:

- a) International Roughness Index (IRI)
- b) Total Rutting
- c) Rutting in Asphalt Layer (only)
- d) Bottom-up Fatigue Cracking and
- e) Top-down Longitudinal Cracking

S(100) PG 64-22

Table 52 lists the mix parameters, aggregate pits, binder suppliers and contractor information of the S(100) PG 64-22 mix. Mix parameters includes V_{be} , V_a , VMA, VFA, and AC. All this information is used while analyzing the performance of different mixes as discussed below.

Table 52. Generic Information of S(100) PG 64-22 Mix

Mix ID	Paving Contractor	Binder Supplier	Region	Date	V_{be} (%)	V_a (%)	VMA (%)	VFA (%)	AC (%)	Pit
18206 P52 14	Aggregate Industries	Aggregate Industries	1	1/2015	12.09	6.78	15.8	72.5	5.00	Morrison, Platte River
18465 P9 14	Asphalt Paving	Frontier Cheyenne	4	7/2014	10.59	6.34	15.8	44.0	4.80	Firestone, Ralston, Lien
18695 P9 15	APC Southern	Suncor	1	4/2016	10.04	6.20	16.3	63.8	5.09	Ralston / Platteville
18695 P13 14	APC Southern	Holly Frontier	1	7/2014	10.78	6.12	17.0	63.7	5.00	Firestone, Ralston, Pete Lien
18695 P25 14	-	Holly Frontier	1	8/2014	10.26	5.84	15.8	63.2	5.00	Firestone, Ralston, Lien
18695 P6 14	-	Holly Frontier	1	4/2014	11.1	6.2	17.0	63.2	5.00	Firestone, Ralston, Pete Lien

Note: Orange highlighted mixes produce statistically the same distress with the CDOT-default mix. This is clarified in the following discussions.

International Roughness Index (IRI): The CDOT-default mix data and the average-fit data produce the IRI in a good agreement with the other dynamic modulus data for both high (AADTT = 7,000) and low traffic (AADTT = 800), Figures 30, and 31 respectively. The other mixes (18206 P52 14, 18465 P9 14, 18695 P9 15, 18695 P13 14, and 18695 P 25 14) produce a consistent IRI. A threshold value of 200 in./mi. is drawn in Figure 30 and shows that the mixes reach the threshold in about seven to eight years for high traffic. Similar observation is obtained for low traffic as shown in Figure 31, where a threshold value of 175 in./mi. is assumed.

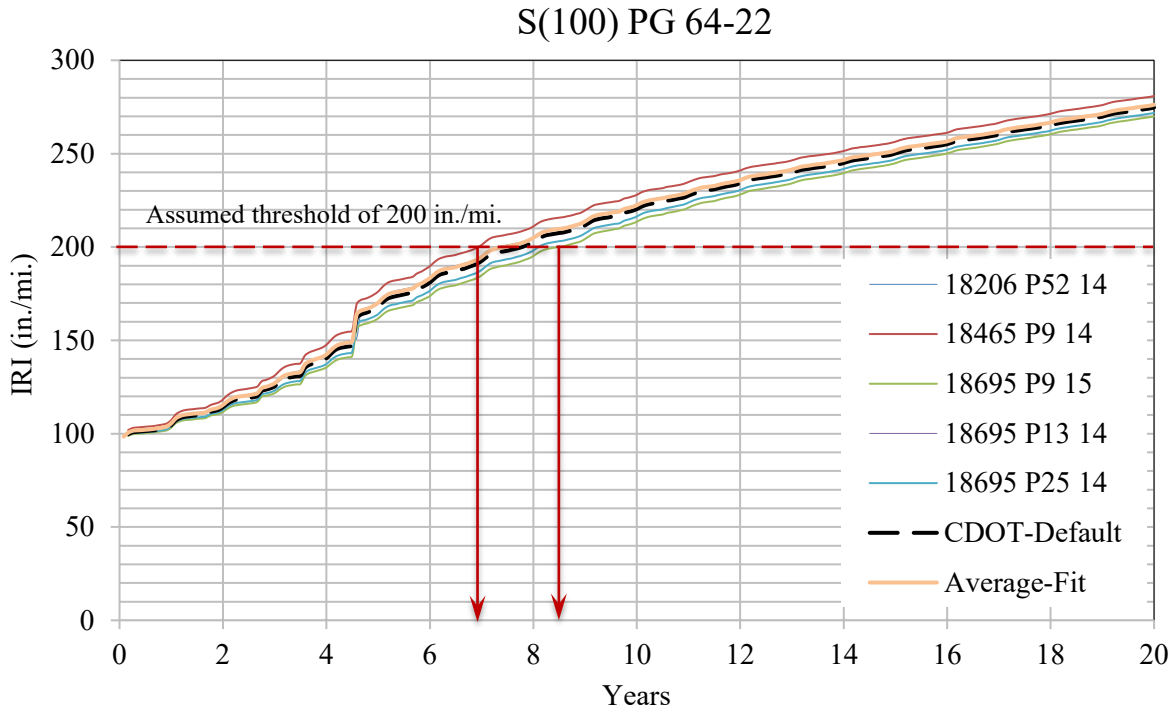


Figure 30. IRI Due to AADTT = 7,000 by S(100) PG 64-22 Mix

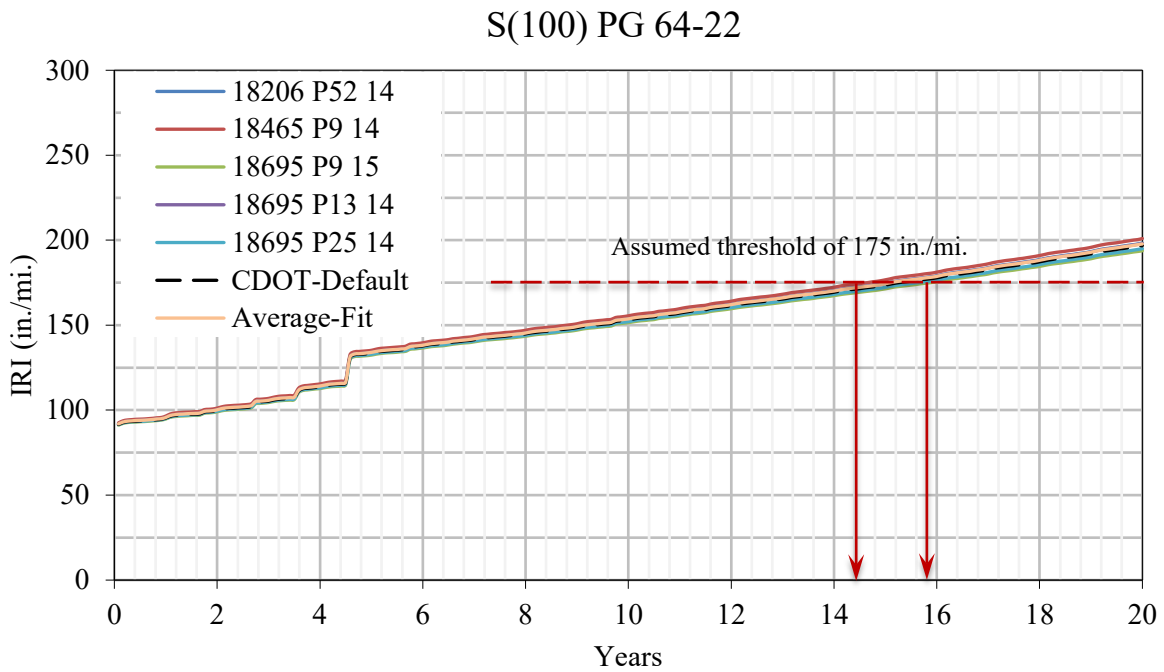


Figure 31. IRI Due to AADTT = 800 by S(100) PG 64-22 Mix

Total Rutting: The predicted total rutting over 20 years of design life of the trial pavement is shown in Figures 32 and 33 for AADTT = 7,000 and AADTT = 800, respectively. Figures 32 and 33 show that the CDOT-default data and the average-fit data produce roughly the average total rutting, and are in good agreement with the other dynamic modulus data. Comparing contractor to contractor, the prediction varies a lot from one rutting result to another. For example, if the threshold total rutting value is assumed 0.6-in, then the prediction reaches the threshold by 18465 P9 14 mix at about five years, whereas the prediction reaches the threshold by 18695 P9 15 mix at about nine years as shown in Figure 32. That means the prediction may differ by about four years from one mix to another, although the mix design is same. Similar low traffic results are seen where the design life differs by four years as shown in Figure 33 for an assumed threshold value of 0.3 in. The statistical 95% CI boundaries show only a single mix, 18465 P9 14, is not within the 95% CI boundaries of the CDOT mix, and thus, is not statistically the same as the CDOT-default mix. The average-fit data produces the total rutting within the 95% CI boundaries of the CDOT mix.

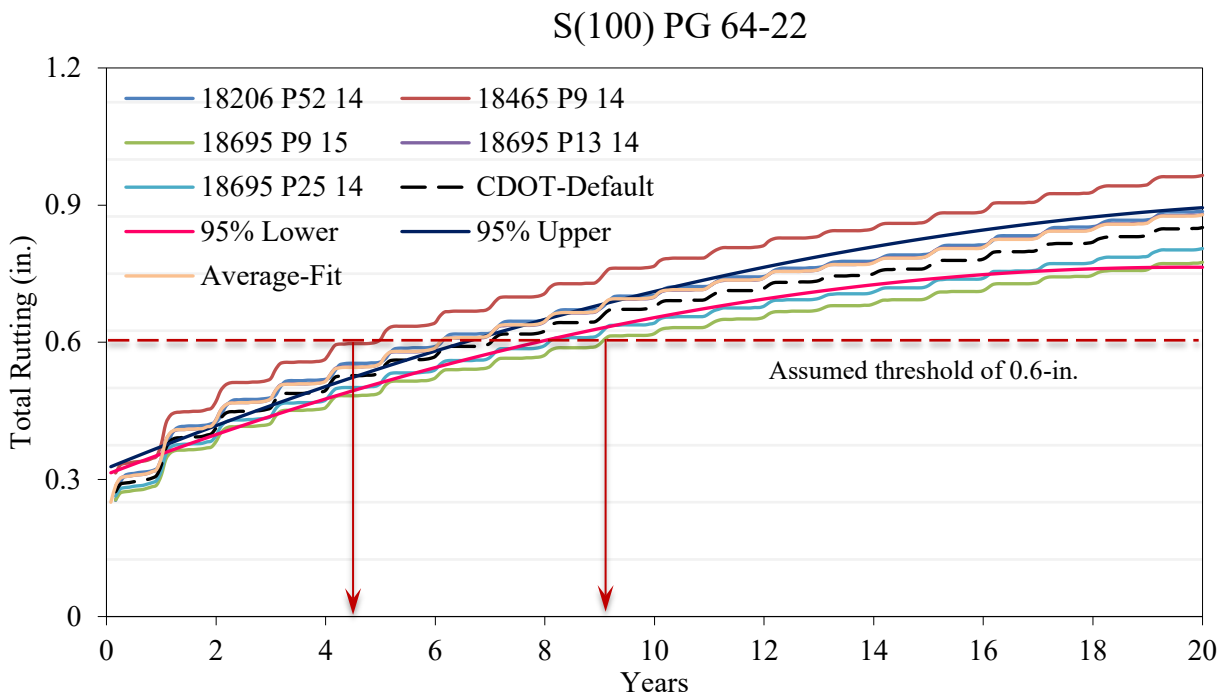


Figure 32. Total Rutting Due to AADTT = 7,000 by S(100) PG 64-22 Mix

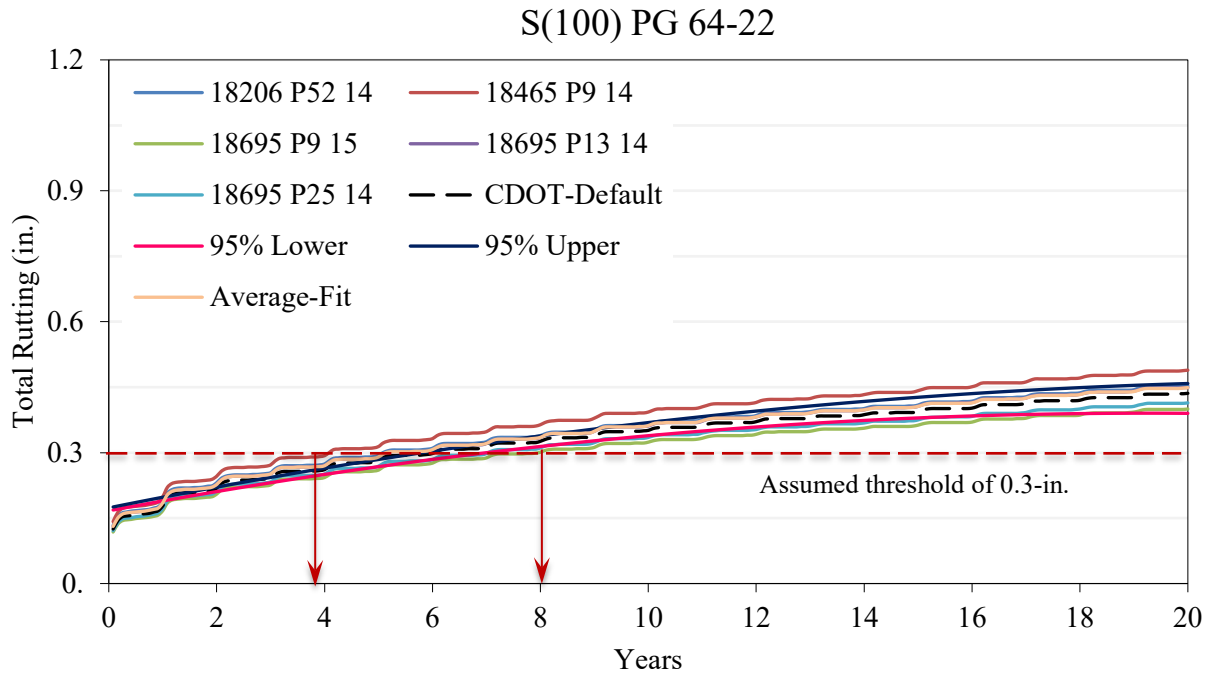


Figure 33. Total Rutting Due to AADTT = 800 by S(100) PG 64-22 Mix

Rutting in Asphalt Layer Only: The rutting variation in asphalt layer (Figures 34, and 35) for both AADTT = 7,000 and AADTT = 800 are similar to total rutting. The CDOT-default data produces roughly the average rutting in asphalt layer and is in a good agreement with the other dynamic modulus data. Comparing contractor to contractor, the prediction may differ by about five years from one mix to another as shown in Figure 34 for an assumed threshold rutting in asphalt layer of 0.50-in. The variation of this prediction is similar for low traffic for an assumed threshold of 0.25-in., as shown in Figure 35. Only a single mix, 18465 P9 14, is not within the statistical 95% CI boundaries of the CDOT mix, and thus, not statistically the same as the CDOT-default mix. The average-fit data produces the rutting in asphalt layer within the 95% CI boundaries of the CDOT mix.

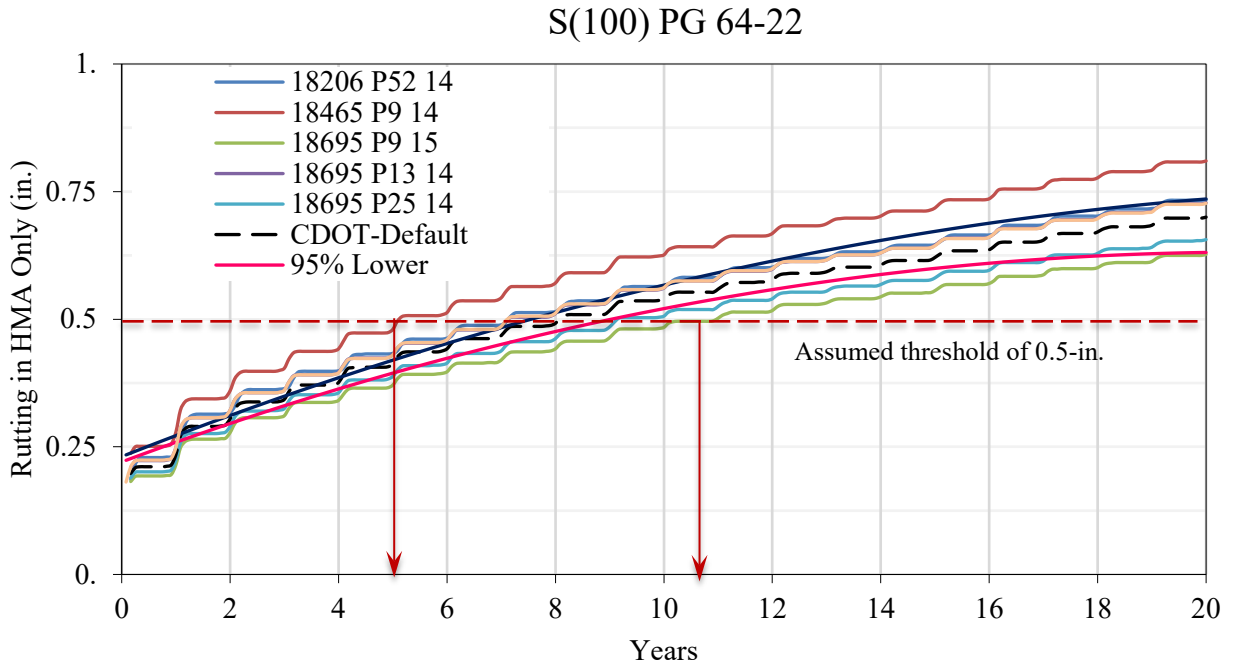


Figure 34. Rutting in Asphalt Layer Due to AADTT = 7,000 by S(100) PG 64-22 Mix

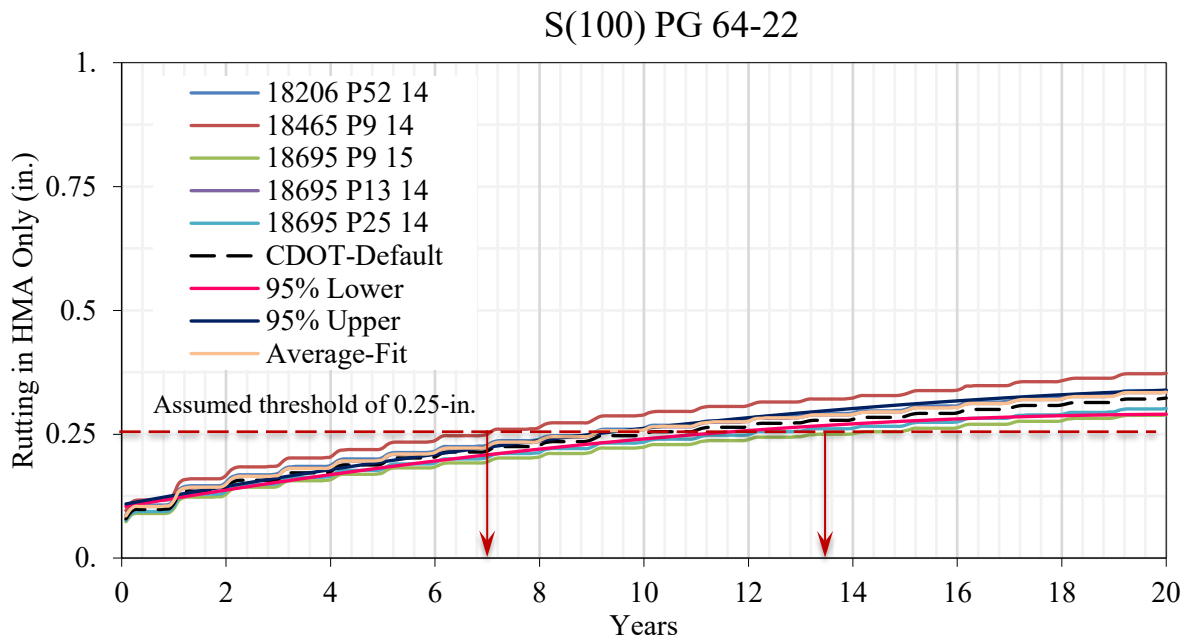


Figure 35. Rutting in Asphalt Layer Due to AADTT = 800 by S(100) PG 64-22 Mix

Bottom-up Fatigue Cracking: The bottom-up fatigue cracking variation during its service life of the trial pavement is shown in Figures 36 and 37 for high (AADTT = 7,000) and low traffic (AADTT = 800), respectively. It shows that the CDOT-default data produces about the average amount of fatigue cracking compared to the other dynamic modulus data. The assumed threshold of 35% of the lane area shown in Figure 36 shows that the mixes reach the threshold between three and four years, which is very close to each other. Similar observation is obtained for low traffic as shown in Figure 37 where the threshold is assumed to be 15% of the lane area. Two mixes, 18465 P9 14 and 18695 P9 15, are not within the statistical 95% CI boundaries of the CDOT mix, and thus, are not statistically the same as the CDOT-default mix.

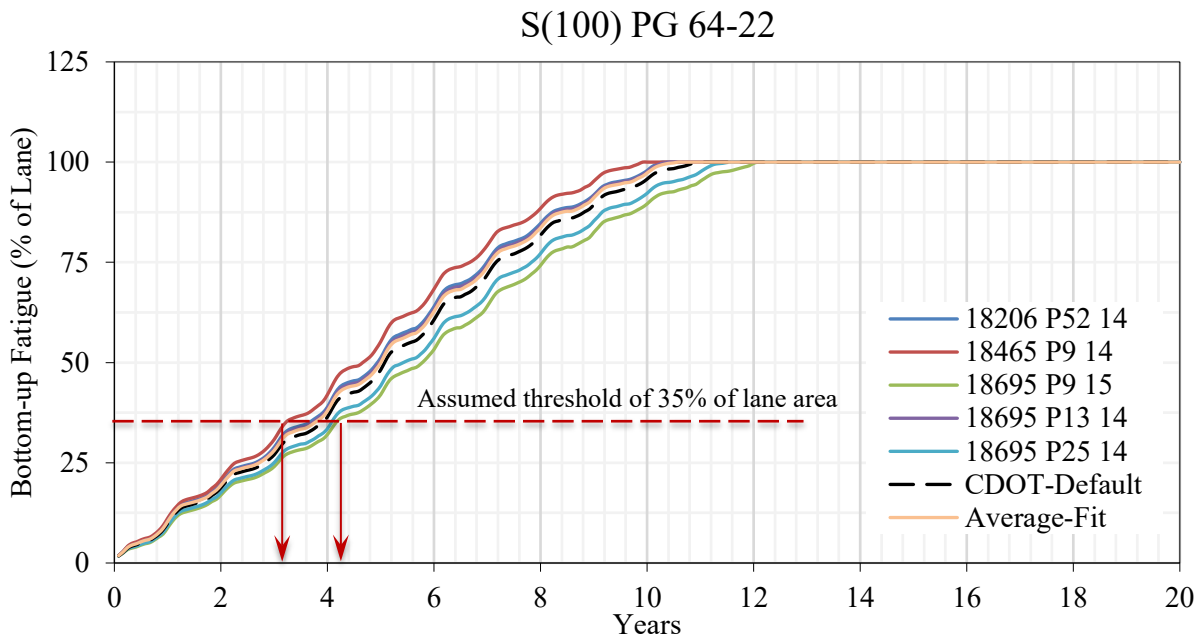


Figure 36. Bottom-up Fatigue Cracking Due to AADTT = 7,000 by S(100) PG 64-22 Mix

S(100) PG 64-22

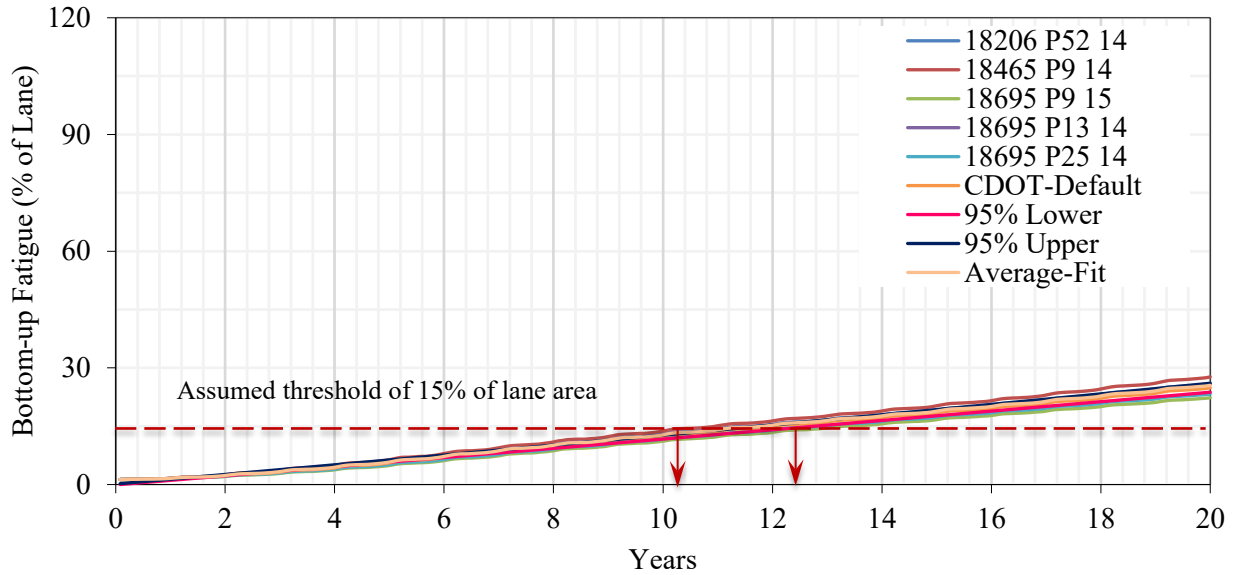


Figure 37. Bottom-up Fatigue Cracking Due to AADTT = 800 by S(100) PG 64-22 Mix

Top-down Longitudinal Cracking: The top-down longitudinal cracking variation during its service life of the trial pavement is shown in Figures 38 and 39 for high (AADTT = 7,000) and low traffic (AADTT = 800), respectively. It shows that the CDOT-default data produces about the average amount of top-down longitudinal cracking compared to the other dynamic modulus data. The assumed threshold of 2,500 ft./mi. shown in Figure 38 shows that the mixes reach the threshold between six and nine years, which is very close to each other. Similar observation is obtained for low traffic as shown in Figure 39 where the threshold is assumed to be 1,250 ft./mi. Two mixes, 18465 P9 14 and 18695 P9 15 as shown in Figure 39, are not within the statistical 95% CI boundaries of the CDOT mix, and thus, are not statistically the same as the CDOT-default mix. The average-fit data produces the top-down longitudinal cracking within the 95% CI boundaries of the CDOT mix.

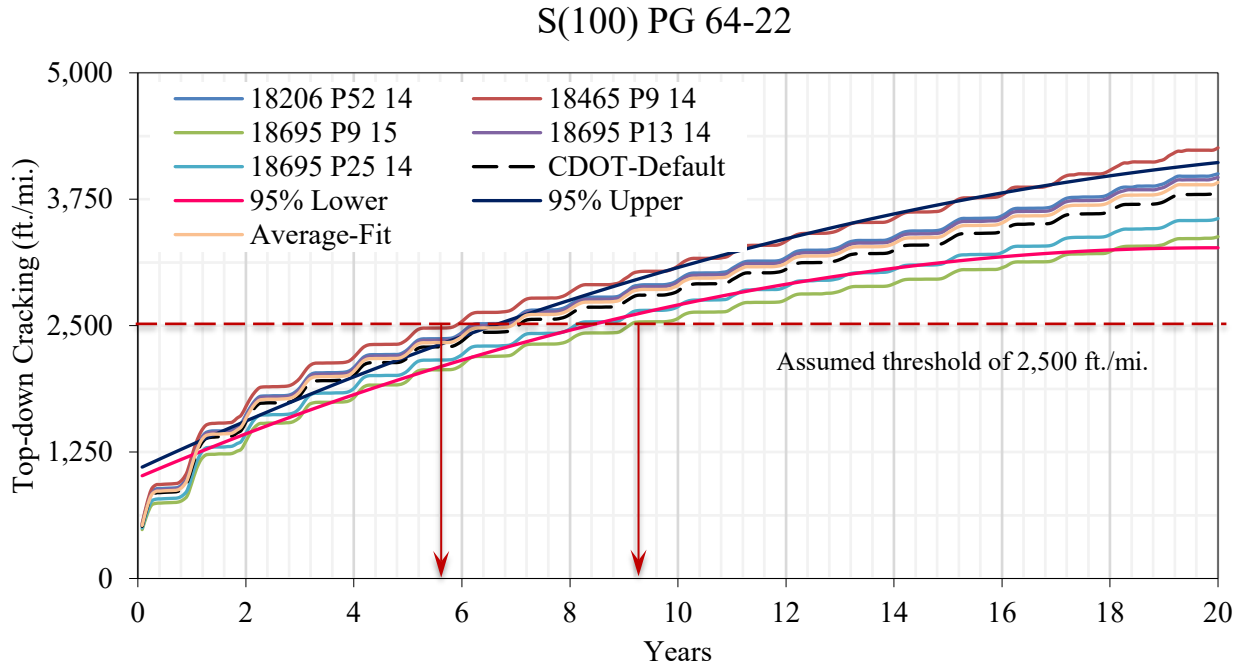


Figure 38. Longitudinal Cracking Due to AADTT = 7,000 by S(100) PG 64-22 Mix

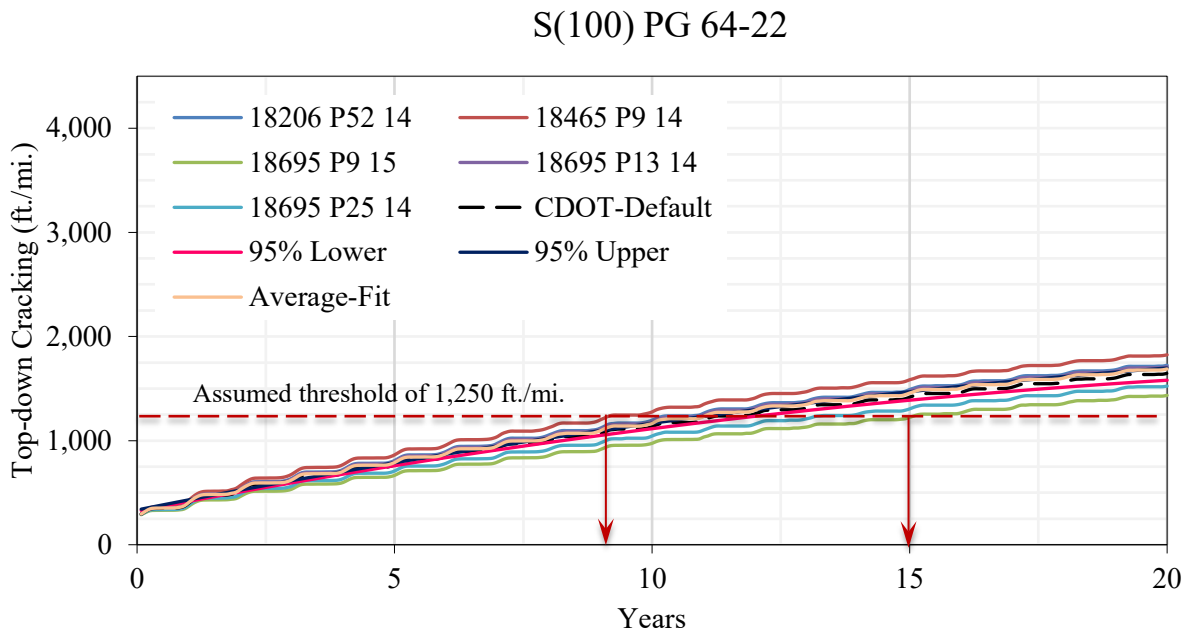


Figure 39. Longitudinal Cracking Due to AADTT = 800 by S(100) PG 64-22 Mix

Referring to Table 52, mixes 18465 P9 14 (Region 4) and 18695 P9 15 (Region 1) are not statistically the same as the CDOT-default mix. Mix 18695 P9 14 produces the lowest distresses

per Figures 32 - 39 compared to all S(100) PG 64-22 mixes. Although this mix has the lowest VFA (44%), the other properties listed in Table 40 are comparable to the other S(100) PG 64-22 mixes. Mixes which are statistically the same with the CDOT-default mix do not have similar properties. For example, 18206 P52 14 has the highest air voids (6.78%), whereas 19695 P25 14 has the lowest air voids (5.84%). Additionally, these two mixes' production dates, effective binder contents, VMAs, VFAs, and aggregate sources are not similar. Therefore, an individual mix parameter's effect may not be appropriately sought out for this mix.

The evaluation of the influence of V_{be} , V_a , VMA, VFA, and AC are performed using a regression analysis. The R^2 of all correlations listed below is 1.0, meaning the correlations are classified as good. Using the following regression equations, the IRI, total rutting, rutting in asphalt layer, bottom-up fatigue cracking (FC), and top-down cracking (TDC) increase with an increase in V_{be} and VMA, but decrease with an increase in V_a and VFA, and are insensitive to AC.

$$\text{IRI (in./mi.)} = 134.5321 + 8.6859 V_{be} - 3.6976 V_a + 3.1705 \text{ VMA} - 0.572 \text{ VFA}$$

$$\text{Total Rutting (in.)} = -0.03244 + 0.0827 V_{be} - 0.0268 V_a + 0.0229 \text{ VMA} - 0.0061 \text{ VFA}$$

$$\text{Rutting in HMA (in.)} = -0.0089 + 0.0861 V_{be} - 0.0449 V_a + 0.0173 \text{ VMA} - 0.0059 \text{ VFA}$$

$$\text{FC (\%)} = -1.7976 + 1.7793 V_{be} - 1.1604 V_a + 0.543 \text{ VMA} - 0.1038 \text{ VFA}$$

$$\text{TDC (ft./mi.)} = -98.6203 + 358.9417 V_{be} - 218.242 V_a + 105.5483 \text{ VMA} - 20.3995 \text{ VFA}$$

S(100) PG 76-28

Table 53 lists the mix parameters, aggregate pits, binder suppliers and contractor information of the S(100) PG 76-28 mix. Mix parameters includes V_{be} , V_a , VMA, VFA, and AC. All this information is used while analyzing the performance of different mixes as discussed below.

Table 53. Generic Information of S(100) PG 76-28 Mix

	Paving Contractor	Binder Supplier	Region	Date	V_{be} (%)	V_a (%)	VMA (%)	VFA (%)	AC (%)	Pit
17800 P17 14	Aggregate Industries	Jebro	4	7/2014	10.61	6.98	16.9	55.5	5.20	Distil, Lien
17800 P26 14	Aggregate Industries	Jebro	4	8/2014	10.61	6.58	16.8	58.6	5.20	Distil, Lien
17800 P38 14	Aggregate Industries	Jebro	4	9/2014	10.79	6.08	16.2	62.2	5.20	Distil, Lien
17800 P53 14	Aggregate Industries	Jebro	4	1/2015	10.61	6.72	16.6	59.3	5.20	Distil, Lien

International Roughness Index: The IRI variation during its service life of the trial pavement is shown in Figures 40 and 41 for AADTT = 7,000 and AADTT = 800, respectively. The IRI data show the CDOT-default mix produces the highest value of IRI comparing to the other mixes listed in Figures 40 and 41. The other mixes produce consistent amounts of IRI. Assumed threshold values of 220 in./mi. and 150 in./mi. are drawn in Figures 40 and 41, respectively. Figure 40 shows that the mixes reach the threshold in about 10 to 13 years for high traffic. Similar observation is obtained for low traffic as shown in Figure 41.

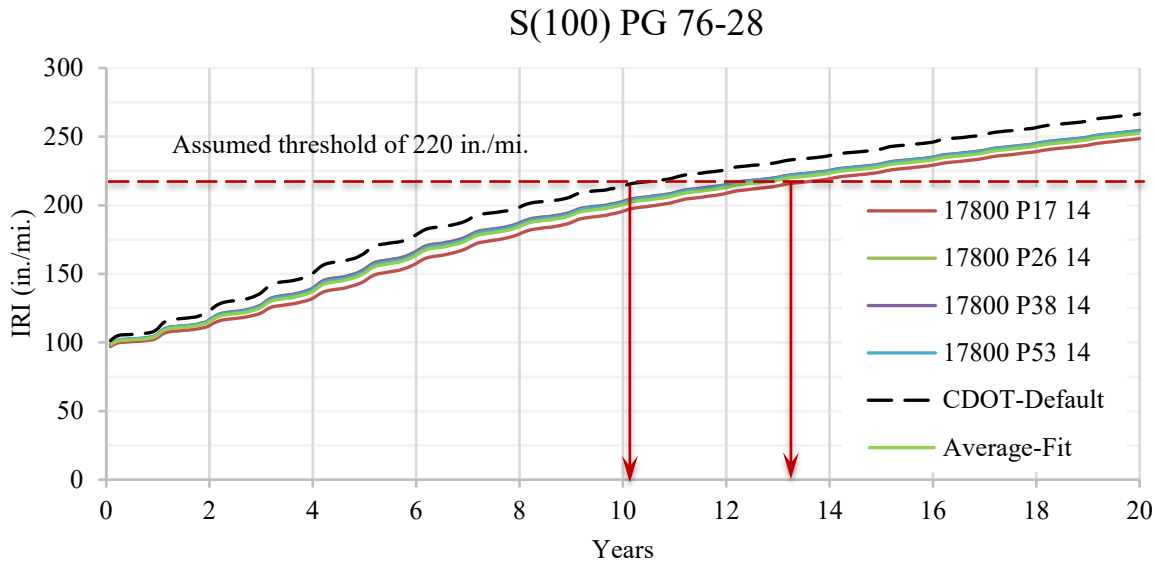


Figure 40. IRI Due to AADTT = 7,000 by S(100) PG 76-28 Mix

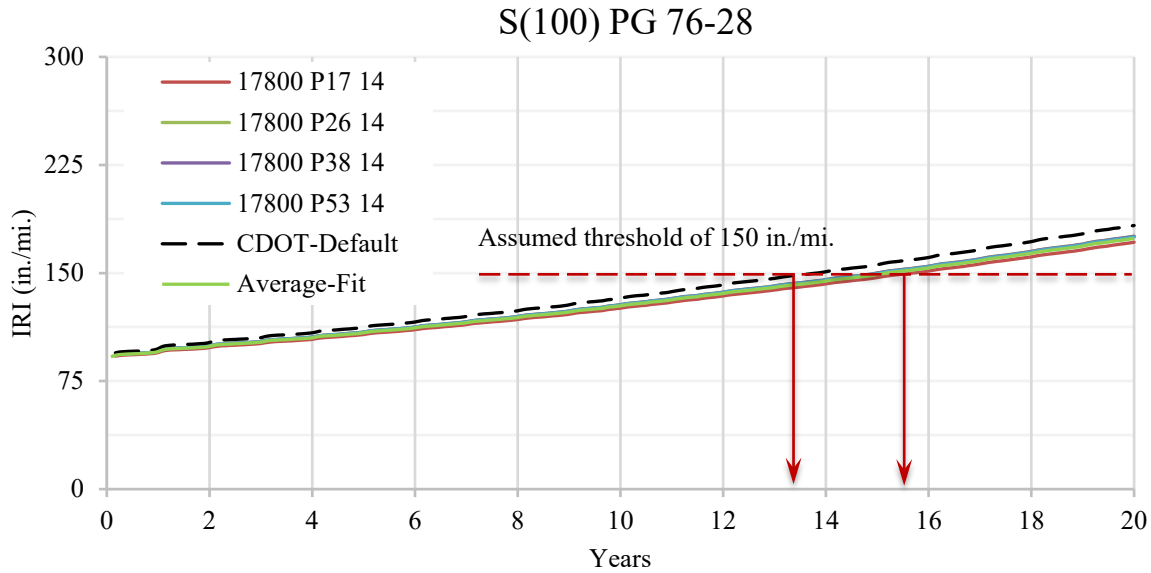


Figure 41. IRI Due to AADTT = 800 by S(100) PG 76-28 Mix

Total Rutting: The total rutting (Figures 42, and 43) shows the CDOT-default mix data produces the highest amount of total rutting comparing to all the mixes' data. The other mixes, except 17800 P17 14, produce a consistent amount of total rutting. However, the statistical 95% CI boundaries show that no mix is within the 95% boundaries for AADTT = 7,000, and statistically are not the same as the CDOT-default mix. If the threshold total value is 0.6 in as shown in Figure 42, then the prediction reaches the threshold by 17800 P14 14 mix at about five years, whereas the prediction reaches the threshold by 17800 P17 14 mix at about eight years. However, the CDOT-default mix reaches the threshold in about three years. The variation of this prediction is similar as shown in Figure 43 for low traffic for an assumed threshold of 0.35 in. That means the total rutting prediction may vary up to three years from mix to mix, despite having the same mix design. The average-fit data produces the total rutting outside the 95% CI boundaries of the CDOT mix.

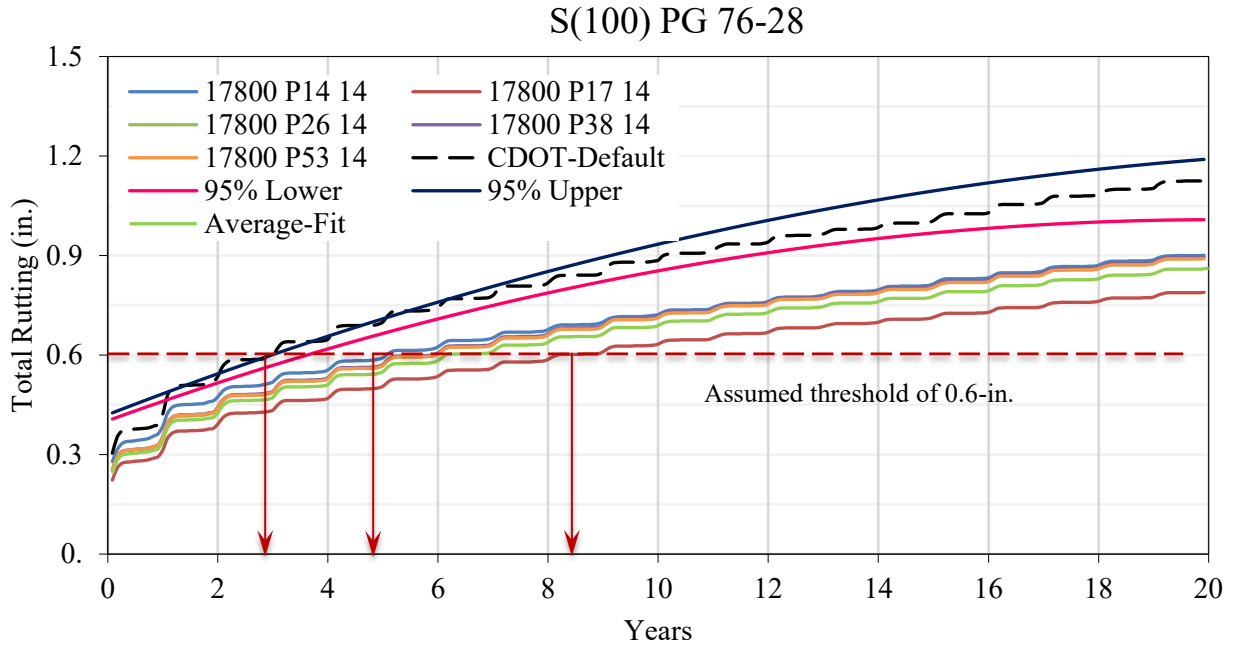


Figure 42. Total Rutting Due to AADTT = 7,000 by S(100) PG 76-28 Mix

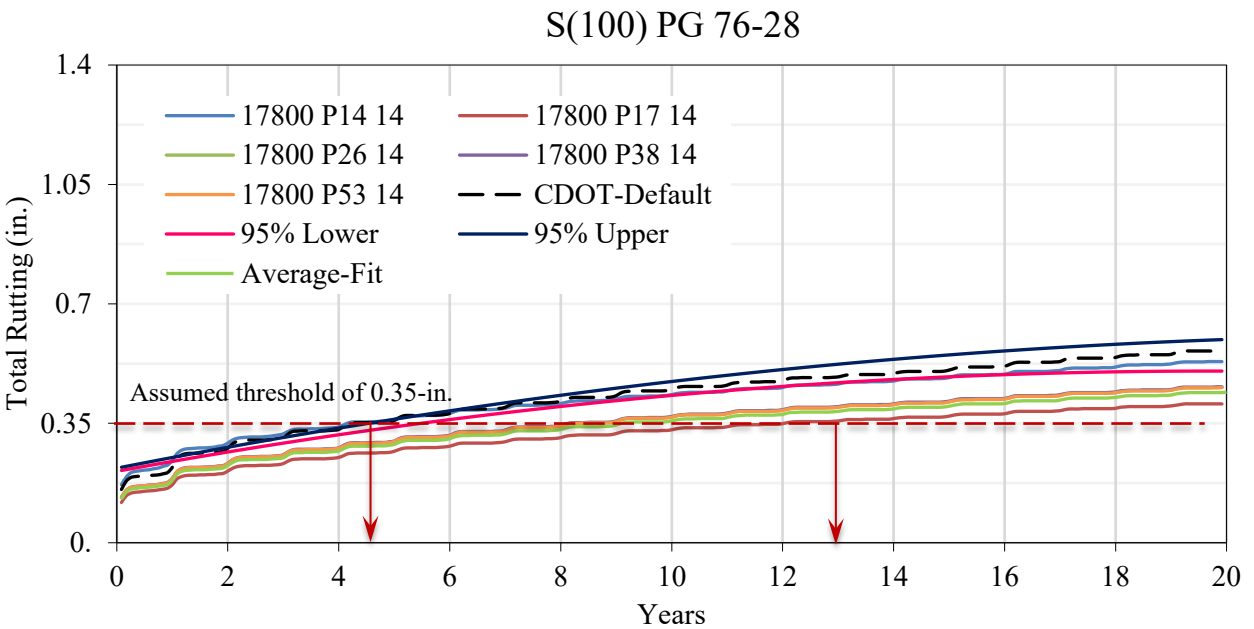


Figure 43. Total Rutting Due to AADTT = 800 by S(100) PG 76-28 Mix

Rutting in Asphalt Layer Only: The rutting in the asphalt layer (Figures 44 and 45) has the same finding of the total rutting that the CDOT-default mix data produces the highest amount of rutting

in the asphalt layer comparing to all the mixes' data. The statistical 95% CI boundaries show that no mix is within the 95% boundaries and is statistically not the same as the CDOT-default mix. The rutting in the asphalt layer prediction may vary up to nine years from mix to mix, despite having the same mix design for an assumed threshold value of 0.50 in. The low traffic shows the similar observation as shown in Figure 45 for an assumed threshold of 0.30 in. The average-fit data produces the rutting in asphalt layer outside the 95% CI boundaries of the CDOT mix.

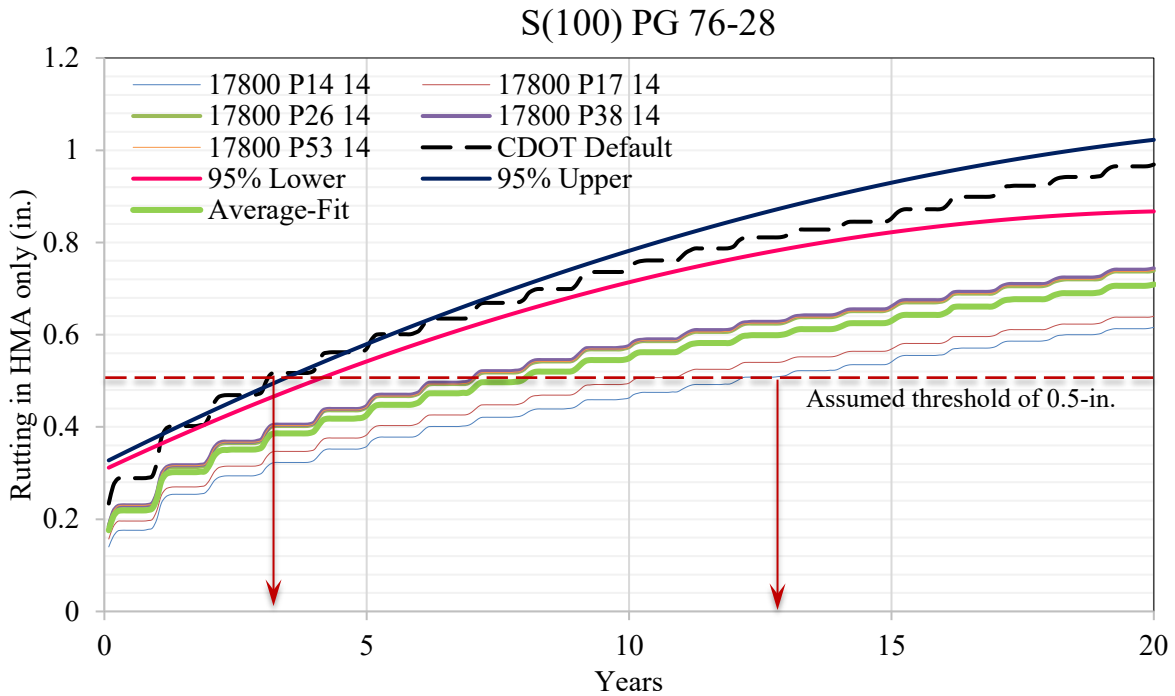


Figure 44. Rutting in Asphalt Layer Due to AADTT = 7,000 by S(100) PG 76-28 Mix

S(100) PG 76-28

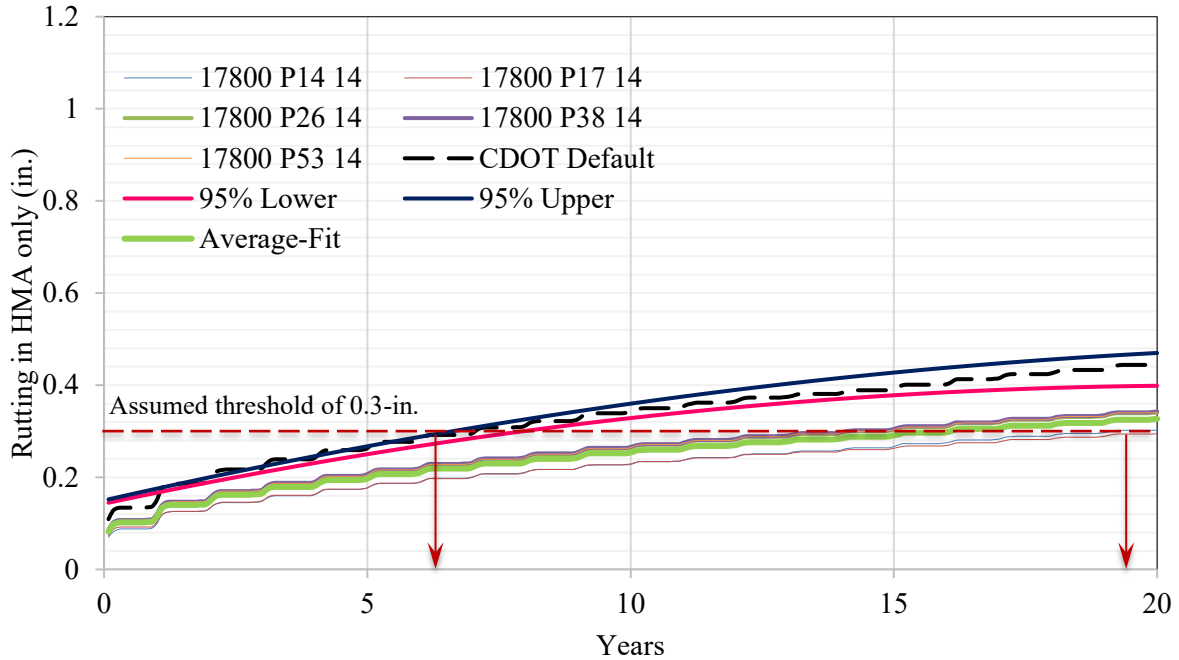


Figure 45. Rutting in Asphalt Layer Due to AADTT = 800 by S(100) PG 76-28 Mix

Bottom-up Fatigue Cracking: The CDOT-default mix data produces the highest amount of bottom-up fatigue cracking in comparison to all the mixes' data (Figures 46 and 47). The assumed threshold of 25% of the lane area shown in Figure 46 shows that the mixes reach the threshold between two and three years, which is very close to each other. Similar observation is obtained for low traffic as shown in Figure 47 where the threshold is assumed to be 15% of the lane area. The statistical test shows that no mix is within the 95% CI boundaries, meaning no mix is statistically not the same as the CDOT-default mix. However, the other mixes produce consistent amounts of bottom-up fatigue cracking.

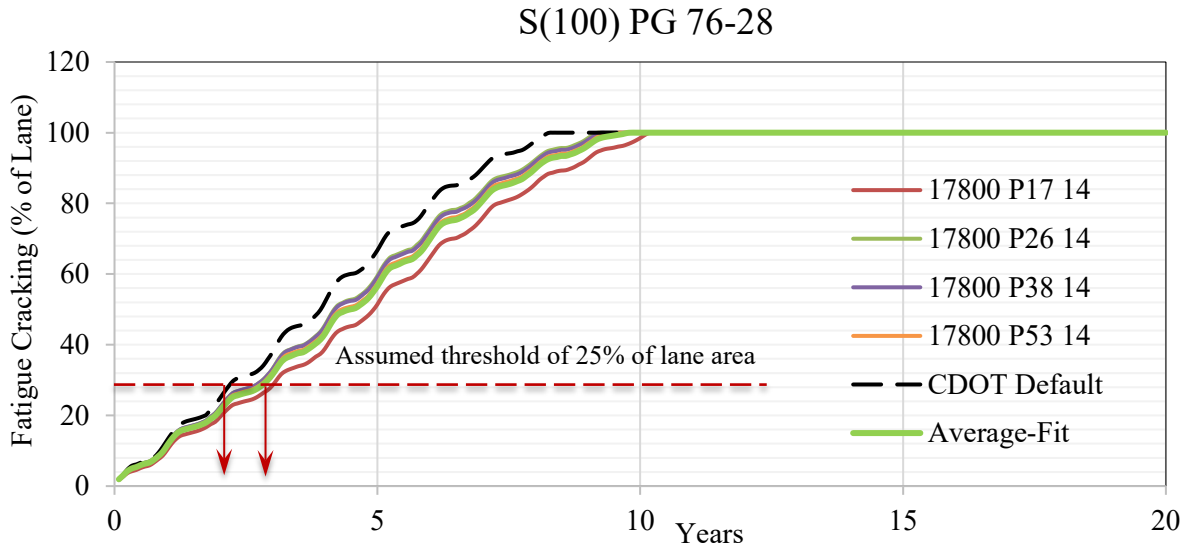


Figure 46. Bottom-up Fatigue Cracking Due to AADTT = 7,000 by S(100) PG 76-28 Mix

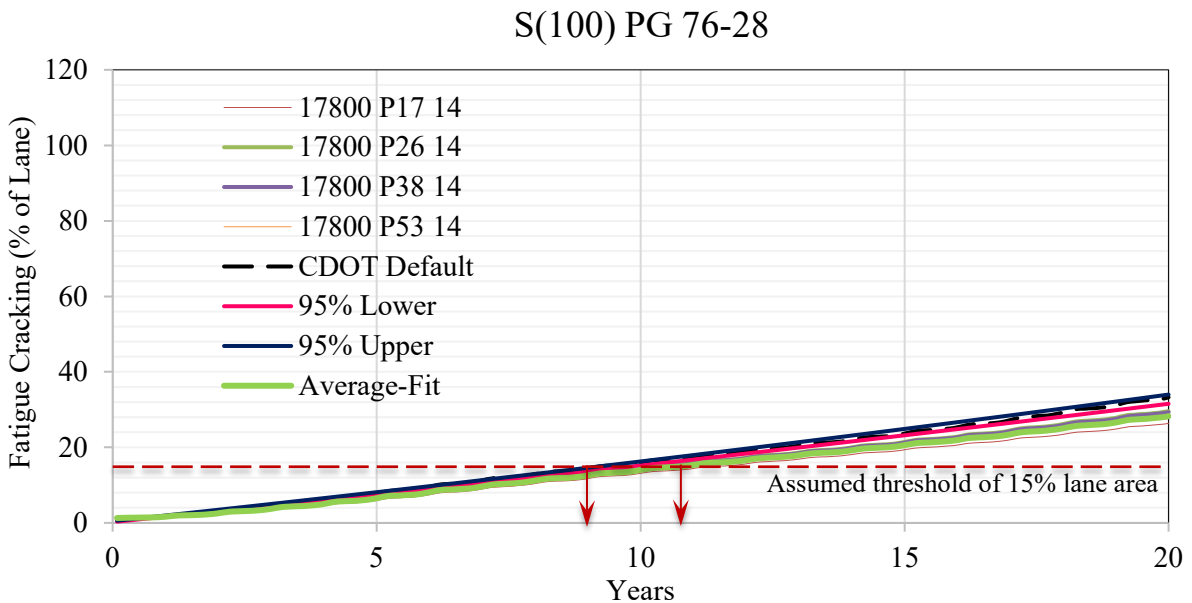


Figure 47. Bottom-up Fatigue Cracking Due to AADTT = 800 by S(100) PG 76-28 Mix

Top-down Longitudinal Cracking: The CDOT-default mix data produces the highest amount of top-down longitudinal cracking in comparison to all the mixes' data (Figures 48 and 49). The statistical 95% CI boundaries show that no mix is within the 95% CI boundaries and is statistically not the same as the CDOT-default mix. However, the other mixes, except for 17800 P17 14, produce consistent amounts of top-down longitudinal cracking. The average-fit data produces the top-down longitudinal cracking outside the 95% CI boundaries of the CDOT mix. Mixes reach the

threshold value of 2,500 ft./mi. from five to eight years for high traffic as shown in Figure 48. This observation is similar for the low traffic where mixes reach the threshold value of 1,500 ft./mi. from 8 to 15 years as shown in Figure 49.

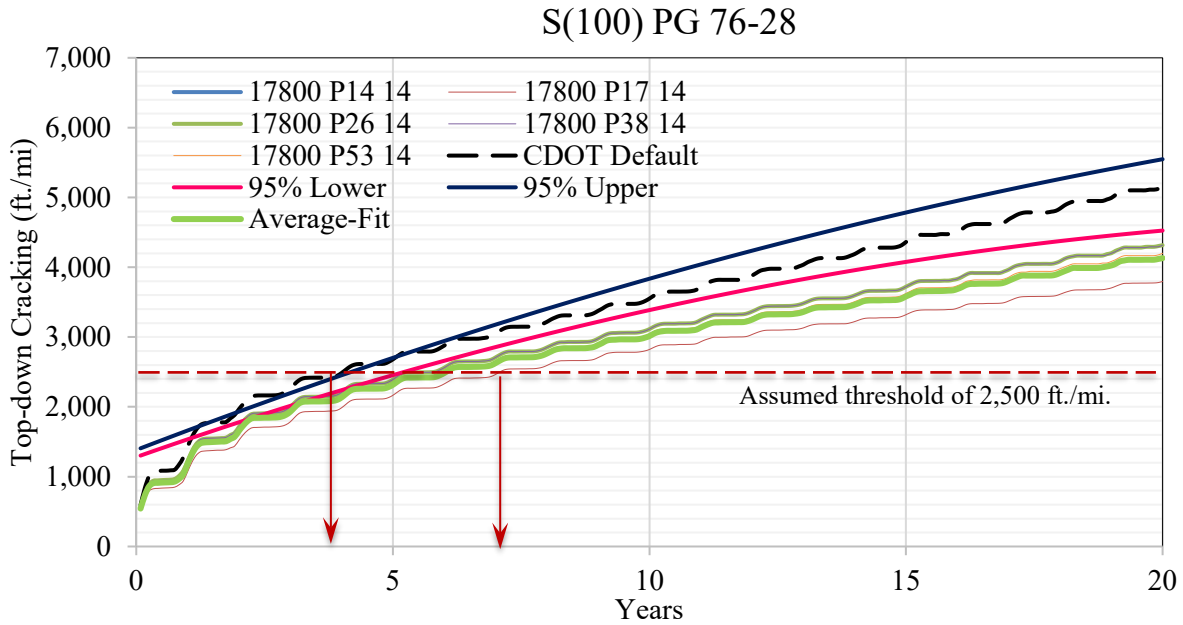


Figure 48. Longitudinal Cracking Due to AADTT = 7,000 by S(100) PG 76-28 Mix

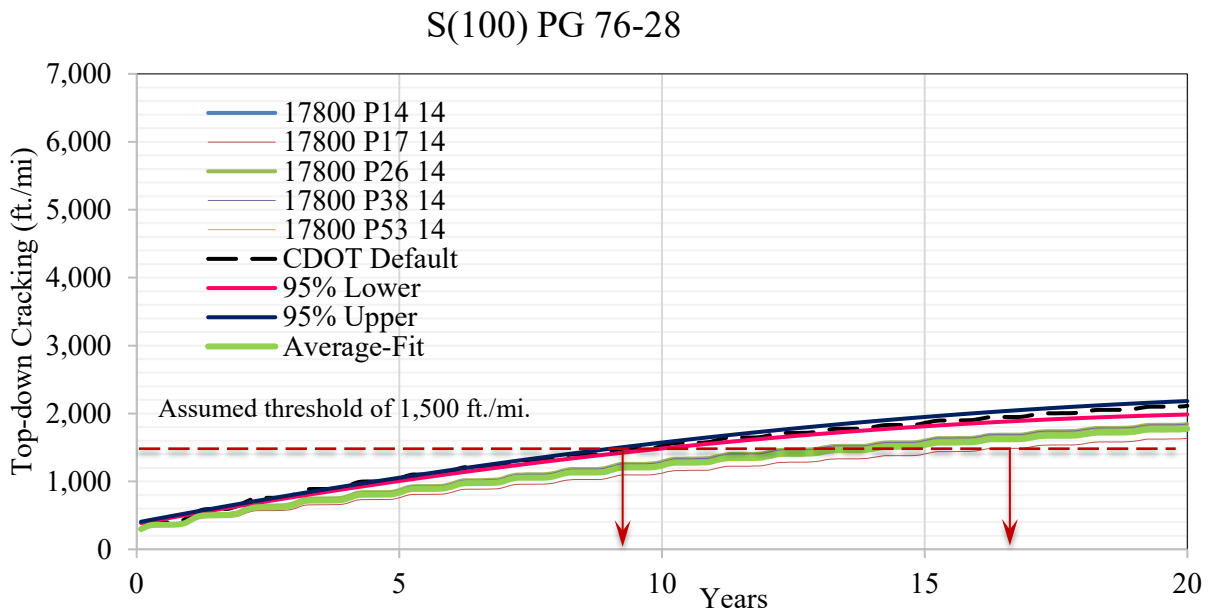


Figure 49. Longitudinal Cracking Due to AADTT = 800 by S(100) PG 76-28 Mix

The above discussion suggests that none of the mixes are statistically the same as the CDOT-default mix data. From Table 53, all mixes are produced by Aggregate Industries with a binder supplied by Jebro, and aggregate collected from the same pit (Distil, Lien) in 2014. Their production dates, effective binder contents, VMAs, VFAs, and aggregate source are almost the same. The 17800 P17 14 produces the lowest distresses; it has the highest air voids, the highest VMA, and the least VFA.

To determine the influence of V_{be} , V_a , VMA, VFA, and AC, a regression analysis is conducted, and the following correlations are obtained. The R^2 of all correlations is 1.0. It is apparent from the following regression equations that that IRI, total rutting, rutting in asphalt layer, FC, and TDC increase with the increase in V_a , VMA, and VFA, and are insensitive to V_{be} and AC.

$$\text{IRI (in./mi.)} = -290.399 + 2.3699 V_a + 17.3129 \text{ VMA} + 3.1868 \text{ VFA}$$

$$\text{Total Rutting (in.)} = -5.0539 + 0.0612 V_a + 0.1813 \text{ VMA} + 0.0396 \text{ VFA}$$

$$\text{Rutting in HMA (in.)} = -4.0493 + 0.0425 V_a + 0.1442 \text{ VMA} + 0.0327 \text{ VFA}$$

$$\text{FC (\%)} = -76.3433 - 0.3280 V_a + 3.6805 \text{ VMA} + 0.5329 \text{ VFA}$$

$$\text{TDC (ft./mi.)} = -14949.8 - 42.7356 V_a + 703.6219 \text{ VMA} + 111.3348 \text{ VFA}$$

SMA PG 76-28

Table 54 lists the mix parameters, aggregate pits, binder suppliers and contractor information of the SMA PG 76-28 mix. Mix parameters includes V_{be} , V_a , VMA, VFA, and AC. All this information is used while analyzing the performance of different mixes as discussed below.

Table 54. Generic Information of SMA(100) PG 76-28 Mix

	Paving Contractor	Binder Supplier	Region	Date	V_{be} (%)	V_a (%)	VMA (%)	VFA (%)	AC (%)	Pit
17800 P70 14	Aggregate Industries	Jebro	4	5/2015	10.0	3.2	17.8	73.7	6.4	Morrison, Lien
17800 P85 14	Aggregate Industries	Jebro	4	10/2015	13.68	4.66	18.5	70.7	6.2	Morrison, Lien
17890 P40 14	Martin Marietta	Suncor	1	10/2014	15.17	4.24	18.0	77.5	6.40	Spec Agg
17890 P56 14	Martin Marietta	Suncor	1	1/2015	15.17	4.66	18.3	75.2	6.20	Spec Agg
17890 P66 14	Martin Marietta	Suncor	1	3/2015	15.17	4.20	17.9	76.8	6.20	Spec Agg
18842 P30 14	Kiewit Construction	Suncor	2	8/2014	13.64	4.64	18.4	75.7	6.3	Parkdale Tezak
18842 P43 14	Kiewit Construction	Suncor	2	11/2014	13.58	5.08	19.1	73.3	6.3	Parkdale Tezak
18842 P44 14	Kiewit Construction	Suncor	2	11/2014	13.29	3.4	18.8	75.0	6.3	Tezak, I-25 Millings
18842 P60 14	Kiewit Construction	Suncor	2	2/2015	13.31	3.4	19.8	65.1	5.2	Parkdale Tezak
18842 P83 14	Kiewit Construction	Suncor	2	9/2015	13.77	3.4	18.9	71.2	6.3	Parkdale Tezak
19314 P7 14	Martin Marietta	Suncor	4	6/2014	13.94	5.24	18.4	71.0	5.65	Granite Canyone, Lien
19807 P32 14	Brannan	Suncor	1	9/2014	13.80	3.0	16.0	74.9	6.3	Frei, Lein

Note: Orange Highlighted mixes produce statistically the same distress with the CDOT-default mix. This is clarified in the following discussion.

International Roughness Index: The CDOT-default mixture produces the lowest IRI during its service life other than 18842 P43 14 (Figures 50, and 51). All mixtures produce consistent amount

of IRI, except for the 19807 P32 14 mix, which produces the highest IRI value. Statistical comparison has not been made to this distress. Assumed threshold values of 200 in./mi. and 160 in./mi. are drawn in Figures 50 and 51, respectively. Figure 50 shows that the mixes reach the threshold in about 8 to 10 years for high traffic. Similar observation is obtained for low traffic as shown in Figure 51.

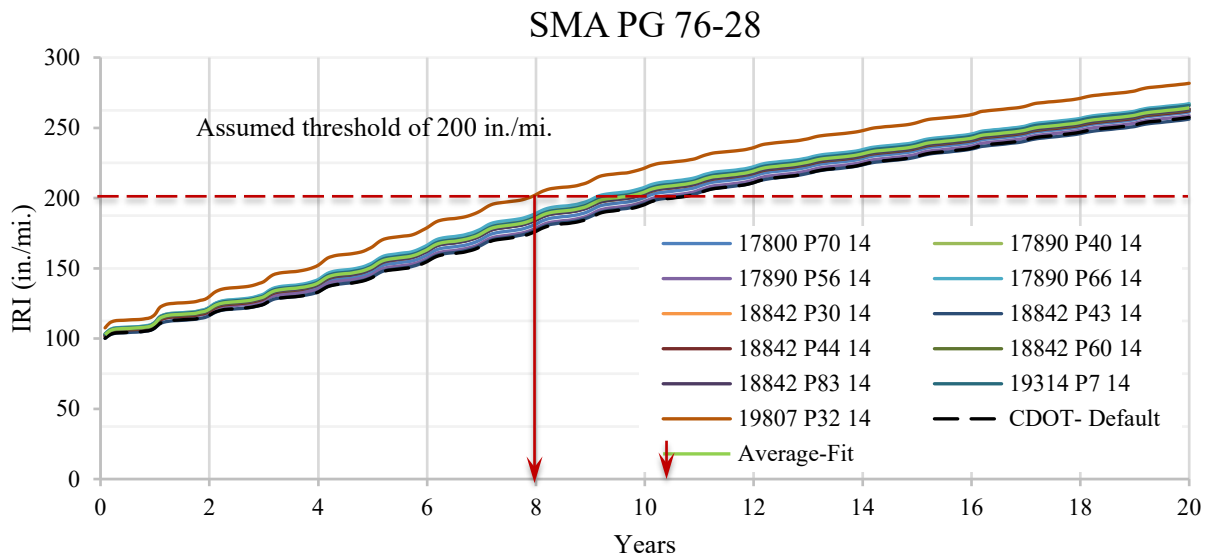


Figure 50. IRI Due to AADTT = 7,000 by SMA PG 76-28 Mix

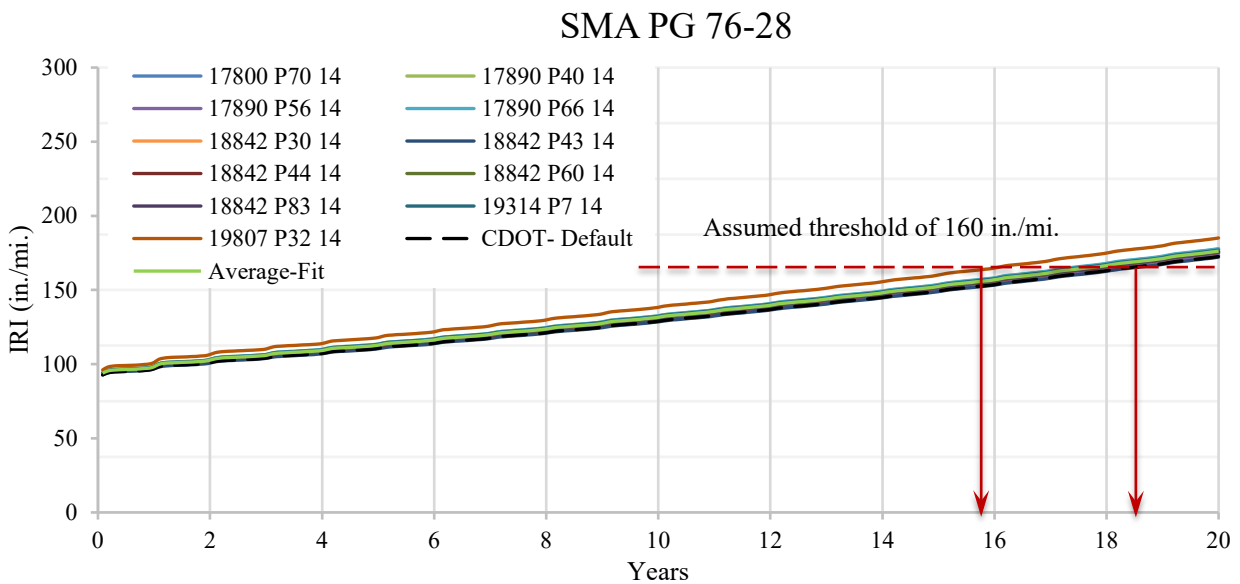


Figure 51. IRI Due to AADTT = 800 by SMA PG 76-28 Mix

Total Rutting: The total rutting variation during the service life of the trial pavement is shown in Figures 52 and 53 for AADTT = 7,000 and AADTT = 800, respectively. Similar to the IRI, the CDOT-default mixture produces the least amount of rutting during its service life except for the 18842 P43 14 mix. The mix, 19807 P32 14 produces the highest IRI rutting value. If the threshold total value is 0.7 in., as shown in Figure 52, then the prediction reaches the threshold by 19807 P32 14 mix at about one year, whereas the prediction reaches the threshold by 18842 P43 14 mix at about seven years. That means the prediction of rutting may differ by about six years from one mix to another, although the mix design is same. The variation of this prediction is similar for low traffic as shown in Figure 53. The statistical 95% CI boundaries show that only two mixes, 18842 P43 14 and 17890 P56 14, are within the 95% CI boundaries of the CDOT mix. The average-fit data produces the total rutting outside the 95% CI boundaries of the CDOT mix.

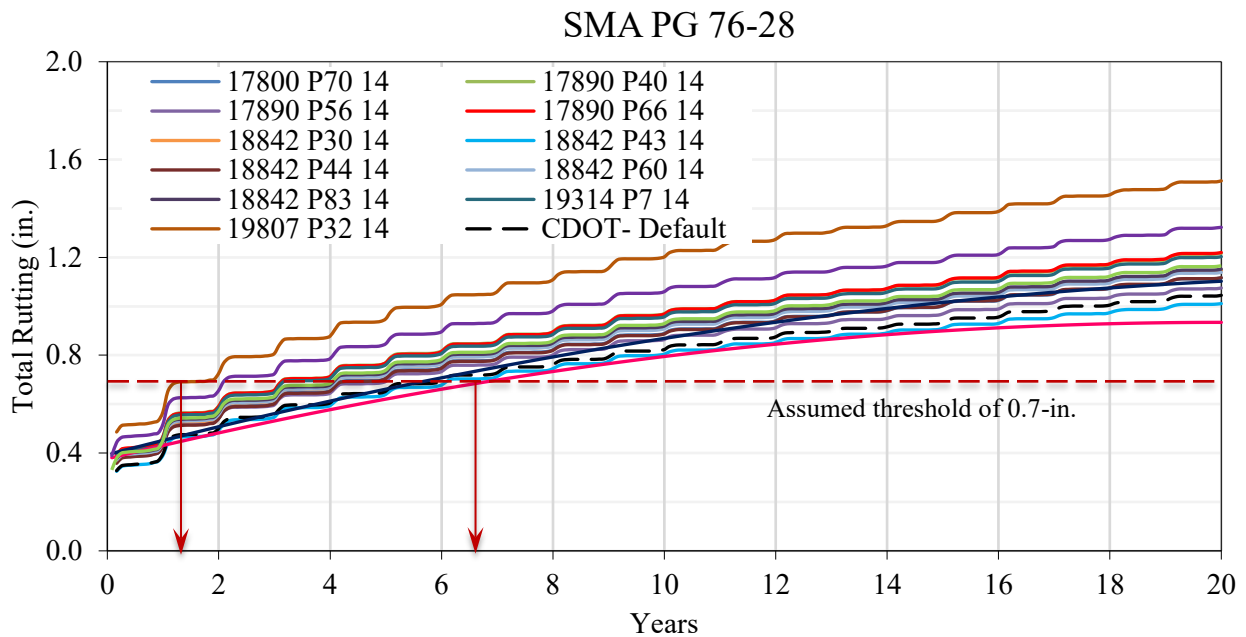


Figure 52. Total Rutting Due to AADTT = 7,000 by SMA PG 76-28 Mix

SMA PG 76-28

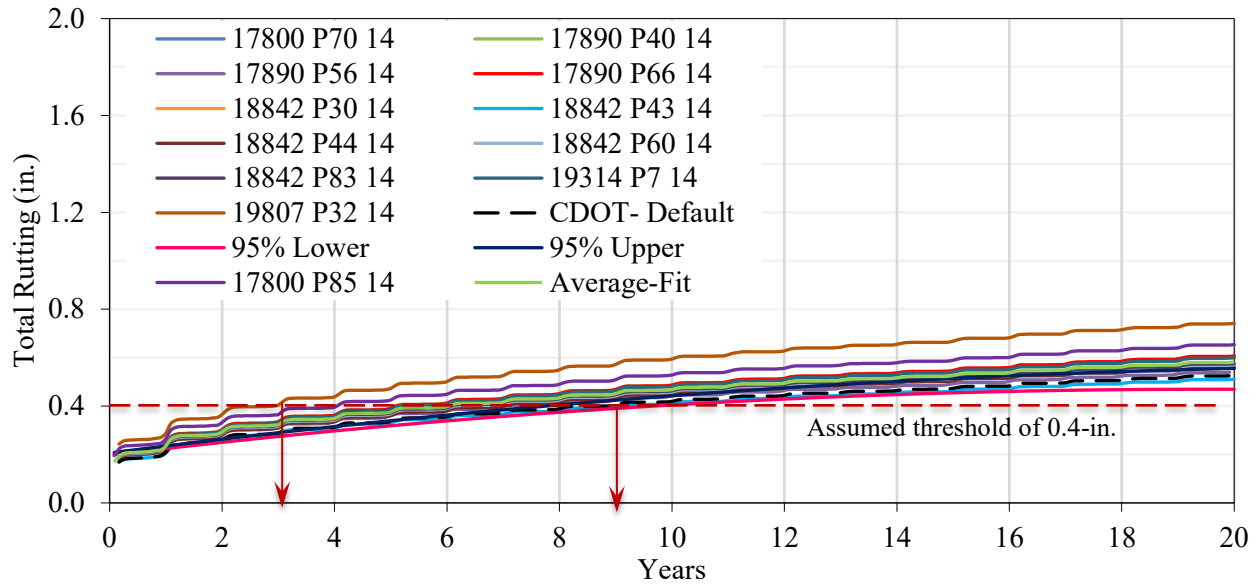


Figure 53. Total Rutting Due to AADTT = 800 by SMA PG 76-28 Mix

Rutting in Asphalt Layer Only: The rutting in asphalt layer variation during its service life of the trial pavement is shown in Figures 54 and 55 for high and low traffic, respectively. The behavior and findings from the rutting in the asphalt layer are similar to those obtained for the total rutting. Assumed threshold values of 0.60 in. and 0.30 in. are drawn in Figures 54 and 55, respectively. Figure 54 shows that the mixes reach the threshold in about 2 to 8 years for high traffic. Similar observation is obtained for low traffic as shown in Figure 55. The statistical 95% CI boundaries show that only two mixes, 18842 P43 14 and 17890 P56 14, are within the 95% CI boundaries of the CDOT mix. The average-fit data produces the rutting in the asphalt layer outside the 95% CI boundaries of the CDOT mix.

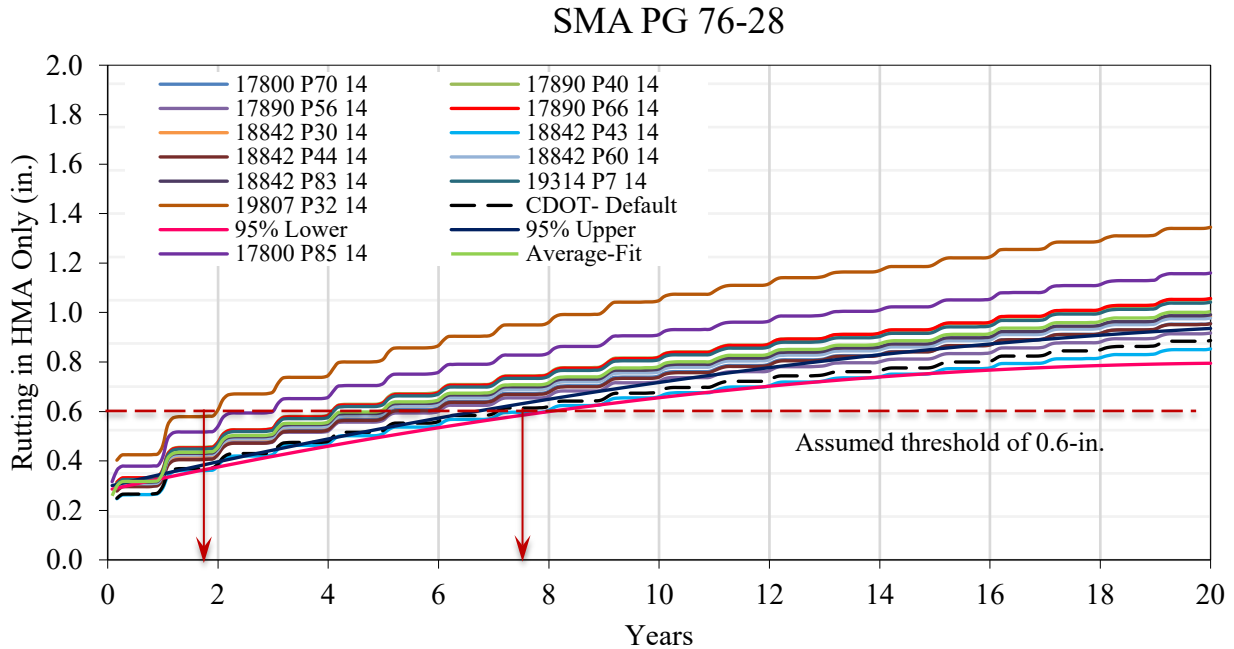


Figure 54. Rutting in Asphalt Layer Due to AADTT = 7,000 by SMA PG 76-28 Mix

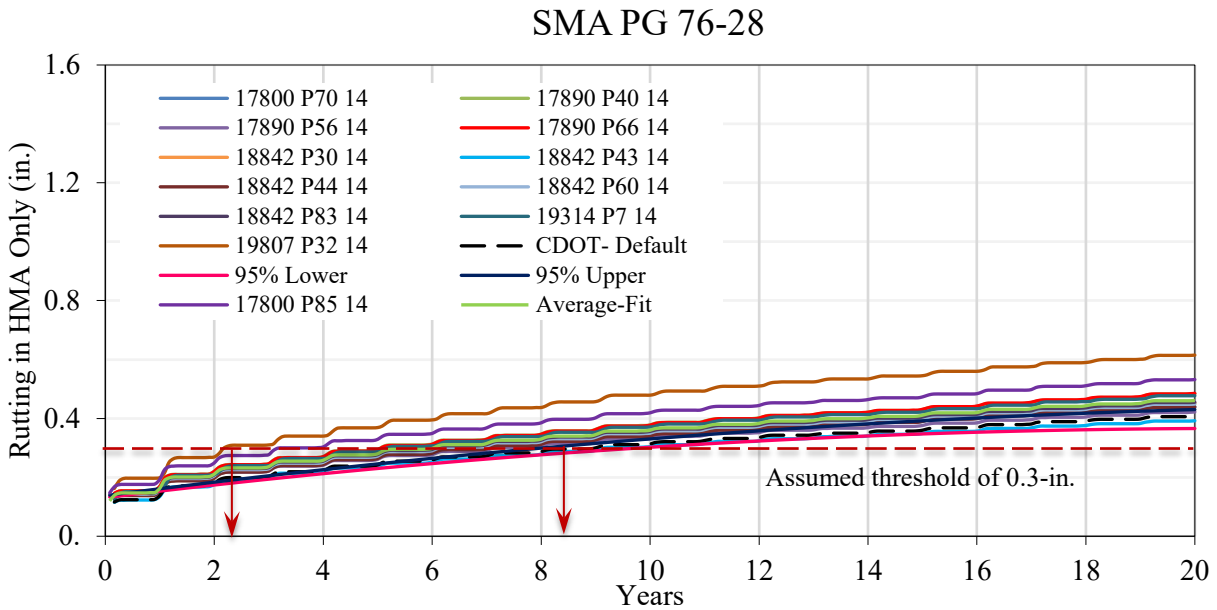


Figure 55. Rutting in Asphalt Layer Due to AADTT = 800 by SMA PG 76-28 Mix

Bottom-up Fatigue Cracking: The CDOT-default dynamic modulus data predicts the lowest amount of bottom-up fatigue cracking (Figures 56, and 57). Thus, a pavement designed with the CDOT-default data may be under-designed considering the top-down cracking. The other dynamic

modulus data produces consistent amounts of cracking, except for 19807 P32 14 mix. The assumed threshold of 25% of the lane area shown in Figure 56 shows that the mixes reach the threshold in about three years, which is very close to each other. A little higher variation in observation is obtained for low traffic as shown in Figure 57 where the threshold is assumed to be 15% of the lane area. This prediction is similar for the low traffic analysis as well. Figure 57 shows that three mixes, 17800 P70 14, 17890 P56 14, and 18842 P43 14, are within the statistical 95% CI boundaries.

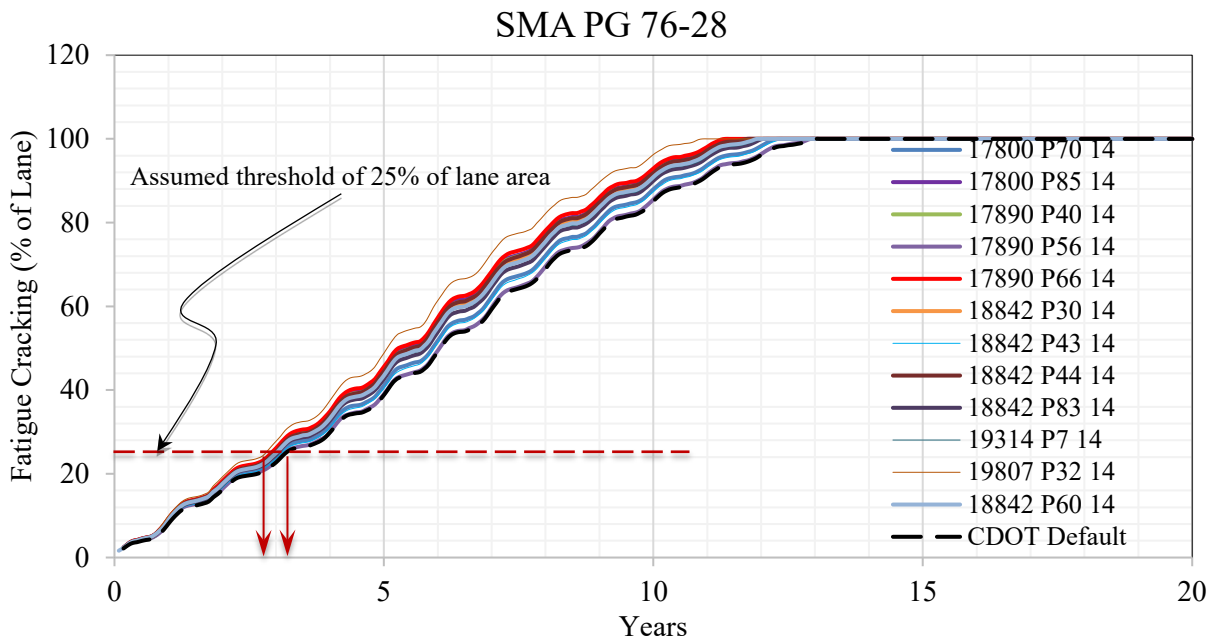


Figure 56. Bottom-up Fatigue Cracking Due to AADTT = 7,000 by SMA PG 76-28 Mix

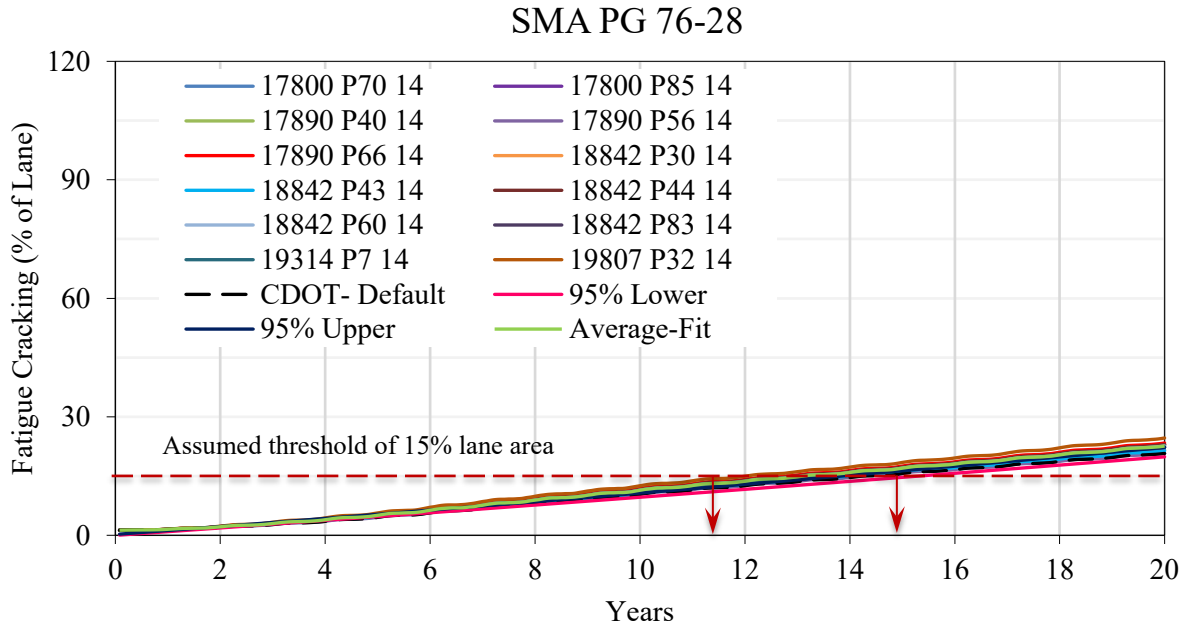


Figure 57. Bottom-up Fatigue Cracking Due to AADTT = 800 by SMA PG 76-28 Mix

Top-down Longitudinal Cracking: As shown in Figures 58 and 59, the default CDOT mixture produces the least amount of top-down cracking, other than the 17890 P56 14 mix. For a threshold value of 2,500 ft./mi., Figure 58, the mixes reach the threshold from five to eight years depending on mix to mix. This observation is similar for the low traffic as shown in Figure 59. Only the 19807 P32 14 mixture is outside the statistical 95% CI boundaries.

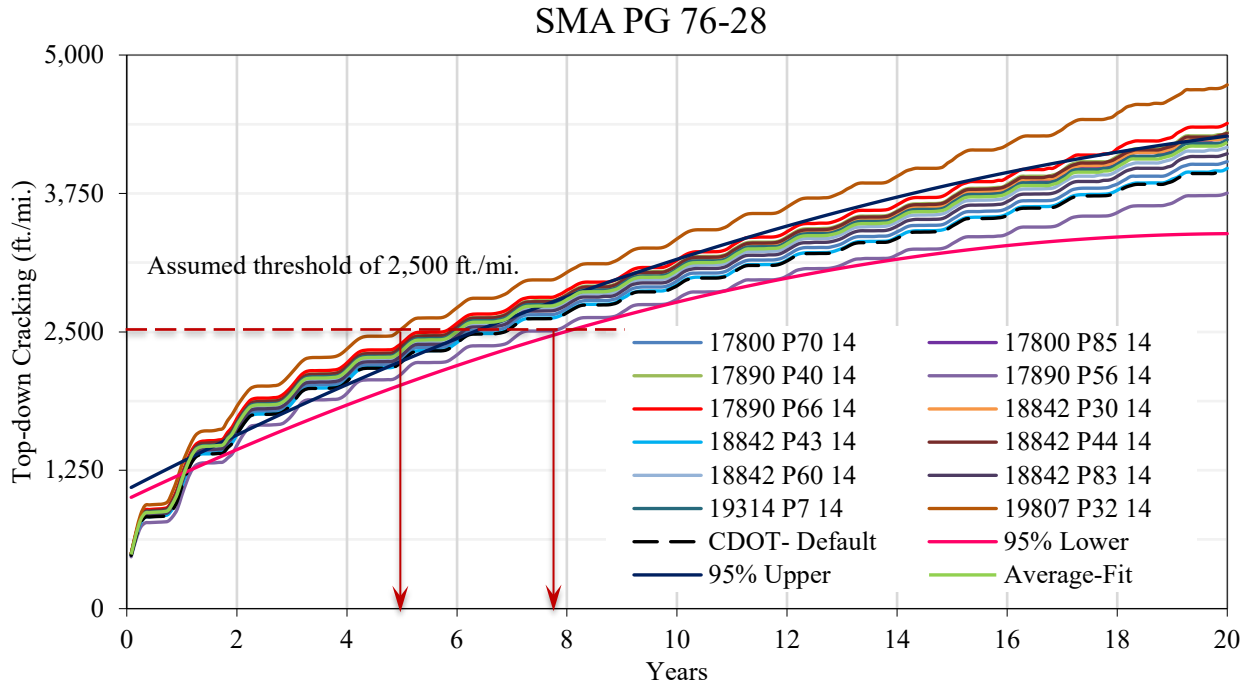


Figure 58. Longitudinal Cracking Due to AADTT = 7,000 by SMA PG 76-28 Mix

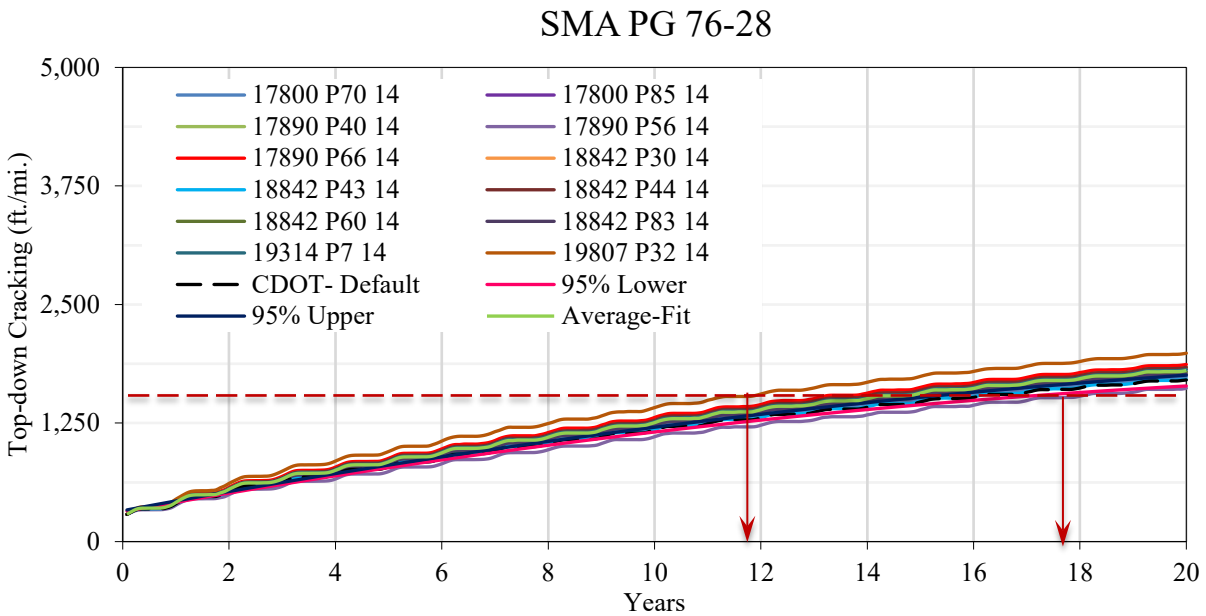


Figure 59. Longitudinal Cracking Due to AADTT = 800 by SMA PG 76-28 Mix

The above distress analysis shows that only two mixes, 18842 P43 14 (Region 2) and 17890 P56 14 (Region 1), are within the 95% CI boundaries of the CDOT mix for all distresses. Table 54 lists

the mix parameters and two distresses, total rutting in in., and bottom-up fatigue cracking in percent lane area, after 10 years of life for comparison. There are many variables in the mix parameters as listed in Table 54. For example, mixes 17890 P56 14 and 17890 P66 14 have different production dates, different voids ratios, VMAs, and VFAs. Although the difference is not so notable, their effects produced different distresses, and one is statistically the same as the CDOT-default mix, while the other is not. Therefore, the effect of the individual mix parameter may be appropriately sought out for this mix. Another observation is that most of mixes from Regions 1, 2, and 4 are statistically different from the CDOT-default mix.

To determine the influence of V_{be} , V_a , VMA, VFA, and AC, a regression analysis is conducted, and the following correlations are obtained. The R^2 of the correlations of IRI, total rutting, rutting in HMA, FC, and TDC are found to be 0.76, 0.84, 0.84, 0.52, and 0.65, respectively. It can be seen from the following regression equations that IRI increases with the increase in V_{be} , VFA, and AC, and decreases with the increase in V_a and VMA. Total rutting, rutting in asphalt layer, and TDC increase with the increase in V_{be} and AC, but decrease with the increase in V_a , VFA, and VMA. FC increases with V_{be} , and decreases with the increase in V_a , VMA, VFA, and AC.

$$\text{IRI (in./mi.)} = 395.01 + 2.0456 V_{be} - 1.4291 V_a - 7.07 \text{ VMA} + 1.3321 \text{ VFA} + 2.4632 \text{ AC}$$

$$\begin{aligned} \text{Total Rutting (in.)} &= 4.209 + 0.03149 V_{be} - 0.0111 V_a - 0.1204 \text{ VMA} - 0.02526 \text{ VFA} \\ &+ 0.0665 \text{ AC} \end{aligned}$$

$$\begin{aligned} \text{Rutting in HMA (in.)} &= 4.0193 + 0.0314 V_{be} - 0.0103 V_a - 0.1189 \text{ VMA} - 0.02499 \text{ VFA} \\ &+ 0.0653 \text{ AC} \end{aligned}$$

$$\text{FC (\%)} = 20.72 + 0.1488 V_{be} - 0.2542 V_a - 0.3707 \text{ VMA} - 0.0289 \text{ VFA} - 0.2312 \text{ AC}$$

$$\begin{aligned} \text{TDC (ft./mi.)} &= 4115.85 + 210.48 V_{be} - 55.05 V_a - 83.03 \text{ VMA} - 35.401 \text{ VFA} + 51.97 \\ &\text{AC} \end{aligned}$$

SX(75) PG 58-28

Table 55 lists the mix parameters, aggregate pits, binder suppliers and contractor information of the SX(75) PG 58-28 mix. Mix parameters includes V_{be} , V_a , VMA, VFA, and AC. All this information is used while analyzing the performance of different mixes as discussed below.

Table 55. Generic Information of SX(75) PG 58-28 Mix

	Paving Contractor	Binder Supplier	Region	Date	V_{be} (%)	V_a (%)	VMA (%)	VFA (%)	AC (%)	Pit
17735 P27 14	United Companies	Suncor	3	8/2014	13.23	5.60	18.1	69.5	6.40	Halderson
19095 P42 14	United Gypsum	Sinclair	3	10/2014	10.96	6.90	16.8	61.0	6.10	Lyster Camilletti
19171 P57 14	Everist Materials	Suncor	3	1/2015	12.58	6.90	18.6	62.8	5.80	Maryland Creek Ranch
19489 P51 14	Elam Construction	Sinclair	3	1/2015	11.25	5.00	15.8	67.5	5.10	Chambers
19633 P94 14	4 Corners	Suncor	5	11/2015	12.57	5.00	17.9	64.0	5.51	Cugnini Bayfield
19707 P92 14	Elam Construction	Suncor	5	11/2015	15.45	6.95	18.6	62.9	6.60	Agri-D Dillon Ranch
19879 P113 14	-	Suncor	1	2/2016	10.34	6.90	17.8	65.6	4.90	Ralston Firestone
20167 P21 15	Grand River	Peak	3	7/2016	9.81	5.90	17.7	65.1	4.94	Sievers

Note: Orange Highlighted mixes produce statistically the same distress with the CDOT-default mix. This is clarified in the following discussion.

International Roughness Index: The IRI variation during its service life of the trial pavement is shown in Figures 60 and 61 for high (AADTT = 3,000) and low traffic (AADTT = 800), respectively. It shows that all mixes, including the default CDOT mixture, produce consistent amounts of IRI during its service life. The CDOT-default mix produces larger than average values of IRI in comparison with all mixes. Assumed threshold values of 200 in./mi. and 160 in./mi. are drawn in Figures 60 and 61, respectively. Figure 60 shows that the mixes reach the threshold in about 14 to 16 years for high traffic. Similar observation is obtained for low traffic as shown in Figure 61.

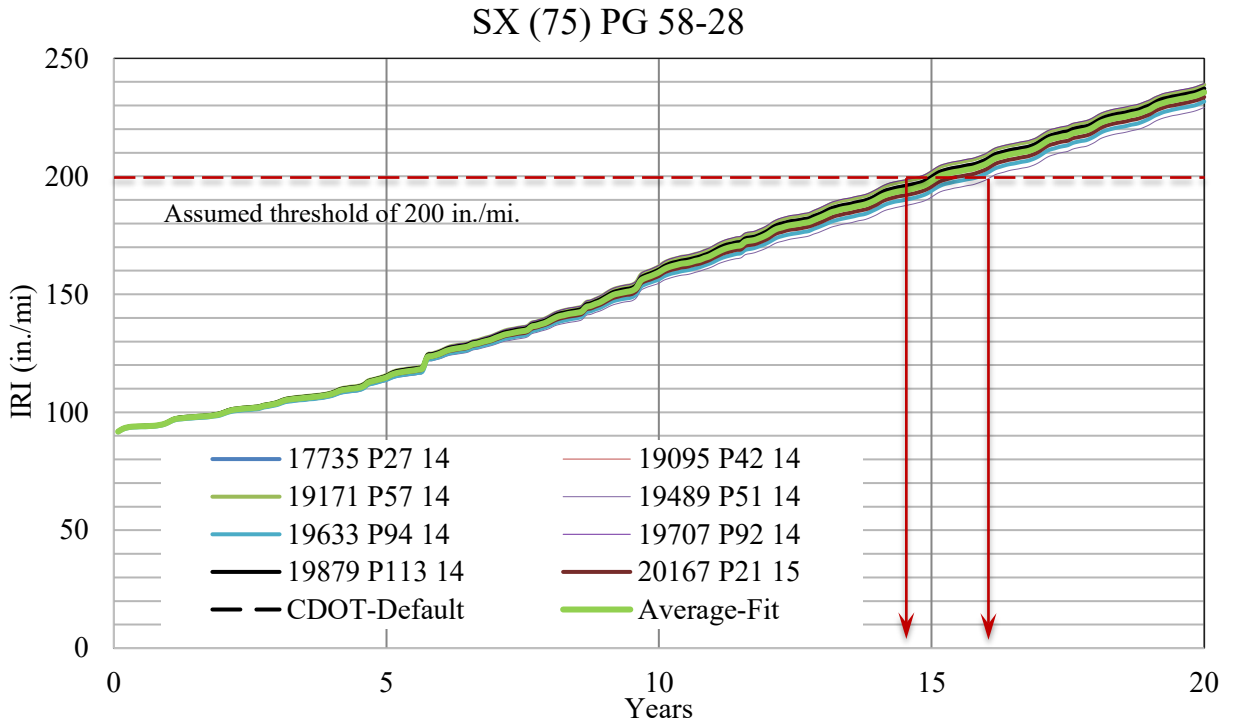


Figure 60. IRI Due to AADTT = 3,000 by SX(75) PG 58-28 Mix

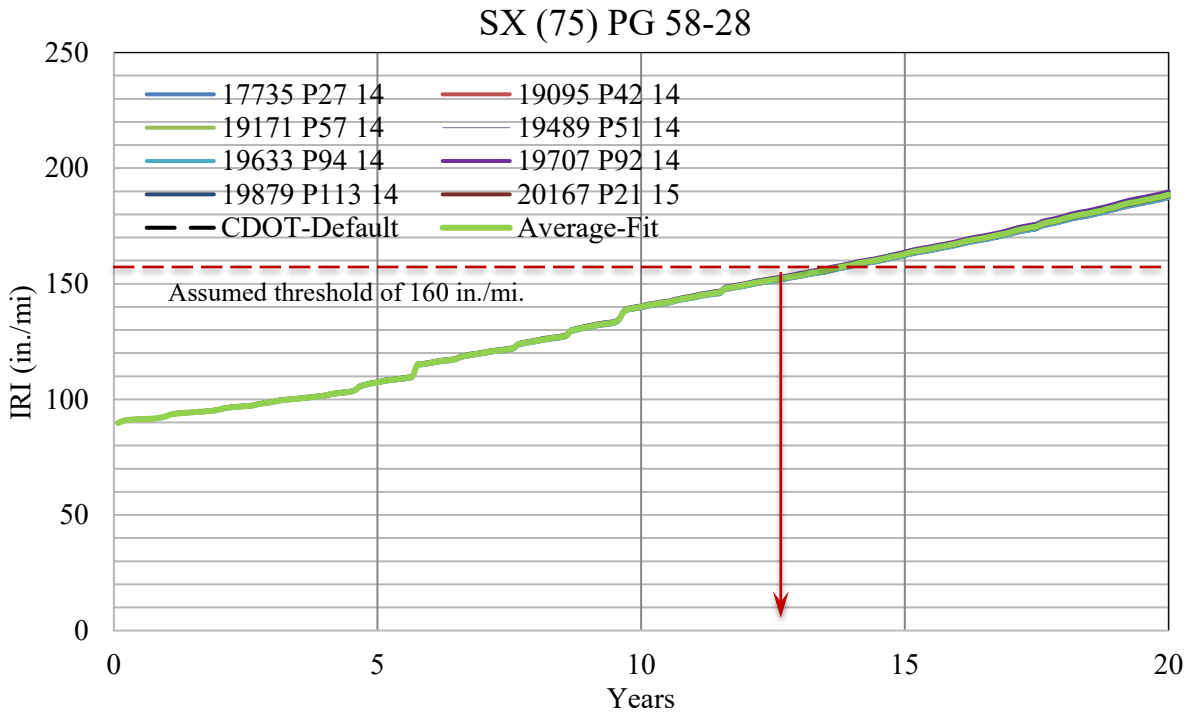


Figure 61. IRI Due to AADTT = 800 by SX(75) PG 58-28 Mix

Total Rutting: The total rutting variation (Figures 62 and 63) for both traffic levels shows that the CDOT-default mix data produce more than average rutting comparing all mixes. For a threshold value of 0.35 in, the mixes reach the threshold from 6 to 10 years as shown in Figure 62 for high traffic. This observation is similar for the low traffic. The statistical 95% CI boundaries show only a single mix, 19489 P51 14, produces rutting outside the boundaries. All other mixes comply with the CDOT-default mix.

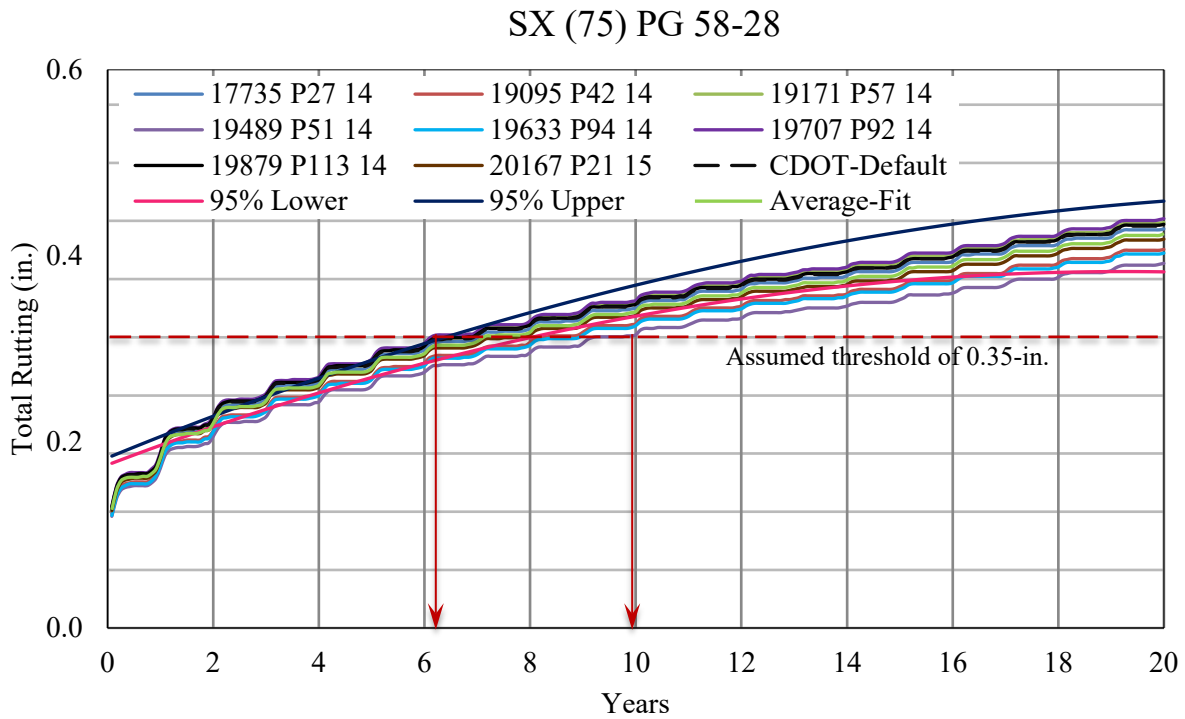


Figure 62. Total Rutting Due to AADTT = 3,000 by SX(75) PG 58-28 Mix

SX (75) PG 58-28

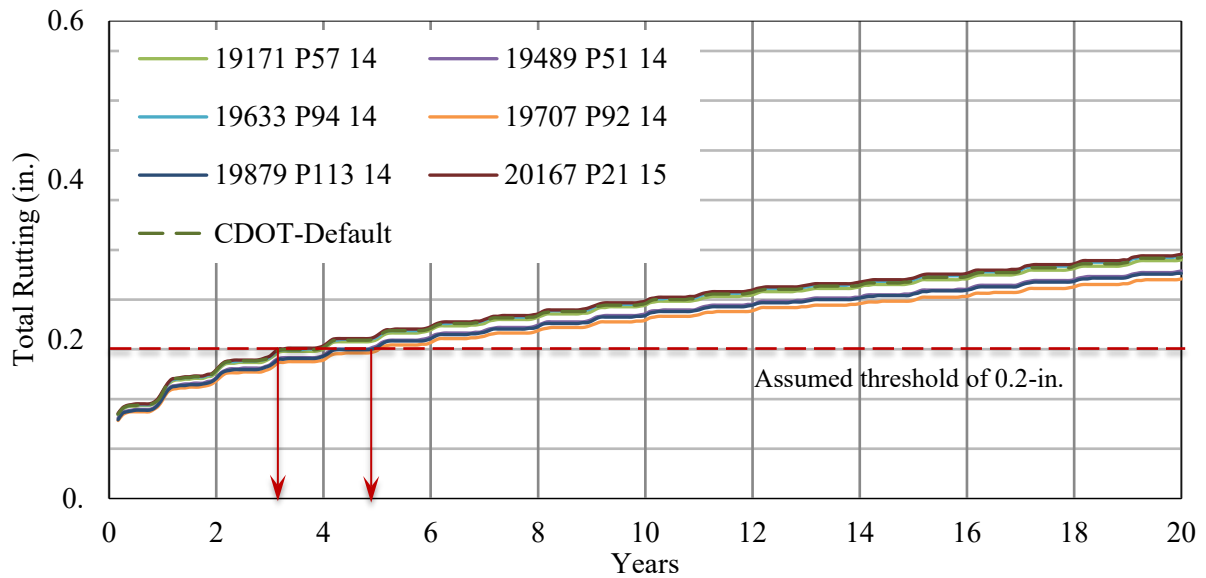


Figure 63. Total Rutting Due to AADTT = 800 by SX(75) PG 58-28 Mix

Rutting in Asphalt Layer Only: As observed for total rutting, the rutting in asphalt layer (Figures 64 and 65) show similar characteristics. For a threshold value of 0.2 in, the mixes reach the threshold from 7 to 11 years as shown in Figure 64 for high traffic. This observation is similar for the low traffic.

SX (75) PG 58-28

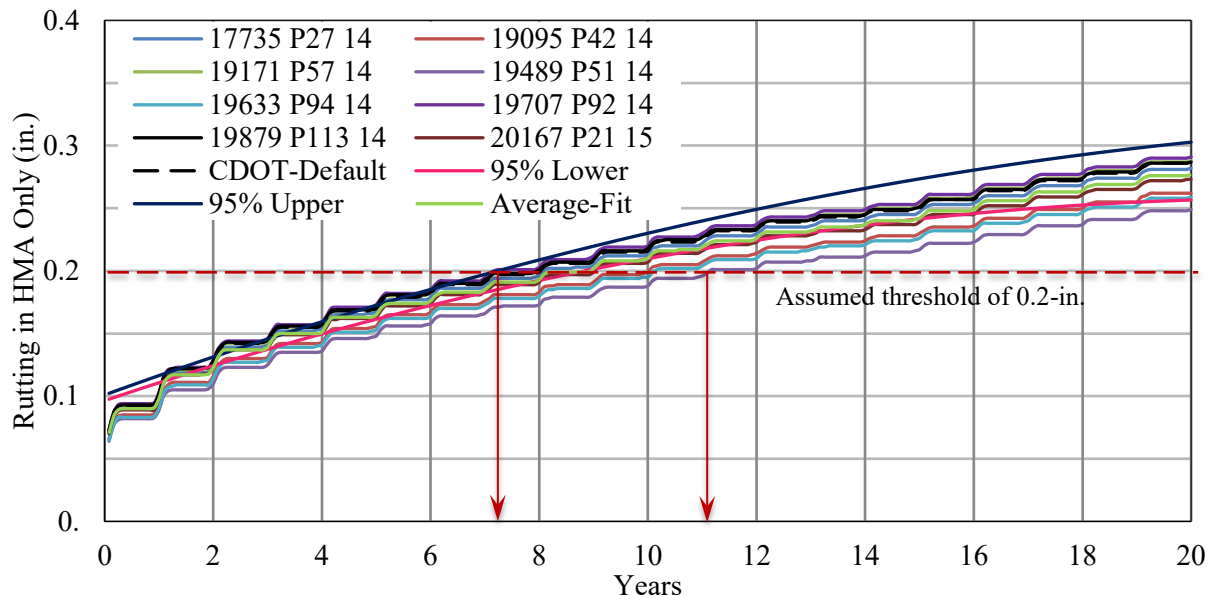


Figure 64. Rutting in Asphalt Layer Due to AADTT = 3,000 by SX(75) PG 58-28 Mix

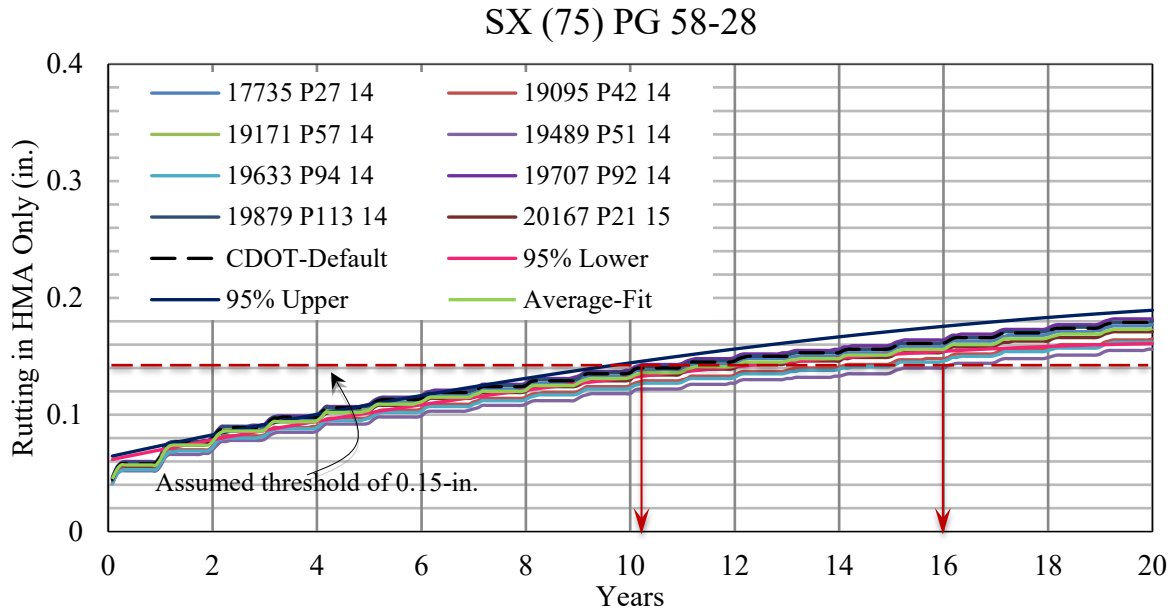


Figure 65. Rutting in Asphalt Layer Due to AADTT = 800 by SX(75) PG 58-28 Mix

Bottom-up Fatigue Cracking: The bottom-up fatigue cracking variation during its service life of the trial pavement is shown in Figures 66 and 67 for high (AADTT = 3,000) and low traffic (AADTT = 800), respectively. The statistical 95% CI boundaries show only the mix, 19489 P51 14, produces bottom-up fatigue cracking outside the boundaries. The assumed threshold of 25% of the lane area shown in Figure 66 shows that the mixes reach the threshold between six and eight years, which is very close to each other. Similar observation is obtained for low traffic as shown in Figure 67 where the threshold is assumed to be 12.5% of the lane area.

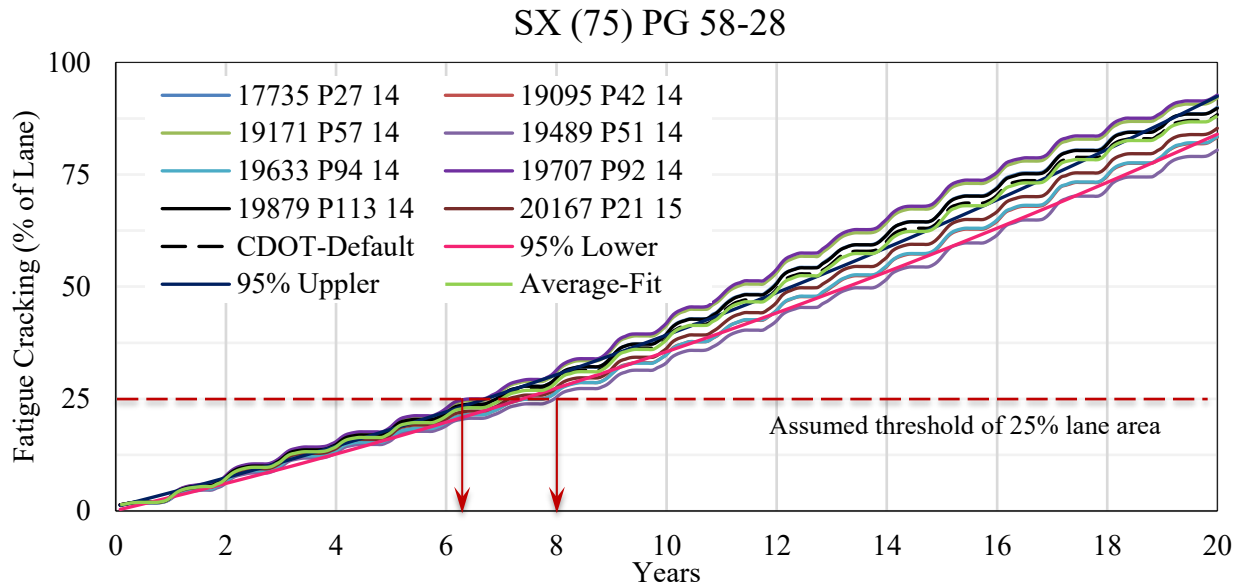


Figure 66. Bottom-up Fatigue Cracking Due to AADTT = 3,000 by SX(75) PG 58-28 Mix

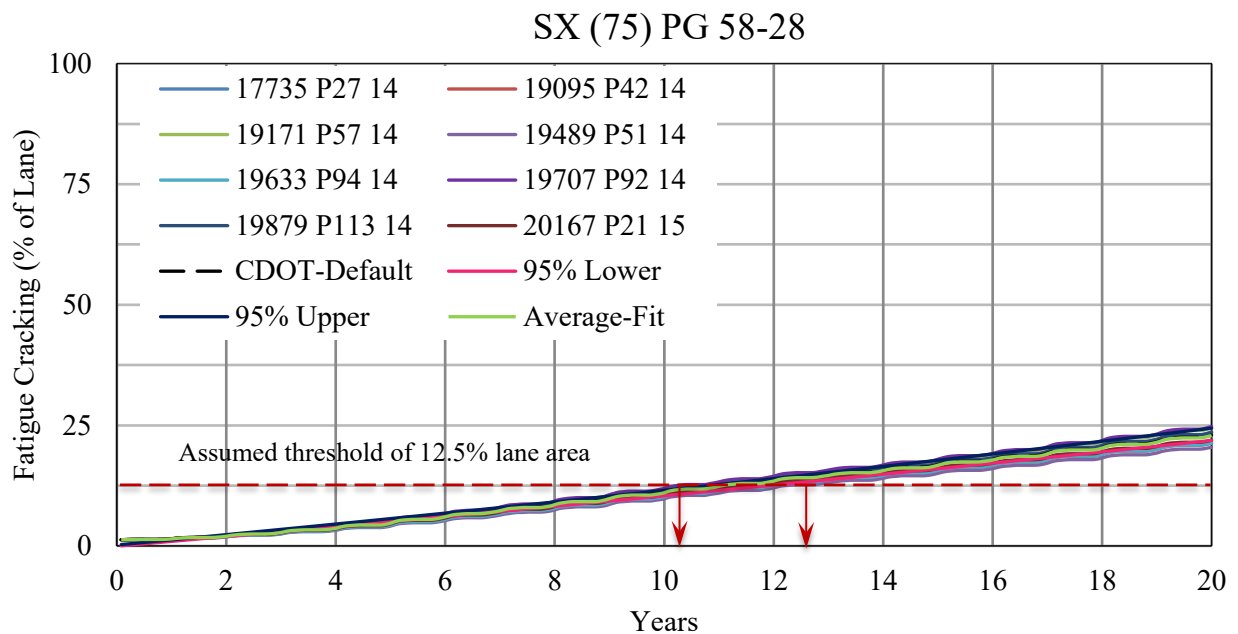


Figure 67. Bottom-up Fatigue Cracking Due to AADTT = 800 by SX(75) PG 58-28 Mix

Top-down Longitudinal Cracking: The top-down longitudinal cracking variation during its service life of the trial pavement is shown in Figures 68 and 69 for high (AADTT = 3,000) and low traffic (AADTT = 800), respectively. Mixes reach the threshold value of 1,500 ft./mi. from 6 to 11 years for high traffic as shown in Figure 68. This observation is similar for the low traffic

where mixes reach the threshold value of 1,000 ft./mi. from 10 to 17 years as shown in Figure 69. The statistical 95% CI boundaries show that the three mixes, 19489 P51 14, 19095 P42 14, and 19633 P94 14, produce top-down longitudinal cracking outside the boundaries. The average-fit data produces the top-down longitudinal cracking along with other distresses mentioned above within the 95% CI boundaries of the CDOT mix.

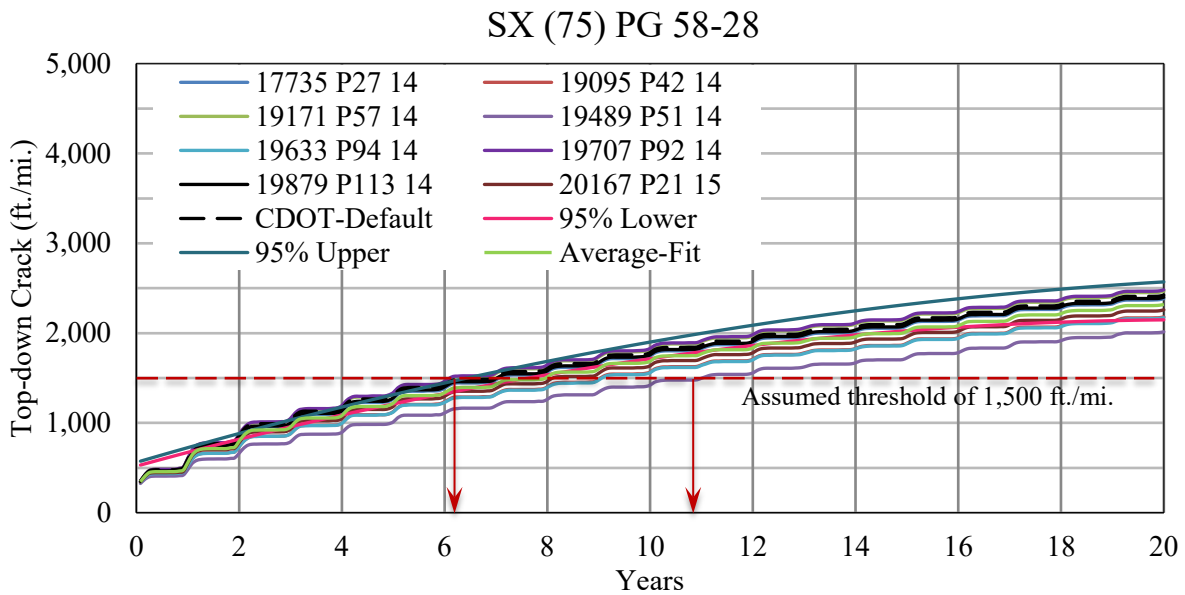


Figure 68. Longitudinal Cracking Due to AADTT = 3,000 by SX(75) PG 58-28 Mix

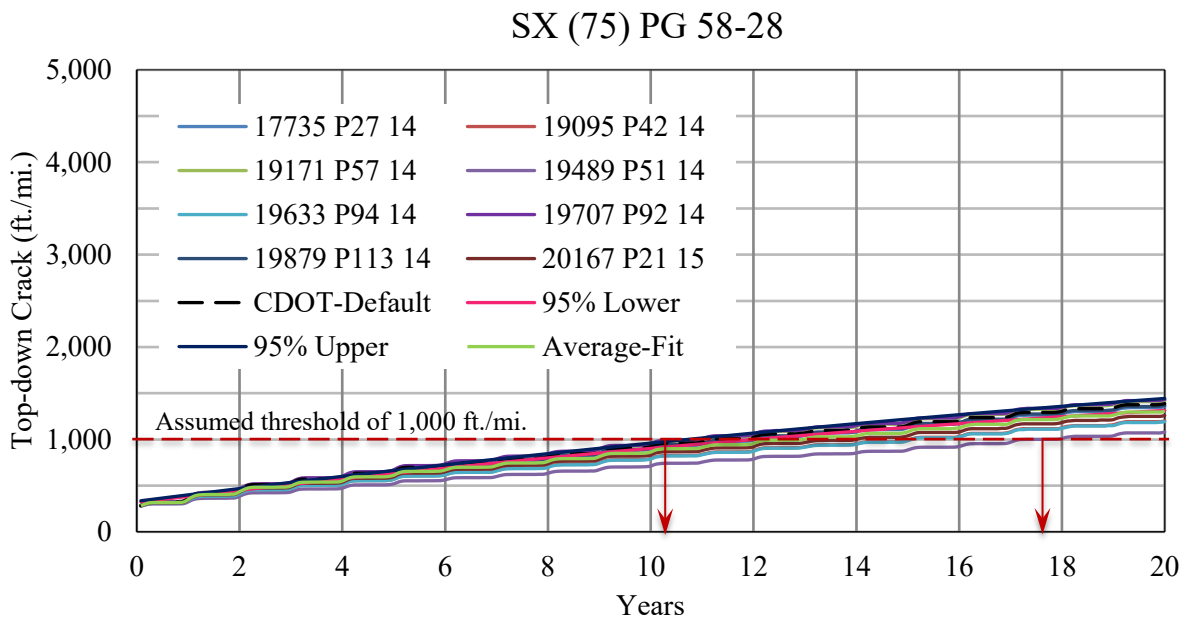


Figure 69. Longitudinal Cracking Due to AADTT = 800 by SX(75) PG 58-28 Mix

The above analysis that the 19489 P51 14, 19095 P42 14, and 19633 P94 14 mixes did not comply with the CDOT-default mix for all distresses. The mix, 19489 P51 14, did not satisfy any single distress; it has the least VMA (15.8%) and a unique aggregate source (Chambers). The causes for the deviations may come from the unique binder supplier (Sinclair) and the unique aggregate sources (Lyster, Camilletti, Chambers, Cugini, and Bayfield), as mentioned in Table 55.

To determine the influence of V_{be} , V_a , VMA, VFA, and AC, a regression analysis is conducted, and the following correlations are obtained. The R^2 of all correlations is 1.0. It is apparent from the regression equations that all distresses increase with the increase in V_{be} , V_a , VMA, and VFA, and decrease with the increase in AC.

$$\text{IRI (in./mi.)} = 86.727 + 0.5809 V_{be} + 2.3731 V_a + 1.5102 \text{ VMA} + 0.443 \text{ VFA} - 0.8613 \text{ AC}$$

$$\text{Total Rutting (in.)} = -0.0266 + 0.0013 V_{be} + 0.0113 V_a + 0.0087 \text{ VMA} + 0.0022 \text{ VFA} - 0.0031 \text{ AC}$$

$$\text{Rutting in HMA (in.)} = -0.0487 + 0.0013 V_{be} + 0.0093 V_a + 0.0077 \text{ VMA} + 0.0013 \text{ VFA} - 0.0062 \text{ AC}$$

$$\text{FC (\%)} = -9.5197 + 0.1817 V_{be} + 0.6578 V_a + 0.4247 \text{ VMA} + 0.1246 \text{ VFA} - 0.2448 \text{ AC}$$

$$\text{TDC (ft./mi.)} = -1967.79 + 12.7944 V_{be} + 104.403 V_a + 97.8032 \text{ VMA} + 18.7019 \text{ VFA} - 17.8014 \text{ AC}$$

SX(75) PG 58-34

Table 56 lists the mix parameters, aggregate pits, binder suppliers and contractor information of the SX(75) PG 58-34 mix. Mix parameters includes V_{be} , V_a , VMA, VFA, and AC. All this information is used while analyzing the performance of different mixes as discussed below.

Table 56. Generic Information of SX(75) PG 58-34 Mix

	Paving Contractor	Binder Supplier	Region	Date	V_{be} (%)	V_a (%)	VMA (%)	VFA (%)	AC (%)	Pit
19217 P41 14	Connell Resources	Suncor	3	10/2014	10.94	6.60	16.5	60.5	5.60	Lyster & Camilletti
19708 P68 14	Connell Resources	Suncor	3	5/2015	11.69	6.90	17.8	60.8	5.50	Camilletti/Duckles

International Roughness Index (IRI): The IRI variation during the service life of the trial pavement is shown in Figures 70 and 71 for AADTT = 3,000 and AADTT = 800, respectively. They show that the default CDOT mixture produces roughly average IRI values compared to 19217 P4114 and 19708 P68 14 mixes.

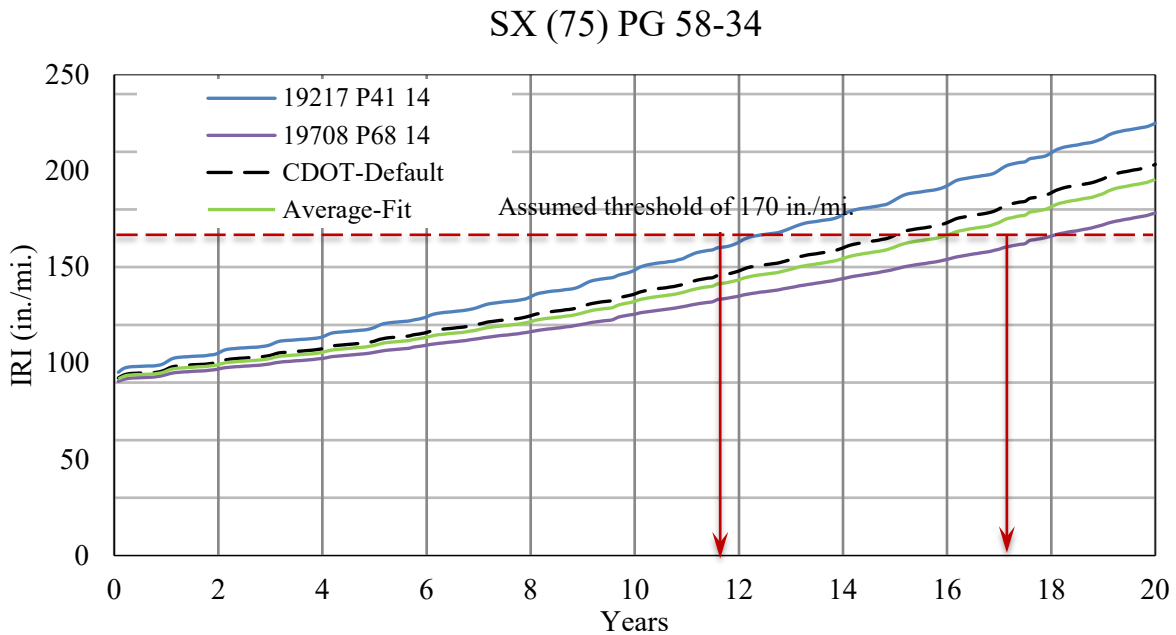


Figure 70. IRI Due to AADTT = 7,000 by SX(75) PG 58-34 Mix

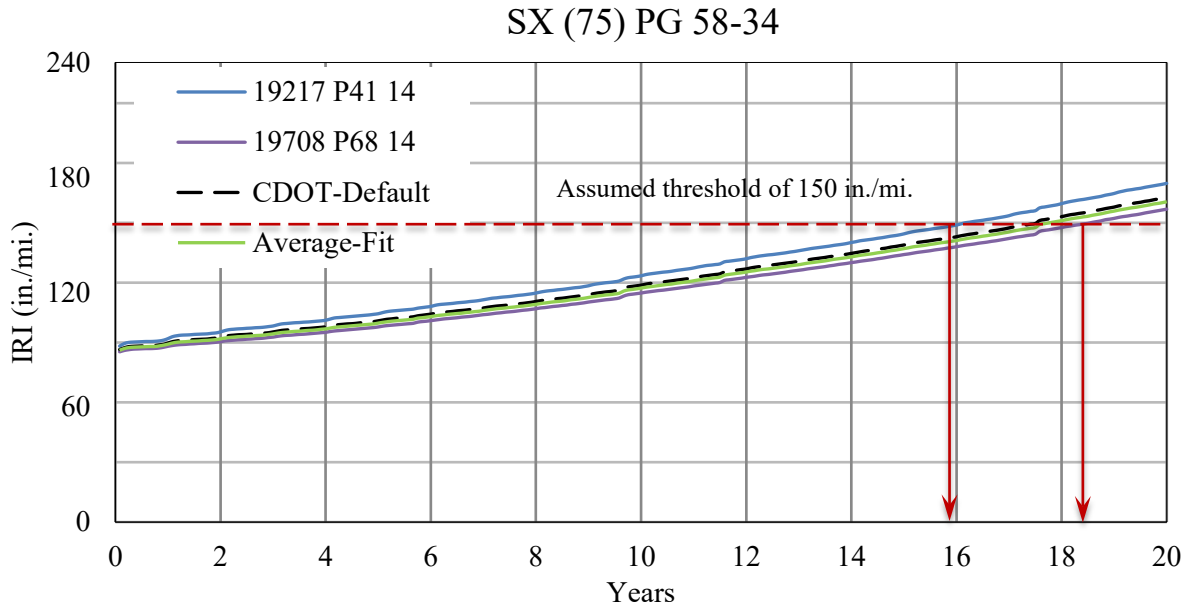


Figure 71. IRI Due to AADTT = 800 by SX(75) PG 58-34 Mix

Total Rutting: The total rutting variations by the default CDOT mixture produce roughly average total rutting values compared to 19217 P4114 and 19708 P68 14 mixes, Figures 72 and 73. Comparing the distress level, the lowest and the highest total rutting predicted are 0.27 and 0.53 in. (96% larger), respectively, at 10-year life for AADTT = 3,000. Both of the moduli data are for mixes prepared by Connell Resources. However, the statistical 95% CI boundaries show that no mix is within the boundaries. For a threshold value of 0.3 in., the mixes reach the threshold from 1 to 16 years as shown in Figure 72 for high traffic. This observation is similar for the low traffic.

SX (75) PG 58-34

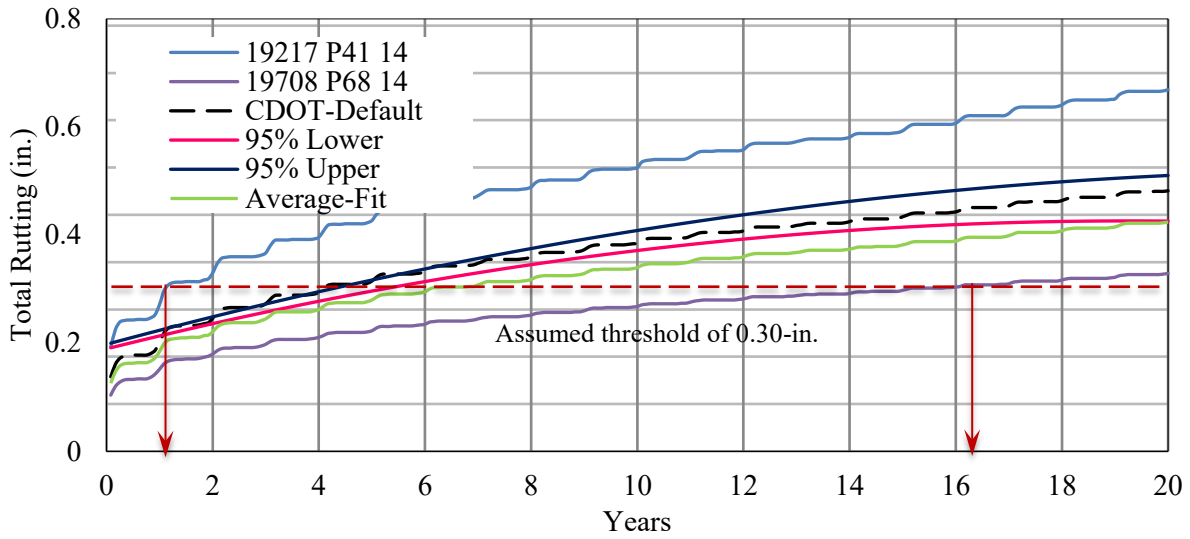


Figure 72. Total Rutting Due to AADTT = 3,000 by SX(75) PG 58-34 Mix

SX (75) PG 58-34

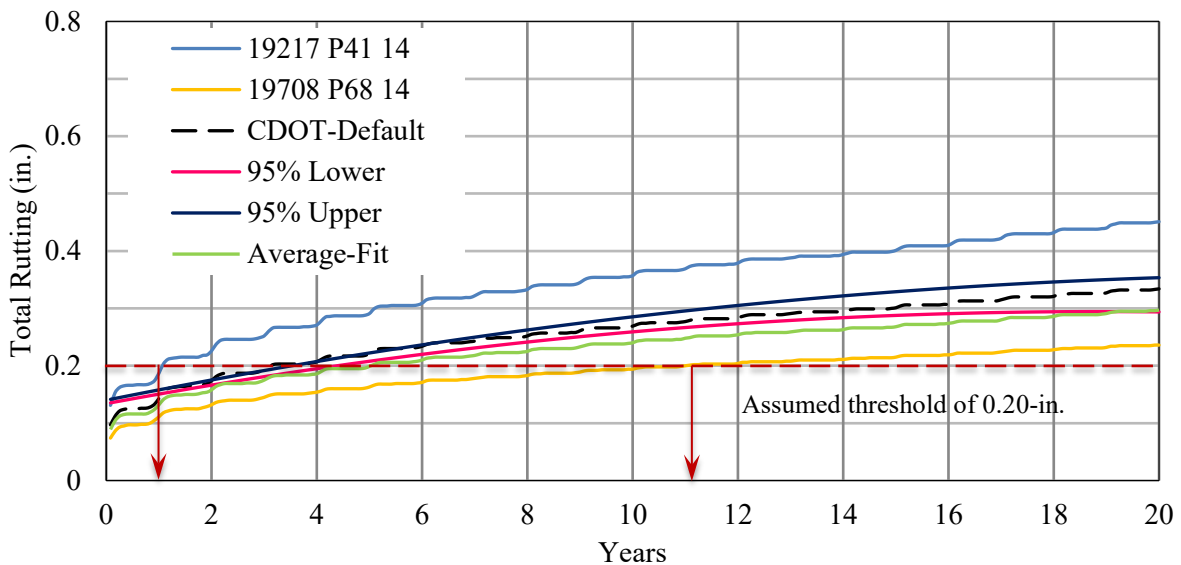


Figure 73. Total Rutting Due to AADTT = 800 by SX(75) PG 58-34 Mix

Rutting in Asphalt Layer Only: Similar to total rutting, the rutting in asphalt layer variations by the default CDOT mixture produces roughly average rutting values, compared to 19217 P4114 and 19708 P68 14 mixes, Figures 74 and 75. Comparing the distress level, the lowest and the highest rutting in asphalt layer predicted are 0.14 and 0.38 in. (170% larger), respectively, at 10-

year life for AADTT = 3,000. For a threshold value of 0.15 in, the mixes reach the threshold from one to 11 years as shown in Figure 74 for high traffic. This observation is similar for the low traffic. The statistical 95% CI boundaries show that no mix is within the boundaries.

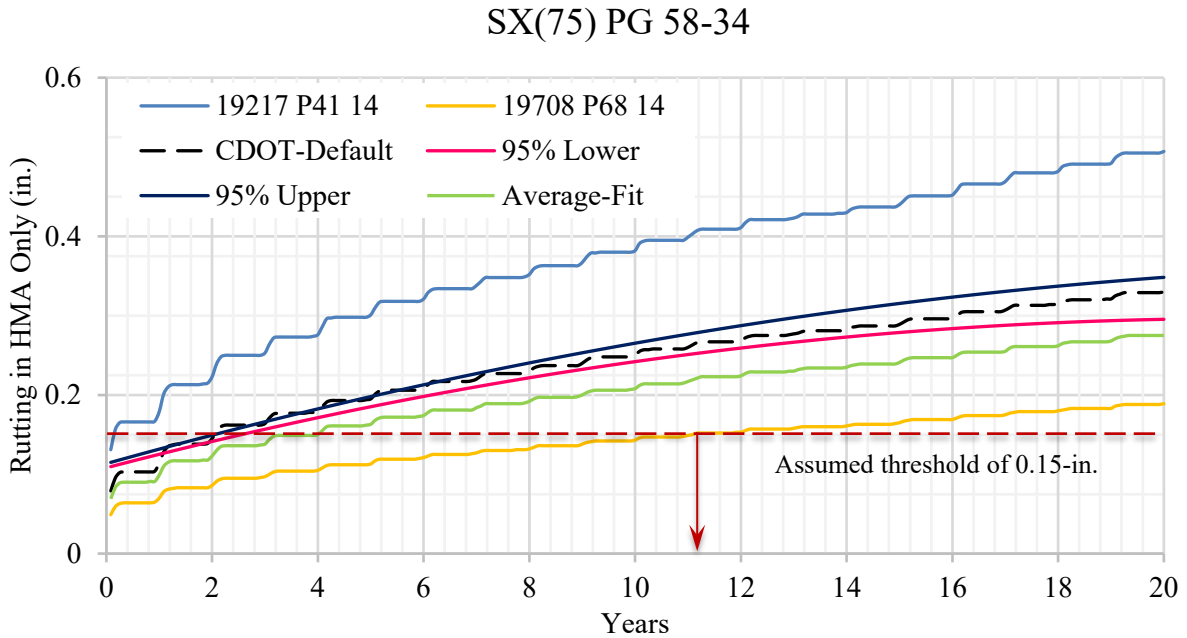


Figure 74. Rutting in Asphalt Layer Due to AADTT = 3,000 by SX(75) PG 58-34 Mix

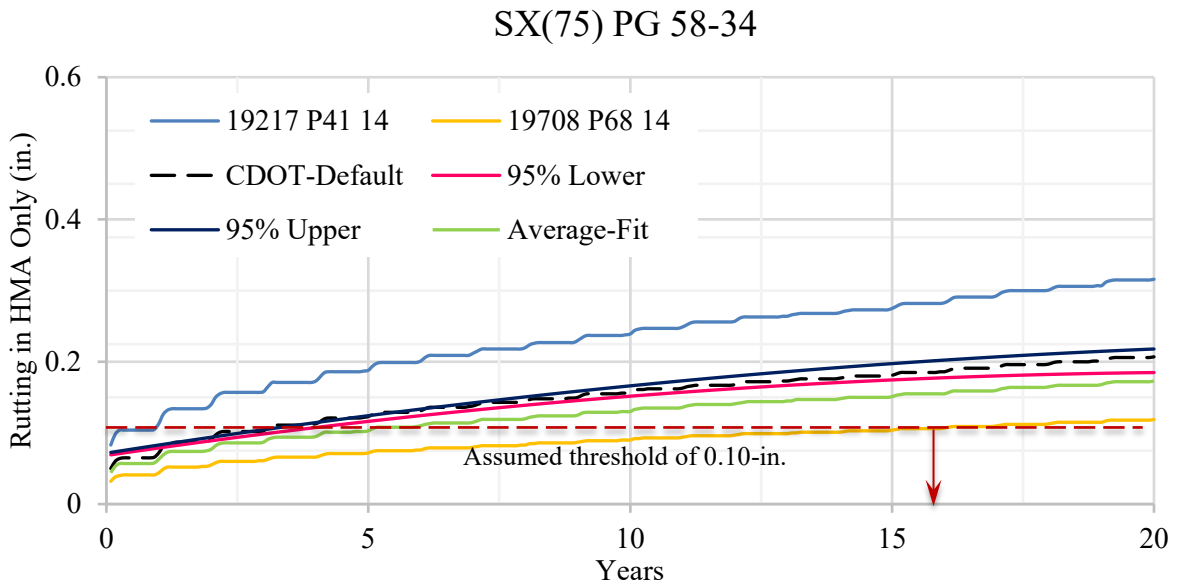


Figure 75. Rutting in Asphalt Layer Due to AADTT = 800 by SX(75) PG 58-34 Mix

Bottom-up Fatigue Cracking: Similar to rutting, the bottom-up fatigue cracking variations by the default CDOT mixture produce roughly average bottom-up fatigue cracking values compared to 19217 P4114 and 19708 P68 14 mixes, Figures 74 and 75. Comparing the distress level, the lowest and the highest bottom-up fatigue cracking predicted are found to be 15% and 31% (107% larger), respectively, at 10-year life for AADTT = 3,000. The assumed threshold of 20% of the lane area shown in Figure 66 shows that the mixes reach the threshold between six and thirteen years. Similar observation is obtained for low traffic as shown in Figure 77 where the threshold is assumed to be 7% of the lane area. The statistical 95% CI boundaries show that no mix is within the boundaries.

SX (75) PG 58-34

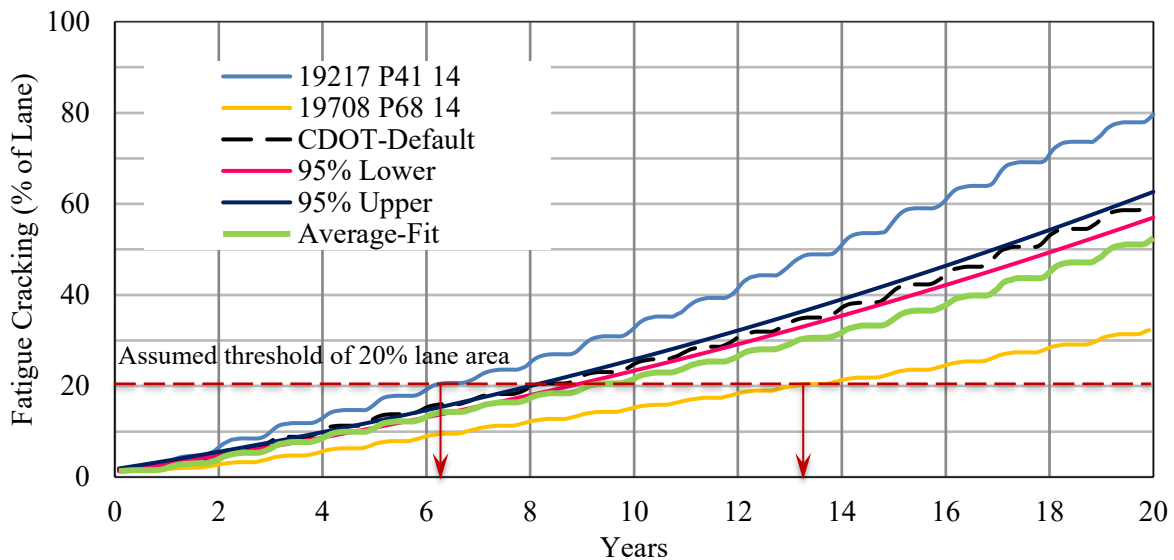


Figure 76. Bottom-up Fatigue Cracking Due to AADTT = 3,000 by SX(75) PG 58-34 Mix

SX (75) PG 58-34

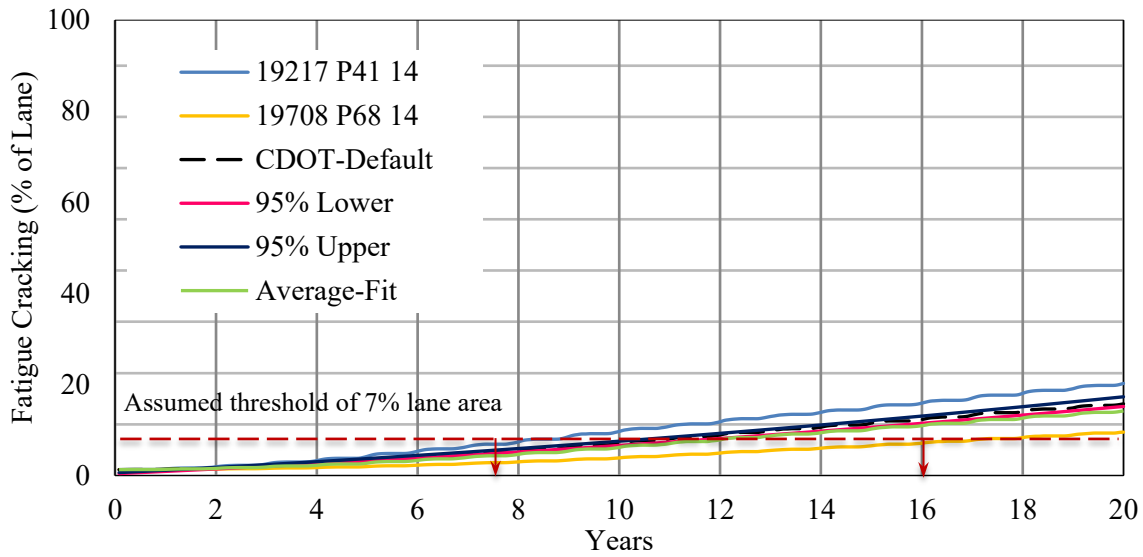


Figure 77. Bottom-up Fatigue Cracking Due to AADTT = 800 by SX(75) PG 58-34 Mix

Top-down Longitudinal Cracking: The top-down longitudinal cracking variation during its service life of the trial pavement is shown in Figures 86 and 87 for high and low traffic, respectively. Only two test mixes' data are available for this category, and their prediction differs by a lot from one mix to another. The average-fit data produces the top-down longitudinal cracking, along with other distresses mentioned above, outside the 95% CI boundaries of the CDOT mix. Mixes reach the threshold value of 750 ft./mi. from one to 11 years for high traffic as shown in Figure 78. This observation is similar for the low traffic where mixes reach the threshold value of 600 ft./mi. from 2 to 19 years as shown in Figure 79.

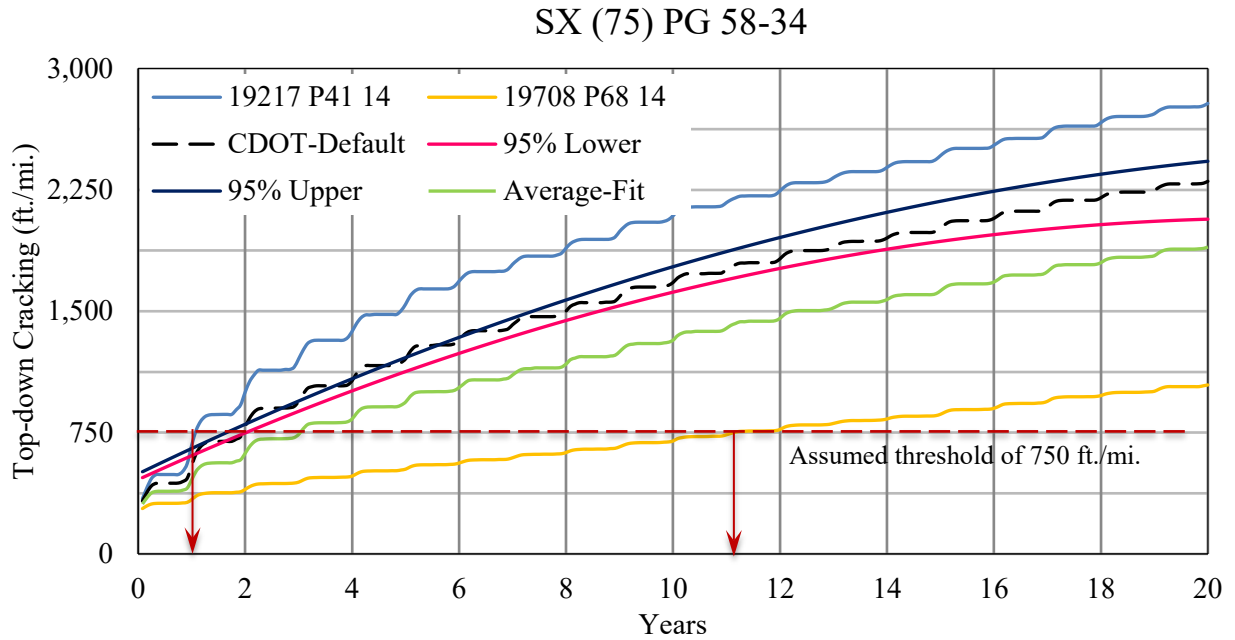


Figure 78. Longitudinal Cracking Due to AADTT = 3,000 by SX(75) PG 58-34 Mix

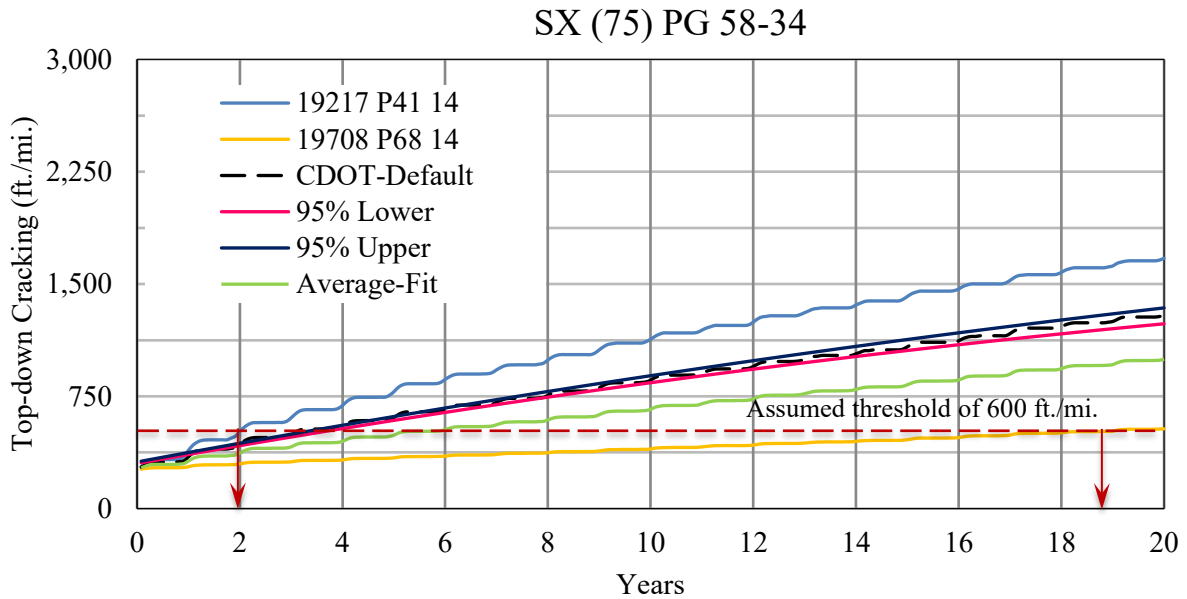


Figure 79. Longitudinal Cracking Due to AADTT = 800 by SX(75) PG 58-34 Mix

The above discussion shows that both mixes produced very different distresses, and the produced distresses are not statistically the same as the CDOT-default mix. From Table 56 below, it can be seen that both mixes are almost the same considering paving contractor, binder source, effective

binder content, air voids, VMA, and VFA. The production dates and aggregate pits are different. Therefore, these two parameters are probably the cause of the deviations between the two mixes.

To determine the influence of V_{be} , V_a , VMA, VFA, and AC, a regression analysis is conducted, and the following correlations are obtained. The R^2 of all correlations is 1.0. It can be seen from the following regression equations that all distresses decrease with the increase in VMA, and are insensitive to V_{be} , V_a , VFA, and AC.

$$\text{IRI (in./mi.)} = 439.0538 - 17.6154 \text{ VMA}$$

$$\text{Total Rutting (in.)} = 3.7869 - 0.1977 \text{ VMA}$$

$$\text{Rutting in HMA (in.)} = 3.4262 - 0.1846 \text{ VMA}$$

$$\text{FC (\%)} = 83.4016 - 4.4685 \text{ VMA}$$

$$\text{TDC (ft./mi.)} = 19757.51 - 1070.76 \text{ VMA}$$

SX(75) PG 64-22

Table 57 lists the mix parameters, aggregate pits, binder suppliers and contractor information of the SX(75) PG 64-22 mix. Mix parameters includes V_{be} , V_a , VMA, VFA, and AC. All this information is used while analyzing the performance of different mixes as discussed below.

Table 57. Generic Information of SX(75) PG 64-22 Mix

	Paving Contractor	Binder Supplier	Region	Date	V_{be} (%)	V_a (%)	VMA (%)	VFA (%)	AC (%)	Pit
19127 P73 14	Beltramo	Suncor	2	6/2015	13.53	7.10	18.4	61.2	5.70	Cesar/Transit Mix/Nepesta
19127 P75 14	Beltramo	Suncor	2	6/2015	13.55	6.93	17.9	61.6	5.70	Cesar/Transit Mix/Nepesta
19458 P105 14	Simon Construction	Suncor	4	12/2015	11.61	6.78	18.1	63.1	5.81	Granite Canyon, Julesburg, Ovid
19935 P58 14	A&S Construction	Suncor	2	2/2015	13.39	6.78	17.5	61.0	5.60	Rocky Ford South
19935 P61 14	A&S Construction	Suncor	2	2/2015	13.31	6.80	18.2	62.8	5.60	Rocky Ford South
19935 P63 14	A&S Construction	Suncor	2	3/2015	13.90	6.73	17.4	61.8	5.60	Rocky Ford South
20189 P7 15	McAtee	Suncor	4	4/2016	11.16	6.80	18.5	62.8	5.48	---

Note: Orange Highlighted mixes produce statistically the same distress with the CDOT-default mix. This is clarified in the following discussion.

International Roughness Index: Figures 80 and 81 show the IRI of the trial pavement with the service life of the pavement for high traffic (AADTT = 7,000) and low traffic (AADTT = 800), respectively. They show that the prediction of IRI of this mix using the dynamic moduli determined by different contractors is very consistent. The produced IRI by the CDOT-default data is the lowest compared to all mixes. Assumed threshold values of 200 in./mi. and 175 in./mi. are drawn in Figures 80 and 81, respectively. Figure 40 shows that the mixes reach the threshold in about 12 to 14 years for high traffic. Similar observation is obtained for low traffic as shown in Figure 81.

SX (75) PG 64-22

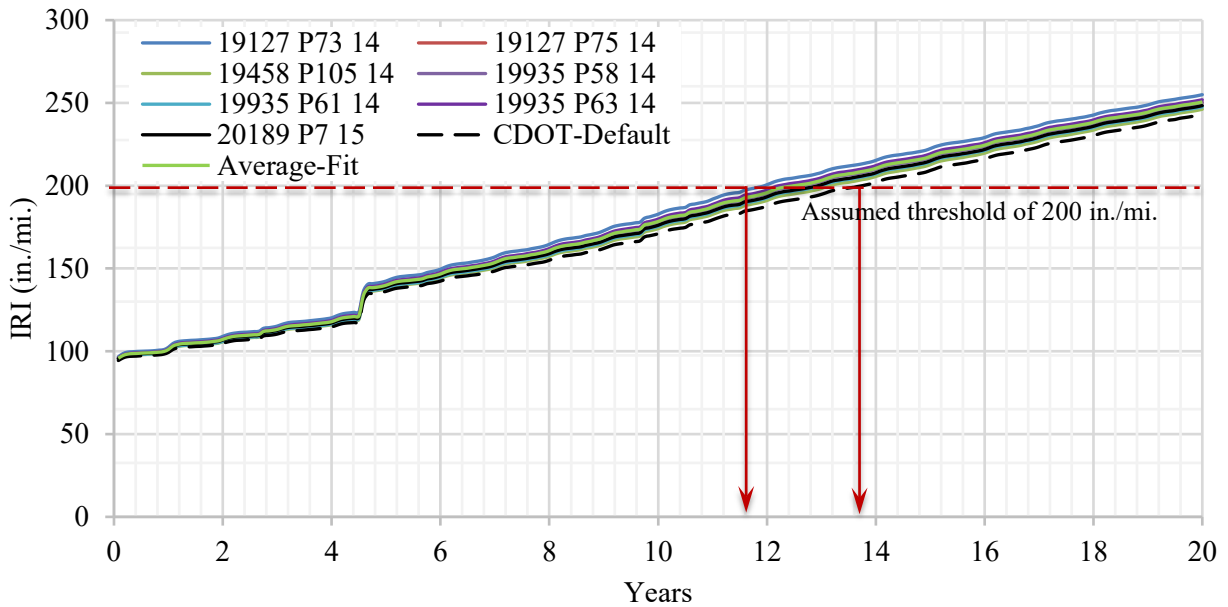


Figure 80. IRI Due to AADTT = 3,000 by SX(75) PG 64-22 Mix

SX (75) PG 64-22

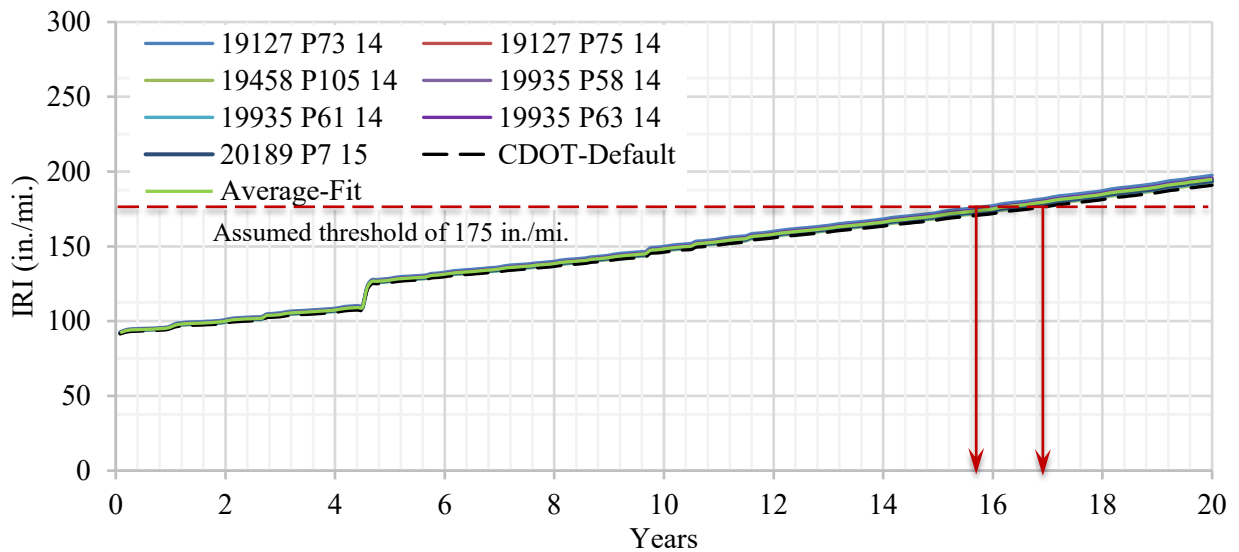


Figure 81. IRI Due to AADTT = 800 by SX(75) PG 64-22 Mix

Total Rutting: Figures 82 and 83 show that the CDOT-default dynamic modulus data produces the lowest rutting compared to the other dynamic modulus data. For a threshold value of 0.4 in, the mixes reach the threshold from two to five years as shown in Figure 82 for high traffic. This

observation is similar for the low traffic. The statistical 95% CI boundaries show only two mixes, 19458 P105 14 and 19935 P61 14, are within the boundary, and statistically the same as the CDOT-default mix data.

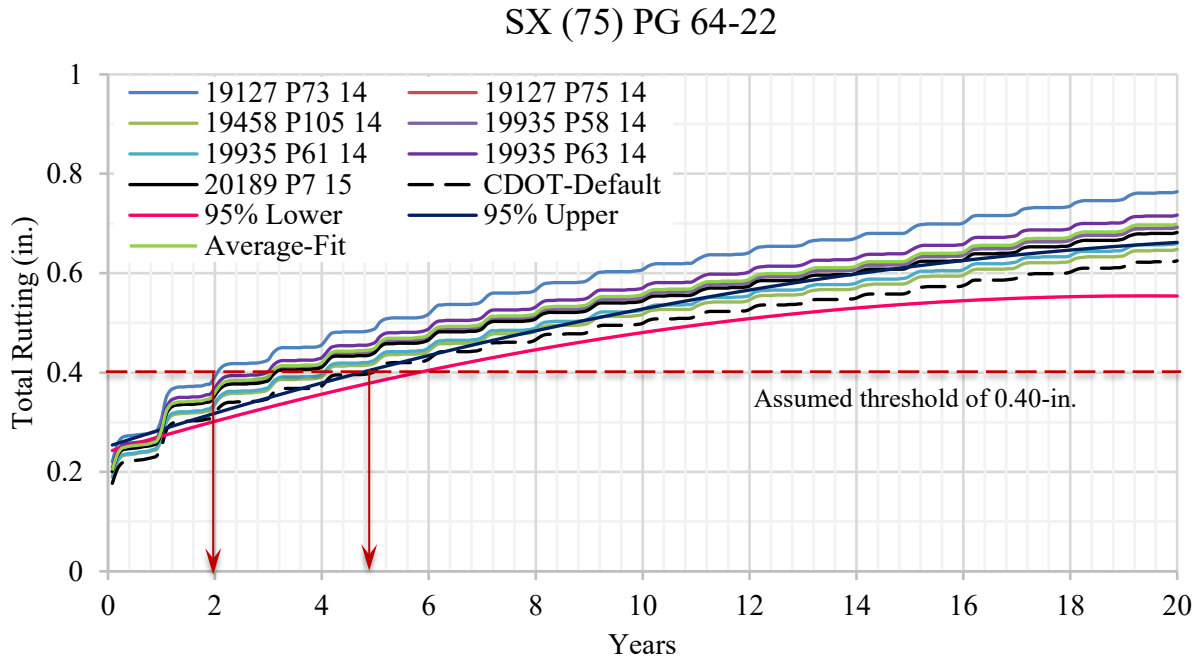


Figure 82. Total Rutting Due to AADTT = 3,000 by SX(75) PG 64-22 Mix

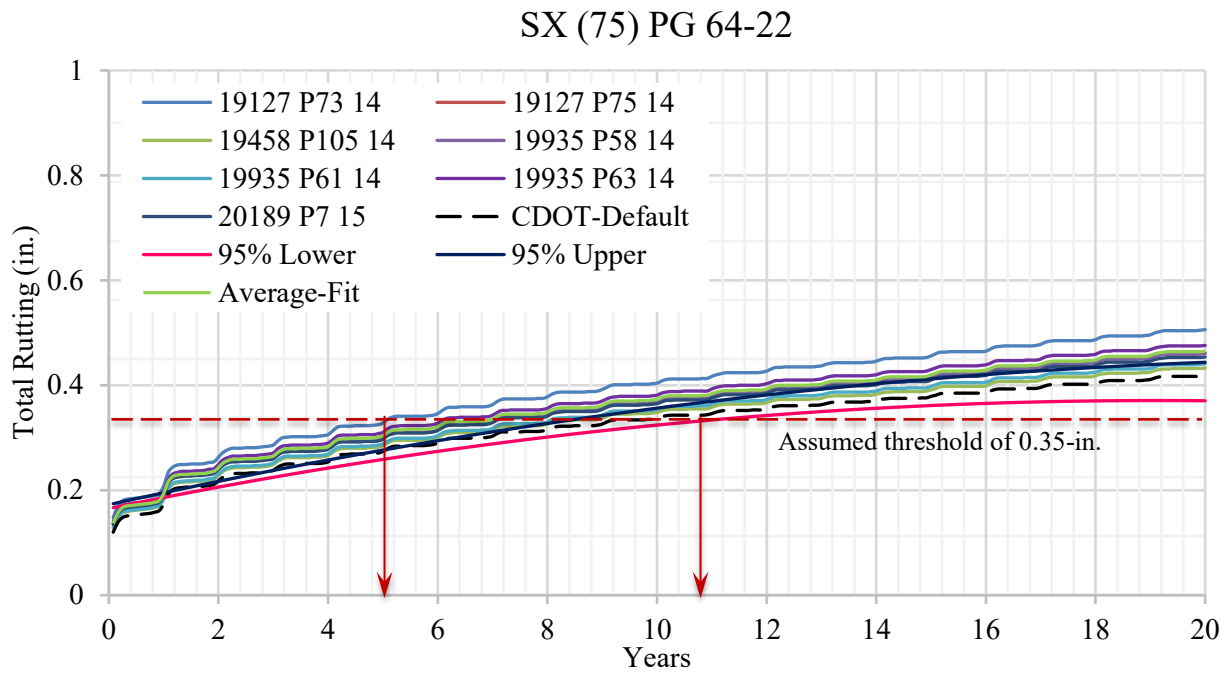


Figure 83. Total Rutting Due to AADTT = 800 by SX(75) PG 64-22 Mix

Rutting in the Asphalt Layer Only: Figures 84 and 85 show that the CDOT-default dynamic modulus data produces the lowest rutting in the asphalt layer compared to the other dynamic modulus data. For a threshold value of 0.2 in, the mixes reach the threshold from two to five years as shown in Figure 84 for high traffic. This observation is similar for the low traffic. The statistical 95% CI boundaries show that the 19458 P105 14 and 19935 P61 14 mixes are within the boundary, and statistically the same as the CDOT-default mix data.

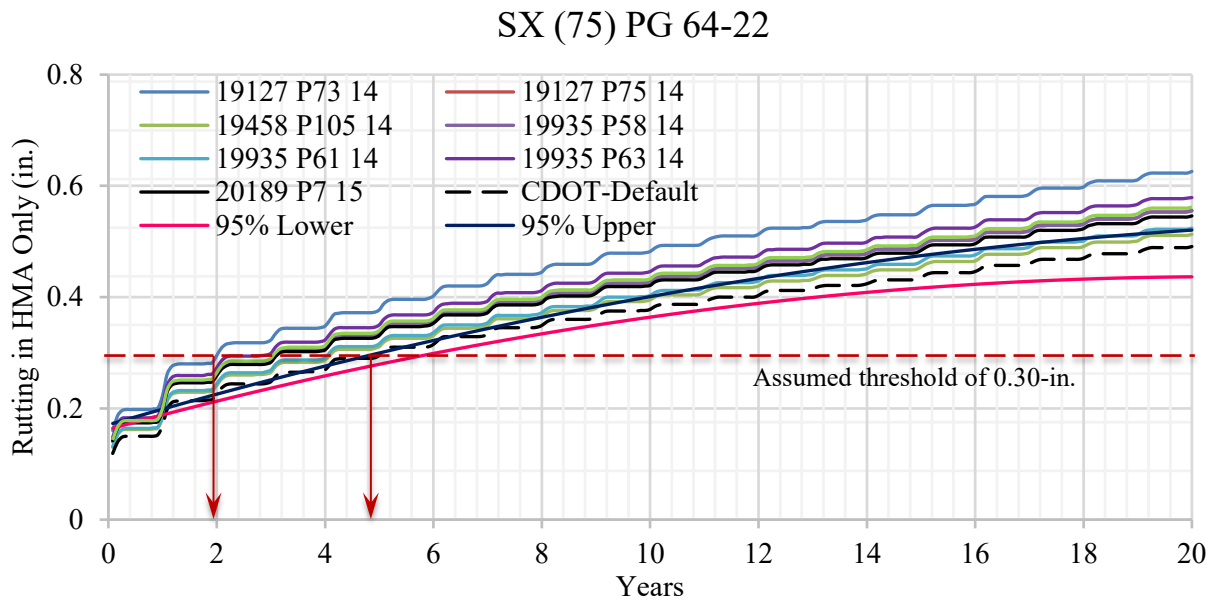


Figure 84. Rutting in Asphalt Layer Due to AADTT = 3,000 by SX(75) PG 64-22 Mix

SX (75) PG 64-22

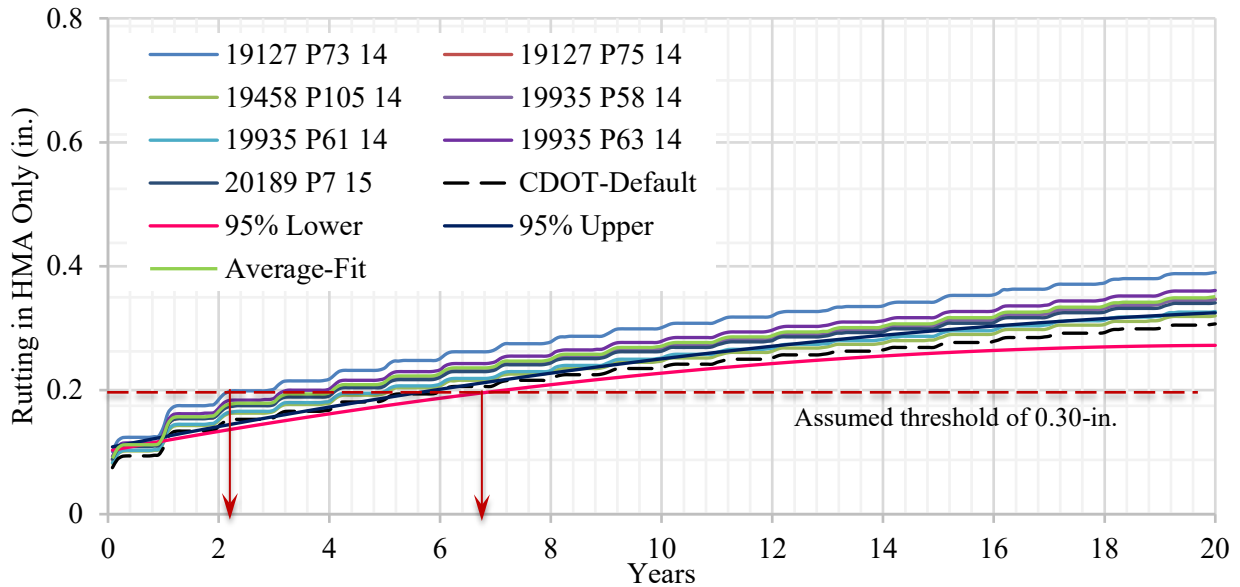


Figure 85. Rutting in Asphalt Layer Due to AADTT = 800 by SX(75) PG 64-22 Mix

Bottom-up Fatigue Cracking: Figures 86 and 87 show the CDOT-default dynamic modulus data produces the lowest bottom-up fatigue cracking compared to the other dynamic modulus data. The assumed threshold of 35% of the lane area shown in Figure 86 shows that the mixes reach the threshold in about eight years. A little higher variation in observation is obtained for low traffic as shown in Figure 87 where the threshold is assumed to be 20% of the lane area. The statistical 95% CI show that the 19458 P105 14 and 19935 P61 14 are barely within the boundary, and statistically the same as the CDOT-default mix data.

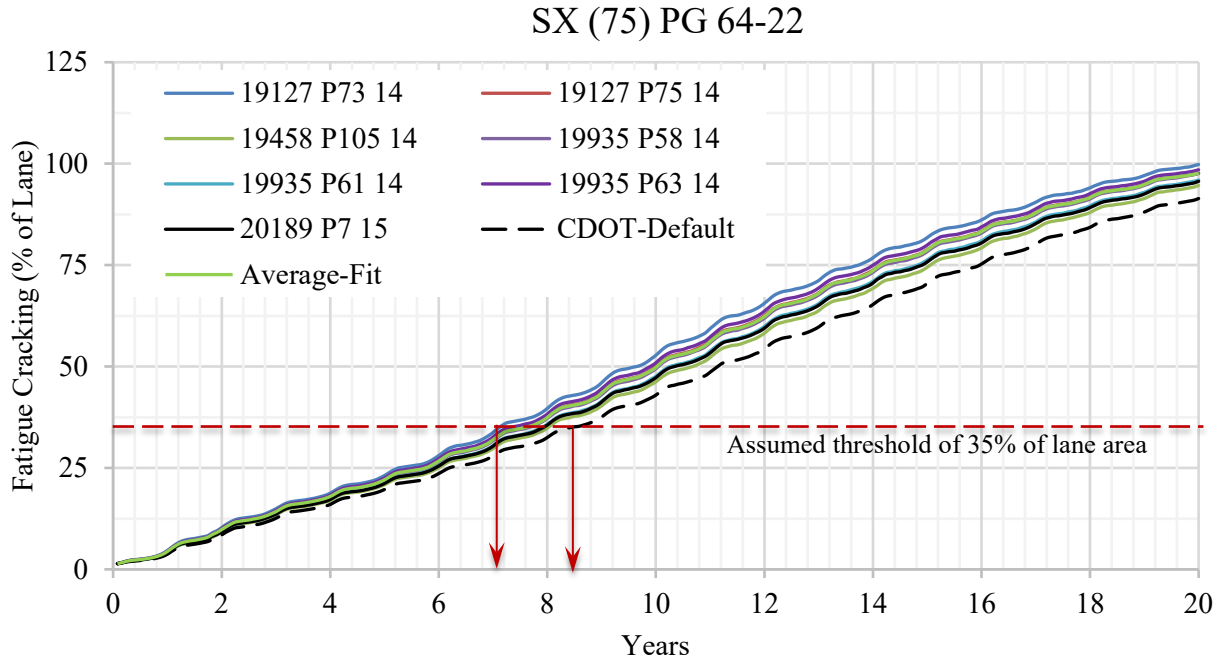


Figure 86. Bottom-up Fatigue Cracking Due to AADTT = 3,000 by SX(75) PG 64-22 Mix

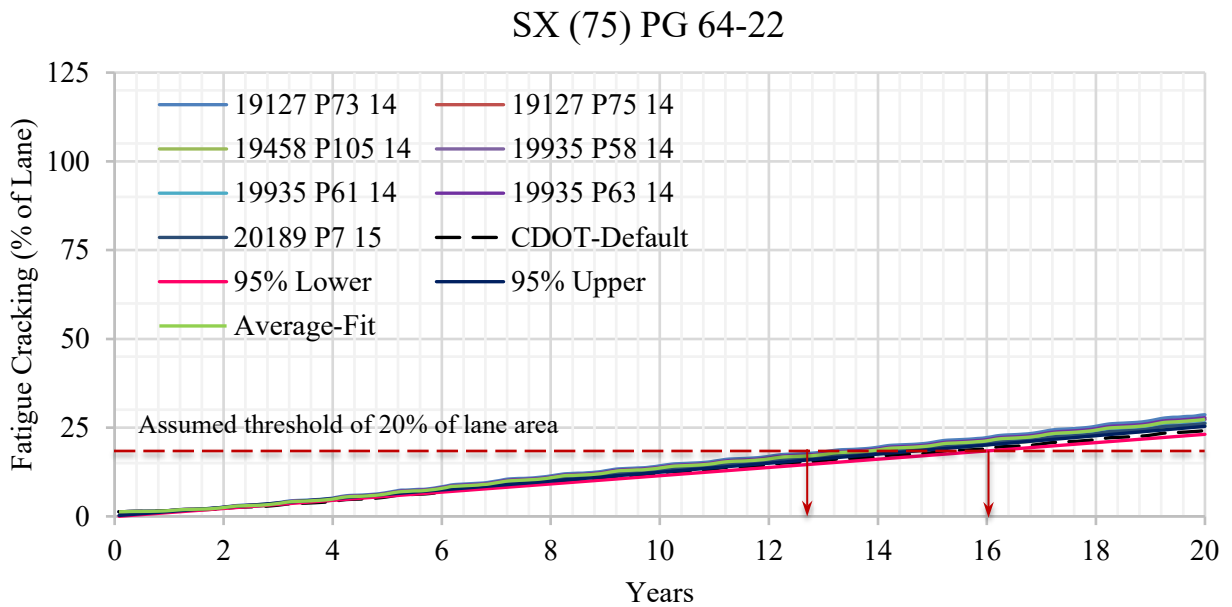


Figure 87. Bottom-up Fatigue Cracking Due to AADTT = 800 by SX(75) PG 64-22 Mix

Top-down Longitudinal Cracking: Figures 86 and 87 show that the CDOT-default dynamic modulus data produces the lowest top-down longitudinal cracking compared to the other dynamic modulus data. Mixes reach the threshold value of 2,000 ft./mi. from six to nine years for high

traffic as shown in Figure 88. This observation is similar for the low traffic where mixes reach the threshold value of 1,250 ft./mi. from 9 to 14 years as shown in Figure 89. The statistical 95% CI boundaries show that the 19458 P105 14, 19935 P61 14, and 19935 P61 14 mixes are barely within the boundary, and statistically the same as the CDOT-default mix data. The average-fit data produces the top-down longitudinal cracking, along with other distresses mentioned above, outside the 95% CI boundaries of the CDOT mix.

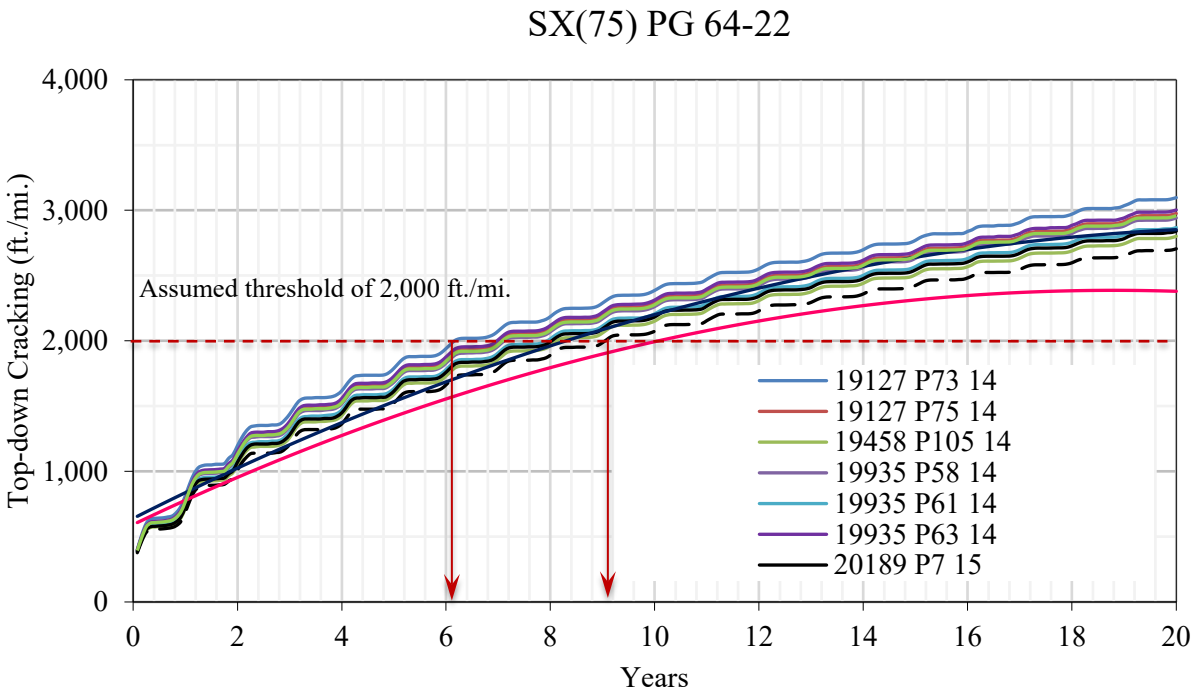


Figure 88. Longitudinal Cracking Due to AADTT = 3,000 by SX(75) PG 64-22 Mix

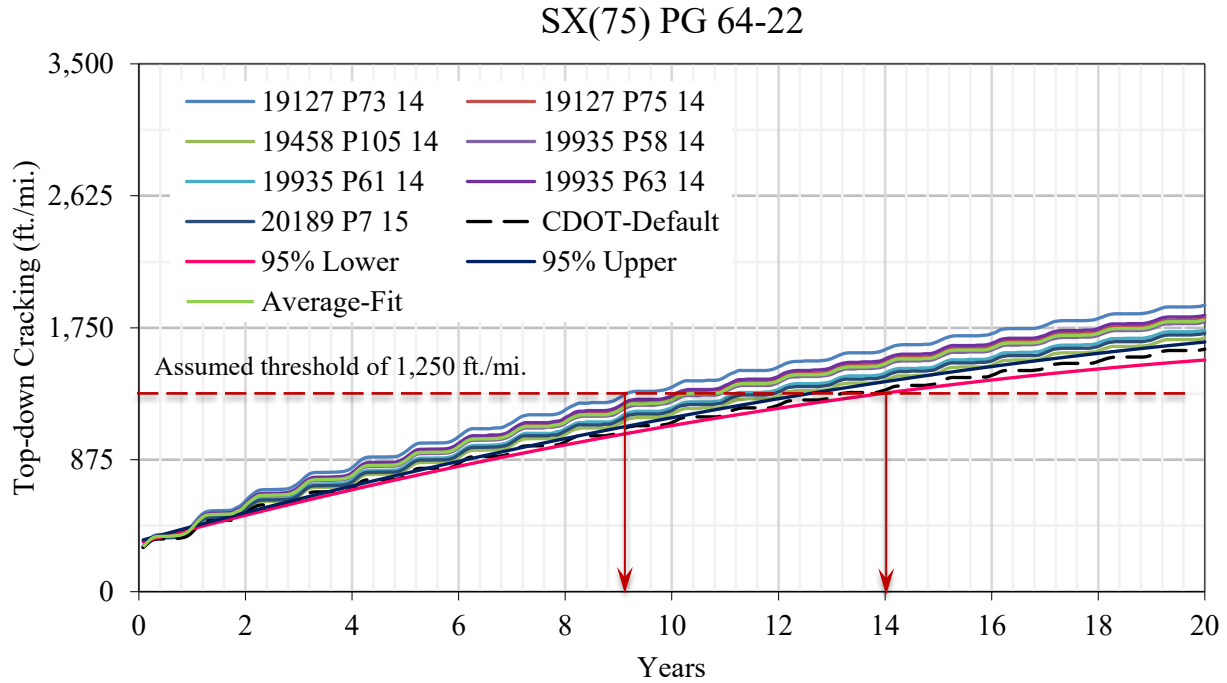


Figure 89. Longitudinal Cracking Due to AADTT = 800 by SX(75) PG 64-22 Mix

The above discussion shows that only the 19458 P105 14 and 19935 P61 14 mixes are barely within the boundary, and statistically the same as the CDOT-default mix data considering all distresses. From Table 57, the mixes that are and that are not statistically the same as the CDOT-default mix do not have different mix parameters, aside from paving contractor and aggregate source. Therefore, it can be said that the causes of the deviations are the paving contractor and the aggregate source.

To determine the influence of V_{be} , V_a , VMA, VFA, and AC, a regression analysis is conducted, and the following correlations are obtained. The R^2 of the correlations for IRI, Total Rutting, Rutting in HMA, FC, and TDC are 0.87, 0.83, 0.79, 0.92, and 0.93, respectively. It can be seen that IRI increases with the increase in V_a , and decreases with the increase in V_a , VMA, VFA, and AC. Total rutting, rutting in asphalt layer, and FC increases with the increase in V_a and VFA, and decreases with the increase in V_{be} , VMA, and AC. TDC increases with the increase in V_{be} , V_a , and VFA, and decreases with the increase in VMA, and AC.

$$\text{IRI (in./mi.)} = 29.6877 - 0.6203 V_{be} + 45.8622 V_a - 10.8097 \text{ VMA} - 2.3045 \text{ VFA} - 18.8364 \text{ AC}$$

$$\text{Total Rutting (in.)} = -0.8255 - 0.0097 V_{be} + 0.4657 V_a - 0.1044 \text{ VMA} + 0.0214 \text{ VFA} - 0.2013 \text{ AC}$$

$$\text{Rutting in HMA (in.)} = -1.0506 - 0.0134 V_{be} + 0.4991 V_a - 0.123 \text{ VMA} + 0.0253 \text{ VFA} - 0.1989 \text{ AC}$$

$$\text{FC (\%)} = -10.7754 - 0.0337 V_{be} + 7.1573 V_a - 1.7398 \text{ VMA} + 0.3717 \text{ VFA} - 2.8436 \text{ AC}$$

$$\text{TDC (ft./mi.)} = -2156.54 + 0.9252 V_{be} + 1150.866 V_a - 269.071 \text{ VMA} + 61.4465 \text{ VFA} - 433.627 \text{ AC}$$

SX(75) PG 64-28

Table 58 lists the mix parameters, aggregate pits, binder suppliers and contractor information of the SX(75) PG 64-28 mix. Mix parameters includes V_{be} , V_a , VMA, VFA, and AC. All this information is used while analyzing the performance of different mixes as discussed below.

Table 58. Generic Information of SX(75) PG 64-28 Mix

	Paving Contractor	Binder Supplier	Region	Date	V_{be} (%)	V_a (%)	VMA (%)	VFA (%)	AC (%)	Pit
16439 P77 14	Everist	Suncor	3	6/2015	12.73	7.08	18.9	62.5	5.80	Maryland Creek Ranch
19356 P22 15	Asphalt Specialties	Suncor	4	7/2016	10.92	5.30	17.7	60.9	5.51	Spec Agg, Turnpike, Bestway Firestone
20098 P19 15	Coulson	Suncor	4	5/2016	10.84	6.52	18.0	62.1	5.37	Bonser, Lien
20098 P23 15	Coulson	Suncor	4	8/2016	11.01	6.52	17.9	61.4	5.61	Bonser, Lien

International Roughness Index: Figures 90 and 91 show the IRI of the trial pavement with the service life of the pavement for high traffic (AADTT = 7,000) and low traffic (AADTT = 800), respectively. They show that the prediction of IRI of this mix using the dynamic moduli determined

by different contractors is very consistent. The produced IRI by the CDOT-default data is the lowest compared to all mixes. Assumed threshold values of 200 in./mi. and 200 in./mi. are drawn in Figures 90 and 91, respectively. Figure 90 shows that the mixes reach the threshold in about 12 years for high traffic. Similar observation is obtained for low traffic as shown in Figure 91.

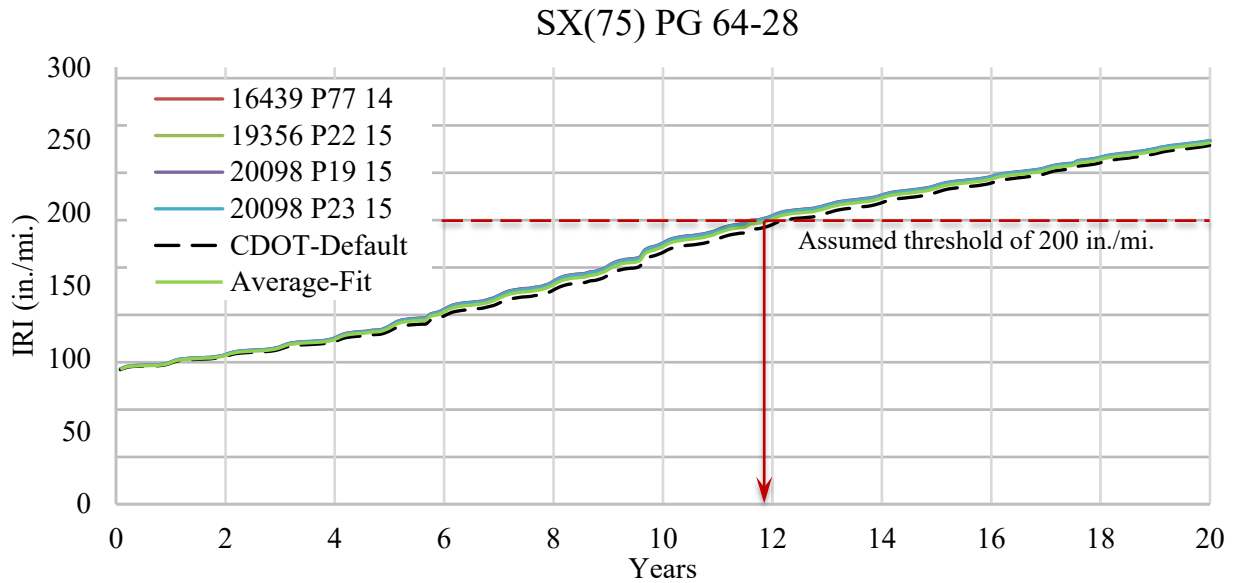


Figure 90. IRI Due to AADTT = 3,000 by SX(75) PG 64-28 Mix

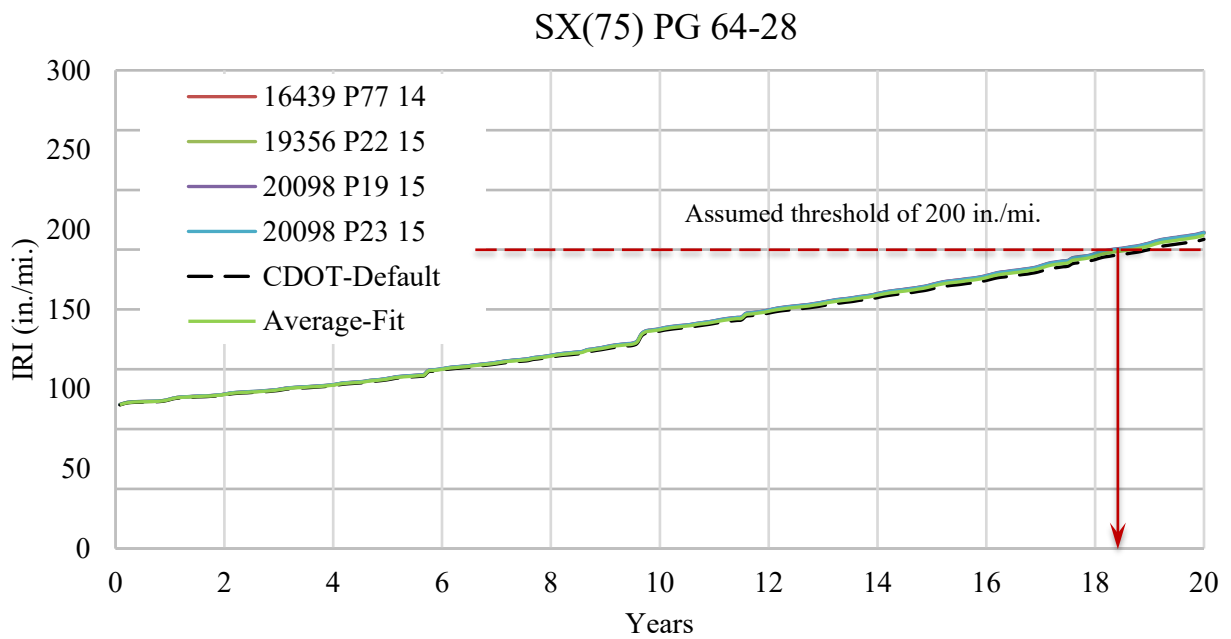


Figure 91. IRI Due to AADTT = 800 by SX(75) PG 64-28 Mix

Total Rutting: The CDOT-default mix produces the lowest amount of total rutting, although very close in value to the others (Figures 92 and 93). For a threshold value of 0.4 in, the mixes reach the threshold from 10 to 12 years as shown in Figure 92 for high traffic. This observation is similar for the low traffic. The statistical analysis shows that distresses produced by all mixes are within the 95% CI boundaries of the CDOT mix.

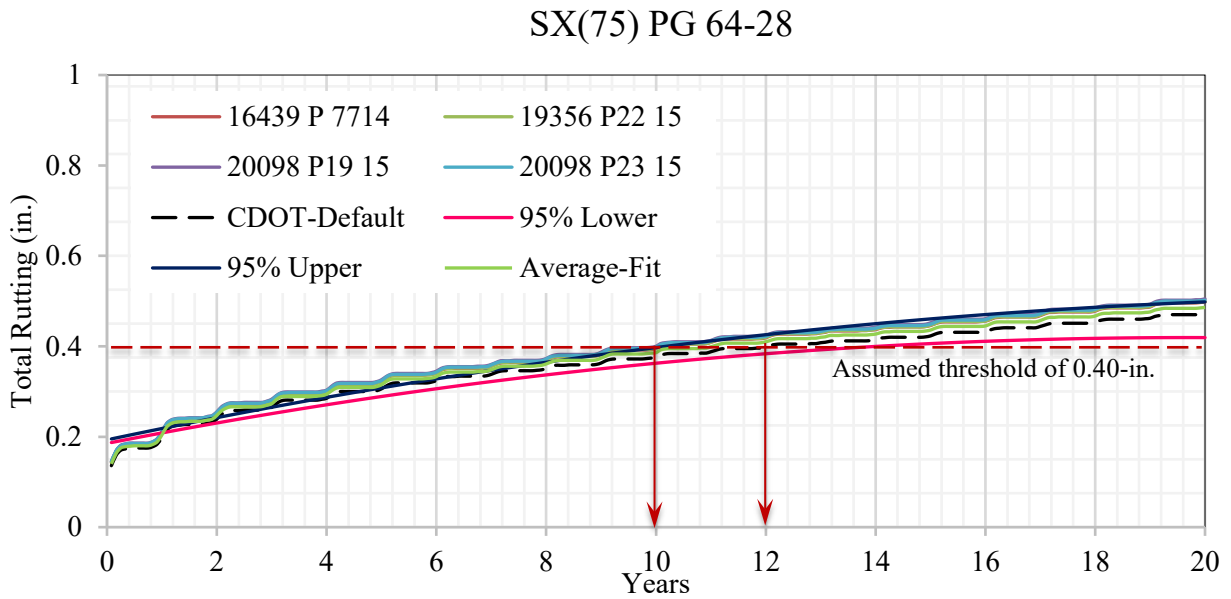


Figure 92. Total Rutting Due to AADTT = 3,000 by SX(75) PG 64-28 Mix

SX(75) PG 64-28

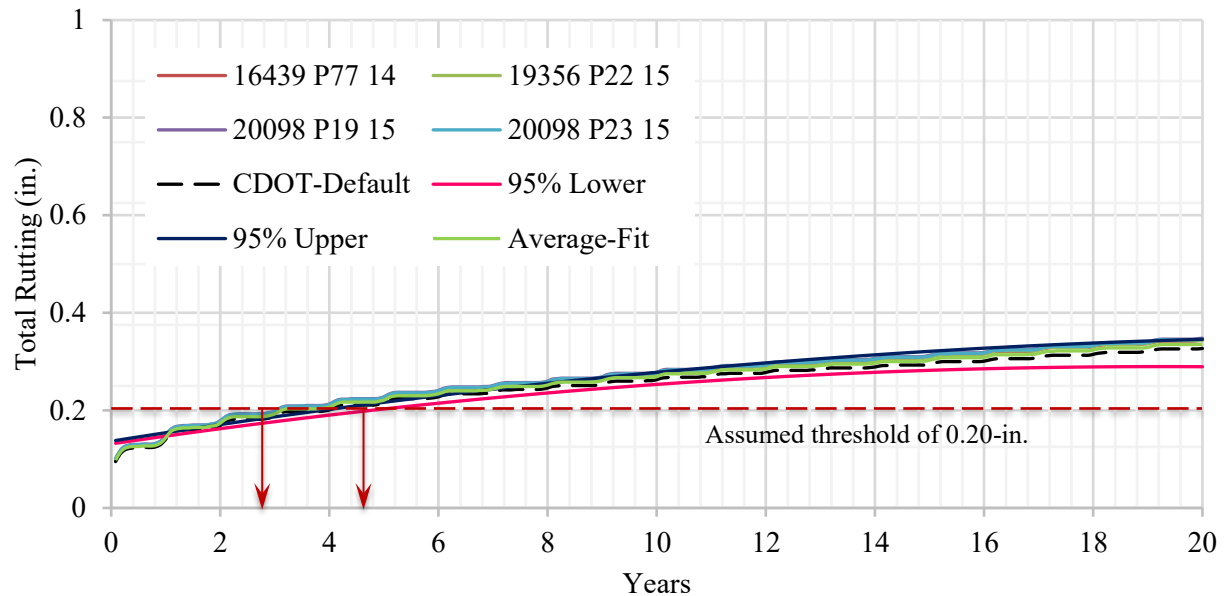


Figure 93. Total Rutting Due to AADTT = 800 by SX(75) PG 64-28 Mix

Rutting in the Asphalt Layer Only: Similar to total rutting, the CDOT-default data produces the lowest amount of total rutting in the asphalt layer, although very close in value to the others (Figures 94 and 95). For a threshold value of 0.3 in, the mixes reach the threshold from 14 to 17 years as shown in Figure 94 for high traffic. This observation is similar for the low traffic. The statistical analysis shows that distresses produced by no mix are within the 95% CI boundaries of the CDOT mix. However, the predictions by different mixes are very consistent with each other.

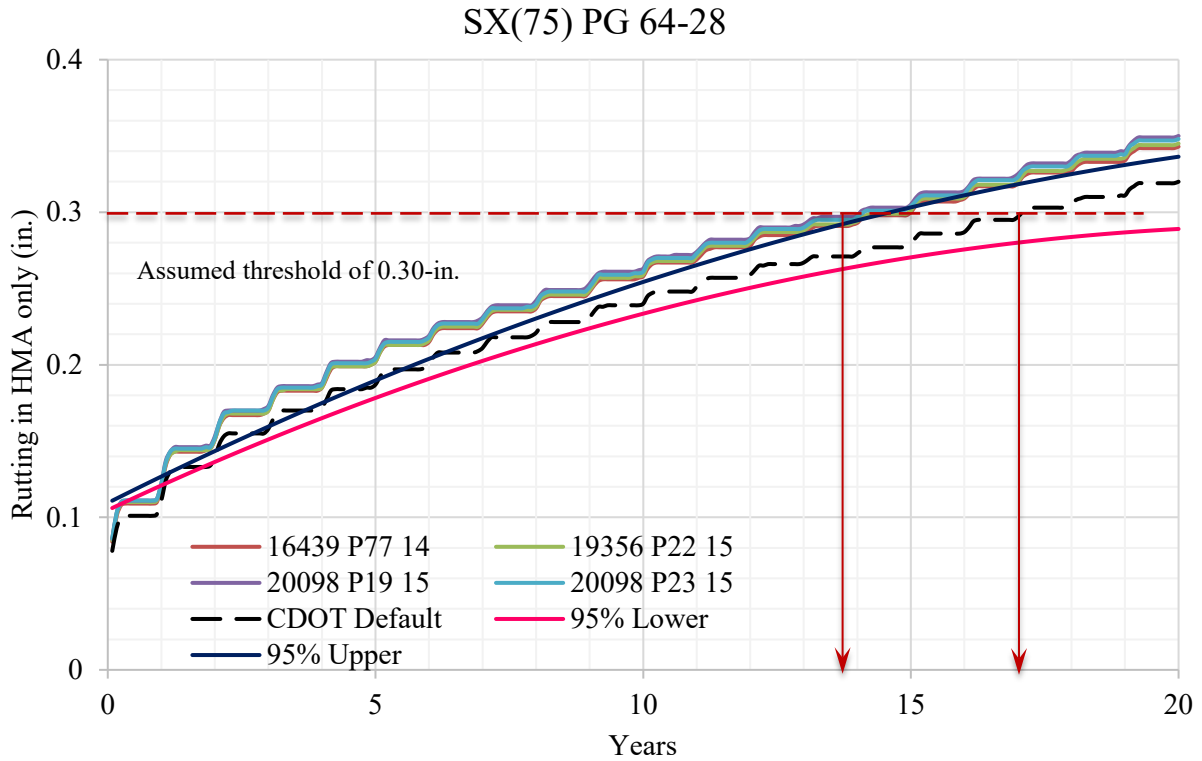


Figure 94. Rutting in Asphalt Layer Due to AADTT = 3,000 by SX(75) PG 64-28 Mix

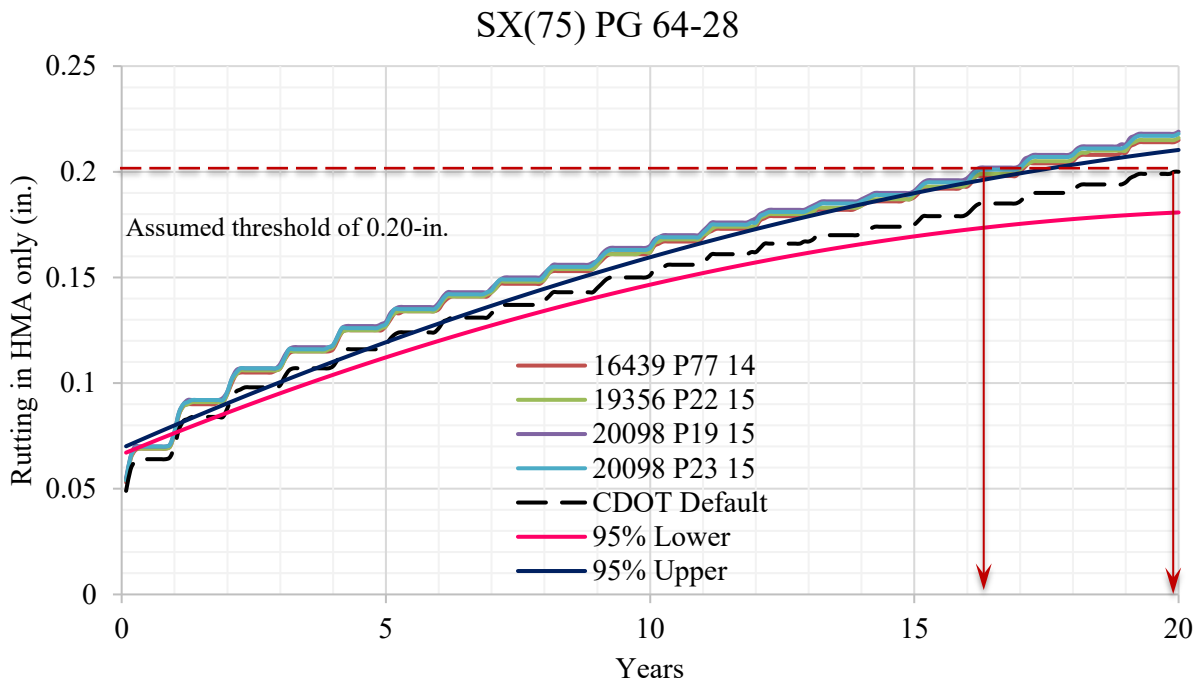


Figure 95. Rutting in Asphalt Layer Due to AADTT = 800 by SX(75) PG 64-28 Mix

Bottom-up Fatigue Cracking: Similar to total rutting, the CDOT-default data produces the amount of bottom-up fatigue cracking in asphalt layer, although very close in value to the others (Figures 96 and 97). The assumed threshold of 30% of the lane area shown in Figure 96 shows that the mixes reach the threshold in about five years. Similar observation is obtained for low traffic as shown in Figure 97 where the threshold is assumed to be 30% of the lane area. The statistical analysis shows that distresses produced by no mix are within the 95% CI boundaries of the CDOT-default mix. However, the predictions by different mixes are very consistent with each other.

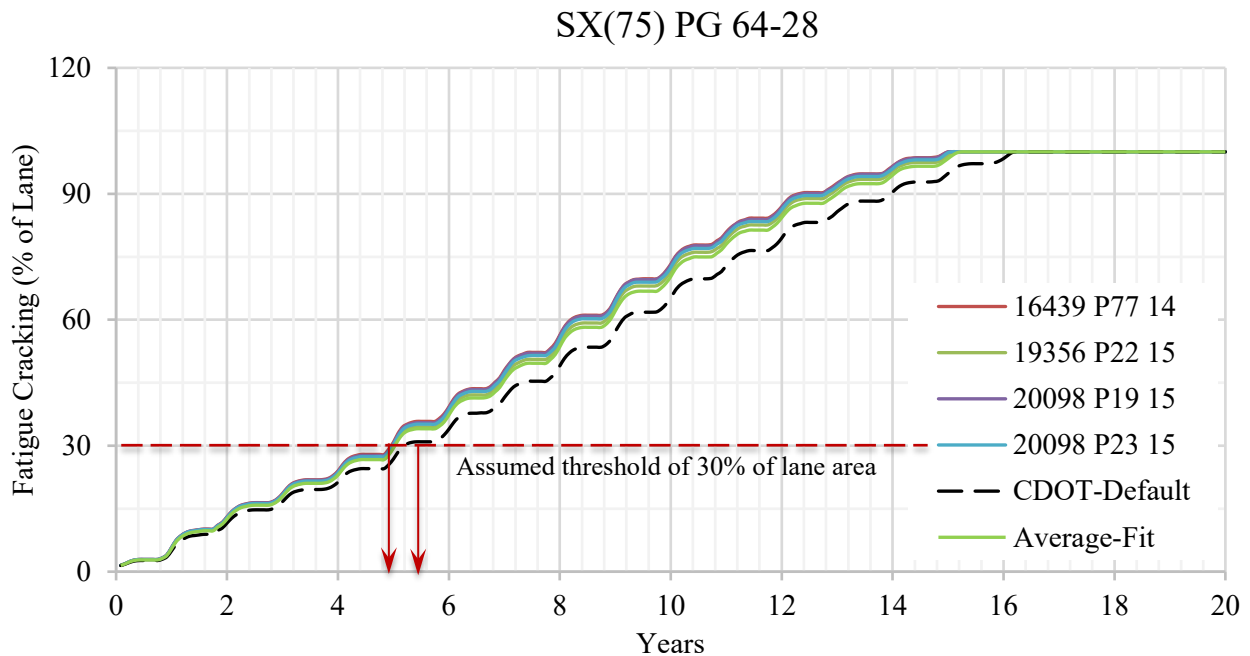


Figure 96. Bottom-up Fatigue Cracking Due to AADTT = 3,000 by SX(75) PG 64-28 Mix

SX(75) PG 64-28

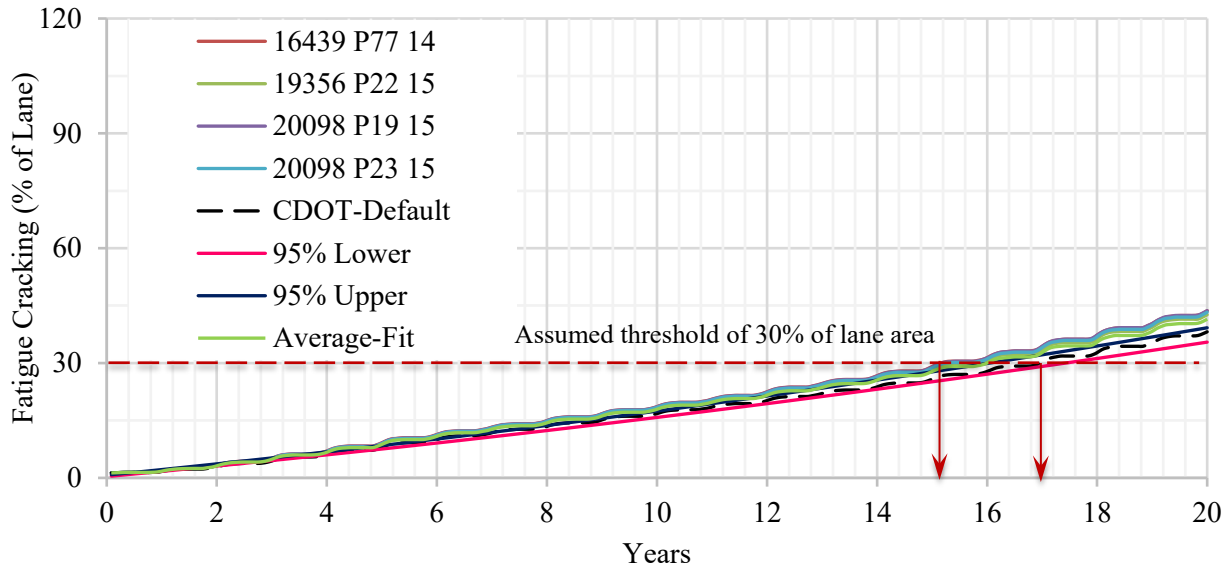


Figure 97. Bottom-up Fatigue Cracking Due to AADTT = 800 by SX(75) PG 64-28 Mix

Top-down Longitudinal Cracking: Similar to other distresses, the CDOT-default data produces the lowest, but very close, amount of total rutting in asphalt layer compared with others (Figures 98 and 99). The statistical analysis shows distresses produced by all mixes are within the 95% CI boundaries of the CDOT mix, and the predictions by different mixes are very consistent with each other. The average-fit data produces the top-down longitudinal cracking, along with other distresses mentioned above, within the 95% CI boundaries of the CDOT mix. Mixes reach the threshold value of 1,500 ft./mi. from three to four years for high traffic as shown in Figure 98. This observation is similar for the low traffic where mixes reach the threshold value of 1,500 ft./mi. from 11 to 14 years as shown in Figure 99.

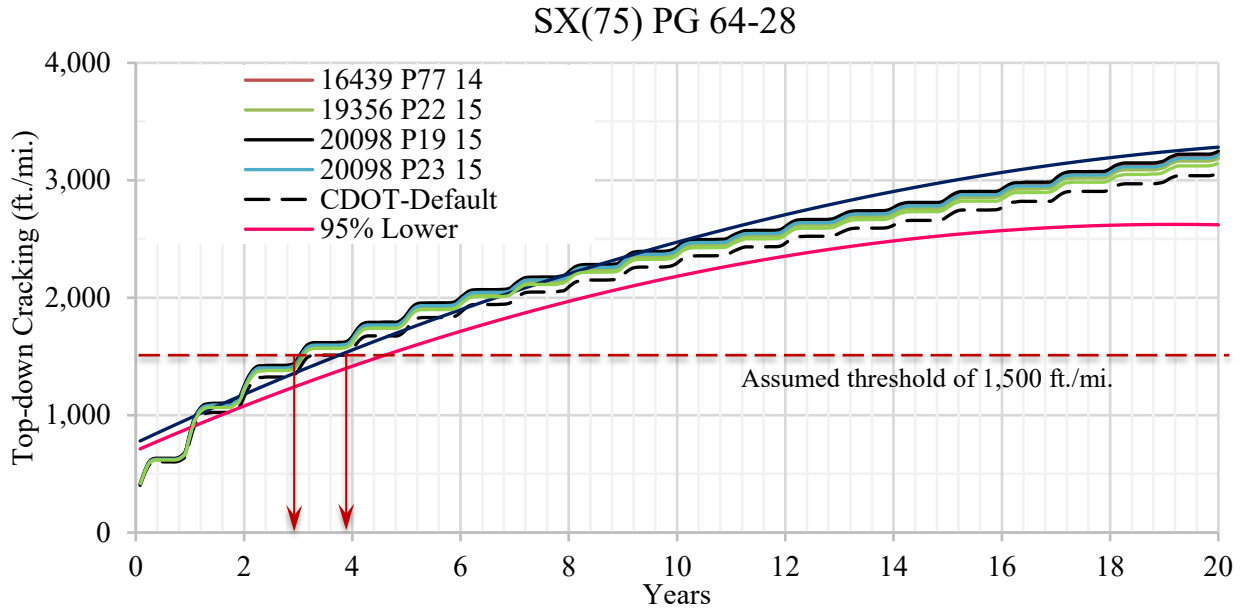


Figure 98. Longitudinal Cracking Due to AADTT = 3,000 by SX(75) PG 64-28 Mix

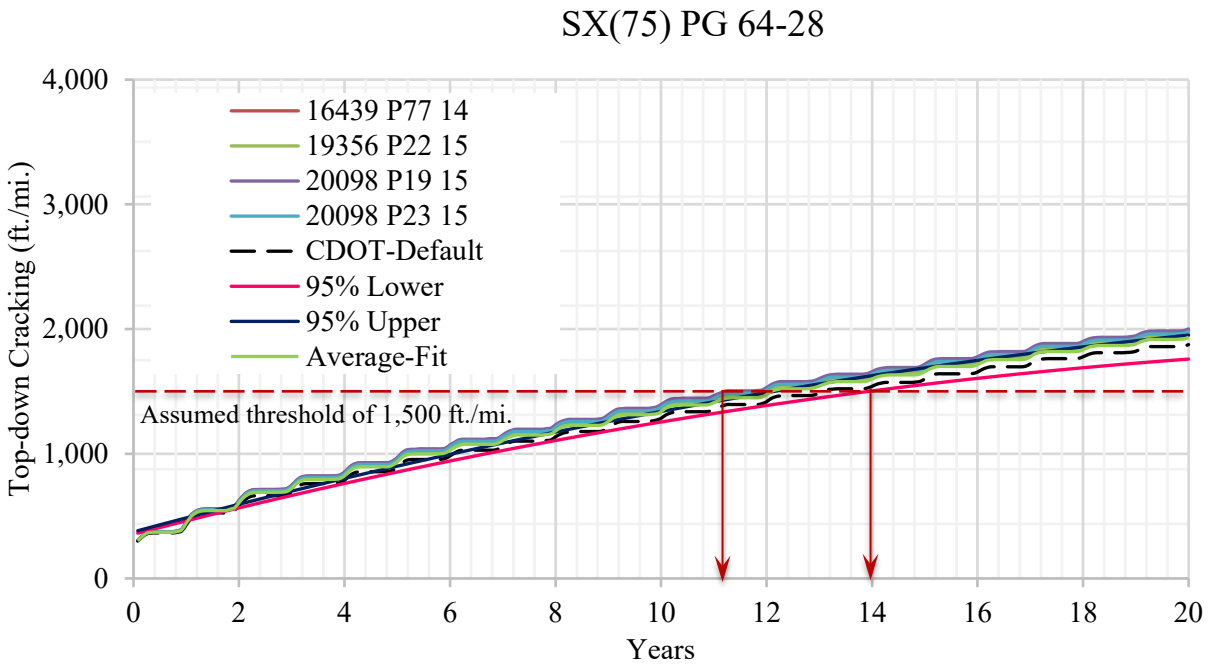


Figure 99. Longitudinal Cracking Due to AADTT = 800 by SX(75) PG 64-28 Mix

The analysis of the distress data shows that all mixes produced distresses outside the statistical 95% CI boundaries, and they are not statistically the same as the CDOT-default mix. The mix

parameters listed in Table 58 show that the mixes have different paving contractors, production dates, effective binder contents, air voids, VMAs, VFAs, asphalt content, and aggregate sources. However, their predictions are very consistent. Therefore, the effect of an individual mix parameter could not be found for this mix.

To determine the influence of V_{be} , V_a , VMA, VFA, and AC, a regression analysis is conducted, and the following correlations are obtained. The R^2 of all correlations is 1.0. It can be seen that IRI, total rutting, FC, and TDC increases with the increase in V_a and VFA, decreases with the increase in V_{be} , and are insensitive to VMA and AC. Correlation for rutting in asphalt layer could not be made due to insufficient data.

$$\text{IRI (in./mi.)} = 140.4017 - 0.3116 V_{be} + 0.417 V_a + 0.6386 \text{ VFA}$$

$$\text{Total Rutting (in.)} = 0.3035 - 0.0034 V_{be} + 0.0011 V_a + 0.002 \text{ VFA}$$

$$\text{FC (\%)} = 5.7163 - 0.0495 V_{be} + 0.0991 V_a + 0.2051 \text{ VFA}$$

$$\text{TDC (ft./mi.)} = 492.5526 - 14.9885 V_{be} + 3.6608 V_a + 33.4457 \text{ VFA}$$

SX(100) PG 58-28

International Roughness Index: Figures 100 and 101 show the IRI of the trial pavement with the service life of the pavement. It shows that the prediction of IRI of this mix, using the dynamic moduli determined by 18887 P15 14 and the CDOT-default mix data, is consistent. Assumed threshold values of 200 in./mi. and 180 in./mi. are drawn in Figures 100 and 101, respectively. Figure 100 shows that the mixes reach the threshold in about 16 years for high traffic. Similar observation is obtained for low traffic as shown in Figure 111.

SX(100) PG 58-28

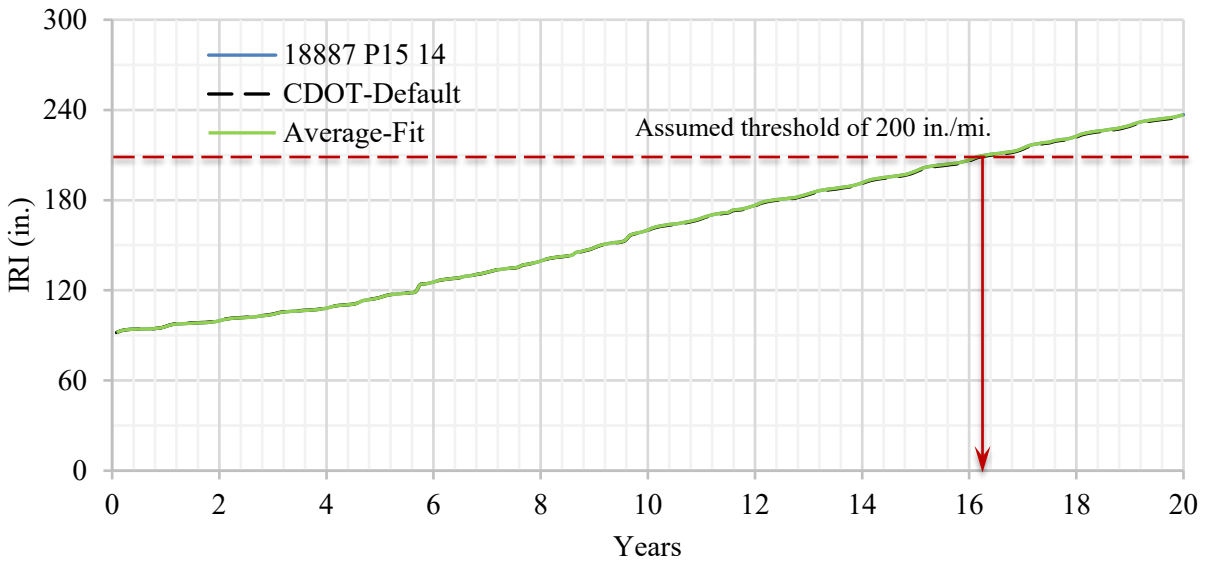


Figure 100. IRI Due to AADTT = 7,000 by SX(100) PG 58-28 Mix

SX(100) PG 58-28

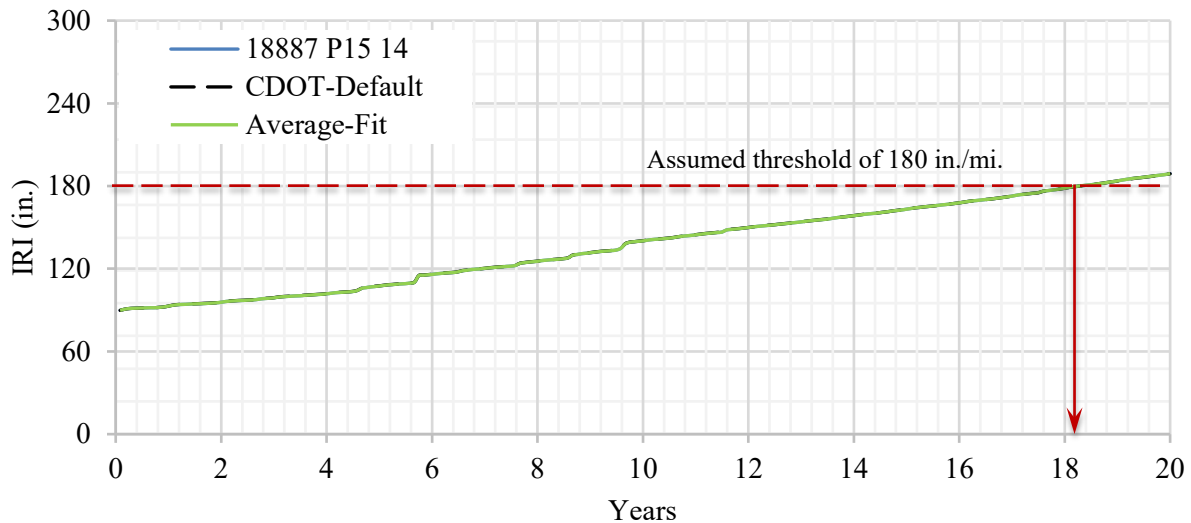


Figure 101. IRI Due to AADTT = 800 by SX(100) PG 58-28 Mix

Total Rutting: Figures 102 and 103 show the total rutting of the trial pavement with the service life of the pavement. It can be seen that the prediction of total rutting of this mix, using the dynamic moduli determined by 18887 P15 14 and the CDOT-default mix data, is consistent. For a threshold value of 0.3 in, the mixes reach the threshold from six to seven years as shown in Figure 102 for

high traffic. This observation is similar for the low traffic. The statistical analysis shows that total rutting produced by both mixes are within the 95% CI boundaries of the CDOT mix, and the 18887 P15 14 mix is statistically the same as the CDOT-default mix.

SX(100) PG 58-28

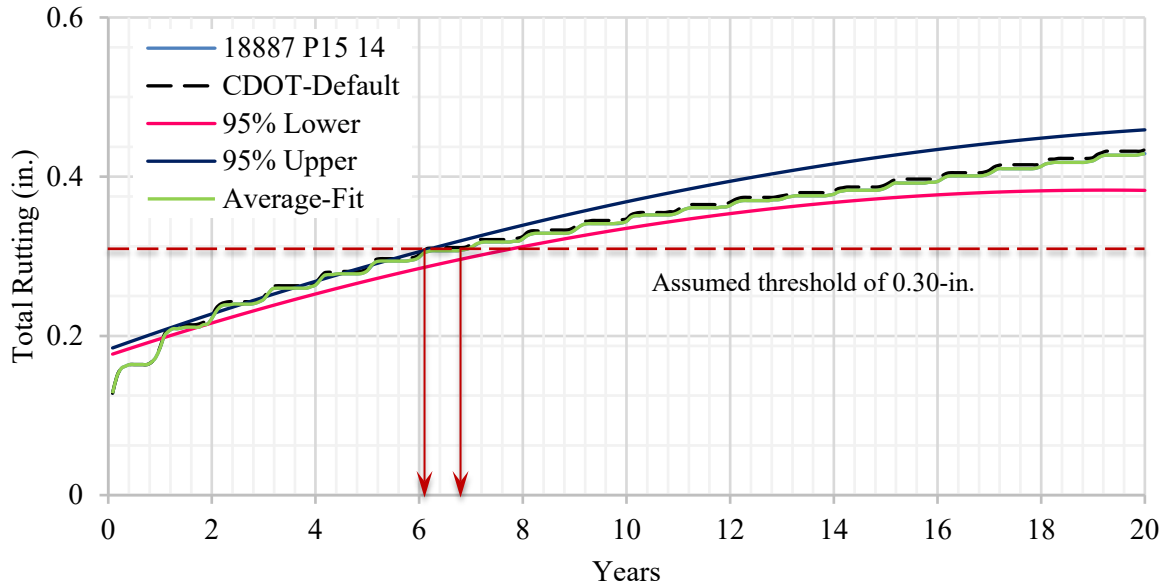


Figure 102. Total Rutting Due to AADTT = 7,000 by SX(100) PG 58-28 Mix

SX(100) PG 58-28

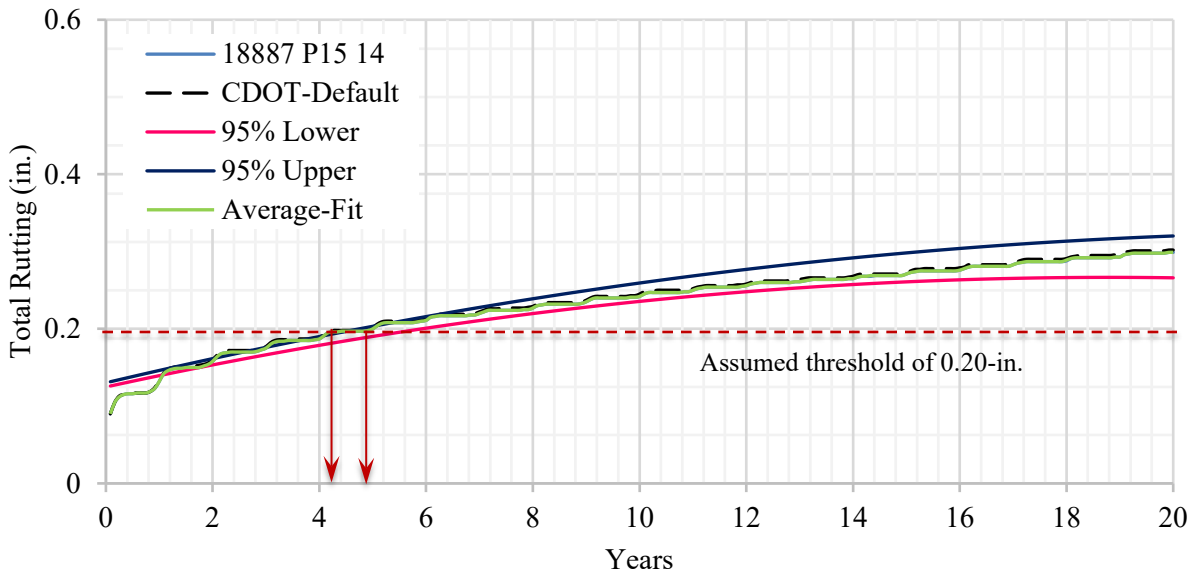


Figure 103. Total Rutting Due to AADTT = 800 by SX(100) PG 58-28 Mix

Rutting in Asphalt Layer Only: Figures 104 and 105 show the rutting in asphalt layer of the trial pavement with the service life of the pavement. It can be seen that the prediction of rutting in asphalt layer of this mix, using the dynamic moduli determined by 18887 P15 14 and the CDOT-default mix data, is consistent. For a threshold value of 0.15 in, the mixes reach the threshold from three to four years as shown in Figure 104 for high traffic. This observation is similar for the low traffic. The statistical analysis shows that rutting in the asphalt layer produced by both mixes are within the 95% CI boundaries of the CDOT mix, and the 18887 P15 14 mix is statistically the same as the CDOT-default mix.

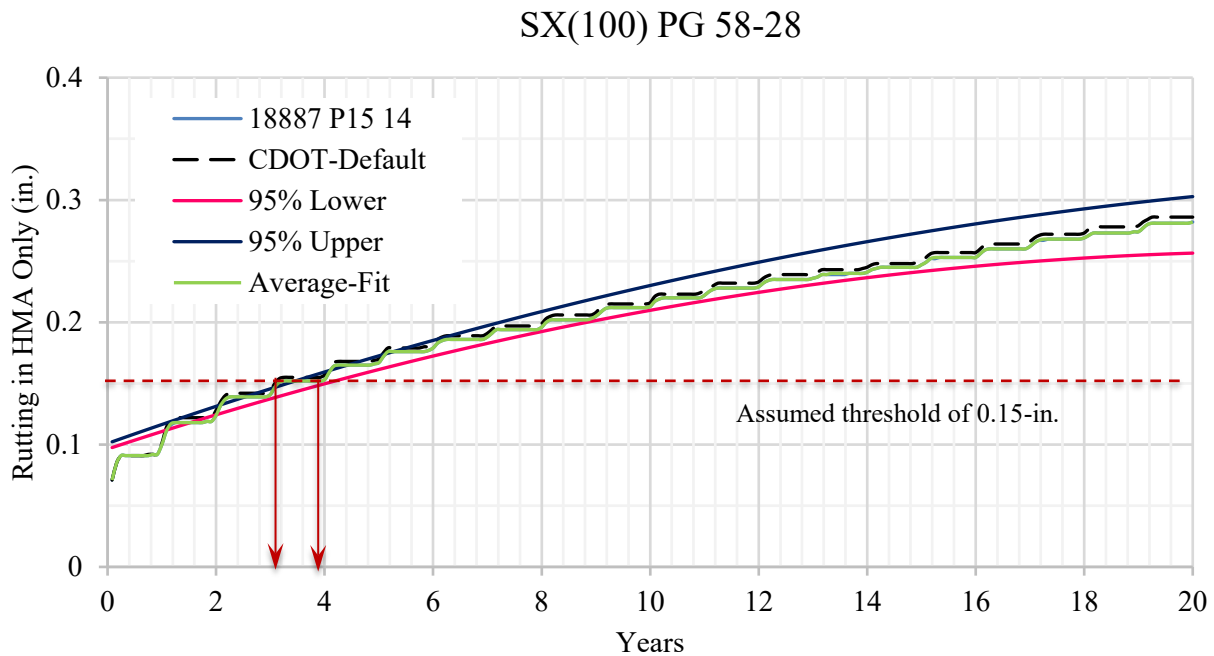


Figure 104. Rutting in Asphalt Layer Due to AADTT = 7,000 by SX(100) PG 58-28 Mix

SX(100) PG 58-28

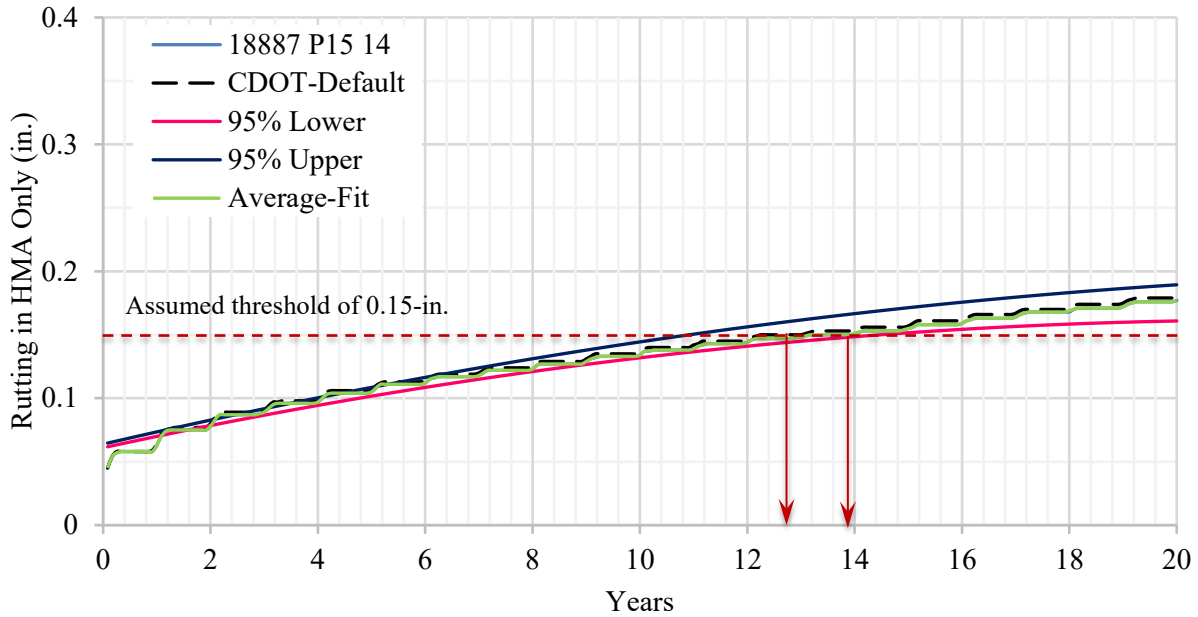


Figure 105. Rutting in Asphalt Layer Due to AADTT = 800 by SX(100) PG 58-28 Mix

Bottom-up Fatigue Cracking: Figures 106 and 107 show the bottom-up fatigue cracking of the trial pavement with the service life of the pavement. It can be seen that the prediction of bottom-up fatigue cracking of this mix, using the dynamic moduli determined by 18887 P15 14 and the CDOT-default mix data, are consistent. The assumed threshold of 25% of the lane area shown in Figure 106 shows that the mixes reach the threshold in about seven years by all mixes, which is very close to each other. Little higher variation in observation is obtained for low traffic as shown in Figure 107 where the threshold is assumed to be 20% of the lane area. The statistical analysis shows that the bottom-up fatigue cracking produced by both mixes are within the 95% CI boundaries of the CDOT mix, and the 18887 P15 14 mix is statistically the same as the CDOT-default mix.

SX(100) PG 58-28

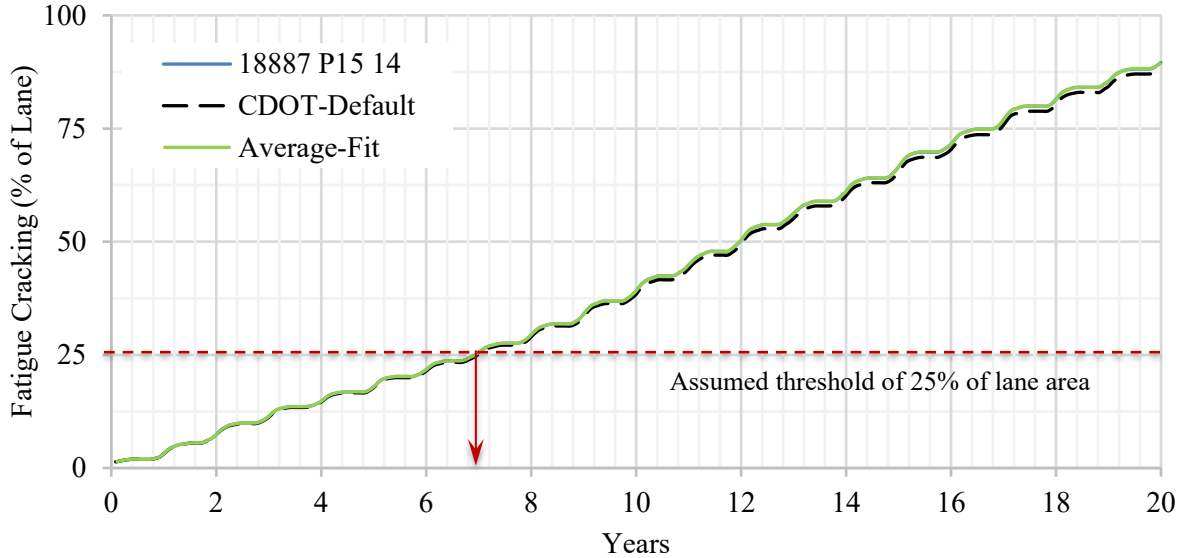


Figure 106. Bottom-up Fatigue Cracking Due to AADTT = 7,000 by SX(100) PG 58-28 Mix

SX(100) PG 58-28

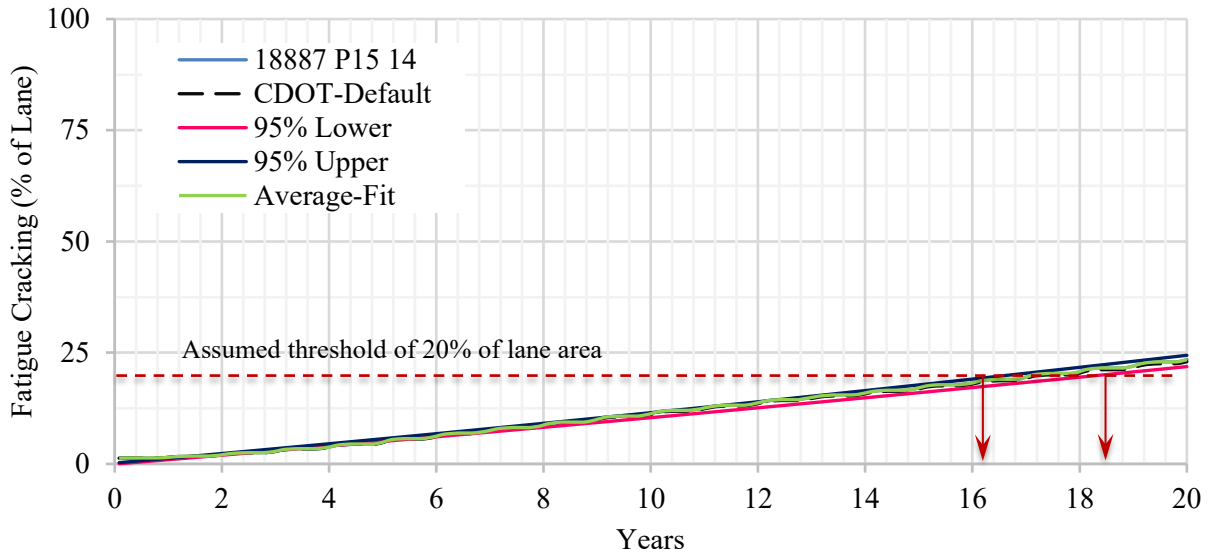


Figure 107. Bottom-up Fatigue Cracking Due to AADTT = 800 by SX(100) PG 58-28 Mix

Top-down Longitudinal Cracking: Figures 108 and 109 show the top-down longitudinal cracking of the trial pavement with the service life of the pavement. It can be seen that the prediction of top-down longitudinal cracking of this mix, using the dynamic moduli determined

by 18887 P15 14 and the CDOT-default mix data, is consistent. The statistical analysis shows that the top-down longitudinal cracking produced by both mixes are within the 95% CI boundaries of the CDOT mix, and the mix 18887 P15 14 is statistically the same as the CDOT-default mix. The average-fit data produces the top-down longitudinal cracking, along with other distresses mentioned above, within the 95% CI boundaries of the CDOT mix. Mixes reach the threshold value of 1,500 ft./mi. in about 7 years for high traffic as shown in Figure 108. This observation is similar for the low traffic where mixes reach the threshold value of 1,250 ft./mi. in about 15 years as shown in Figure 109.

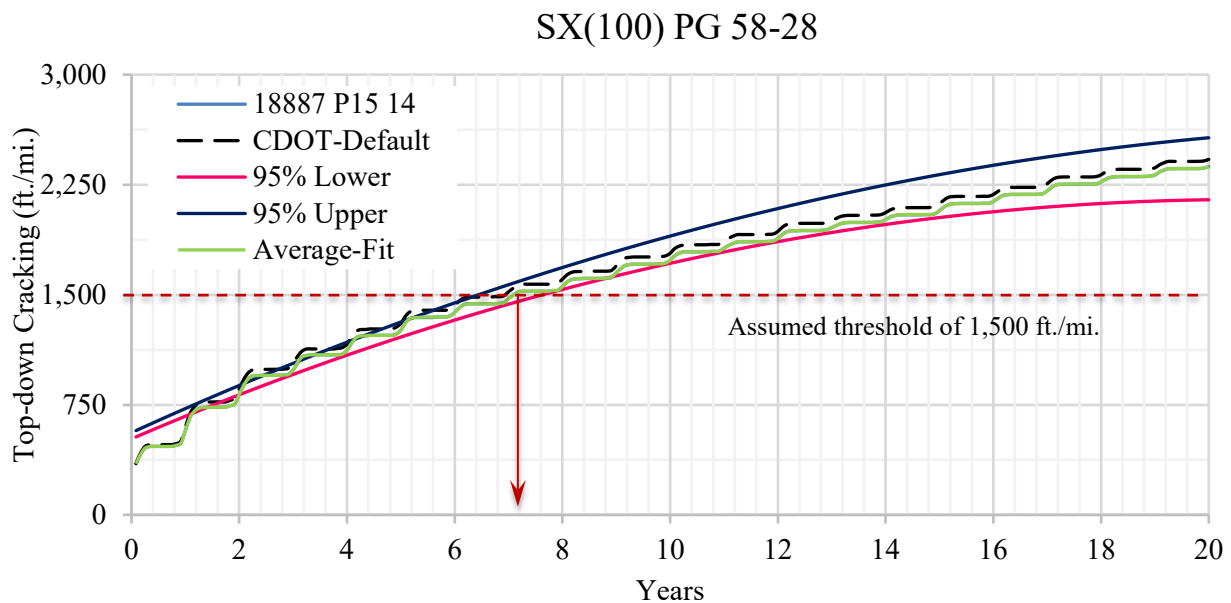


Figure 108. Longitudinal Cracking Due to AADTT = 7,000 by SX(100) PG 58-28 Mix

SX(100) PG 58-28

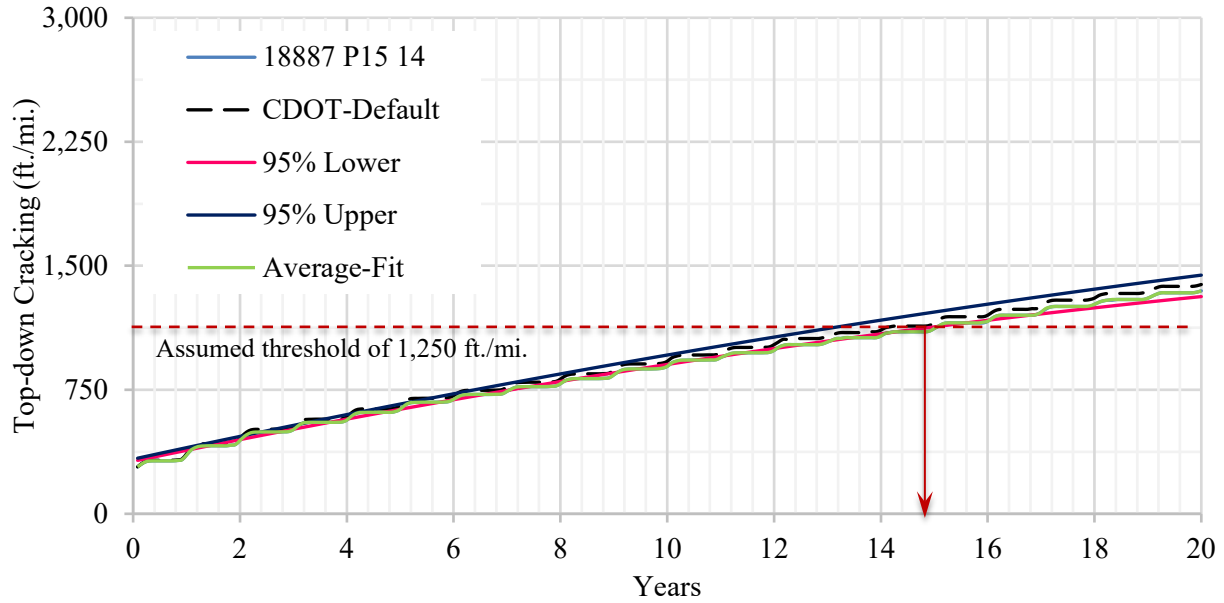


Figure 109. Longitudinal Cracking Due to AADTT = 800 by SX(100) PG 58-28 Mix

SX(100) PG 64-22

Table 59 lists the mix parameters, aggregate pits, binder suppliers and contractor information of the SX(100) PG 64-22 mix. Mix parameters includes V_{be} , V_a , VMA, VFA, and AC. All this information is used while analyzing the performance of different mixes as discussed below.

Table 59. Generic Information of SX(100) PG 64-22 Mix

	Paving Contractor	Binder Supplier	Region	Date	V_{be} (%)	V_a (%)	VMA (%)	VFA (%)	AC (%)	Pit
18180 P3 14	Aggregate Industries	Aggregate Industries	1	6/2014	12.24	6.66	17.1	61.2	5.00	Morrison, Plate River
18180 P4 14	Aggregate Industries	Suncor	--	6/2014	10.31	6.66	17.9	63.4	5.00	Morrison, Plate River
18842 P10 14	Kiewit Construction	Suncor	2	7/2014	11.63	5.00	18.3	62.8	5.30	Tezak Fountain / I25
18842 P16 14	Kiewit Construction	Suncor	2	7/2014	11.39	6.98	18.4	62.4	5.30	Tezak Fountain / I25
18842 P22 14	Kiewit Construction	Suncor	2	8/2014	11.44	6.52	18.1	64.3	5.30	Tezak Fountain / I25
19128 P81 14	Martin Marietta	Suncor	2	7/2015	13.18	6.90	17.6	60.8	5.50	Evans
19202 P107 14	Skanska	Suncor	5	1/2015	11.94	6.00	18.8	64.2	6.34	Four Corners
19202 P112 14	Skanska	Suncor	5	1/2015	11.29	6.00	18.3	61.2	5.95	Four Corners
19275 P1 14	APC Southern	Holly Frontier	2	6/2014	13.41	5.78	17.0	66.3	5.65	---
19275 P2 14	APC Southern	Holly Frontier	2	6/2014	13.41	6.60	18.1	65.9	5.65	---
19275 P5 14	Aggregate Industries	Holly Frontier	2	6/2014	13.41	6.14	17.3	65.2	5.65	---
19300 P34 14	United Companies	Suncor	3	9/2014	12.04	5.64	16.7	66.4	6.00	Craig Ranch
19655 P18 14	APC Southern	Holly Frontier	2	7/2014	11.05	6.06	16.7	64.3	5.60	Valardi
19904 P14 15	Martin Marietta	Suncor	1	5/2016	13.43	6.40	17.1	62.5	5.50	Spec Agg / Riverbend / Cottonwood

International Roughness Index: Figures 110 and 111 show the IRI of the trial pavement with the service life of the pavement for high traffic (AADTT = 7,000) and low traffic (AADTT = 800), respectively. They show that the prediction of IRI by the CDOT-default mix (except 19128 P81 14) data is the lowest. The IRI prediction by the other mixes are consistent. Assumed threshold values of 200 in./mi. and 150 in./mi. are drawn in Figures 110 and 111, respectively. Figure 110 shows that the mixes reach the threshold from seven to nine years for high traffic. Similar observation is obtained for low traffic as shown in Figure 111.

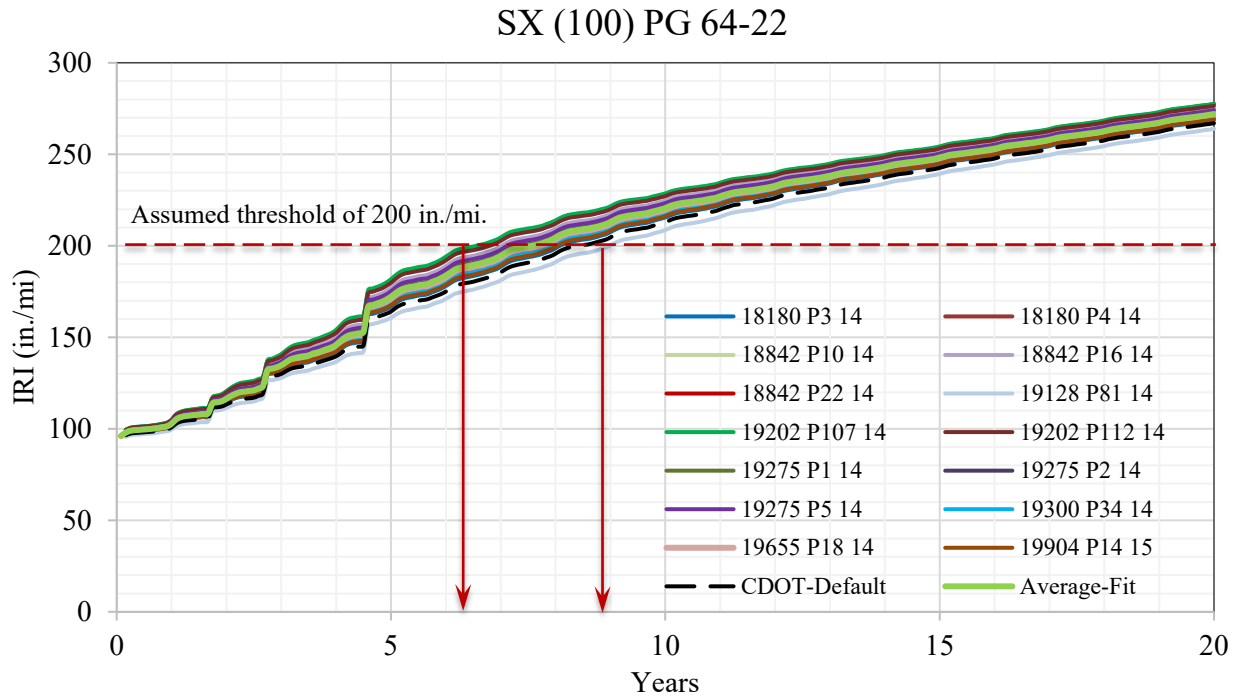


Figure 110. IRI Due to AADTT = 7,000 by SX(100) PG 64-22 Mix

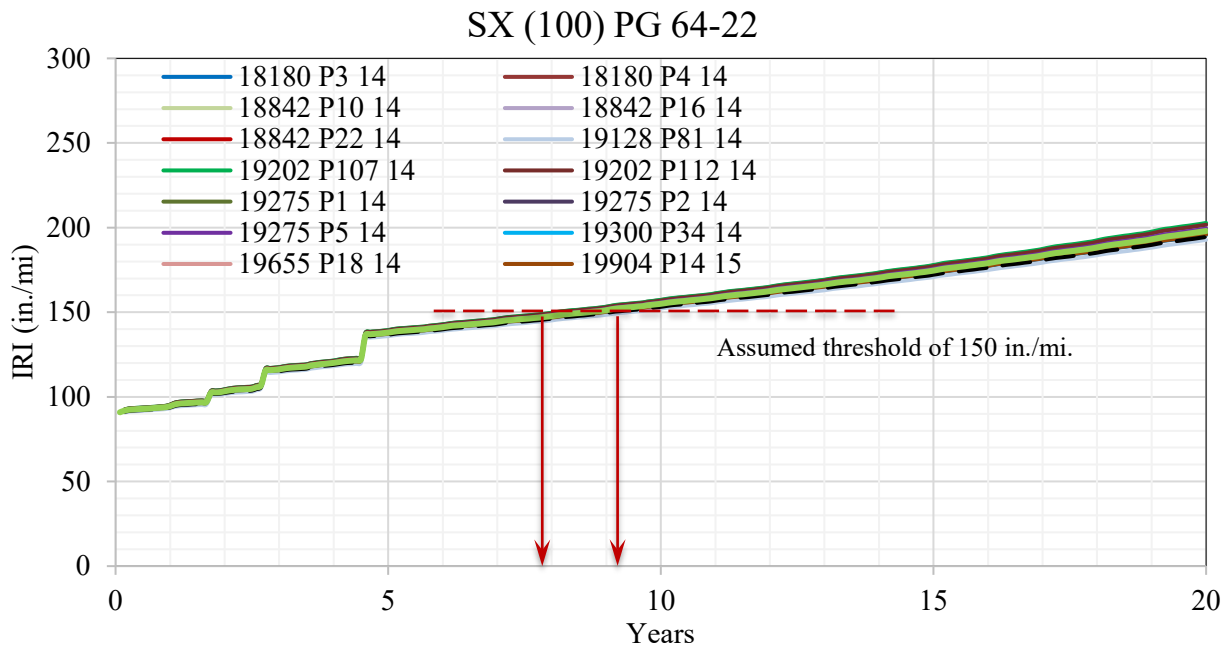


Figure 111. IRI Due to AADTT = 800 by SX(100) PG 64-22 Mix

Total Rutting: Figures 112 and 113 show the total rutting of the trial pavement with the service life of the pavement for high traffic (AADTT = 7,000) and low traffic (AADTT = 800), respectively. They show that the prediction of total rutting by the CDOT-default mix (except 19128 P81 14) data is the lowest. This means the CDOT-default dynamic modulus data for the PG 62-22 binder predicts a lower rutting compared to that of the actual tested dynamic modulus (except for 19128 P81 14). Comparing contractor to contractor, the prediction varies a lot, especially for high traffic. For example, if the threshold total value is 0.6 in. as shown in Figure 112, then the prediction reaches the threshold from four years to nine years. For low traffic, the variation of this prediction is similar. The statistical analysis shows that several mixes are within the 95% CI boundaries.

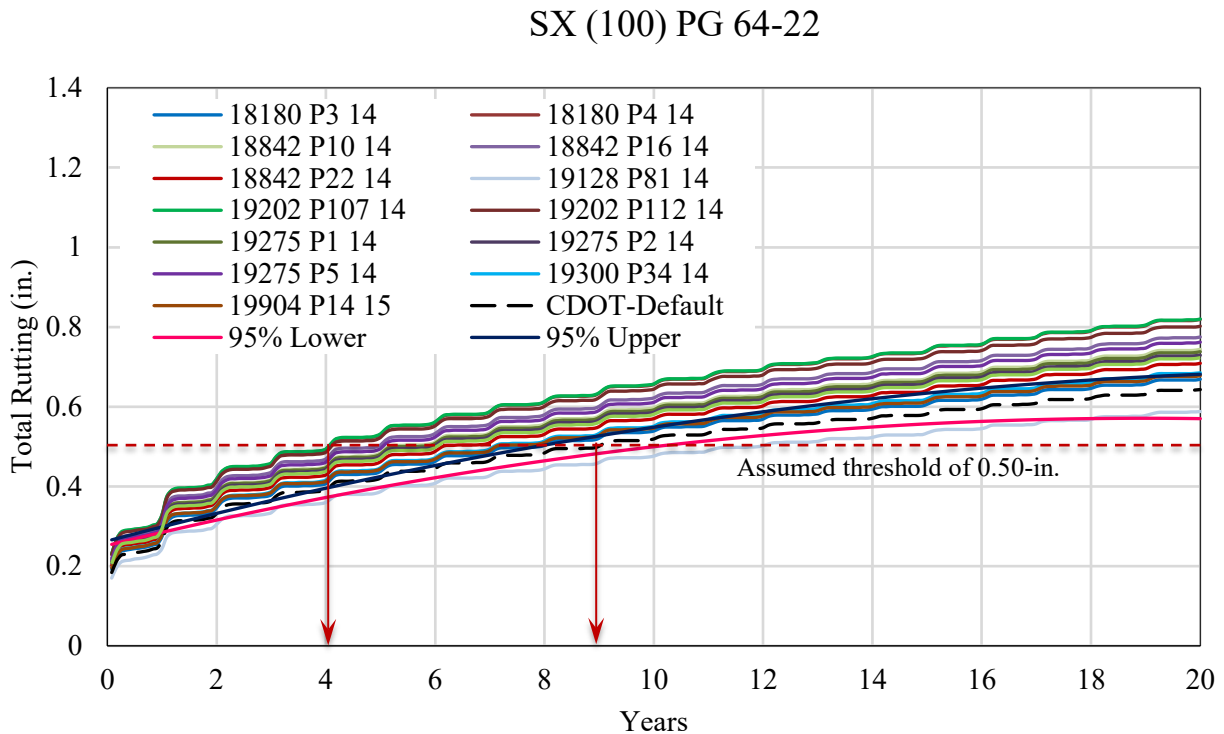


Figure 112. Total Rutting Due to AADTT = 7,000 by SX(100) PG 64-22 Mix

SX (100) PG 64-22

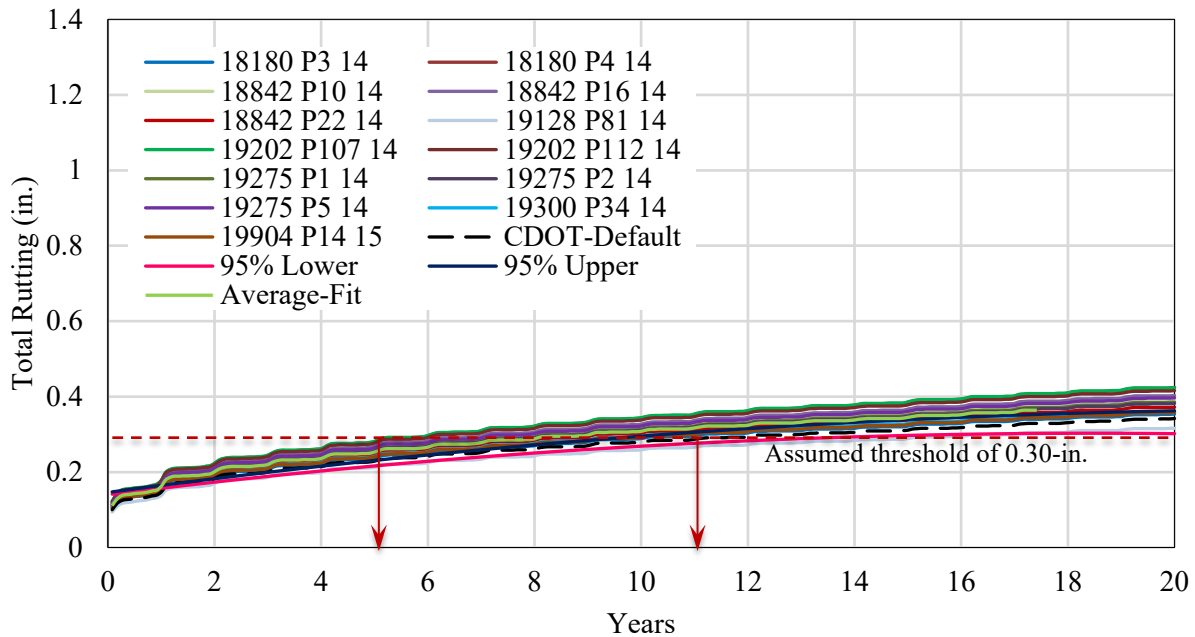


Figure 113. Total Rutting Due to AADTT = 800 by SX(100) PG 64-22 Mix

Rutting in the Asphalt Layer only: Figures 114 and 115 show the rutting in the asphalt layer of the trial pavement with the service life of the pavement for high traffic (AADTT = 7,000) and low traffic (AADTT = 800), respectively. They show that the prediction of rutting in the asphalt layer by the CDOT-default mix (except for 19128 P81 14) data is the lowest. This means that the CDOT-default dynamic modulus data for the PG 62-22 binder predicts lower rutting in the asphalt layer compared to that of the actual tested dynamic modulus (except for 19128 P81 14). Comparing contractor to contractor, the prediction varies a lot, especially for high traffic. For example, if the threshold total value is 0.3 in. as shown in Figure 114, then the prediction reaches the threshold from two to seven years. For low traffic, the findings are similar. The statistical analysis shows that several mixes are within the 95% CI boundaries.

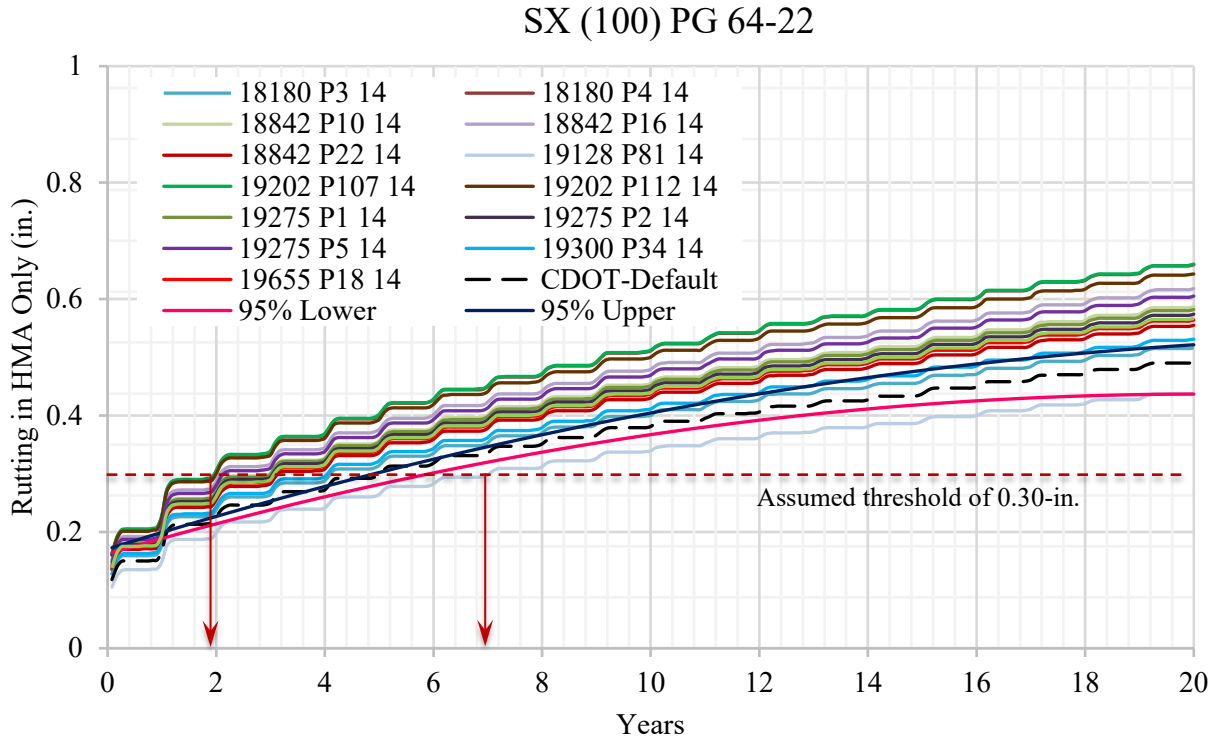


Figure 114. Rutting in Asphalt Layer Due to AADTT = 7,000 by SX(100) PG 64-22 Mix

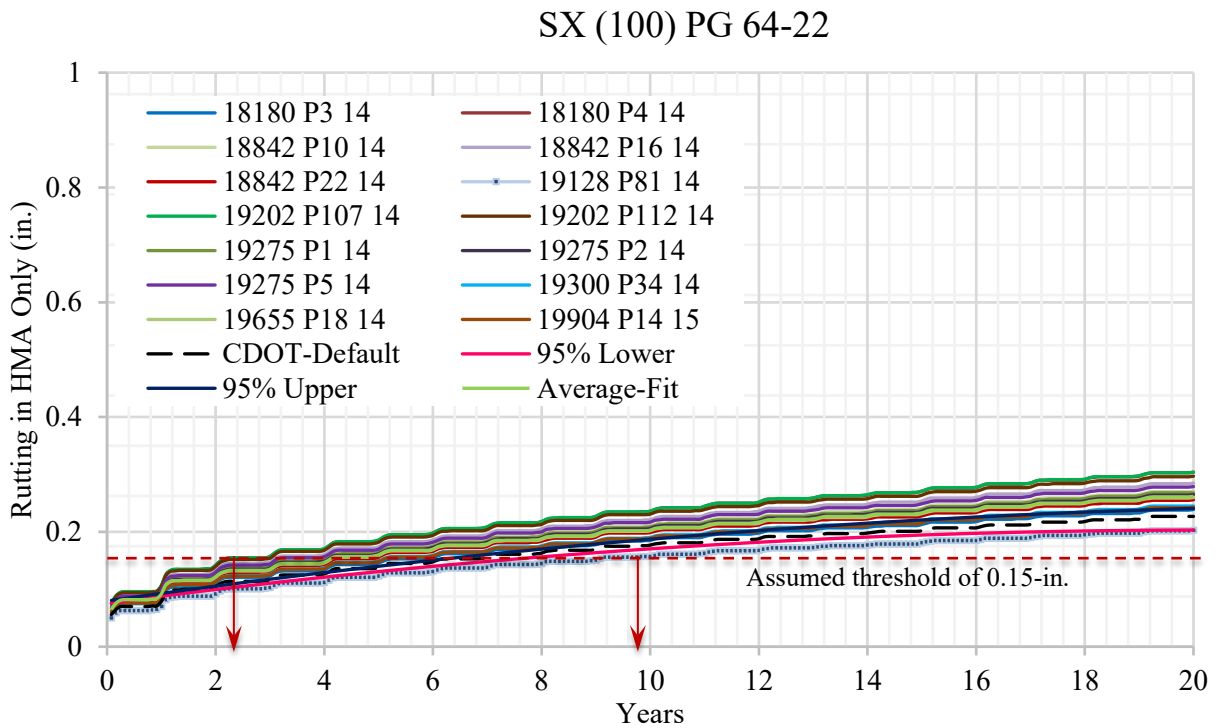


Figure 115. Rutting in Asphalt Layer Due to AADTT = 800 by SX(100) PG 64-22 Mix

Bottom-up Fatigue Cracking: Figures 114 and 115 show the bottom-up fatigue cracking of the trial pavement with the service life of the pavement for high traffic (AADTT = 7,000) and low traffic (AADTT = 800), respectively. They show that the prediction of bottom-up fatigue cracking by the CDOT-default mix data (except for 19128 P81 14) is the lowest. This means that the CDOT-default dynamic modulus data for the PG 62-22 binder predicts lower bottom-up fatigue cracking compared to that of the actual tested dynamic modulus (except for 19128 P81 14). The assumed threshold of 35% of the lane area shown in Figure 116 shows that the mixes reach the threshold between three and four years, which is very close to each other. Similar observation is obtained for low traffic as shown in Figure 117 where the threshold is assumed to be 20% of the lane area. The statistical analysis shows that none of the mix listed in Figure 117 is within the 95% CI boundaries.

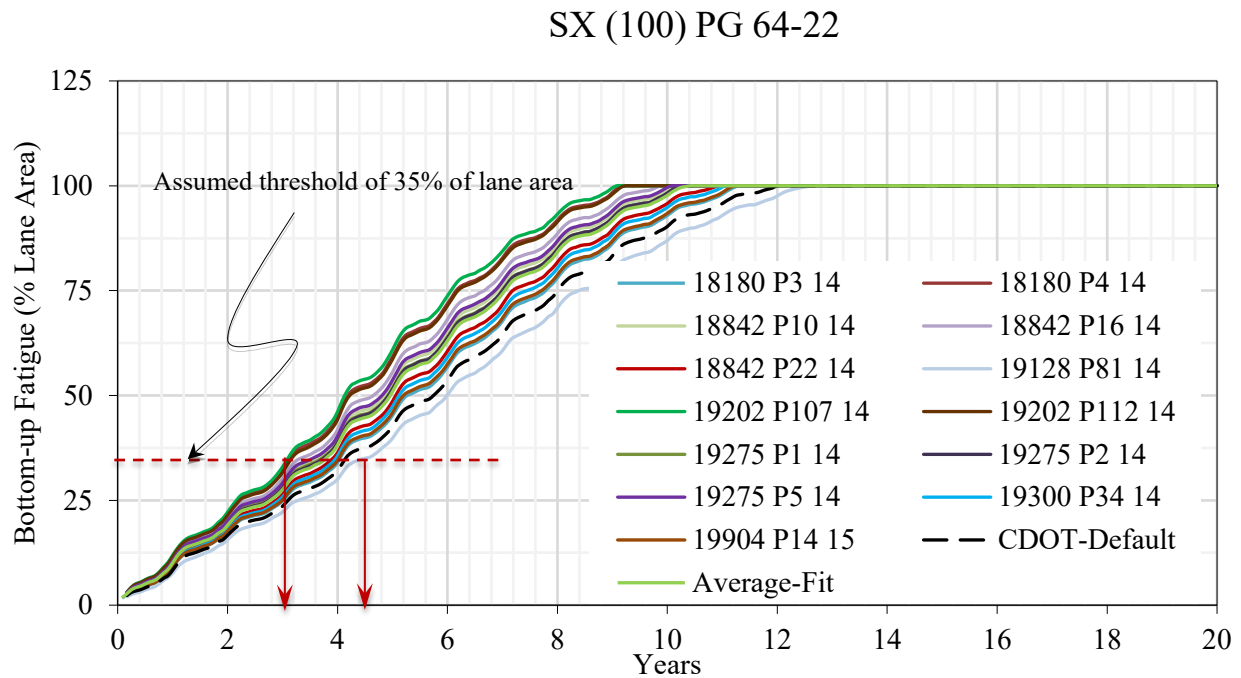


Figure 116. Bottom-up Fatigue Cracking Due to AADTT = 7,000 by SX(100) PG 64-22 Mix

SX (100) PG 64-22

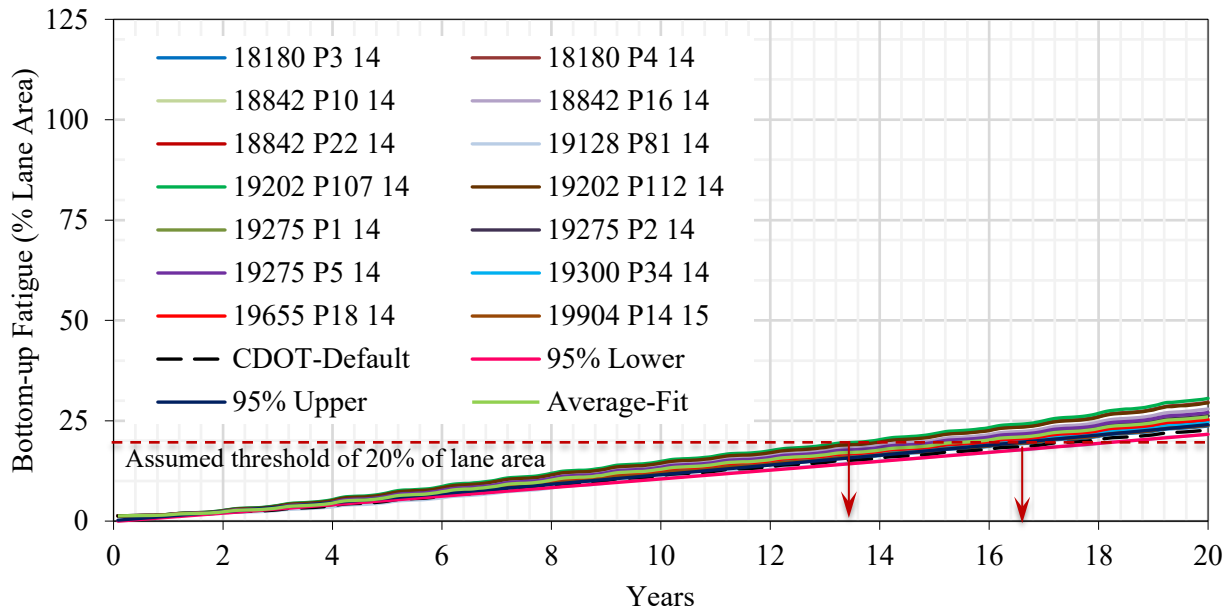


Figure 117. Bottom-up Fatigue Cracking Due to AADTT = 800 by SX(100) PG 64-22 Mix

Top-down Longitudinal Cracking: Figures 118 and 119 show the top-down longitudinal cracking of the trial pavement with the service life of the pavement for high traffic (AADTT = 7,000) and low traffic (AADTT = 800), respectively. They show that the prediction of top-down longitudinal cracking by the CDOT-default mix (except for 19128 P81 14) data is the lowest. This means that the CDOT-default dynamic modulus data for the PG 62-22 binder predicts lower top-down longitudinal cracking compared to that of the actual tested dynamic modulus (except 19128 P81 14). Mixes reach the threshold value of 2,000 ft./mi. from three to eight years for high traffic as shown in Figure 118. This observation is similar for the low traffic where mixes reach the threshold value of 1,000 ft./mi. from 6 to 15 years as shown in Figure 119. The statistical analysis shows that none of the mixes (Figure 119) is within the 95% CI boundaries. The average-fit data produces the top-down longitudinal cracking, along with other distresses mentioned above, outside the 95% CI boundaries of the CDOT mix.

SX (100) PG 64-22

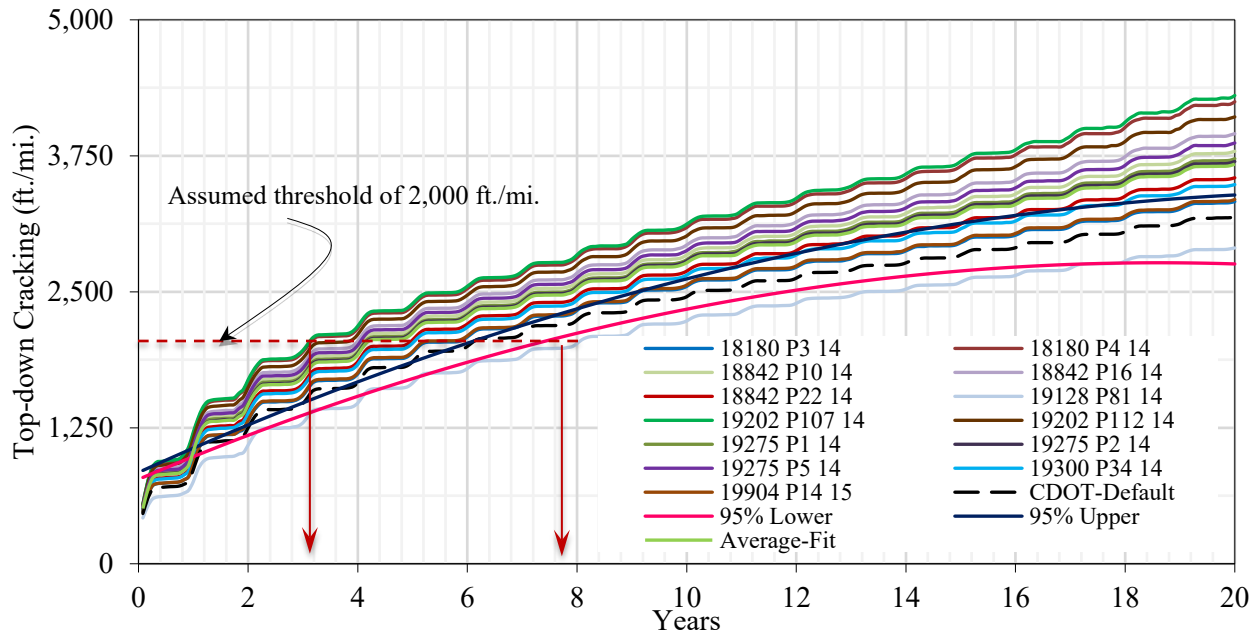


Figure 118. Longitudinal Cracking Due to AADTT = 7,000 by SX(100) PG 64-22 Mix

SX (100) PG 64-22

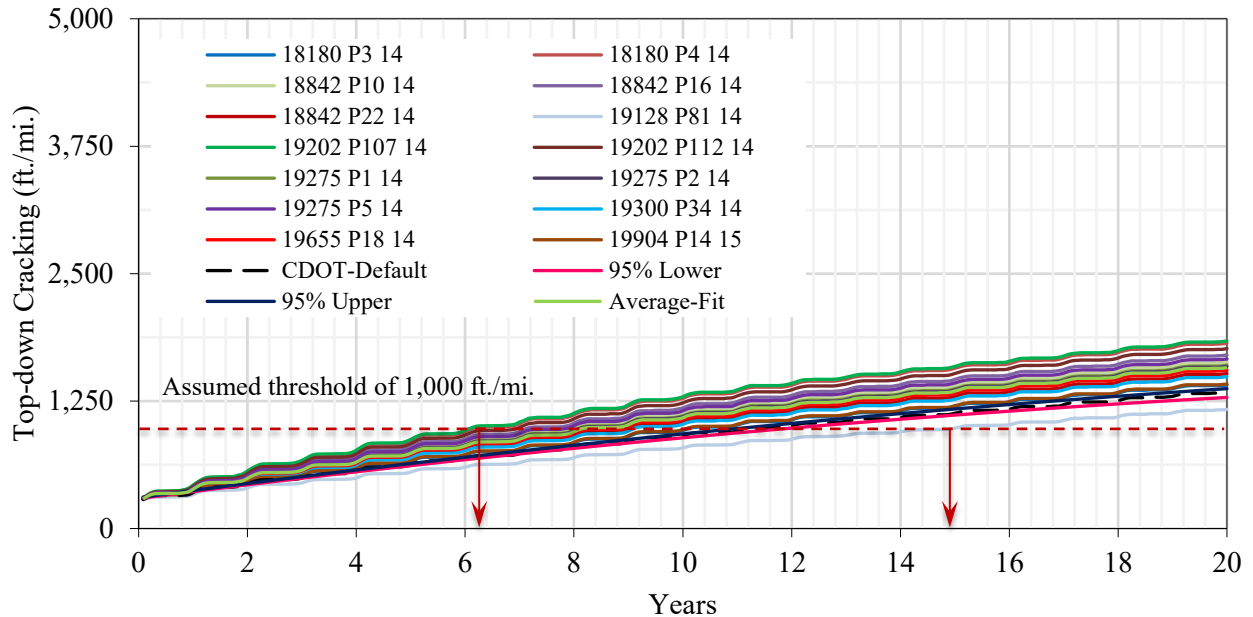


Figure 119. Longitudinal Cracking Due to AADTT = 800 by SX(100) PG 64-22 Mix

The above discussion concludes none of the mixes is within the 95% CI boundaries from all the distress data. From Table 59, their production dates, effective binder contents, VMAs, VFAs, aggregate sources are also not the same. Therefore, the effect of an individual mix parameter may not be appropriately determined for this mix, SX(100) PG 64-22.

To determine the influence of V_{be} , V_a , VMA, VFA, and AC, a regression analysis is conducted, and the following correlations are obtained. The R^2 of the correlations of IRI, total rutting, rutting in HMA, FC, and TDC are 0.65, 0.60, 0.59, 0.65, and 0.64, respectively. It can be seen that all distresses increase with the increase in VMA, VFA, and AC, and decrease with the increase in V_{be} and V_a .

$$\text{IRI (in./mi.)} = 100.104 - 2.1776 V_{be} - 0.9101 V_a + 4.1934 \text{ VMA} + 1.1154 \text{ VFA} + 1.4207 \text{ AC}$$

$$\text{Total Rutting (in.)} = -0.4769 - 0.0207 V_{be} - 0.0065 V_a + 0.0375 \text{ VMA} + 0.0099 \text{ VFA} + 0.012 \text{ AC}$$

$$\text{Rutting in HMA (in.)} = -0.5629 - 0.0188 V_{be} - 0.0078 V_a + 0.0363 \text{ VMA} + 0.0094 \text{ VFA} + 0.0084 \text{ AC}$$

$$\text{FC (\%)} = -13.1366 - 0.461 V_{be} - 0.1364 V_a + 0.9536 \text{ VMA} + 0.2036 \text{ VFA} + 0.5026 \text{ AC}$$

$$\text{TDC (ft./mi.)} = -2467.43 - 100.956 V_{be} - 40.7568 V_a + 175.263 \text{ VMA} + 51.8374 \text{ VFA} + 59.2621 \text{ AC}$$

SX(100) PG 64-28

Table 60 lists the mix parameters, aggregate pits, binder suppliers and contractor information of the SX(100) PG 64-28 mix. Mix parameters includes V_{be} , V_a , VMA, VFA, and AC. All this information is used while analyzing the performance of different mixes as discussed below.

Table 60. Generic Information of SX(100) PG 64-28 Mix

	Paving Contractor	Binder Supplier	Region	Date	V_{be} (%)	V_a (%)	VMA (%)	VFA (%)	AC (%)	Pit	Total Rutting after 10 years (in.)	Fatigue Cracking after 10 years (% of lane)
19655 P20 14	APC Southern	Suncor	2	7/2014	10.59	6.06	17.0	64.0	5.58	Valardi	1.133	19.2
19655 P21 14	APC Southern	Suncor	2	7/2014	10.85	6.06	17.1	63.5	5.80	Valardi	0.96	23.0
19655 P23 14	APC Southern	Suncor	2	8/2014	10.56	6.06	16.7	65.1	5.70	Valardi	0.89	22.4
19655 P24 14	APC Southern	Suncor	2	8/2014	10.97	6.06	16.0	64.2	5.78	Valardi	0.92	21.9
19655 P28 14	APC Southern	Suncor	2	8/2014	10.71	6.06	16.1	63.0	5.61	Valardi	0.52	15.4
19655 P37 14	APC Southern	Suncor	2	9/2014	10.48	6.06	15.8	62.4	5.65	Valardi	0.90	21.7
19655 P48 14	APC Southern	Suncor	2	12/2014	13.18	6.60	17.4	62.0	5.50	Valardi	0.75	18.7
19655 P87 14	APC Southern	Suncor	2	10/2015	13.18	6.30	17.1	63.2	5.50	Valardi	0.87	21.6
19879 P114 14	-	Suncor	1	3/2016	10.05	6.90	17.5	63.5	4.90	Ralston, Firestone	0.93	21.6

Note: Orange highlighted mixes produce statistically the same distress with the CDOT-default mix. This is clarified in the following discussion.

International Roughness Index: Figures 120 and 121 show the IRI of the trial pavement with the service life of the pavement for high traffic (AADTT = 7,000) and low traffic (AADTT = 800), respectively. They show that the prediction of IRI of this mix, using the dynamic moduli determined by different contractors, including the CDOT-default data, are close to each other, except for 19655 P28 14 and 19655 P48 14. Assumed threshold values of 200 in./mi. and 180 in./mi. are drawn in Figures 120 and 121, respectively. Figure 120 shows that the mixes reach the

threshold in about 6 to 11 years for high traffic. Similar observation is obtained for low traffic as shown in Figure 121.

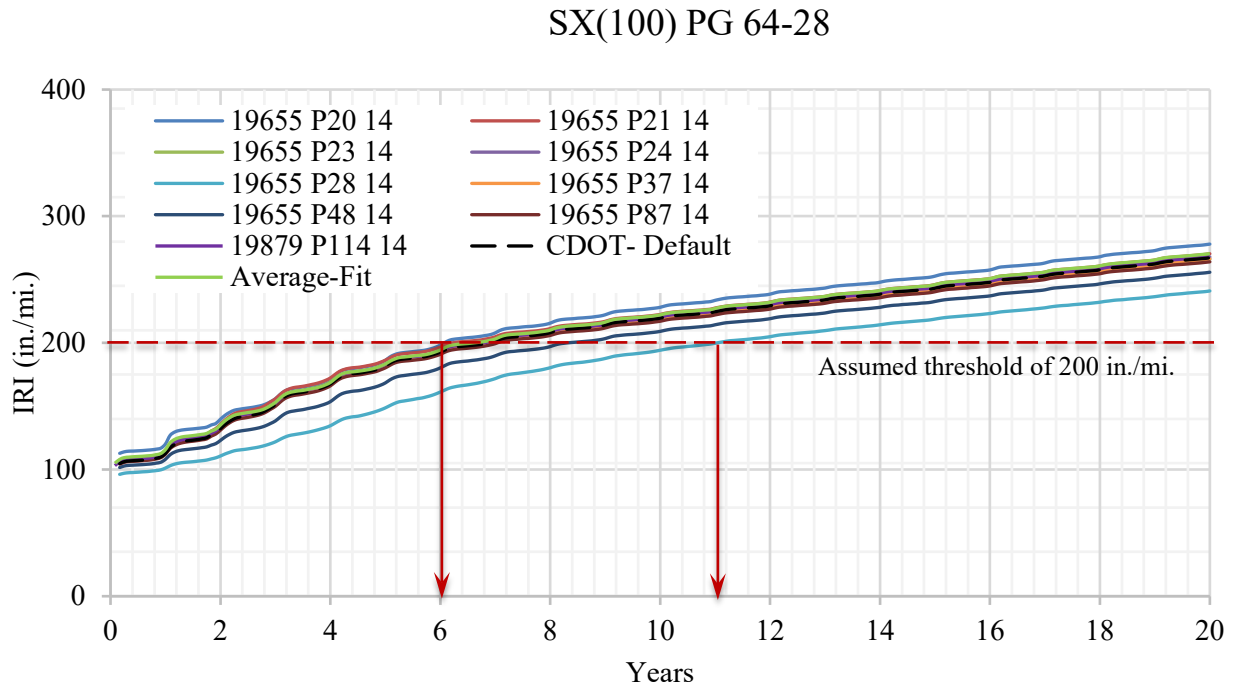


Figure 120. IRI Due to AADTT = 7,000 by SX(100) PG 64-28 Mix

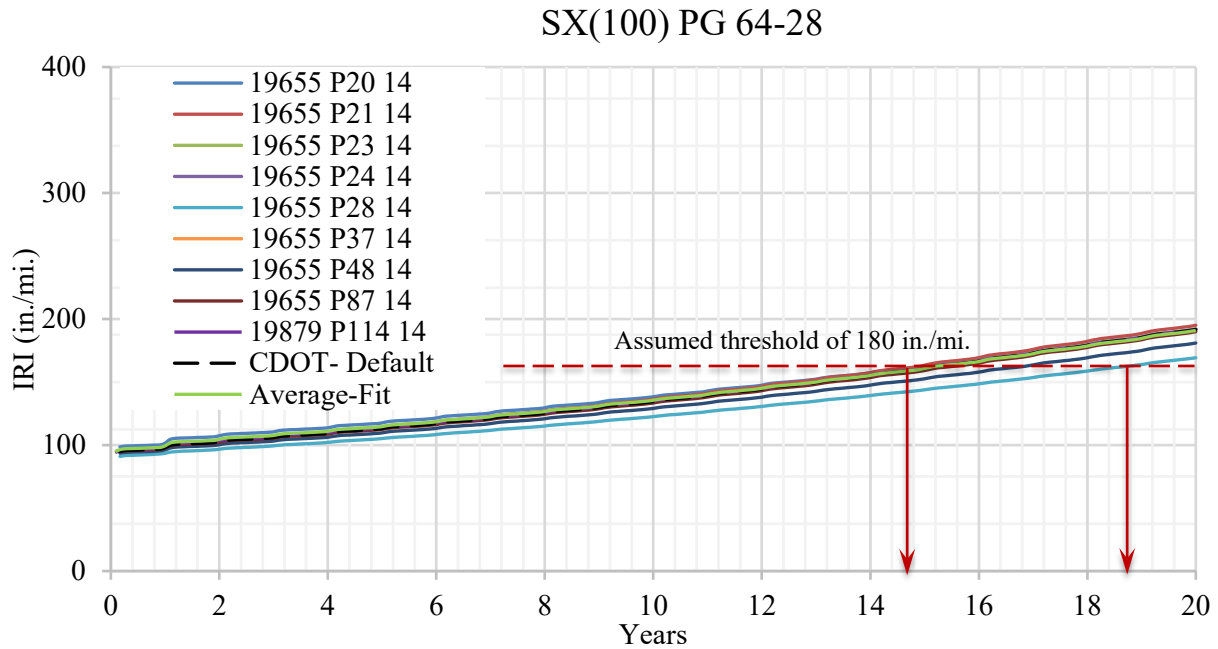


Figure 121. IRI Due to AADTT = 800 by SX(100) PG 64-28 Mix

Total Rutting: The total rutting variation (Figures 122 and 123) during its service life shows that the prediction of total rutting of this mix, using the dynamic moduli determined by different contractors, including the CDOT-default data, are close to each other, except for 19655 P20 14, 19655 P28 14, and 19655 P48 14. The prediction reaches the threshold of 0.60-in. from about one year to 16 years for mix to mix for high traffic as shown in Figure 122. The statistical 95% CI boundaries also testifies that these three mixtures, 19655 P20 14, 19655 P28 14, and 19655 P48 14, are not statistically the same with the CDOT-default mix.

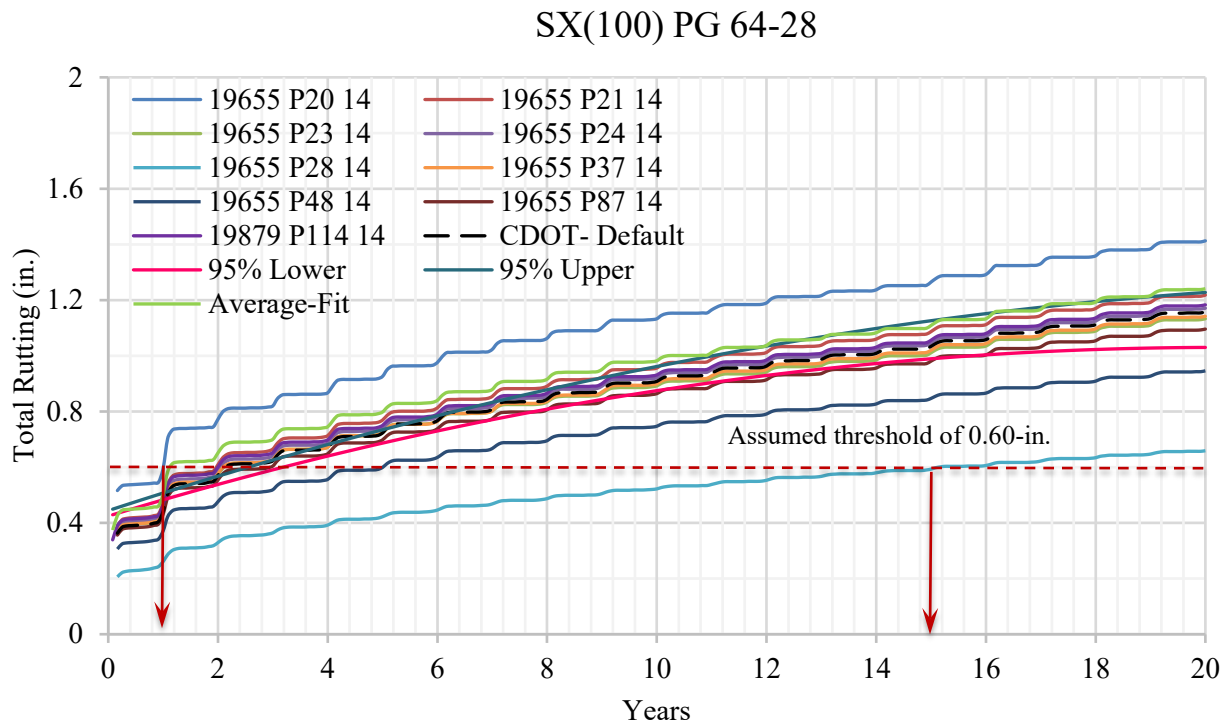


Figure 122. Total Rutting Due to AADTT = 7,000 by SX(100) PG 64-28 Mix

SX(100) PG 64-28

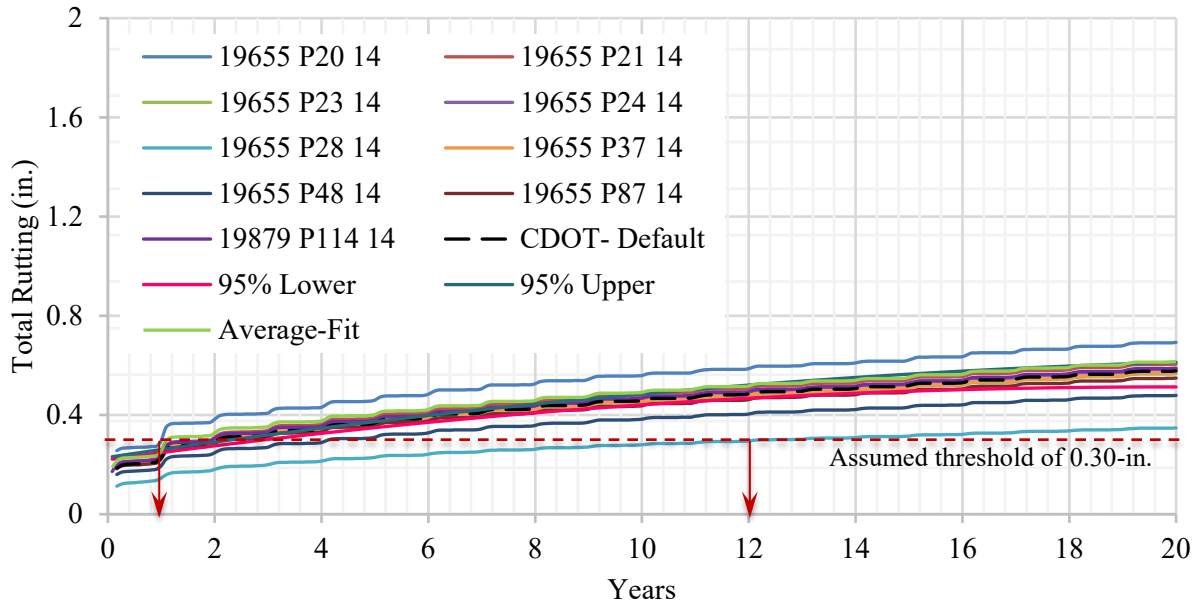


Figure 123. Total Rutting Due to AADTT = 800 by SX(100) PG 64-28 Mix

Rutting in the Asphalt Layer Only: The rutting in the asphalt layer variation (Figures 124 and 125) during its service life shows that the prediction of rutting in the asphalt layer of this mix, using the dynamic moduli determined by different contractors, including the CDOT-default data, are consistent with each other, except for 19655 P20 14, 19655 P28 14, and 19655 P48 14. The prediction reaches the threshold of 0.40-in. from about one year to 11 years for mix to mix for high traffic as shown in Figure 124. The statistical 95% CI boundaries also testify that these three mixtures, 19655 P20 14, 19655 P28 14, and 19655 P48 14, are not same with the CDOT-default mix.

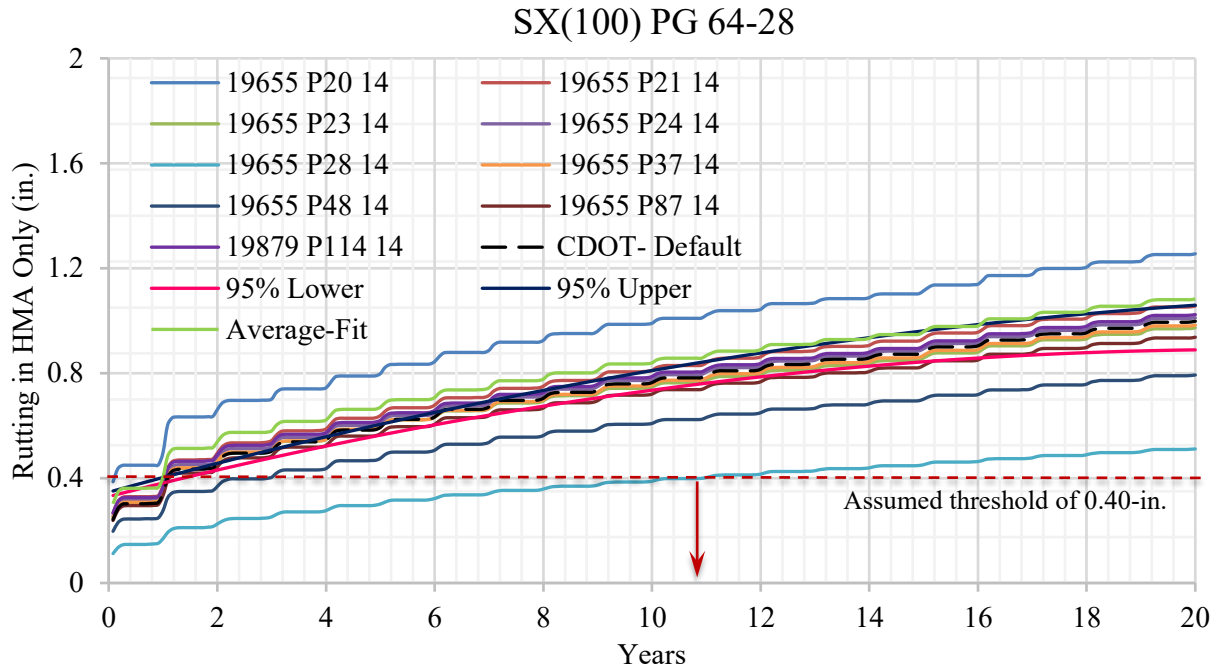


Figure 124. Rutting in the Asphalt Layer Due to AADTT = 7,000 by SX(100) PG 64-28 Mix

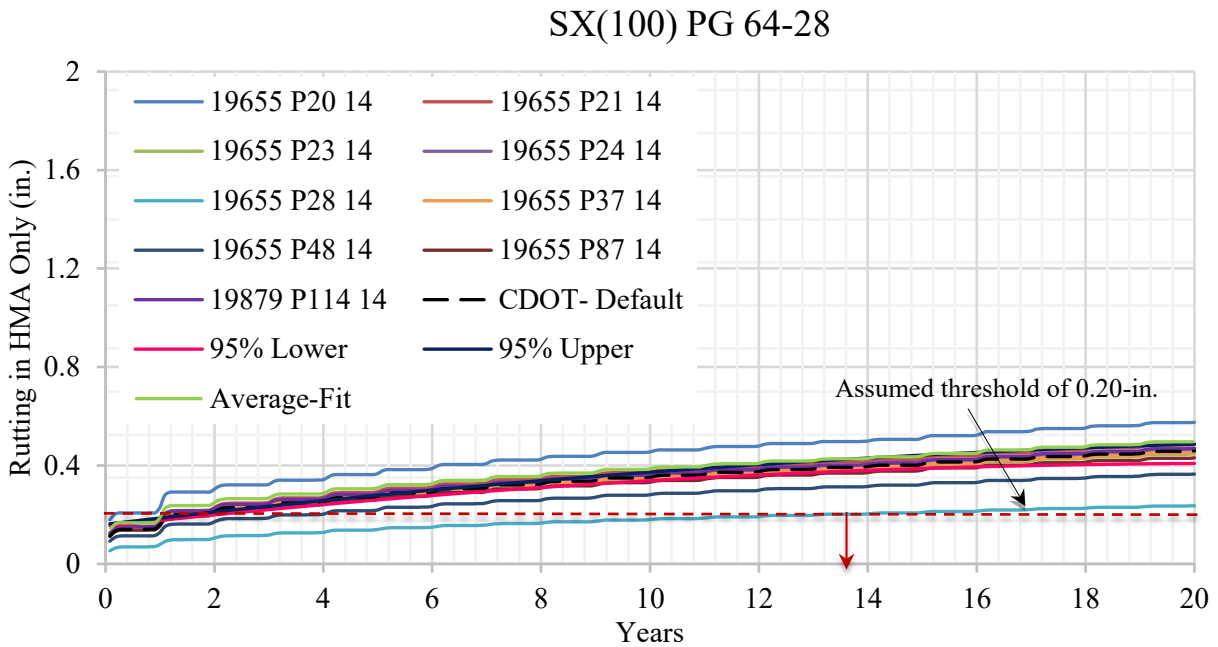


Figure 125. Rutting in the Asphalt Layer Due to AADTT = 800 by SX(100) PG 64-28 Mix

Bottom-up Fatigue Cracking: The bottom-up fatigue cracking variation during the service life of the trial pavement is shown in Figures 126 and 127 for AADTT = 7,000 and AADTT = 800,

respectively. They show that the prediction of bottom-up fatigue cracking of this mix, using the dynamic moduli determined by different contractors, including the CDOT-default data, are consistent with each other, except for 19655 P20 14, 19655 P28 14, and 19655 P48 14. The assumed threshold of 30% of the lane area shown in Figure 126 shows that the mixes reach the threshold between three and four years, which is very close to each other. Similar observation is obtained for low traffic as shown in Figure 127 where the threshold is assumed to be 30% of the lane area. The statistical 95% CI boundaries also testifies that these three mixtures, 19655 P20 14, 19655 P28 14, and 19655 P48 14, are not statistically the same with the CDOT-default mix.

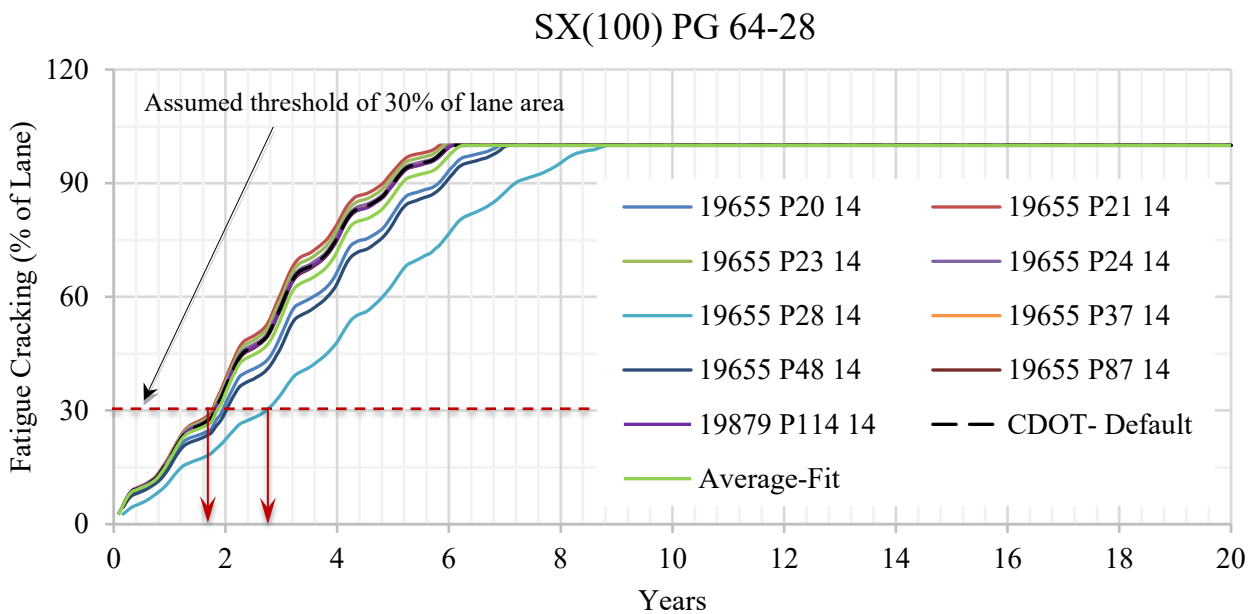


Figure 126. Bottom-up Fatigue Cracking Due to AADTT = 7,000 by SX(100) PG 64-28 Mix

SX(100) PG 64-28

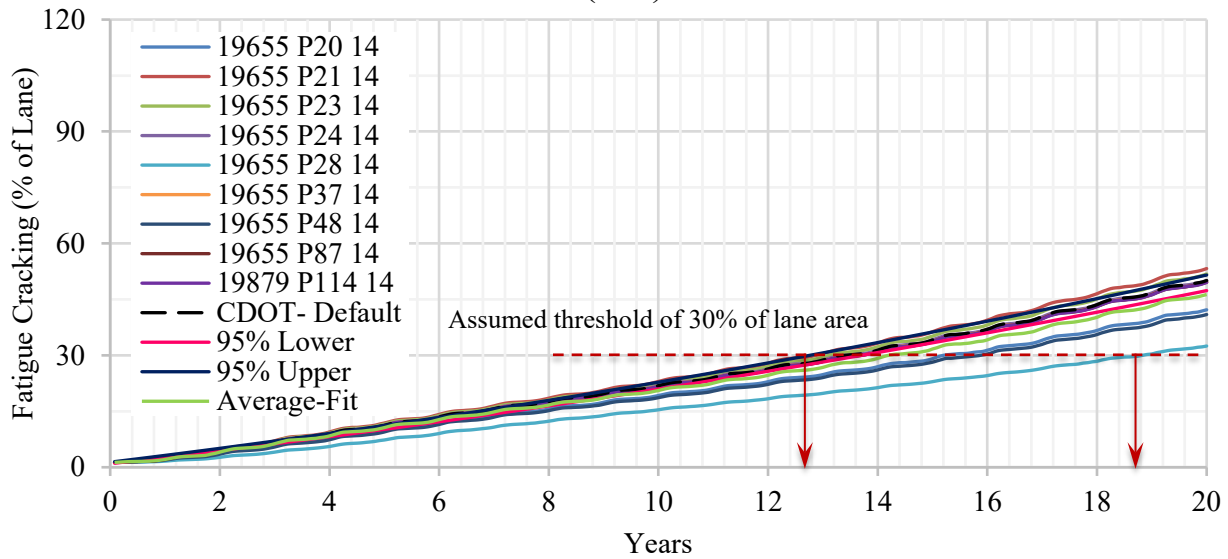


Figure 127. Bottom-up Fatigue Cracking Due to AADTT = 800 by SX(100) PG 64-28 Mix

Top-down Longitudinal Cracking: The top-down longitudinal cracking variation during the service life of the trial pavement is shown in Figures 128 and 129 for high and low traffic, respectively. They show that the prediction of top-down longitudinal cracking of this mix, using the dynamic moduli determined by different contractors, including the CDOT-default data, are consistent with each other, except for 19655 P20 14, 19655 P28 14, and 19655 P48 14. The prediction reaches the threshold of 3,000 ft./mi. from about 4 to 10 years for mix to mix for high traffic as shown in Figure 138. The statistical 95% CI boundaries also indicate that these three mixtures, 19655 P20 14, 19655 P28 14, and 19655 P48 14, are not statistically the same with the CDOT-default mix. The average-fit data produces the top-down longitudinal cracking, along with other distresses mentioned above, marginally within the 95% CI boundaries of the CDOT mix.

SX(100) PG 64-28

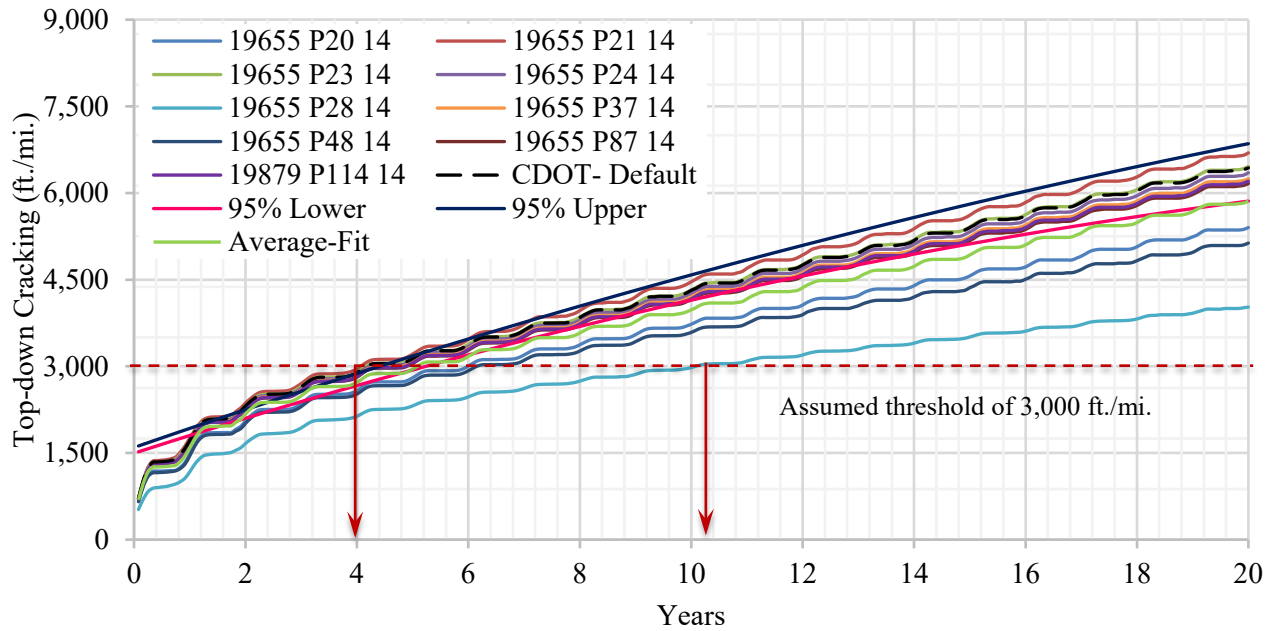


Figure 128. Longitudinal Cracking Due to AADTT = 7,000 by SX(100) PG 64-28 Mix

SX(100) PG 64-28

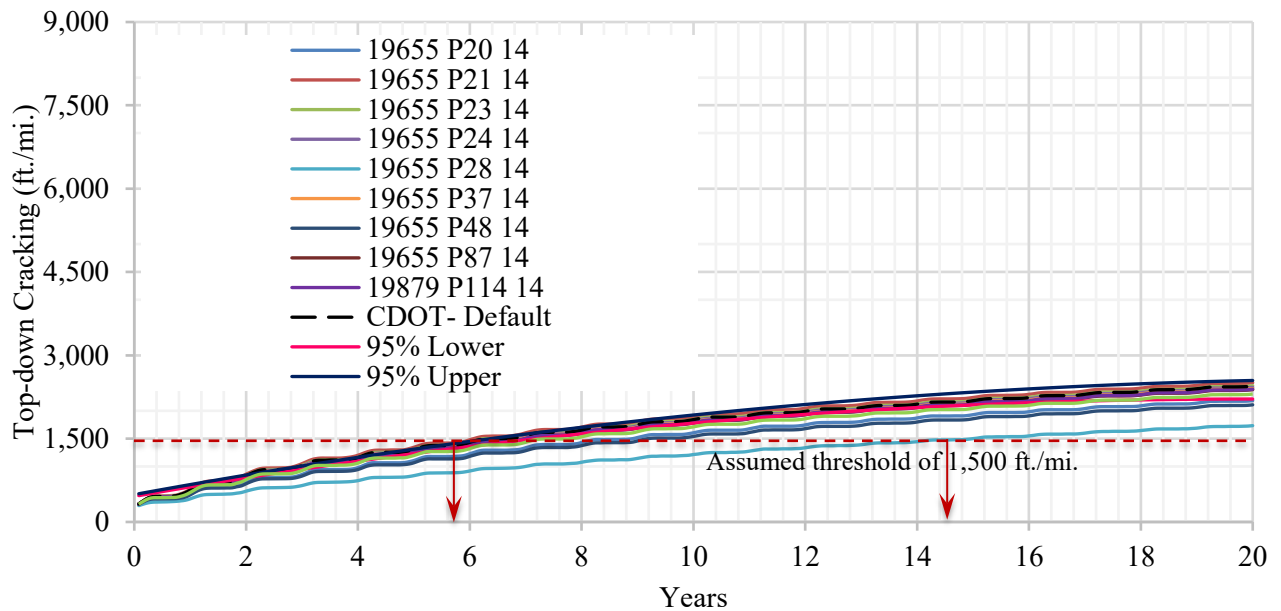


Figure 129. Longitudinal Cracking Due to AADTT = 800 by SX(100) PG 64-28 Mix

The above discussion shows that only three mixtures, 19655 P20 14, 19655 P28 14, and 19655 P48 14, are not statistically the same with the CDOT-default mix. From the mix parameters listed in Table 60, the mixes which are not statistically the same with the CDOT-default mix do have properties which vary from the mixes that are statistically the same with the CDOT-default mix. Therefore, the effect of individual mix parameters may not be appropriately sought out for this mix.

To determine the influence of V_{be} , V_a , VMA, VFA, and AC, a regression analysis is conducted, and the following correlations are obtained. The R^2 of the correlations of IRI, total rutting, rutting in HMA, FC, and TDC are 0.31, 0.34, 0.33, 0.27, and 0.27, respectively. It can be seen that IRI increases with the increase in VMA, VFA, and AC, and decreases with the increase in V_{be} and V_a . Total rutting and rutting in the asphalt layer increase with the increase in VMA and VFA, and decrease with the increase in V_{be} , V_a , and AC. FC and TDC increase with the increase in V_a , VMA, VFA, and AC, and decrease with the increase in V_{be} .

$$\text{IRI (in./mi.)} = -88.8899 - 2.2939 V_{be} - 2.5538 V_a + 8.0307 \text{ VMA} + 2.7866 \text{ VFA} + 6.4381 \text{ AC}$$

$$\text{Total Rutting (in.)} = -2.1945 - 0.0416 V_{be} - 0.2047 V_a + 0.162 \text{ VMA} + 0.0348 \text{ VFA} - 0.0201 \text{ AC}$$

$$\text{Rutting in HMA (in.)} = -2.1758 - 0.0414 V_{be} - 0.2005 V_a + 0.1572 \text{ VMA} + 0.0334 \text{ VFA} - 0.0226 \text{ AC}$$

$$\text{FC (\%)} = -142.342 - 0.4119 V_{be} + 7.3635 V_a + 0.2285 \text{ VMA} + 1.1732 \text{ VFA} + 7.8005 \text{ AC}$$

$$\text{TDC (ft./mi.)} = -27701.1 - 91.5988 V_{be} + 1450.335 V_a + 41.0239 \text{ VMA} + 224.3789 \text{ VFA} + 1572.199 \text{ AC}$$

SX(100) PG 76-28

Table 61 lists the mix parameters, aggregate pits, binder suppliers and contractor information of the SX(100) PG 76-28 mix. Mix parameters includes V_{be} , V_a , VMA, VFA, and AC. All this information is used while analyzing the performance of different mixes as discussed below.

Table 61. Generic Information of SX(100) PG 76-28 Mix

	Paving Contractor	Binder Supplier	Region	Date	V_{be} (%)	V_a (%)	VMA (%)	VFA (%)	AC (%)	Pit
18842 P29 14	Kiewit Construction	Suncor	2	7/2014	12.61	6.68	18.1	64.3	6.30	Tezak / Fountain / I-25 Millings
18842 P36 14	Kiewit Construction	Suncor	2	8/2014	14.32	4.56	15.8	72.5	6.30	Parkdale/Tezak
18842 P45 14	Tezak	Suncor	2	8/2014	12.53	6.93	18.2	62.2	5.20	Tezak / Fountain / I-25 Millings
18842 P64 14	Kiewit Construction	Suncor	2	9/2014	12.53	6.85	18.2	62.4	6.30	Tezak / Fountain / I-25 Millings
18842 P71 14	Kiewit Construction	Suncor	2	10/2014	15.23	4.88	18.5	73.5	6.30	Parkdale/Tezak
18842 P82 14	Kiewit Construction	Suncor	2	10/2014	12.53	6.93	18.3	62.3	5.20	Tezak / Fountain / I-25 Millings
18970 P106 14	APC Southern	Suncor	5	11/2014	12.72	5.60	18.2	67.4	6.12	King Pit
19082 P65 14	ACA Buena Vista	Suncor	5	3/2015	13.84	6.85	18.8	63.2	5.70	Avery Pit, ACA Buena Vista
19128 P35 14	Martin Marietta	Suncor	2	8/2014	10.96	6.32	17.1	62.5	5.60	Evans
19128 P47 14	Evans	Suncor	2	8/2014	10.90	6.82	17.6	61.4	5.60	Evans
19128 P59 14	Martin Marietta	Suncor	2	9/2014	10.90	6.82	17.6	60.9	5.60	Evans
19128 P72 14	Martin Marietta	Suncor	2	9/2014	10.00	6.82	17.9	60.2	5.10	Evans
19128 P80 14	Martin Marietta	Suncor	2	10/2014	10.00	6.82	17.6	60.7	5.10	Evans/slate
19128 P88 14	Martin Marietta	Suncor	2	10/2014	10.82	6.83	17.6	61.6	5.60	Evans/slate
19458 P10 15	Simon Construction	Suncor	4	5/2015	9.90	5.30	16.8	61.5	5.05	Granite Canyon, Julesburg, Sedgwick
19458 P13 15	Simon Construction	Suncor	4	6/2015	9.47	5.30	16.5	61.7	4.96	Granite Canyon, Julesburg, Sedgwick
19458 P17 15	Simon Construction	Suncor	4	6/2015	9.55	5.30	16.1	60.7	4.93	Granite Canyon, Julesburg, Sedgwick
19458 P20 15	Simon Construction	Suncor	4	6/2015	10.32	4.40	16.6	60.0	5.30	Granite Canyon, Julesburg, Sedgwick

19458 P76 14	Simon Construction	Suncor	4	6/2015	11.57	6.43	17.3	62.6	5.20	Granite Canyon, Julesburg, Sedgwick
19458 P79 14	Simon Construction	Suncor	4	7/2015	11.57	6.80	17.6	61.4	5.20	Granite Canyon, Julesburg, Sedgwick
19458 P84 14	Simon Construction	Suncor	4	9/2015	11.57	6.75	17.6	61.2	5.20	Granite Canyon, Julesburg, Sedgwick
19458 P86 14	Simon Construction	Suncor	4	10/2015	11.57	6.78	17.6	61.3	5.20	Granite Canyon, Julesburg, Sedgwick
19557 P111 14	A&S Construction	Suncor	2	11/2014	11.71	5.00	17.7	64.6	5.38	Tezak/Transit Mix
19654 P24 15	Martin Marietta	Suncor	2	7/2015	10.31	5.00	17.6	60.6	5.25	Evans/slate
19669 P78 14	A&S Construction	Suncor	2	10/2014	10.72	6.93	17.7	61.0	5.40	Rocky Ford South/La Junta
19677 P54 14	Elam Construction	Suncor	3	1/2015	10.25	5.18	14.9	65.4	5.50	23 Road
19677 P55 14	Elam Construction	Suncor	3	1/2015	10.54	5.04	15.1	66.6	5.50	23 Road
19677 P62 14	Elam Construction	Suncor	3	2/2015	10.69	5.00	15.2	66.5	5.50	23 Road
19677 P69 14	Elam Construction	Suncor	3	5/2015	11.71	4.43	15.6	71.7	5.50	23 Road
19677 P89 14	Elam Construction	Suncor	3	10/2015	10.69	6.83	16.8	58.9	5.50	23 Road
19677 P90 14	Elam Construction	Suncor	3	10/2015	11.71	5.98	17.0	64.6	5.50	23 Road
19677 P91 14	Elam Construction	Suncor	3	11/2015	11.71	5.88	16.9	65.3	5.50	23 Road
19677 P104 14	Elam Construction	Suncor	3	11/2014	11.02	5.88	18.6	57.6	5.74	23 Road

Note: Orange highlighted mixes produce statistically the same distress with the CDOT-default mix. This is clarified in the following discussion.

International Roughness Index: Figures 130 and 131 show the IRI of the trial pavement with the service life of the pavement for high traffic (AADTT = 7,000) and low traffic (AADTT = 800), respectively. It shows that the prediction of IRI of this mix, using the dynamic moduli determined by different contractors, including the CDOT-default data, are close to each other. The IRI prediction differs by about four years from mix to mix as shown in Figures 130 and 131.

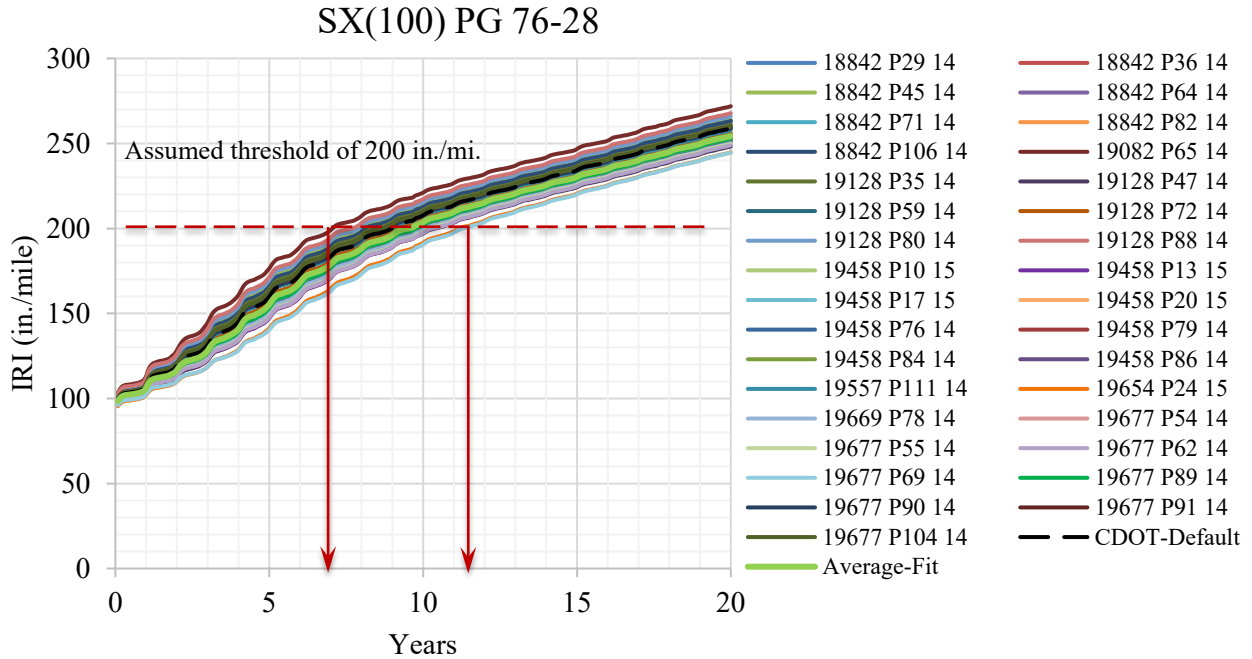


Figure 130. IRI Due to AADTT = 7,000 by SX(100) PG 76-28 Mix

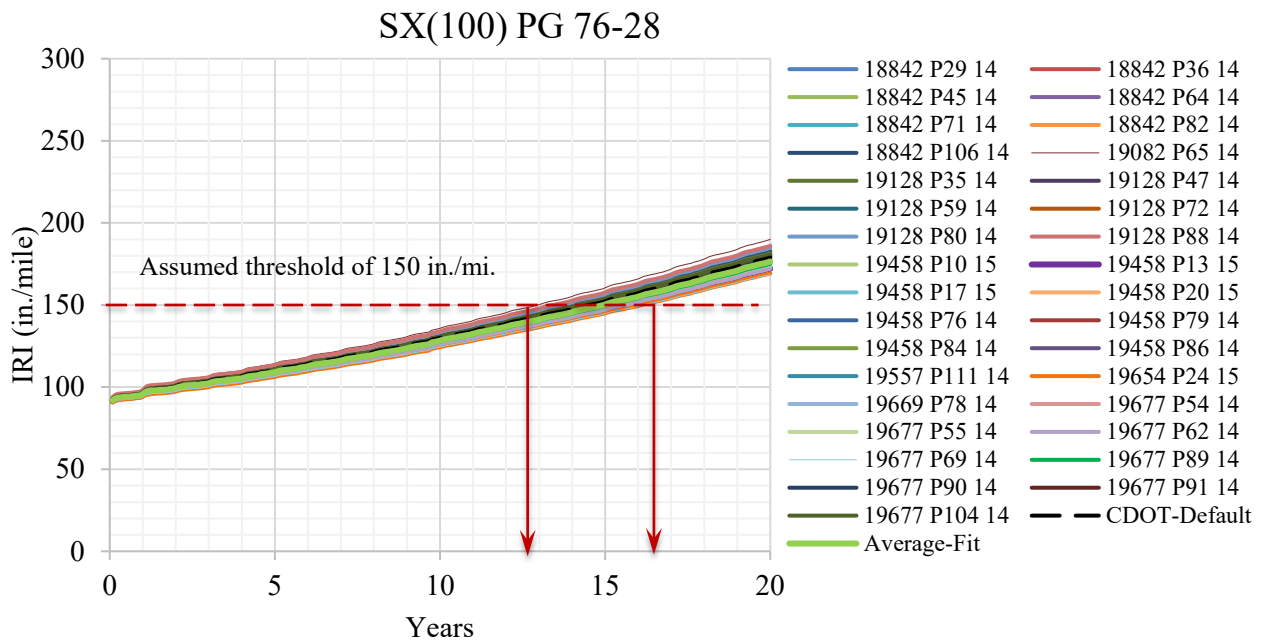


Figure 131. IRI Due to AADTT = 800 by SX(100) PG 76-28 Mix

Total Rutting: The total rutting variation during the service life of the trial pavement is shown in Figures 132 and 133 for high and low traffic, respectively. It shows that the default CDOT mixture

produces roughly the average amount of rutting compared to the other dynamic modulus data. Comparing contractor to contractor, the prediction varies a lot. For example, if the threshold total rutting value is 0.6 in. as shown in Figure 132, then the prediction reaches the threshold from two years to twelve years. The variation of this prediction is similar for low traffic as shown in Figure 133. This means that the total rutting prediction may vary up to ten years from mix to mix, if the threshold total rutting value is 0.6 in.. This variation may be larger for higher threshold values. Comparing the distress level, the lowest and the highest total rutting predicted are 0.57 in. (19654 P24 15 by Martin Marietta) and 0.97 in. (19082 P65 14 by ACA Buena Vista), respectively, at 10-year life for AADTT = 7,000. The statistical 95% CI boundaries show that most of the mixes are outside the 95% CI boundaries.

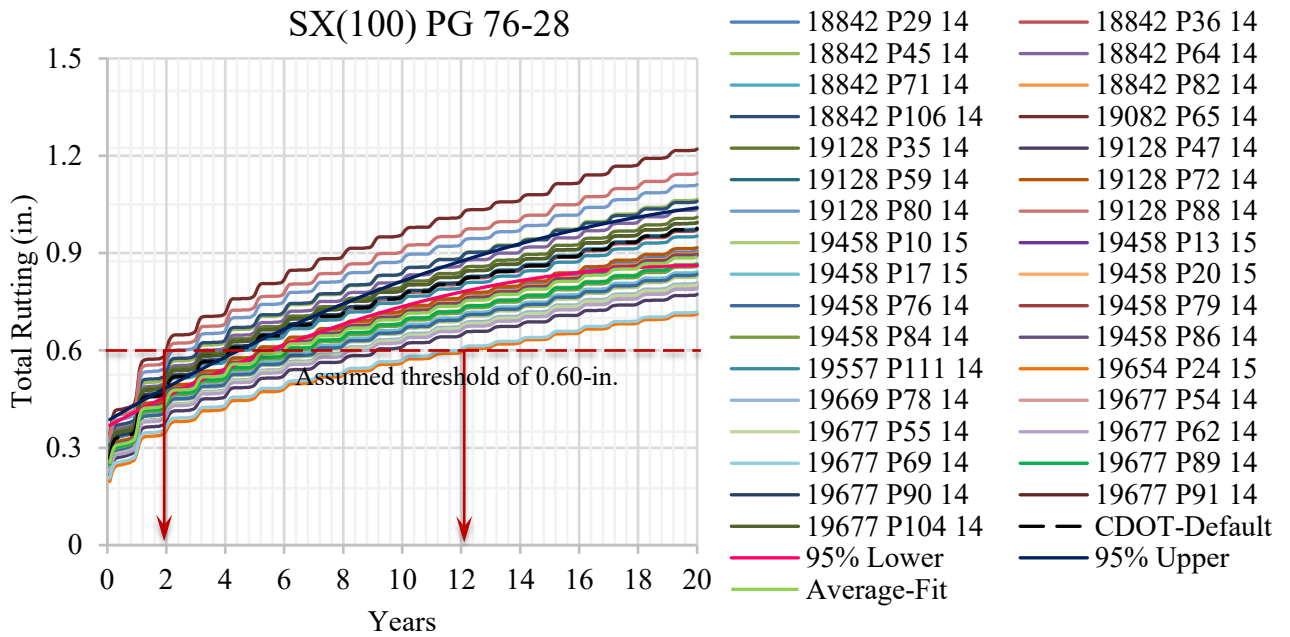


Figure 132. Total Rutting Due to AADTT = 7,000 by SX(100) PG 76-28 Mix

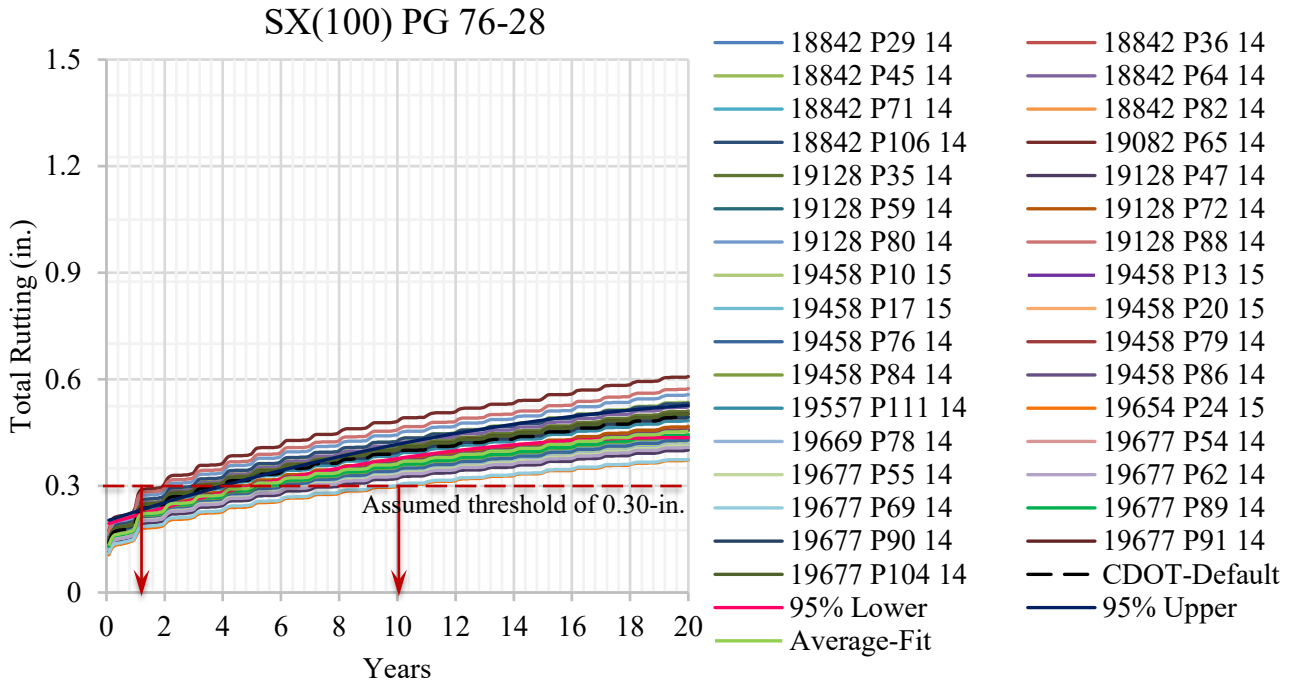


Figure 133. Total Rutting Due to AADTT = 800 by SX(100) PG 76-28 Mix

Rutting in the Asphalt Layer Only: The total rutting variation during the service life of the trial pavement is shown in Figures 143 and 144 for high and low traffic, respectively. The figures show that the CDOT-default data produces the lowest amount of rutting compared to the other dynamic modulus data, for both high and low traffic. Comparing contractor to contractor, the prediction varies a lot especially for high traffic. For example, if the threshold total value is 0.4 in. as shown in Figure 134, then the threshold rutting value is reached in one year for one of the mixes but reached in 10 years for another mix. For low traffic, the variation of this prediction varies about 12 years as shown in Figure 135 for an assumed threshold value of 0.2-in. This means that the total rutting prediction may vary up to eight years from mix to mix. Comparing the distress level, the lowest and the highest rutting in the asphalt layer predicted are 0.43 in. (19654 P24 15 by Martin Marietta) and 0.81 in. (19082 P65 14 by ACA Buena Vista), respectively, at 10-year life for AADTT = 7,000. The highest rutting value is 88% larger than the lowest rutting value. The statistical 95% CI boundaries show that many mixes are outside the 95% CI boundaries.

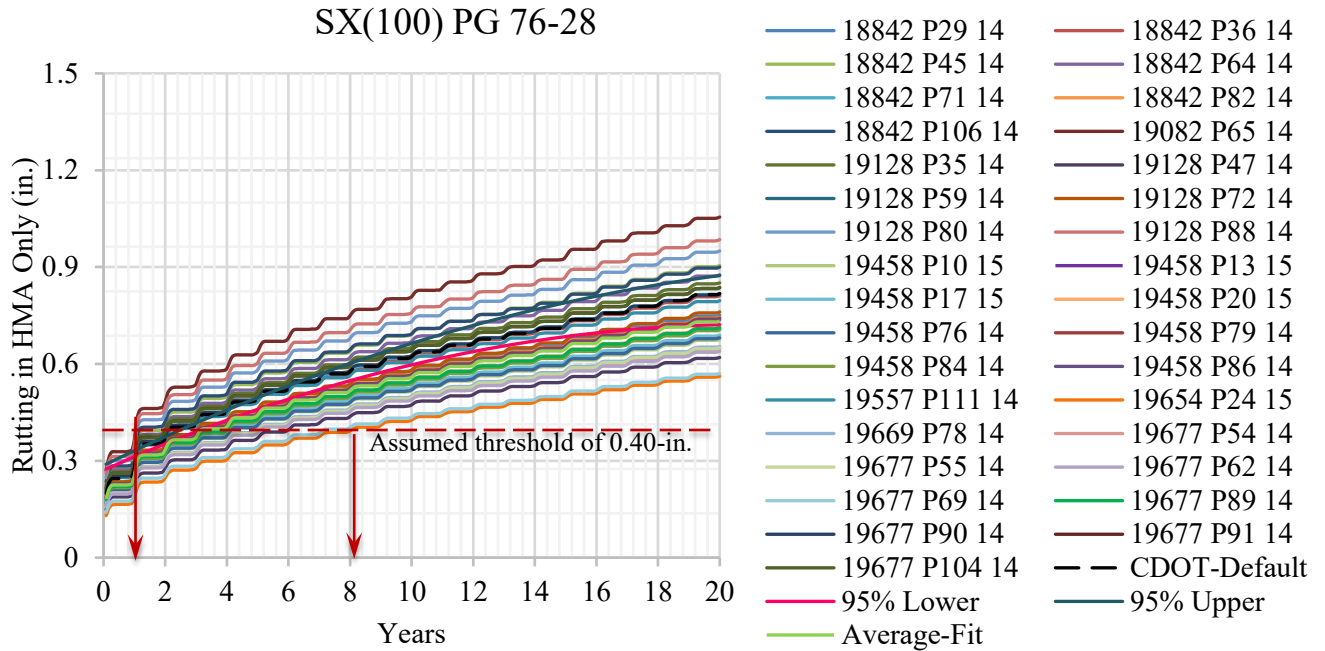


Figure 134. Rutting in the Asphalt Layer Due to AADTT = 7,000 by SX(100) PG 76-28 Mix

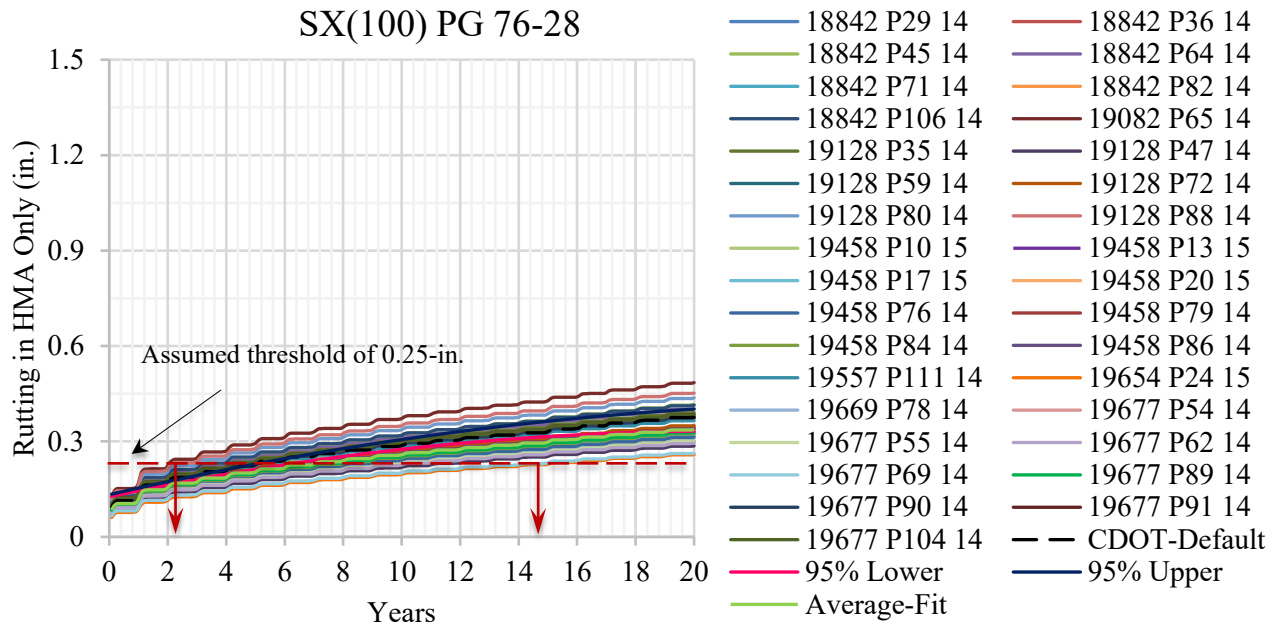


Figure 135. Rutting in the Asphalt Layer Due to AADTT = 800 by SX(100) PG 76-28 Mix

Bottom-up Fatigue Cracking: The bottom-up fatigue cracking variation during its service life of the trial pavement is shown in Figures 136 and 137 for AADTT = 7,000 and AADTT = 800, respectively. They show that the default CDOT mixture produces about the average amount of

bottom-up fatigue cracking. Comparing the distress level, the lowest and the highest bottom-up fatigue cracking predicted are 12.23%, and 17.98%, respectively, at 10-year life for AADTT = 800, which differs by 47%. The assumed threshold of 25% of the lane area shown in Figure 136 shows that the mixes reach the threshold between two and three years, which is very close to each other. For low traffic as shown in Figure 137, mixes reach the threshold between thirteen and nineteen years with the threshold of 25% of the lane area. The statistical 95% CI boundaries show that many mixes are outside the 95% CI boundaries. The bottom-up fatigue cracking prediction may vary from about five years as shown in Figure 137 for low traffic.

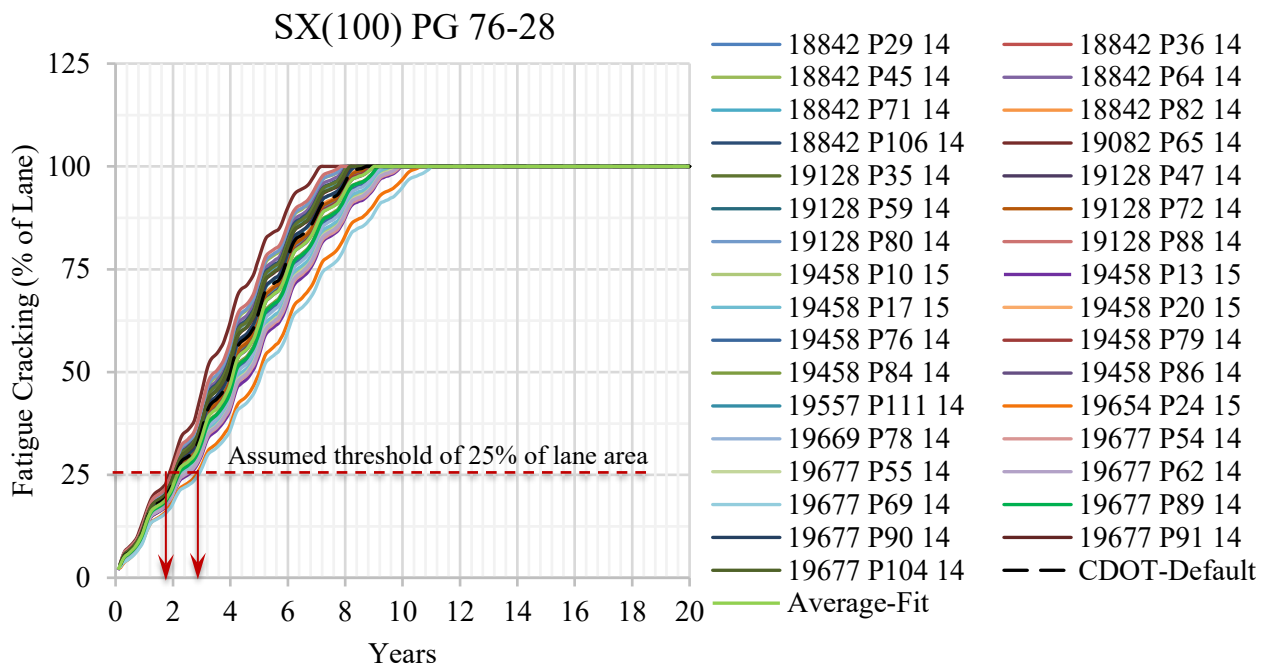


Figure 136. Bottom-up Fatigue Cracking Due to AADTT = 7,000 by SX(100) PG 76-28 Mix

SX(100) PG 76-28

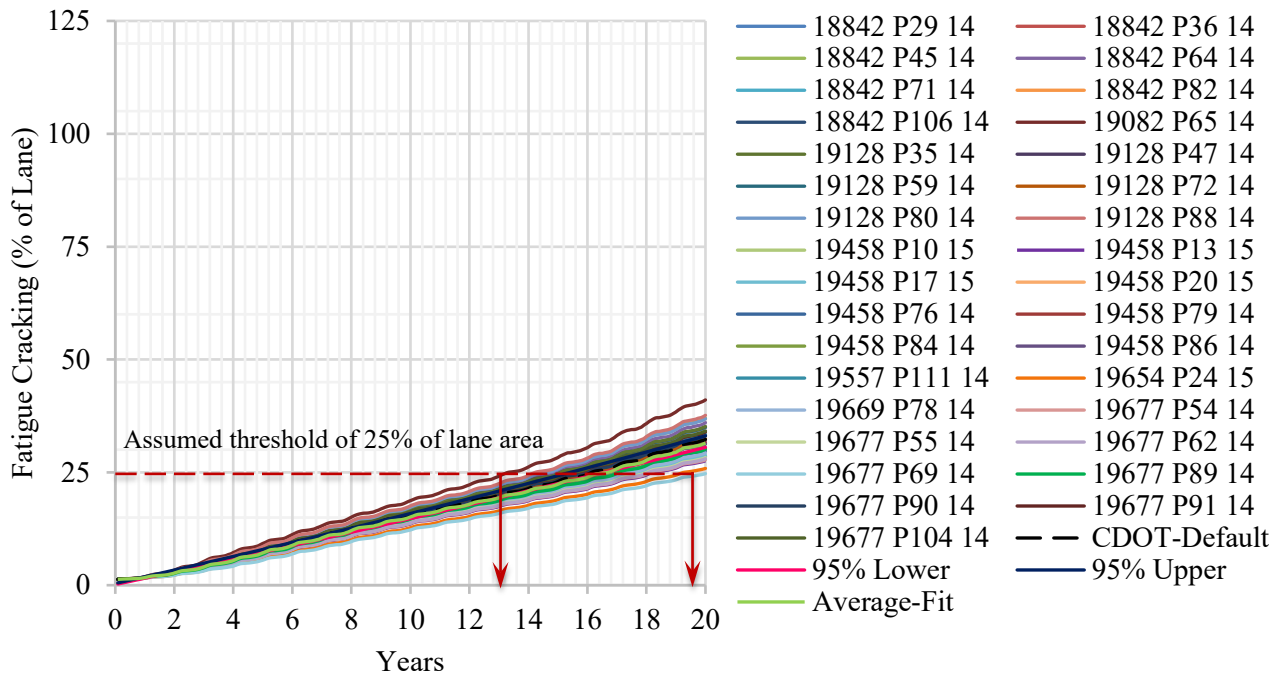


Figure 137. Bottom-up Fatigue Cracking Due to AADTT = 800 by SX(100) PG 76-28 Mix

Top-down Longitudinal Cracking: The top-down longitudinal cracking variation during the service life of the trial pavement is shown in Figures 138 and 139 for AADTT = 7,000 and AADTT = 800, respectively. They show that the default CDOT mixture produces about the average amount of top-down longitudinal fatigue cracking. Comparing the distress level, the lowest and the highest top-down longitudinal cracking predicted are 2673 and 3709 ft./mi., respectively, at 10-year life for AADTT = 800. The highest top-down longitudinal cracking is 39% larger than the lowest top-down longitudinal cracking. The prediction reaches the threshold of 3,000 ft./mi. from about 6 to 14 years for mix to mix for high traffic as shown in Figure 138. The mix reaches the threshold of 1,500 ft./mi. from eight years to 19 years from mix to mix for low traffic. The statistical 95% CI boundaries show that many mixes are outside the 95% CI boundaries. The average-fit data produces the top-down longitudinal cracking, along with other distresses mentioned above, marginally within the 95% CI boundaries of the CDOT mix.

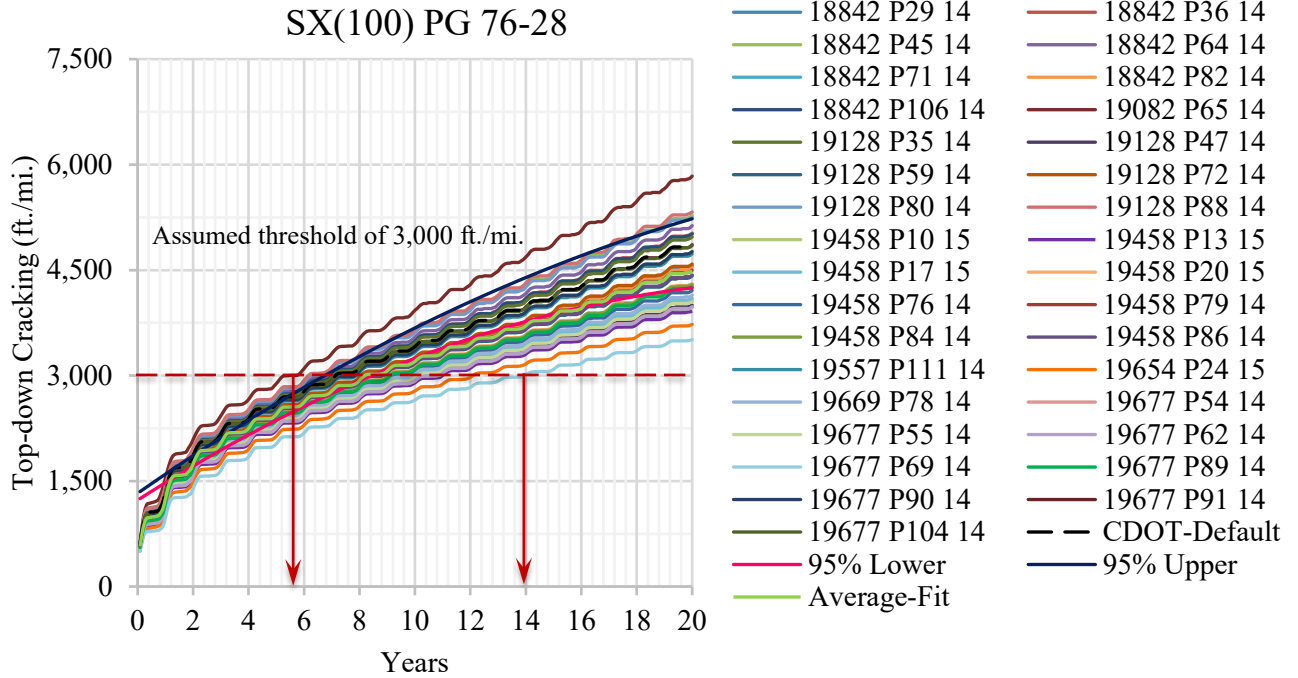


Figure 138. Longitudinal Cracking Due to AADTT = 7,000 by SX(100) PG 76-28 Mix

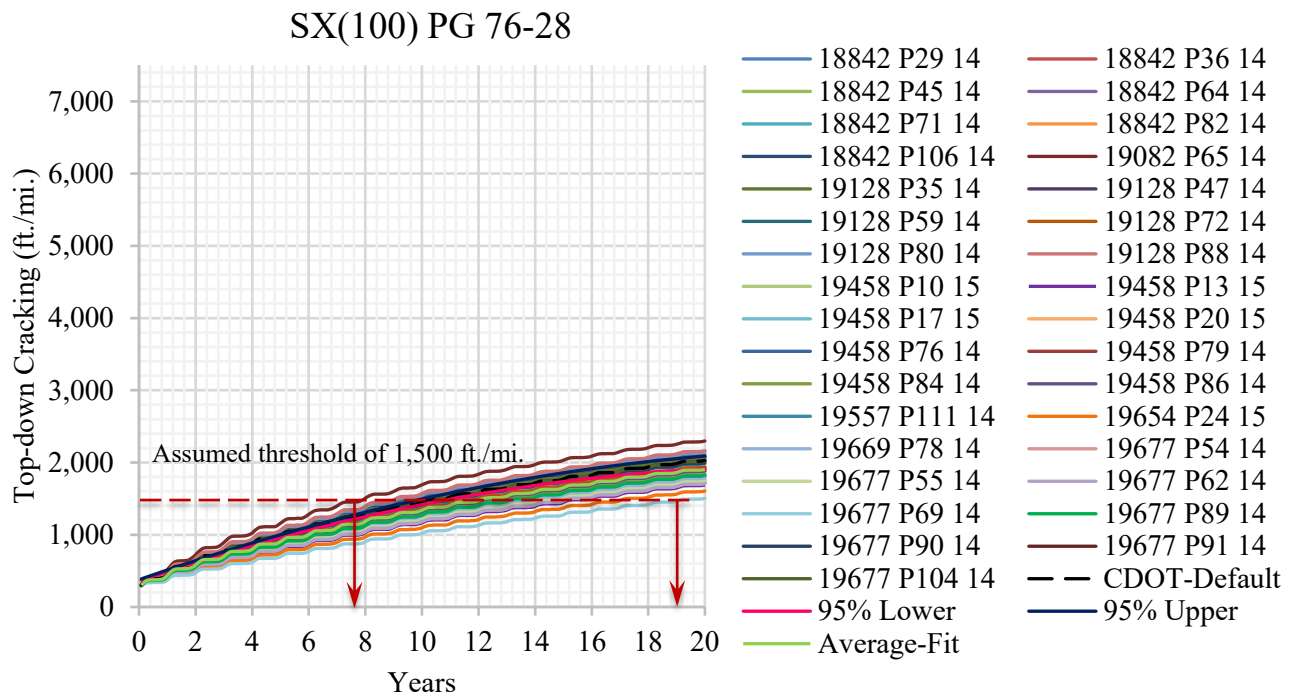


Figure 139. Longitudinal Cracking Due to AADTT = 800 by SX(100) PG 76-28 Mix

From the mix parameters listed in Table 61, the mixes which are not statistically the same with the CDOT-default mix do have properties that vary from those mixes, having statistically the same with the CDOT-default mix. Therefore, the effect of an individual mix parameter may not be appropriately determined for this mix.

To determine the influence of V_{be} , V_a , VMA, VFA, and AC, a regression analysis is conducted, and the following correlations are obtained. The R^2 of the correlations of IRI, total rutting, rutting in HMA, FC, and TDC are 0.44, 0.38, 0.37, 0.51, and 0.31, respectively. It can be seen that all distresses increase with the increase in V_{be} , V_a , VMA, and AC, and decrease with the increase in AC.

$$\text{IRI (in./mi.)} = 148.9982 + 2.0406 V_{be} + 1.5794 V_a + 1.5638 \text{ VMA} - 0.2927 \text{ VFA} + 2.642 \text{ AC}$$

$$\text{Total Rutting (in.)} = -0.074 + 0.0218 V_{be} + 0.0192 V_a + 0.0235 \text{ VMA} - 0.0022 \text{ VFA} + 0.0309 \text{ AC}$$

$$\text{Rutting in HMA (in.)} = -0.1364 + 0.0216 V_{be} + 0.017 V_a + 0.0218 \text{ VMA} - 0.0025 \text{ VFA} + 0.0273 \text{ AC}$$

$$\text{FC (\%)} = 4.4372 + 0.5244 V_{be} + 0.3415 V_a + 0.2786 \text{ VMA} + 0.0771 \text{ VFA} + 0.5284 \text{ AC}$$

$$\text{TDC (ft./mi.)} = -8467.06 - 151.464 V_{be} + 6.3975 V_a + 367.4666 \text{ VMA} + 69.5876 \text{ VFA} + 498.2458 \text{ AC}$$

Analysis Summary

Tables 62–66 show a summary of the analysis of different regions of Colorado and the recommended mix based on the performance on the trial pavements. For example, the Average-Fit mix is recommended for pavement design in Region 1 using S(100) PG 64-22, SMA PG 76-28, SX(75) PG 58-28, and SX(100) PG 64-22 mixes. The CDOT-Default mix is good for pavement design in Region 1 using S(100) PG 64-22, SX(75) PG 58-28, and SX(100) PG 64-28 mixes. The mix, 19879 P113 14 is also good for pavement design using a SX(75) PG 58-28 mix in Region 1.

Table 62. Summary of Region 1 Mixes Using the Statistical Analysis

Mix Type	Mix ID	Paving Contractor	Recommended Mix
S(100) PG 64-22	18206 P52 14*	Aggregate Industries	Average-Fit CDOT-Default
	18695 P9 15	APC Southern	
	18695 P13 14*	APC Southern	
	18695 P25 14*	-	
	18695 P6 14	-	
	Avergae-Fit*	-	
S(100) PG 76-28	-	-	-
SMA PG 76-28	17890 P40 14	Martin Marietta	Average-Fit
	17890 P56 14*	Martin Marietta	
	17890 P66 14	Martin Marietta	
	19807 P32 14	Brannan	
	Avergae-Fit*	-	
SX(75) PG 58-28	19879 P113 14*	-	19879 P113 14 CDOT-Default Average-Fit
	Avergae-Fit*	-	
SX(75) PG 58-34	-	-	-
SX(75) PG 64-22	-	-	-
SX(75) PG 64-28	-	-	-
SX(100) PG 58-28	-	-	-
SX(100) PG 64-22	18180 P3 14	Aggregate Industries	Average-Fit
	19904 P14 15	Martin Marietta	
	Avergae-Fit	-	
SX(100) PG 64-28	19879 P114 14	-	CDOT-Default
	Avergae-Fit*	-	
SX(100) PG 76-28	-	-	-

*Note: * Indicates mix is statistically similar to the CDOT-Default Mix*

The Average-Fit mix is recommended for pavement design in Region 2 using SMA PG 76-28, SX(75) PG 64-22, and SX(100) PG 64-22 mixes. The CDOT-Default mix is good for pavement design in Region 2 using SX(100) PG 64-28 and SX(100) PG 76-28 mixes.

Table 63. Summary of Region 2 Mixes Using the Statistical Analysis

Mix Type	Mix ID	Paving Contractor	Recommended Mix
S(100) PG 64-22	-	-	-
S(100) PG 76-28	-	-	-
SMA PG 76-28	18842 P30 14	Kiewit	Avergae-Fit
	18842 P43 14*	Kiewit	
	18842 P44 14	Kiewit	
	18842 P60 14	Kiewit	
	18842 P83 14	Kiewit	
	Avergae-Fit*	-	
SX(75) PG 58-28	-	-	-
SX(75) PG 58-34	-	-	-
SX(75) PG 64-22	19127 P73 14	Beltramo	Avergae-Fit
	19127 P75 14	Beltramo	
	19935 P58 14	A&S	
	19935 P61 14*	A&S	
	19935 P63 14	A&S	
	Avergae-Fit	-	
SX(75) PG 64-28	-	-	-
SX(100) PG 58-28	-	-	-
SX(100) PG 64-22	18842 P10 14	Kiewit Construction	Avergae-Fit
	18842 16 14	Kiewit Construction	
	18842 P22 14	Kiewit Construction	
	19128 P81 14	Martin Marietta	
	19275 P1 14	APC Southern	
	19275 P2 14	APC Southern	
	19275 P5 14	Aggregate Industries	
	19655 P18 14	APC Southern	
	Avergae-Fit	-	
SX(100) PG 64-28	19655 P20 14	APC Southern	CDOT-Default
	19655 P21 14*	APC Southern	
	19655 P23 14*	APC Southern	
	19655 P24 14*	APC Southern	
	19655 P28 14	APC Southern	
	19655 P37 14*	APC Southern	

	19655 P48 14	APC Southern	
	19655 P87 14*	APC Southern	
	Average-Fit*	-	
SX(100) PG 76-28	18842 P29 14	Kiewit Construction	CDOT-Default
	18842 P36 14*	Kiewit Construction	
	18842 P45 14	Tezak	
	18842 P64 14*	Kiewit Construction	
	18842 P71 14*	Kiewit Construction	
	18842 P82 14	Kiewit Construction	
	19128 P35 14*	Martin Marietta	
	19128 P47 14	Evans	
	19128 P59 14	Martin Marietta	
	19128 P72 14	Martin Marietta	
	19128 P80 14	Martin Marietta	
	19128 P88 14	Martin Marietta	
	19557 P111 14*	A&S Construction	
	19654 P24 15	Martin Marietta	
	19669 P78 14	A&S Construction	
	Average-Fit*	-	

*Note: * Indicates mix is statistically similar to the CDOT-Default Mix*

The Average-Fit mix is recommended for pavement design in Region 3 using SX(75) PG 58-28, SX(75) PG 64-28, and SX(100) PG 64-22 mixes. The CDOT-Default mix is good for pavement design in Region 3 using SX(75) PG 58-28, SX(75) PG 58-34, and SX(100) PG 76-28 mixes.

Table 64. Summary of Region 3 Mixes Using the Statistical Analysis

Mix Type	Mix ID	Paving Contractor	Recommended Mix
S(100) PG 64-22	-	-	-
S(100) PG 76-28	-	-	-
SMA PG 76-28	-	-	-
SX(75) PG 58-28	17735 P27 14	United Companies	CDOT-Default (better) Average-Fit (About average)
	19095 P42 14	United Gypsum	
	19171 P57 14	Everist Materials	
	19489 P51 14	Elam	
	20167 P21 15	Grand River	
	Average-Fit*	-	
SX(75) PG 58-34	19217 P41 14	Connell Resources	CDOT-Default
	19708 P68 14	Connell Resources	
	Average-Fit	-	
SX(75) PG 64-22	-	-	-
SX(75) PG 64-28	16439 P77 14	Everist	Average-Fit
	Average-Fit	-	
SX(100) PG 58-28	-	-	-
SX(100) PG 64-22	19300 P34 14	United Companies	Average-Fit
	Average-Fit	-	
SX(100) PG 64-28	-	-	-
SX(100) PG 76-28	19677 P54 14	Elam	CDOT-Default
	19677 P55 14	Elam	
	19677 P62 14	Elam	
	19677 P69 14	Elam	
	19677 P89 14	Elam	
	19677 P90 14*	Elam	
	19677 P91 14*	Elam	
	19677 P104 14*	Elam	
Average-Fit*	-		

*Note: * Indicates mix is statistically similar to the CDOT-Default Mix*

The Average-Fit is recommended for Region 4 for S(100) PG 76-28 mix. The CDOT-Default Mix is over designed.

The Average-Fit mix is recommended for pavement design in Region 4 using S(100) PG 76-28, SMA PG 76-28, SX(75) PG 64-22, and SX(75) PG 64-28 mixes. The CDOT-Default mix is good for pavement design in Region 4 using SMA PG 76-28, SX(100) PG 58-28, and SX(100) PG 76-28 mixes. Mixes, 18465 P9 14 and 18887 P15 14 mixes can be used for S(100) PG 64-22 and SX(100) PG 58-28, respectively, for pavement design in Region 4.

Table 65. Summary of Region 4 Mixes Using the Statistical Analysis

Mix Type	Mix ID	Paving Contractor	Recommended Mix
S(100) PG 64-22	18465 P9 14	Asphalt Paving	18465 P9 14 (conservative)
S(100) PG 76-28	17800 P17 14	Aggregate Industries	Average-Fit
	17800 P26 14	Aggregate Industries	
	17800 P38 14	Aggregate Industries	
	17800 P53 14	Aggregate Industries	
	Average-Fit	-	
SMA PG 76-28	17800 P70 14	Aggregate Industries	Average-Fit CDOT-Default (Acceptable but under predicts)
	17800 P85 14	Aggregate Industries	
	19314 P7 14	Martin Marietta	
	Average-Fit*	-	
SX(75) PG 58-28	-	-	-
SX(75) PG 58-34	-	-	-
SX(75) PG 64-22	19458 P105 14*	Simon	Average-Fit
	20189 P7 15	McAtee	
	Average-Fit	-	
SX(75) PG 64-28	19356 P22 15	Asphalt Specialties	Average-Fit
	20098 P19 15	Coulson	
	20098 P23 15	Coulson	
	Average-Fit	-	
SX(100) PG 58-28	18887 P15 14*	United Companies	18887 P15 14 CDOT-Default
SX(100) PG 64-22	-	-	-
SX(100) PG 64-28	-	-	-
SX(100) PG 76-28	19458 P10 15	Simon Construction	CDOT-Default
	19458 P13 15	Simon Construction	
	19458 P17 15	Simon Construction	
	19458 P20 15	Simon Construction	
	19458 P76 14	Simon Construction	
	19458 P79 14	Simon Construction	
	19458 P84 14	Simon Construction	
	19458 P86 14	Simon Construction	
	Average-Fit *	-	

Note: * Indicates mix is statistically similar to the CDOT-Default Mix

The Average-Fit mix is recommended for pavement design in Region 5 using SX(75) PG 58-28, and SX(100) PG 64-22 mixes. The CDOT-Default mix is good for pavement design in Region 5 using SX(75) PG 58-28 and SX(100) PG 76-28.

Table 66. Summary of Region 5 Mixes Using the Statistical Analysis

Mix Type	Mix ID	Paving Contractor	Recommended Mix
S(100) PG 64-22	-	-	-
S(100) PG 76-28	-	-	-
SMA PG 76-28	-	-	-
SX(75) PG 58-28	19633 P94 14	4 Corners	CDOT-Default (better) Average-Fit (About average)
	19707 P92 14*	Elam	
	Average-Fit*	-	
SX(75) PG 58-34	-	-	-
SX(75) PG 64-22	-	-	-
SX(75) PG 64-28	-	-	-
SX(100) PG 58-28	-	-	-
SX(100) PG 64-22	19202 P107 14	Skanska	Average-Fit
	19202 P112 14	Skanska	
	Average-Fit	-	
SX(100) PG 64-28	-	-	-
SX(100) PG 76-28	18970 P106 14	APC Southern	CDOT-Default
	19082 P65 14	ACA Buena Vista	
	Average-Fit *	-	

*Note: *Indicates mix is statistically similar to the CDOT-Default Mix*

Regarding contractors, mixes by Asphalt Paving, Brannan, United Gypsum, Everist Materials, Grand River, 4 Corners, Connell Resources, Beltramo, McAtee, Everist, Asphalt Specialties, Coulson, Skanska, Tezak, Evans and ACA Buena Vista are not statistically the same as the CDOT-default mix, regardless of group. The other contractors such as Kiewit, APC Southern, United Companies, Martin Marietta, A&S, and Elam are sometimes statistically the same as the CDOT-default mix.

The average-fit dynamic moduli curves yield statistically the same distress as the CDOT-default mix data for S(100) PG 64-22, SX(75) PG 58-28, SX(75) PG 64-28, SX(100) PG 58-28, SX(100) PG 64-28, and SX(100) PG 76-28. For other mixtures, S(100) PG 76-28, SMA PG 76-28, SX(75) PG 58-28, SX(75) PG 64-22, and SX(100) PG 64-22, the average-fit dynamic moduli curves do not yield statistically the same distress as the CDOT-default mix data.

The influences of different mix parameters are not consistent, as observed in the group analysis. The summary of the influence of different mix parameters is provided in Table 67. All distresses except rutting in HMA increase with an increase in V_a , VMA, and VFA, and are insensitive to V_{be} and AC in the study range of these parameters. Rutting in HMA increases with an increase in VMA and VFA, and is insensitive to V_{be} , V_a , and AC.

Table 67. Summary of the Influence of Different Mix Parameters

	V_{be} (%)	V_a (%)	VMA (%)	VFA (%)	AC (%)
IRI (in./mi.)	4 Increases 4 Decreases 3 N/A	5 Increases 4 Decreases 2 N/A	6 Increases 3 Decreases 2 N/A	6 Increases 3 Decreases 2 N/A	4 Increases 2 Decreases 5 N/A
Total Rutting (in.)	4 Increases 4 Decreases 3 N/A	5 Increases 4 Decreases 2 N/A	6 Increases 3 Decreases 2 N/A	6 Increases 3 Decreases 2 N/A	3 Increases 3 Decreases 5 N/A
Rutting in HMA (in.)	4 Increases 3 Decreases 4 N/A	4 Increases 4 Decreases 3 N/A	7 Increases 3 Decreases 1 N/A	5 Increases 3 Decreases 3 N/A	3 Increases 3 Decreases 5 N/A
FC (%)	4 Increases 4 Decreases 3 N/A	5 Increases 4 Decreases 2 N/A	6 Increases 3 Decreases 2 N/A	6 Increases 3 Decreases 2 N/A	3 Increases 3 Decreases 5 N/A
TDC (ft./mi.)	4 Increases 4 Decreases 3 N/A	5 Increases 4 Decreases 2 N/A	6 Increases 3 Decreases 2 N/A	7 Increases 2 Decreases 2 N/A	4 Increases 2 Decreases 5 N/A

SECTION 7: CONCLUSIONS AND RECOMMENDATIONS

Conclusions

The following conclusions can be made from the study:

- a) S(100) PG 76-28 is the most durable mix for rutting, and SX(75) PG 58-34 is the most durable mix for transverse cracking.
- b) SX(75) PG 64-28 is the most susceptible mix for rutting, and S(100) PG 64-22 is the most susceptible mix for transverse cracking.
- c) The dynamic modulus of an HMA mix can vary from 200 ksi to about 1,000 ksi.
- d) The E^* increases with an increase in V_{be} , V_a , and VFA, and decreases with an increase in VMA and AC. However, the effects of VFA and AC on E^* are less sensitive compared to V_{be} , V_a , and VFA.
- e) There are effects of aggregate pit, paving contractor, effective binder content, air voids, VMA, VFA, etc. on the prediction of distresses using the PMED software. However, the effect of each individual parameter is still unknown.
- f) The prediction of distresses using the PMED software by a mix prepared by a single contractor may differ by up to eleven years, although most of the data reveals three to seven years.
- g) IRI, total rutting, fatigue cracking, and top-down cracking increase with V_a , VMA, but not VFA, and are insensitive to V_{be} and AC.
- h) Rutting in HMA increases with the increase in VMA and VFA, but is insensitive to V_{be} , V_a , and AC.
- i) There are mixes in all Regions of Colorado which are sometimes statistically the same as the CDOT default mix.
- j) Mixes by Asphalt Paving, Brannan, United Gypsum, Everist Materials, Grand River, 4 Corners, Connell Resources, Beltramo, McAtee, Everist, Asphalt Specialties, Coulson, Skanska, Tezak, Evans and ACA Buena Vista are not statistically the same as the CDOT-default mix, regardless of group. The other contractors such as Kiewit, APC Southern, United Companies, Martin Marietta, A&S, and Elam are sometimes

- statistically the same as the CDOT-default mix. The prediction of distresses using the PMED software may differ by up to 170%, although most data show that the difference is less than 100%.
- k) The average-fit dynamic moduli curves yield statistically the same distress as the CDOT-default mix data for S(100) PG 64-22, SX(75) PG 58-28, SX(75) PG 64-28, SX(100) PG 58-28, SX(100) PG 64-28, and SX(100) PG 76-28.
 - l) The same mix may have statistically different flow numbers and is independent of contractor.
 - m) Flow number increases with an increase in V_{be} , V_a , VMA, VFA, and AC.
 - n) Only two types of mixtures, SX(100) PG 76-28 and SMA PG 76-28, have flow numbers greater than 740. Thus, only these mixtures are considered good for traffic greater than 30 million ESALs.
 - o) S(100) PG 76-28 has an average flow number of more than 190; thus, it is considered good for traffic between 10 to 30 million ESALs.
 - p) SX(100) PG 64-22, SX(100) PG 64-28 and SX(100) PG 58-28 are considered good for traffic between 3 to 10 million ESALs.
 - q) Other five mixtures: S(100) PG 64-22, SX(75) PG 58-28, SX(75) PG 58-34, SX(75) PG 64-22 and SX(75) PG 64-28 have a flow number less than 50; thus, they are considered good for traffic less than 3 million ESALs.

Recommendations for Future Studies

Recommendations for a future research are summarized below:

- a) A revised E^* predictive model can be developed which may be used for Level 2 or Level 3 pavement analysis and design.
- b) Determine the effect of individual mix parameters on the pavement performance. A designed test matrix should be developed.
- c) A flow number predictive model can be developed for Colorado's mixtures to determine the flow number of a new mix.

Implementation Plans

Some implementation plans proposed by the study are listed below:

- a) The developed dynamic modulus mastercurves can be used in the PMED software for analyzing and designing pavements for S(100) PG 64-22, S(100) PG 76-28, SMA PG 76-28, SX(75) PG 58-28, SX(75) PG 58-34, SX(75) PG 64-22, SX(75) PG 64-28, SX(100) PG 58-28, SX(100) PG 64-22, SX(100) PG 64-28 and SX(100) PG 76-28 mixtures.
- b) In selecting a contractor, binder source, and aggregate pit, care needs to be taken as pavement performance varies highly due to these parameters.
- c) The flow number can be directly used to choose a mixture for a pavement whose design ESALs is known.

REFERENCES

1. Clyne, T. R., X. Li, M. O. Marasteanu, and E. L. Skok. (2003). *Dynamic and Resilient Modulus of Mn/DOT Asphalt Mixtures*. Report No. MN/ RC-2003-09, 2003, Minnesota Department of Transportation, St. Paul, MN.
2. Rahman, A., Islam, M. R., and Tarefder, R. A. (2016). “Modifying the Viscosity Based Witzcak Model and Developing Phase Angle Predictive Model for New Mexico’s Superpave Mixes.” *Transportation Research Board (TRB) 95th Annual Meeting*, Jan. 10–14, 2016, Arehington, D.C., Paper ID. 16-3180.
3. Birgisson, B., G. Sholar, and R. Roque. Evaluation of Predicted Dynamic Modulus for Florida Mixtures. 84th Annual Meeting of the Transportation Research Board, Paper No. 05-1309, 2005, Washington D.C.
4. Ceylan, H., Schwartz, C., Kim, S. and Gopalakrishnan, K. (2009). Accuracy of Predictive Models for Dynamic Modulus of Hot-Mix Asphalt, *Journal of Materials in Civil Engineering*, Vol. 21, No. 6, pp. 286–293.
5. Christensen, D. W., T. K. Pellinen, and R. F. Bonaquist. Hirsch Model for Estimating the Modulus of Asphalt Concrete. *Journal of Association Asphalt Paving Technologists*, Vol. 72, 2003, pp. 97–121.
6. Kim, Y.R., M. King, and M. Momen. Typical Dynamic Moduli Values of Hot Mix Asphalt in North Carolina and Their Prediction. *84th Annual Meeting of the Transportation Research Board*, Paper No. 05-2568, 2005, Arehington D.C.
7. Mohammad, L.N., Z. Wu, L. Myers, S. Cooper, and C. Abadie. A Practical Look at Simple Performance Tests: Louisiana’s Experience. *Journal of the Association of Asphalt Paving Technologists*, Vol. 74, 2005, pp. 557-600.
8. Sakhaeifar, M., Kim, Y. and Kabir, P. (2015). New predictive models for the dynamic modulus of hot mix asphalt, *Construction and Building Materials*, Vol. 76, pp. 221–231.
9. Tran, N.H., and K.D. Hall. Evaluating the Predictive Equation in Determining Dynamic Moduli of Typical Asphalt Mixtures Used in Arkansas. *Journal of the Association of Asphalt Paving Technologists*, Volume 74, 2005, pp. 1-17.

10. Hu, H., and Shen, S. (2012). An Investigation of Dynamic Modulus and Flow Number Properties of Asphalt Mixtures in Washington State, Final Report, No. 709867, USDOT, Office of the Secretary of Transportation, Washington D.C.
11. AASHTO TP 79. Standard Method of Test for Determining the Dynamic Modulus and Flow Number for Asphalt Mixtures Using the Asphalt Mixture Performance Tester (AMPT), 2015, American Association of State Highway and Transportation Officials (AASHTO), Washington D.C. DC, pp. 1- 21.
12. Kaloush, K.E., (2001), Simple performance test for permanent deformation of asphalt mixtures. Doctoral Dissertation, Department of Civil and Environmental Engineering, Arizona State University, Tempe, Arizona.
13. Kvasnak et al. (2007), Statistical development of a flow number predictive equation for the Mechanistic-Empirical Pavement Design Guide, TRB Annual Meeting, Washington D.C., Paper 07-1000.
14. Christensen, D. et al. (2009). A Mix Design Manual for Hot-Mix Asphalt, NCHRP 9-33 Report, National Cooperative Highway Research Program (NCHRP), Washington D.C.
15. Rodezno, M. C., Kaloush, K.K. and Corrigan, M. R. (2010), Development of a Flow Number Predictive Model. 2010 Transportation Research Board CD-ROM, TRB, Washington D.C.
16. AASHTO TP 62, Standard Method of Test for Determining Dynamic Modulus of Hot Mix Asphalt (HMA), 2007, American Association of State Highway and Transportation Officials (AASHTO), Washington D.C. DC, pp. 1- 21.
17. Biligiri, K. and Way, G. (2013), Predicted E^* dynamic moduli of the Arizona mixes using asphalt binders placed over a 25-year period, Construction and Building Materials, Vol. 54, pp. 520–532.